UNIVERSIDAD COMPLUTENSE DE MADRID
FACULTAD DE CIENCIAS ECONÓMICAS Y EMPRESARIALES

TESIS DOCTORAL

Energy Commodities: New Approaches For Pricing Options

Materias Primas de Energía: Nuevos Enfoques para la Valoración de Opciones

MEMORIA PARA OPTAR AL GRADO DE DOCTOR

PRESENTADA POR

María del Carmen Frau Gomila

Directores

John Crosby
María Dolores Robles Fernández

Madrid

UNIVERSIDAD COMPLUTENSE DE MADRID

FACULTAD DE CIENCIAS ECONÓMICAS Y EMPRESARIALES

TESIS DOCTORAL

Energy Commodities: New Approaches For Pricing Options
Materias Primas de Energía: Nuevos Enfoques para la Valoración de Opciones

MEMORIA PARA OPTAR AL GRADO DE DOCTORA

PRESENTADA POR

María del Carmen Frau Gomila

DIRECTORES

John Crosby

María Dolores Robles Fernández

UNIVERSIDAD COMPLUTENSE DE MADRID

FACULTAD DE CIENCIAS ECONÓMICAS Y EMPRESARIALES

TESIS DOCTORAL

Energy Commodities: New Approaches For Pricing Options

Materias Primas de Energía: Nuevos Enfoques para la Valoración de Opciones

MEMORIA PRESENTADA EN CUMPLIMIENTO DE LOS REQUISITOS
PARA OPTAR AL GRADO DE DOCTORA

María del Carmen Frau Gomila

DIRECTORES

John Crosby
María Dolores Robles Fernández

COMPLUTENSE UNIVERSITY OF MADRID
FACULTY OF ECONOMICS AND BUSINESS

DOCTORAL THESIS

Energy Commodities: New Approaches For Pricing Options
Materias Primas de Energía: Nuevos Enfoques para la Valoración de Opciones

A THESIS SUBMITTED IN FULLFILMENT OF THE REQUIREMENTS
FOR THE DEGREE OF DOCTOR OF PHILOSOPHY

María del Carmen Frau Gomila

SUPERVISORS

John Crosby
María Dolores Robles Fernández

To my family

Acknowledgements

First and foremost, I would like to thank my supervisor John Crosby for supporting and believing in me during all this time, even before this adventure begun back in our days in London. He has also been a mentor and I have learned a lot from him.

I would also like to thank many others, primarilly my local supervisor at UCM and tutor Lola Robles, for helping me so much during the last year of this endeavour – yours have been the wisest pieces of advice, most of all in difficult moments. A special thank you to Viviana Fanelli, for trusting and encouraging me, listening to me in difficult times, and making me laugh (almost) every day.

I would also like to thank both Gianluca Fusai and Ioannis Kyriakou for hosting me during my international research stay in the summer of 2021. Unfortunately due to the Covid-19 pandemic, it was impossible for me to be physically in London at Bayes Business School. Albeit on-line, I learned a lot.

I want to dedicate another warm thank you to my other academic mentor Lourdes Moreno, for guiding me in my incipient career in academia since we first met and for always being by my side – you have been a superb host in office N-315 during the time I worked at UCM as adjunct professor (2018-2020). I also want to mention the department colleagues, with whom I shared many lunches and challenging conversations.

And last but not at all least to my family, who have always been by my side. My son Jordi, who was so patient waiting to be with me untill I finished working in this thesis in the evenings. My partner Agustín, who takes care of me, accompanies me in his superb way and always encourages me to think big. My mum Catalina, for being the best mum in the world and hosting us in the wonderful country house where we live in now. And my dad Pedro, who passed away during the writting of this thesis; he was always wondering when I would stop studying – I am afraid that moment is yet to come. I also want to mention those family members who travelled with me to Bilbao in July 2010 showing their support when I was presenting my M.Sc. dissertation – it meant a lot to me. And a warm thank you to my cousin Rosa – without that phone call, I don't know if this work would have ever existed.

I also would like to thank all other family, colleagues or friends who showed interest in my research in one way or another. To all of you, thank you!

Resumen

UNIVERSIDAD COMPLUTENSE DE MADRID
Facultad de Ciencias Económicas y Empresariales
Grado de Doctora

Materias Primas Energéticas: Nuevos Enfoques para la Valoración de Opciones

por María del Carmen Frau Gomila

En esta tesis nos centramos en la valoración de opciones de compra y venta europeas estándar cuyo subyacente son los precios de los contratos de futuros sobre dos materias primas energéticas: el petróleo West Texas Intermediate (WTI) (Capítulo 1) y el gas natural Henry Hub (HH) (Capítulo 2). Ambos cotizan en dólares USD en la Bolsa de materias primas de Nueva York (NYMEX) especializada en activos derivados (futuros y opciones) sobre productos agrícolas, metales preciosos y materias primas energéticas. También consideramos opciones europeas del tipo diferencial de precios (Capítulo 3).

Para poder plantear la valoración es necesario partir de un modelo para los precios del subyacente en cada caso, por lo que al tratarse de futuros, nos centramos en modelos de estructura temporal en los que el plazo a vencimiento de los contratos es relevante. Partimos del modelo de estructura temporal propuesto por Trolle y Schwartz (2009) como *benchmark*, el cual considera las siguientes características: (i) los precios son estocásticos; (ii) la tasa de rendimiento de los activos es estocástica; (iii) la correlación es negativa entre los precios al contado y su tasa de rendimiento; (iv) hay una reversión a la media de los precios al contado (debido a la correlación negativa anteriormente mencionada); y (v) la volatilidad de los precios de los futuros es estocástica e inversamente proporcional al vencimiento del contrato (efecto Samuelson).

Tanto el petróleo como el gas natural presentan otras características que no están recogidas en este modelo. Los precios del petróleo han presentado saltos hacia abajo importantes en los últimos años, especialmente en el 2014 (*fracking*) y el 2020 (inicio de la pandemia del Covid-19), cuya magnitud se aprecia como inversamente proporcional al vencimiento del contrato. Los precios del gas natural son estacionales en media y varianza; la primera viene implícitamente recogida en la curva de precios de los futuros, no ocurre lo mismo con la segunda.

El modelo presentado en Trolle y Schwartz (2009) así como otros modelos similares existentes en la literatura no son capaces de reproducir simultáneamente todas las características menciona-

das anteriormente, por lo que el objetivo de esta tesis es proponer nuevos modelos que recojan todos estos hechos estilizados y permitan mejorar la valoración de opciones sobre las dos materias primas en cuestión. Esta capacidad es de gran interés en diversos ámbitos: ofrece al ámbito académico un avance en el conocimiento sobre modelos de estructura temporal y permite replicar más exactamente la superficie de volatilidad implícita en las opciones cotizadas; mientras que a diversos actores de la industria les proporciona herramientas para valorar y cubrir los libros de negociación de forma consistente. Una vez especificados los nuevos modelos, se procede a estudiar las dinámicas de los precios y a la valoración de opciones europeas sobre estos activos, para lo cual requerimos conocer la expresión matemática de las funciones características de los precios.

En el Capítulo 1 se incorporan saltos al modelo *benchmark* para investigar posibles mejoras de adecuación a las características del petróleo, proponiendo seis sub-especificaciones. En el Capítulo 2 se extiende el modelo *benchmark* con estacionalidad en la varianza y se estudia su comportamiento aplicado al gas natural, proponiendo dos sub-especificaciones. En estos capítulos se valoran opciones europeas estándar mediante el procedimiento descrito en Carr y Madan (1999) mediante el algoritmo *fast Fourier transform* (FFT). En el Capítulo 3 se valoran opciones europeas sobre diferenciales de precios, en concreto opciones calendario y *crack*; las primeras dependen de la diferencia de precios de dos futuros sobre el mismo activo observado en fechas diferentes, mientras que las segundas dependen de la diferencia de precios de dos futuros sobre diferentes activos observados en una única fecha. Para valorar opciones sobre un diferencial de precios utilizamos los procedimientos propuestos en Carr y Madan (1999) y en Caldana y Fusai (2013).

Obtenemos soluciones analíticas para todos los términos de la función característica del primer modelo, mientras que para el segundo son "cuasi-analíticas" dado que la mayoría de los componentes de la expresión que recoge la estacionalidad presentan una solución cerrada, salvo uno que hemos aproximado por expansiones de Taylor. Comparamos la bondad de ajuste de nuestras propuestas con un panel de modelos bien conocidos en la literatura. En los dos primeros capítulos, trabajamos con series de 10 años (2011-2020) de datos de futuros y opciones para calibrar los parámetros de los modelos a mercado. El análisis se realiza con series mensuales y diarias, logrando con estas últimas mejores resultados en término medio. Los modelos propuestos mejoran todos los del panel incluyendo el *benchmark*, especialmente en contratos de menor duración y cuánto más fuera de dinero.

En cuanto a las opciones de tipo calendario, calculamos la expresión general que sigue la correspondiente función característica conjunta y, para cada modelo, presentamos las expresiones que siguen cada uno de sus términos. Para opciones de tipo *crack*, también proporcionamos las expresiones que siguen los términos de las correspondientes funciones características conjuntas para los modelos más recientes. Todo esto supone una importante contribución ya que permite llenar una laguna en la literatura. En este tercer capítulo desarrollamos una comparativa de los procedimientos de valoración de Carr y Madan (1999) y Caldana y Fusai (2013), concluyendo que el segundo es más robusto y hasta 26.5 veces más rápido en promedio que el primero.

Summary

COMPLUTENSE UNIVERSITY OF MADRID
Faculty of Economics and Business
Doctor of Philosophy
Energy Commodities: New Approaches for Pricing Options
by María del Carmen Frau Gomila

This thesis focuses on the valuation of standard European call and put options, of which the underlyings are the prices of futures contracts on two energy commodities, specifically West Texas Intermediate (WTI) crude oil (Chapter 1) and Henry Hub (HH) natural gas (Chapter 2). Both are quoted in USD and listed in the New York Commodities Exchange (NY MEX), which specialises in derivatives (futures and options) of agricultural products, precious metals and energy commodities. European spread options are also considered (Chapter 3).

In order to define pricing, it is necessary to start by establishing a model for the underlying prices in each case; working with futures prices, the focus is on term-structure models where the time to maturity will be relevant. The starting point is the model proposed in Trolle & Schwartz (2009), considered as the benchmark. The stylised facts represented in this model are the following: (i) prices are stochastic; (ii) the cost of carry is stochastic; (iii) the correlation is negative between spot prices and their cost of carry; (iv) there is a mean-reversion in spot prices (due to the aforementioned negative correlation); and (v) the volatility of futures prices is stochastic and declining with the expiration of the contract (Samuelson effect).

Oil and natural gas present some characteristics which neither Trolle & Schwartz (2009) nor other relevant models in the literature to date are capable of simultaneously reproducing. Notably, oil prices have shown significant downward jumps in recent years, especially in 2014 (fracking) and 2020 (start of the Covid-19 pandemic) in which the magnitude is observed to decline in line with the expiration of the contract. Natural gas prices are seasonal in mean and variance; while the mean is implicitly included in the futures price curve, this does not occur with the variance.

Given that the model presented in Trolle & Schwartz (2009) and similar ones existing in the literature are not capable of simultaneously reproducing all the features previously listed, the objective of this thesis is to propose new models which collect all these stylised facts and improve the valuation of options on the two commodities. This capability is of great interest for different actors:

for academia, it offers an advance in the understanding of term-structure models and the ability of more accurately replicating the implied volatility surface of listed options; as well, it provides tools for industry players to value and hedge trading books consistently. After defining new models, a study is conducted on the price dynamics and the valuation of European options on these assets. The valuation methodologies used require knowing the mathematical expression followed by the characteristic functions of the prices.

In Chapter 1, jumps are incorporated to the benchmark model to investigate possible improvements in line with the characteristics of oil, proposing six sub-specifications. In Chapter 2, the benchmark model is extended with seasonal variance and its behaviour is studied applied to natural gas, proposing two sub-specifications. In these chapters, plain vanilla options on oil and natural gas are valued by means of the method described in Carr & Madan (1999) through the fast Fourier transform (FFT) algorithm. Chapter 3 discusses spread options, specifically calendar and crack; the former depends on the difference in prices of two futures on the same asset observed on different dates, while the latter on the difference in prices of two futures on different assets observed on a common date. The methods proposed in Carr & Madan (1999) as well as Caldana & Fusai (2013) are leveraged to value spread options.

Analytical solutions are presented for all the terms of the characteristic function of the first model. The second model can be described as ”quasi-analytical” since most of the components of the expression that collects the seasonality have a closed-form solution, except one that has been approximated by Taylor expansions. The performance of the newly proposed models is compared with a panel of alternatives well established in the literature. The first two chapters utilise a dataset consisting of 10-year time series (2011-2020) of futures and options to calibrate the models' parameters to market. The analysis is carried out with monthly and daily series, the latter of which yields better results on average. Newly proposed models improve all those in the panel including the benchmark, outperforming them in shorter duration contracts and deep out-of-the-money (OTM) options.

Regarding calendar options, this work calculates the general expression followed by the joint characteristic function aimed for valuing European options for each model, presenting also the expressions followed by each of the terms. In relation to crack options, expressions are provided followed by each of the terms of the joint characteristic functions required to value them through the most recent models. This provides a significant contribution towards filling in a gap in the literature. In the third chapter, a comparison is developed between the different pricing methods in Carr & Madan (1999) and Caldana & Fusai (2013), concluding that the latter is more robust and up to 26.5 times faster on average.

Contents

List of Figures

List of Tables

CHAPTER

1

Jumps in Commodity Prices: New Approaches for Pricing Plain Vanilla Options

Abstract[1]

In this work we present a new term-structure model for commodity futures prices based on Trolle & Schwartz (2009), which we extend by incorporating multiple jump processes. Our work explores the valuation of plain vanilla options on futures prices when the spot price follows a log-normal process, the forward cost of carry curve and the volatility are stochastic variables, and the spot price and the forward cost of carry allow for time-dampening jumps. We obtain an analytical representation of the characteristic function of the futures prices and, hence, also for plain vanilla option prices using the fast Fourier transform (FFT) methodology. We price options on WTI crude oil futures contracts using our model and extant models. We obtain higher accuracy than earlier models and save significantly in computing time.

[1]Co-author: John Crosby, University of Maryland. This chapter refers to an article which is currently under a first R&R at the journal Energy Economics. It can be found at SSRN (id=3754835).

1.1 Introduction

To obtain accurate estimates of the convenience yield of each commodity, it is crucial to adopt a futures pricing model that is capable of matching the different shapes of the term-structure of commodity futures and can explain a large part of their fluctuations.

There are two major approaches to describe the futures price dynamics for pricing options on commodities, spot models and term-structure models. The spot-based approach relies on specifying the dynamics of a limited set of state variables and deriving futures prices endogenously. According to Schwartz (1997), a single-factor model is not suitable for accurately explaining the variations in futures prices (see, e.g., Brennan & Schwartz (1985)). The inclusion of a second state variable (the convenience yield) substantially enhances the model performance and the model is capable of better describing the forward curve. Typically, two-factor models (see, e.g., Gibson & Schwartz (1990), Brennan (1991) and Schwartz (1997)) let the price of a futures contract depend on the specific dynamics of the spot price and the convenience yield, but they typically assume constant interest rates. Several authors suggest the inclusion of stochastic interest rates as a third state variable. Such three-factor models are discussed in Schwartz (1997), Hilliard & Reis (1998), Miltersen & Schwartz (1998), Cortázar & Schwartz (2003), and Nielsen & Schwartz (2004), among others. Richter & Sørensen (2002), in a model focused on agricultural products, explicitly allow for stochastic volatility. Yan (2002) presents a four-factor model which also allows for stochastic volatility, additionally it allows for jumps in the spot price returns and in the volatility.

The term-structure approach relies on specifying the evolution of the futures curve directly, taking the current market futures prices as given. The futures price is the risk-neutral expectation, conditional on the information of the future spot price available at a given time. Within this approach, models have been focused mostly on deterministic volatility functions, but with a major drawback: they produce flat implied volatility surfaces with respect to strike and time to maturity while we observe smile- and skew-shaped surfaces in the market. The inclusion of stochastic volatility allows us to calibrate the model to option volatility smiles and skews, typically seen in option markets. Models that assume deterministic volatilities are discussed in Reisman (1991), Cortázar & Schwartz (1994), Amin, Ng & Pirrong (1995), Hilliard & Reis (1998), Miltersen & Schwartz (1998), Clewlow & Strickland (1999b), Clewlow & Strickland (1999a), Miltersen (2003) and Crosby (2008), among others. Andersen (2010) considers a multi-factor diffusion model based on the Heath, Jarrow & Morton (1992) (HJM hereafter) framework,[2] paying careful attention to the specification of volatility and to issues of seasonality.

[2]Endogenous conditions are imposed on the drift of the futures price process so that it matches the forward curve.

There have been two important extensions in the term-structure literature so far: the inclusion of jumps in the futures dynamics, as in Crosby (2008), and the adaptation of the volatility to be stochastic, as in Trolle & Schwartz (2009) and Trolle (2014). Trolle & Schwartz (2009) is specified under the risk-neutral probability measure and it is based on the HJM framework. Commodity futures prices are driven by two stochastic factors, the spot price and the forward cost of carry curve. They are original in presenting a new stochastic volatility HJM-type model for pricing commodity options. In their three-factor formulation SV1, the volatility of the spot price and that of the cost of carry curve may depend on one volatility factor, whereas in their four-factor general formulation SV2gen, option prices are driven by a short- and a long-term volatility. The advantage of working in an HJM setting is that, as Trolle & Schwartz (2009) point out, unspanned stochastic volatility arises naturally. An analytical representation of the characteristic function of the futures price is derived for the computation of standard European options using Fourier transforms. They compute options numerically.

Jumps in the spot price abound in the literature (see, e.g., Merton (1976), Bates (1996) and Trolle (2014)), as do models that present jumps in the variance process (e.g., Duffie, Pan & Singleton (2000) proposes the SVJJ model which extends Bates (1996) by the addition of exponential jumps in the variance). In the scope of commodity models, however, jumps in the cost of carry have scarcely (if ever) been up to date in the literature. Implicitly, they exist in Crosby (2008).[3]

In this work we present a novel term-structure commodity model which is based on the model of Trolle & Schwartz (2009)-SV1. It presents jumps in those factors that affect the futures price, that is, the spot price and the forward cost of carry curve; this idea is inspired by Crosby (2008). We derive an analytical representation of the characteristic function of futures prices, and compute standard European options analytically using the fast Fourier transform algorithm.

The remainder of this article is structured as follows: in Section 1.2 we present a new three-factor model specification that allows for jumps and describe how to price plain vanilla options on futures contracts; in Section 1.3 we present an alternative characterisation of the parameters or set-up of our model; in Section 1.4 we describe the market data set we use and the estimation method; in Section 1.5 we discuss the values of the calibrated parameters and the pricing performance; and in Section 1.6 we present our conclusions and ideas for further research.

[3]Jumps enter the specification in equal number as futures contracts are considered. Jumps do not enter directly into the spot or cost of carry dynamics, but in the futures dynamics. This model is of the HJM-type but with deterministic volatility.

1.2 A New Three-Factor Model for Futures Prices on Commodities

Let S_t denote the time-t spot price of the commodity, and let $y(t,T)$ denote the time-t instantaneous forward cost of carry that matures at time T, with $y(t,t) = y_t$ the time-t instantaneous spot cost of carry. We model the evolution of the entire futures curve by specifying one process for S_t and another for $y(t,T)$. Also, let v_t denote the instantaneous variance, which follows a mean-reverting process as in Cox, Ingersoll & Ross (1985).

Trolle & Schwartz (2009) extends the existing framework to accommodate unspanned stochastic volatility, which we also incorporate in our model. In this work, we introduce simultaneous jumps in S_t returns and in $y(t,T)$, which are uncorrelated with any standard Wiener process present in the equations that describe the factors dynamics.

1.2.1 The Model Under the Risk-Neutral Measure $\mathbb{Q}$

Consider the following three-factor model. Let (Ω,$\mathcal{F}$,$\mathbb{Q}$) be a probability space on which three Brownian motion processes, W_t^S, W_t^y and W_t^v, are defined for all $0 \leq t \leq T$. On the same probability space, a Poisson process N_t is also defined for all $0 \leq t \leq T$, with a constant intensity parameter $\lambda > 0$. Furthermore, we know that N_t is independent of all Brownian motion processes, W_t^S, W_t^y and W_t^v. Let $\mathcal{F}$ be the filtration generated by these Brownian motions. We also define two random variables, J_S and $J_y(t,T)$, which represent the jump sizes of the Poisson processes in each factor.

The absence of arbitrage implies the existence of a risk-neutral probability $\mathbb{Q}$ under which the drift-adjusted processes followed by $S_t, y(t,T)$ and v_t are governed by the following dynamics

$$\frac{dS_t}{S_t} = \left(y_t - \lambda E_t^{\mathbb{Q}}\left[e^{J_S} - 1\right]\right) dt + \sigma_S \sqrt{v_t}\, dW_t^S + \left(e^{J_S} - 1\right) dN_t, \tag{1.1}$$

$$dy(t,T) = \left(\mu_y(t,T) - \lambda E_t^{\mathbb{Q}}\left[J_y(t,T)\right]\right) dt + \sigma_y(t,T)\sqrt{v_t}\, dW_t^y + J_y(t,T)\, dN_t, \tag{1.2}$$

$$dv_t = \kappa\left(\theta - v_t\right) dt + \sigma_v \sqrt{v_t}\, dW_t^v, \tag{1.3}$$

allowing W_t^S, W_t^y and W_t^v to be correlated with ρ_{Sy}, ρ_{Sv} and ρ_{yv}, which denote pairwise correlations.

The dynamics in (1.1)-(1.3) can also be expressed in an array form

$$d\begin{pmatrix} S_t \\ y(t,T) \\ v_t \end{pmatrix} = \begin{pmatrix} \left(y_t - \lambda E_t^{\mathbb{Q}}\left[e^{J_S}-1\right]\right) S_t \\ \mu_y(t,T) - \lambda E_t^{\mathbb{Q}}\left[J_y(t,T)\right] \\ \kappa(\theta - v_t) \end{pmatrix} dt + \sqrt{v_t}\begin{pmatrix} \sigma_S S_t & 0 & 0 \\ 0 & \sigma_y(t,T) & 0 \\ 0 & 0 & \sigma_v \end{pmatrix} d\begin{pmatrix} W_t^S \\ W_t^y \\ W_t^v \end{pmatrix}$$
$$+ \begin{pmatrix} \left(e^{J_S}-1\right) S_t \\ J_y(t,T) \\ 0 \end{pmatrix} dN_t.$$

The forward cost of carry is defined by the difference between the forward interest rate and the forward convenience yield. Our model could be extended with separate processes. Notwithstanding, and as Trolle & Schwartz (2009) indicate, "for pricing most commodity futures contracts, this extension is of minor importance. Furthermore, for pricing short-term or medium-term options on most commodity futures, the pricing error that arises from not explicitly modeling stochastic interest rates is negligible – since the volatility of interest rates is typically orders of magnitudes smaller than the volatility of futures returns, and the correlation between interest rates and futures returns tends to be very low."

Intuitively, the long-term forward cost of carry rates should be less volatile than the short-term ones. Following Trolle & Schwartz (2009), this requirement is satisfied using the following exponentially-dampened specification for the volatility of the forward cost of carry curve[4]

$$\sigma_y(t,T) \equiv \alpha e^{-\gamma(T-t)}, \tag{1.4}$$

with $\alpha, \gamma > 0$.

The specification followed by the dynamics of the variance v_t guarantees the positiveness of the volatility factor at all times only if the Feller condition is met.[5]

Jump Specifications

The jump component will affect mainly the tails of the distribution of futures returns. We assume that the intensity of the jumps λ is constant. We consider the following cases to specify the nature of jump sizes:

- Jumps in S_t are as in Merton (1976)

[4] With this specification, the parameters σ_S, α, θ and σ_v are not simultaneously identified. Trolle & Schwartz (2009) normalise $\eta = \kappa\theta$ to one to achieve identification whereas we, seeking the same objective and inspired by Heston (1993) and Bates (1996), decide to set σ_S to one instead.

[5] In Heston (1993), the parameters obey that $2\kappa\theta > \sigma_v$, which is when the values of v_t are strictly positive. We also consider this restriction is met in Bates (1996), Trolle & Schwartz (2009), Trolle (2014) and in our model.

Jump assumption (a_1): We assume that $J_S \sim \mathcal{N}(\mu_{J_S}, \sigma^2_{J_S})$ with $\sigma_{J_S} \geq 0$, that is, jumps in S_t are i.i.d. random variables over time.

Jump assumption (a_2): Jumps in S_t are constant in magnitude, $J_S \equiv \mu_{J_S}$, which is equivalent to imposing $\sigma_{J_S} = 0$ in jump assumption (a_1). This can be seen as an special case of jump assumption (b_2).

- Jumps in $y(t,T)$ are as in Crosby (2008)

$$J_y(t,T) \equiv ae^{-b(T-t)}. \tag{1.5}$$

Jump assumption (b_1): We assume that jumps in $y(t,T)$ are as in Merton (1976). The jump amplitude parameter a is assumed to be an i.i.d. random variable over time, the distribution of which is defined with respect to $\mathbb{Q}$, satisfying $-\infty < a < \infty$, all of which are independent of the Brownian motions and the Poisson processes. With this, we allow the mean jump to be positive or negative. In this case, the jump-decay parameter b is assumed to be identically equal to zero (i.e., $b \equiv 0$). We assume that $J_y(t,T) \sim \mathcal{N}(\mu_{J_Y}, \sigma^2_{J_Y})$ with $\sigma_{J_Y} \geq 0$.

Jump assumption (b_2): We assume that jumps in $y(t,T)$ present an exponentially-dampened functional form. The jump amplitude parameter a is assumed to be a finite constant and the jump-decay parameter b is assumed to be any non-negative number. a determines the size of the jump conditional on a jump in N_t, whereas b controls, when jumps occur, how much less long-dated futures contracts jump relative to short-dated futures contracts.

- There can also be a combination of the jumps presented above occurring simultaneously, with the parameters and conditions as previously described (we do not consider mixed jump types):

Jump assumption (1): We assume i.i.d. jumps in S_t and in $y(t,T)$.

Jump assumption (2): We assume jumps of constant magnitude in S_t and an exponentially-dampened functional form for jumps in $y(t,T)$.

Their corresponding expressions for expected values and transforms are represented in Table 1.5.

Futures Dynamics

Let $F(t,T)$ denote the time-t price of a futures contract that matures at time T. By definition, we have

$$F(t,T) \equiv S_t e^{\int_t^T y(t,u)du} = S_t e^{Y(t,T)}. \tag{1.6}$$

In the absence of arbitrage opportunities, the process followed by $F(t,T)$ must be a martingale under $\mathbb{Q}$ (see Duffie (2001)). As such, we obtain the following condition for the drift of the forward cost of carry process:

Proposition 1.1 *The absence of arbitrage implies that the drift term in equation (1.2) is given by*

$$\mu_y(t,T) = -v_t\sigma_y(t,T)\Big(\sigma_Y(t,T) + \sigma_S\rho_{Sy}\Big) + \lambda E_t^{\mathbb{Q}}\left[\left(e^{J_S} + J_y(t,T) - 1\right) - \left(e^{J_S + J_y(t,T)} - 1\right)\right], \tag{1.7}$$

where

$$\sigma_Y(t,T) \equiv \int_t^T \sigma_y(t,u)du = \frac{\alpha}{\gamma}\left(1 - e^{-\gamma(T-t)}\right). \tag{1.8}$$

Proof. See Appendix 1A.1 for proof. ■

Despite the existence of jumps, this condition is analogous to the drift condition in forward interest rate term-structure models such as Heath et al. (1992).

From applying Itô's Lemma for jump diffusion processes (see (Cont & Tankov 2003, Sec. 8.3.2)) to (1.6), given (1.7) and setting the drift to zero, it follows that the dynamics of $F(t,T)$ are given by

$$\frac{dF(t,T)}{F(t,T)} = \sqrt{v_t}\Big(\sigma_S dW_t^S + \sigma_Y(t,T)dW_t^y\Big) - \lambda E_t^{\mathbb{Q}}\left[e^{J_S + J_Y(t,T)} - 1\right]dt + \left(e^{J_S + J_Y(t,T)} - 1\right)dN_t, \tag{1.9}$$

where

$$J_Y(t,T) \equiv \int_t^T J_y(t,u)du = \frac{a}{b}\left(1 - e^{-b(T-t)}\right). \tag{1.10}$$

The volatility of the futures prices depends on v_t, a factor driven by W_t^v which does not appear in the expression followed by the futures dynamics (1.9). The volatility risk and the options on futures contracts cannot be completely hedged by trading in futures contracts alone, for which reason the model features unspanned stochastic volatility. To the extent that W_t^v is correlated with W_t^S and W_t^y, the variance factor contains a spanned component and volatility risk is partly hedgeable. As special cases, if this correlation is 0, the volatility risk is completely unhedgeable, and if this correlation is ± 1, the volatility risk is completely hedgeable.

In the following proposition, we show that the cost of carry rates are affine jump-diffusion functions of two state variables, namely χ_t and ϕ_t, plus the jump-related terms; the log-futures prices $f(t,T) \equiv \ln F(t,T)$ are also affine jump-diffusion functions of the same variables and terms, plus the log-spot prices $s_t \equiv \ln S_t$:

Proposition 1.2 *The forward and the instantaneous cost of carry rates and log-futures prices are given by*

$$y(t,T) = y(0,T) - \lambda \int_0^t E_u^{\mathbb{Q}}\left[J_y(u,T)\right] du + \int_0^t J_y(u,T) dN_u + \sigma_y(t,T)\chi_t + \frac{\sigma_y^2(t,T)}{\alpha}\phi_t, \quad (1.11)$$

$$y_t = y(0,t) - \lambda \int_0^t E_u^{\mathbb{Q}}\left[J_y(u,t)\right] du + \int_0^t J_y(u,t) dN_u + \alpha\left(\chi_t + \phi_t\right). \quad (1.12)$$

$$f(t,T) = s_t + f(0,T) - f(0,t) + \sigma_Y(t,T)\chi_t + \frac{\hat{\sigma}_Y(t,T)}{\alpha}\phi_t + \int_0^t \left(y_u - \frac{\sigma_S^2}{2}v_u\right) du + \sigma_S \int_0^t \sqrt{v_u} dW_u^S - \lambda \int_0^t E_u^{\mathbb{Q}}\left[e^{J_S} + J_Y(u,T) - 1\right] du + \int_0^t \left(J_S + J_Y(u,T)\right) dN_u. \quad (1.13)$$

with $\hat{\sigma}_Y(t,T)$ as in (1A.21), the dynamics for $f(t,T), \chi_t$ and ϕ_t as in (1A.10),(1A.15) and (1A.16).

Proof. See Appendix 1A.2 for proof. ■

In the following proposition we present the expressions followed by futures and spot prices:

Proposition 1.3 *With y_u as in (1.12), the expressions followed by the spot and futures prices are given by*

$$F(t,T) = F(0,T) \times \exp\left\{\int_0^t \left(\sqrt{v_u}\left(\sigma_S dW_u^S + \sigma_Y(u,T) dW_u^y\right) - \frac{v_u}{2}\left(\sigma_S dW_u^S + \sigma_Y(u,T) dW_u^y\right)^2\right) du\right\} \exp\left\{-\lambda \int_0^t E_u^{\mathbb{Q}}\left[e^{J_S} + J_Y(u,T) - 1\right] du + \int_0^t \left(e^{J_S + J_Y(u,T)} - 1\right) dN_u\right\}, \quad (1.14)$$

$$S_t = S_0 \exp\left\{\int_0^t \left(y_u - \frac{\sigma_S^2}{2}v_u - \lambda E_u^{\mathbb{Q}}\left[e^{J_S} - 1\right]\right) du + \sigma_S \int_0^t \sqrt{v_u} dW_u^S + J_S \int_0^t dN_u\right\}. \quad (1.15)$$

Proof. See Appendix 1A.3 for proof. ■

1.2.2 Deriving the Characteristic Function

As with most exchange-traded products, options on oil expire (T_{Opt}) slightly before the expiration date of the underlying futures contract (T). The Fourier transform for the time-t standard European option price can be expressed in terms of the characteristic function (hereafter CF) $\psi(iu,t,T_{Opt},T)$, so it can be obtained by applying the Fourier inversion theorem. We define $\tau \equiv T_{Opt} - t$ and the process $f(T_{Opt},T) \equiv \ln F(T_{Opt},T)$ with dynamics as in (1A.10). To price options on futures, we introduce the transform

$$\psi_t(iu,t,T_{Opt},T) \equiv E_t^{\mathbb{Q}}[e^{iuf(T_{Opt},T)}], \tag{1.16}$$

which has an exponential affine solution as demonstrated in the following proposition:

Proposition 1.4 *The transform in (1.16) is given by*

$$\psi_t(iu,t,T_{Opt},T) = e^{A(\tau)+B(\tau)v_t+C(\tau)\lambda+iuf(t,T)}, \tag{1.17}$$

with $C(\tau)$ the new term connected with the jumps. $A(\tau)$, $B(\tau)$ and $C(\tau)$ solve the following system of ODEs

$$\frac{\partial A(\tau)}{\partial \tau} = B(\tau)\kappa\theta, \tag{1.18}$$
$$\frac{\partial B(\tau)}{\partial \tau} = b_0 + b_1 B(\tau) + b_2 B^2(\tau), \tag{1.19}$$
$$\frac{\partial C(\tau)}{\partial \tau} = n_{a_j b_j}(\tau) - iu\, m_{a_j b_j}(\tau), \tag{1.20}$$

with

$$\begin{aligned} b_0 &= -\frac{1}{2}(u^2+iu)\big(\sigma_S^2 + \sigma_Y^2(t,T) + 2\rho_{Sy}\sigma_S\sigma_Y(t,T)\big), \\ b_1 &= -\kappa + iu\,\sigma_v\big(\rho_{Sv}\sigma_S + \rho_{yv}\sigma_Y(t,T)\big), \\ b_2 &= \frac{\sigma_v^2}{2}, \end{aligned} \tag{1.21}$$

subject to the initial conditions $A(0) = B(0) = C(0) = 0$, for $j = 1,2$ and following the jump assumptions in Subsection 1.2.1. The analytical expressions followed by the expected value terms ($m_{a_1}, m_{a_2}, m_{b_1}, m_{b_2}, m_{a_1 b_1}$ and $m_{a_2 b_2}$) and the transform terms ($n_{a_1}, n_{a_2}, n_{b_1}, n_{b_2}, n_{a_1 b_1}$ and $n_{a_2 b_2}$) are represented in Table 1.5.

Proof. See Appendix 1A.4 for proof. ■

The terms $A(\tau)$ and $B(\tau)$ are defined in Trolle & Schwartz (2009). In a recent work, Sitzia (2018) derives an analytical representation followed by the transform of the futures prices

$F(t,T)$ for Trolle & Schwartz (2009)-SV1 and Trolle (2014). Equations (1.18) and (1.19) have analytical solutions which are given by

$$A(\tau) = \frac{2\kappa\theta}{\sigma_v^2}\Big(\beta\gamma\tau - \mu z - \ln g(z)\Big) + k_3, \tag{1.22}$$

$$B(\tau) = \frac{2\gamma}{\sigma_v^2}\Big(\beta + \mu z + z\frac{g'(z)}{g(z)}\Big), \tag{1.23}$$

where $g(z)$ is a linear combination of Kummer's (M) and Tricomi's (U) hypergeometric functions. The expressions followed by $g(z), g'(z), \beta, \mu$ and z can be found in equations (1B.4)-(1B.7) in Appendix 1B.1. To match the initial condition $A(0) = 0$, we have that

$$k_3 = \frac{2\kappa\theta\mu}{\sigma_v^2\omega}. \tag{1.24}$$

The following proposition provides the analytic expression followed by the term $C(\tau)$ in equation (1.17):

Proposition 1.5 *Equation (1.20) has an analytical solution which is given by*

$$C(\tau) = n_{A_jB_j}(\tau) - iu\, m_{A_jB_j}(\tau), \tag{1.25}$$

subject to the initial condition $C(0) = 0$, for $j = 1, 2$ and following the jump assumptions in Subsection 1.2.1. The analytical expressions followed by the expected value terms ($m_{A_1}, m_{A_2}, m_{B_1}, m_{B_2}, m_{A_1B_1}$ and $m_{A_2B_2}$) and the transform terms ($n_{A_1}, n_{A_2}, n_{B_1}, n_{B_2}$, $n_{A_1B_1}$ and $n_{A_2B_2}$) are represented in Table 1.5.

The inclusion of jumps in the model does not have any impact on the computation of the hypergeometric functions, which are part of the expressions followed by $A(\tau)$ and $B(\tau)$.

Model Sub-Specifications

We denote our model by SYSVJ.[6] We consider six model sub-specifications to which we refer with an identifier based on the jump assumption made, as described in Subsection 1.2.1:

- **SYSVJ**^{a_1}: i.i.d. jumps in S_t – equivalent to Trolle (2014)
- **SYSVJ**^{b_1}: i.i.d. jumps in $y(t,T)$
- **SYSVJ**^{1}: i.i.d. jumps in S_t and in $y(t,T)$
- **SYSVJ**^{a_2}: jumps of constant magnitude in S_t
- **SYSVJ**^{b_2}: exponentially-dampened jumps in $y(t,T)$
- **SYSVJ**^{2}: jumps of constant magnitude in S_t and exponentially-dampened jumps in $y(t,T)$

[6]SYSVJ is the acronym for Stochastic cost of carry $Y(t,T)$, Stochastic Volatility v_t and Jumps.

Nested Models

Modeling the futures dynamics using jumps and stochastic volatility causes the futures prices to have non-Gaussian returns – a stylised fact in the energy markets. In Table 1.3 we present the values for the first four moments of the distribution and we perform the Jarque-Bera normality test: Sub-table 1.3(a) refers to monthly observations, whereas Sub-table 1.3(b) refers to daily observations. We reject the null hypothesis of normality in returns for each of the labeled contracts M2-Q2, and all the contracts taken together. This implies that jumps and stochastic volatility are required, providing skewness and kurtosis to the distribution of returns. Earlier models did not include dynamics of both kinds.

We consider one-, two- and three-factor models, a mix of spot-based models such as Merton (1976), Heston (1993) and Bates (1996), and term-structure models such as Trolle & Schwartz (2009)-SV1 and Trolle (2014). By setting $m_{B_1}, m_{B_2}, n_{B_1}$ and n_{B_2} to zero in the jump term $C(\tau)$ in (1.25), Trolle (2014) is replicated; by setting the jump term $C(\tau)$ to zero, Trolle & Schwartz (2009)-SV1 is replicated. Further modifications to $A(\tau)$, $B(\tau)$ and $C(\tau)$ need to be put in place to replicate the nested models we present.

To compare different models from a commodity perspective, we transform the original spot-based specifications and get the corresponding futures prices dynamics. These models were not originally meant for commodities but rather for equities or exchange rates and they do not consider a stochastic cost of carry rate. We adapt their specifications to commodity assets accordingly. We will hereafter refer to their equivalent term-structure models, though naming them under the original form.

Given (1.16), we present the corresponding Fourier transforms to the extant models considered:

1. **Merton (1976)** or **Mer76** hereafter:

$$\psi_t(iu, t, T_{Opt}, T) = e^{A(\tau)+C(\tau)\lambda+iuf(t,T)}. \tag{1.26}$$

   This model extends Black & Scholes (1973) incorporating jumps in the spot price S_t, where the constant term $A(\tau)$ in both models coincides. The jump-related term $C(\tau)$ corresponds to our jump assumption (a_1) in Subsection 1.2.1.

2. **Heston (1993)** or **Hes93** hereafter:

$$\psi_t(iu, t, T_{Opt}, T) = e^{A(\tau)+B(\tau)v_t+iuf(t,T)}. \tag{1.27}$$

   In this case, a volatility term $B(\tau)$ is necessary as this model extends Black & Scholes (1973) incorporating stochastic volatility v_t; the independent term $A(\tau)$ in both models coincides.

3. **Bates (1996)** or **Bat96** hereafter:

$$\psi_t(iu, t, T_{Opt}, T) = e^{A(\tau)+B(\tau)v_t+C(\tau)\lambda+iuf(t,T)}. \tag{1.28}$$

   This model is a combination of Hes93 and Mer76. $A(\tau)$ and $B(\tau)$ are as in Hes93, and the jump term $C(\tau)$ is as in Mer76.

4. **Trolle & Schwartz (2009)-SV1** or **TS09-SV1** hereafter:

$$\psi_t(iu, t, T_{Opt}, T) = e^{A(\tau)+B(\tau)v_t+iuf(t,T)}. \tag{1.29}$$

   This model consists of the extension of Hes93 with a stochastic forward cost of carry curve $y(t,T)$, where $A(\tau)$ and $B(\tau)$ follow (1.22) and (1.23), respectively.

5. **Trolle (2014)** or **Tro14** hereafter:

$$\psi_t(iu, t, T_{Opt}, T) = e^{A(\tau)+B(\tau)v_t+C(\tau)\lambda+iuf(t,T)}. \tag{1.30}$$

   This model consists of the extension of TS09-SV1 with i.i.d. jumps in the spot price S_t. $A(\tau)$ and $B(\tau)$ are as in TS09-SV1; $C(\tau)$ is as in Mer76. This theoretical model has yet to be subjected to an empirical application.

In Table 1.1 we present the dynamics followed by the models presented in this list together with our model, providing both the spot and the futures price dynamics. Table 1.2 shows a classification based on the factors and jumps considered. The expressions followed by the ODEs and the solution to the terms in (1.26)-(1.30) and in our model in (1.17) can be found in Sub-tables 1.4(a) and 1.4(b), respectively. Table 1.5 presents the jump assumptions described in Subsection 1.2.1, their corresponding expressions for expected values and jump transforms. Given that Tro14 is equivalent to our model sub-specification (a_1), it does not explicitly appear in Tables 1.2, 1.4 and 1.6.

Key advantages of the most recent models (TS09-SV1, Tro14 and our model) include improved approximation to the real price behaviour and better description of the implied volatility surface. In our case, adding up to five jump parameters provides even more flexibility to replicate the market implied volatilities, allowing for a wider range of possible shapes (e.g., long-dated contracts jump more than those closer to maturity – a stylised fact in the energy markets). Its implementation is not especially difficult, requiring only the addition of one new term $C(\tau)$ to the CF in TS09-SV1.[7]

[7] Observe that this new term can present six different forms, as many as the number of model sub-specifications.

1.2.3 Pricing of Standard European Options

Let $\mathcal{C}(t, T_{Opt}, T, K)$ and $\mathcal{P}(t, T_{Opt}, T, K)$ denote the time-t prices of a standard European call (hereafter, call) option and a standard European put (hereafter, put) option that expire at time T_{Opt} with strike K on a futures contract that expires at time T, and let $P(T_{Opt}, t)$ denote the time-t price of a zero-coupon bond that matures at time T_{Opt}. This option can be priced quasi-analytically within the framework we describe in this section. In our empirical work, we follow the fast Fourier transform (FFT hereafter) methodology.

We use the Carr & Madan (1999) approach for pricing options which permits the use of the computationally efficient FFT algorithm. Its popularity stems from its remarkable speed: while a naive computation needs N^2 operations, the FFT requires only $N \ln(N)$ steps.

In the following proposition we present the expressions followed by the prices of a European call and put option:

Proposition 1.6 *The time-t price of a call and a put option that expires at time T_{Opt} with strike K on a futures contract that expire at T are given by*

$$\mathcal{C}(t, T_{Opt}, T, K) = P(t, T_{Opt}) \frac{e^{-\alpha \ln(K)}}{\pi} \int_0^\infty \Re \left[\frac{e^{-iu \ln(K)} \psi_t(u - i(1+\alpha), t, T_{Opt}, T)}{\alpha(\alpha+1) - u^2 + iu(1+2\alpha)} \right] du, \quad (1.31)$$

$$\mathcal{P}(t, T_{Opt}, T, K) = P(t, T_{Opt}) \frac{e^{-\alpha \ln(K)}}{\pi} \int_0^\infty \Re \left[\frac{e^{-iu \ln(K)} \psi_t(u - i(1-\alpha), t, T_{Opt}, T)}{\alpha(\alpha-1) - u^2 + iu(1-2\alpha)} \right] du, \quad (1.32)$$

where α is the control parameter.[8]

Proof. The proof is in Carr & Madan (1999). ■

This approach presents two advantages: firstly, it permits the use of the computationally efficient FFT; secondly, it requires the evaluation of only one integral, as opposed to the two integrals required when using earlier methods such as in Heston (1993) or Duffie et al. (2000), among others.

1.3 Alternative Characterisation

We have reinterpreted some parameters presented in this work for the sake of model simplicity. In fact, it consists of an equivalent way of understanding the nature of the volatilities and the

[8] α has to be chosen to ensure that it makes the modified option price square-integrable and to obtain good numerical accuracy – a sufficient condition for the Fourier transform to exist. This parameter has to be wisely chosen as it might produce very oscillatory arguments of the integral if too big, or it might approach a point mass around 0 if too small. This parameter is often set to 0.75, seeming to achieve very good numerical results on practically all occasions. We also set it to 0.75.

jumps of the spot price S_t and the forward cost of carry curve $y(t,T)$ and, as a result, the futures dynamics too. The option prices are equivalent no matter whether we use this alternative parameter characterisation or the original set. This alternative set-up is a novel feature in this work, which reduces calibration time by approximately 50%.

1.3.1 Futures Dynamics

In this subsection we present the alternative expressions for the volatility functions, jump expressions and the futures dynamics. The idea beyond this modification consists of considering a single expression for the volatilities of the factors that affect futures prices $F(t,T)$. It is based in the fact that the spot price S_t does not have a maturity whereas the forward cost of carry curve $y(t,T)$ does. As such, when $t = T$, we have that $\sigma_y(t,t) = \alpha$, and by matching the parameters $\sigma_S = 0$ we allow a single expression to hold for the volatilities of both factors. We do the same with the jumps.

Next, we present the new expressions we refer to and their integrals. We denote the volatility of $F(t,T)$ by $\sigma_f(t,T)$ and the jumps in $F(t,T)$ by $J_f(t,T)$.

Alternative Volatility Functions

We consider that $\sigma_f(t,T)$ follows an exponentially-dampened functional form, with (1.4) and (1.8) becoming

$$\sigma_f(t,T) \equiv \alpha e^{-\gamma(T-t)}, \tag{1.33}$$

$$\sigma_F(t,T) \equiv \int_t^T \sigma_f(t,u)du = \frac{\alpha}{\gamma}\left(1 - e^{-\gamma(T-t)}\right). \tag{1.34}$$

Observe that in Subsection 1.2.1 we imposed $\sigma_S = 1$ given that the parameters σ_S, α, θ and σ_v were not simultaneously identified. This implies that the calibrated values for σ_S and α will not be close at all to each other when comparing their values in the original characterisation with the alternative one.

Alternative Jump Specifications

We consider the jumps in $F(t,T)$ as in Crosby (2008), with expressions (1.5) and (1.10) becoming

$$J_f(t,T) \equiv a e^{-b(T-t)}, \tag{1.35}$$

$$J_F(t,T) \equiv \int_t^T J_f(t,u)du = \frac{a}{b}\left(1 - e^{-b(T-t)}\right), \tag{1.36}$$

for which we contemplate two alternatives:

Jump assumption (1): Jumps as in Mer76, i.e., $J_f(t,T) \sim \mathcal{N}(\mu_{J_F}, \sigma^2_{J_F})$ with $\sigma_{J_F} \geq 0$. The jump amplitude parameter a is assumed to be an i.i.d. random variable over time, the distribution of which is defined with respect to $\mathbb{Q}$. The jump-decay parameter b is assumed to be zero.

Jump assumption (2): Jumps with an exponentially-dampened functional form, where the jump amplitude parameter a is assumed to be a finite constant and the jump-decay parameter b is assumed to be any non-negative number.

Alternative Futures Dynamics and Model Sub-Specifications

As a result, equation (1.9) becomes

$$\frac{dF(t,T)}{F(t,T)} = \sqrt{v_t}\sigma_F(t,T)dW_t^F - \lambda E_t^{\mathbb{Q}}\left[e^{J_F(t,T)} - 1\right]dt + \left(e^{J_F(t,T)} - 1\right)dN_t. \tag{1.37}$$

In this set-up we consider two model sub-specifications:

- **SYSVJ**^{1}: i.i.d. jumps in $F(t,T)$
- **SYSVJ**^{2}: exponentially-dampened jumps in $F(t,T)$

1.3.2 Characteristic Function

The coefficients in the dynamics of $B(\tau)$ in equation (1.19) result in the new expressions

$$\begin{aligned} b_0 &= -\frac{1}{2}(u^2 + iu)\sigma_F^2(t,T), \\ b_1 &= -\kappa + iu\,\sigma_v\rho_{Fv}\sigma_F(t,T), \\ b_2 &= \frac{\sigma_v^2}{2}, \end{aligned} \tag{1.38}$$

whereas the expressions followed by $A(\tau)$ and $B(\tau)$ in (1.22) and (1.23) remain the same. Their coefficients can be found in Annexes 1B.1 and 1B.2.

Subject to the initial condition $C(0) = 0$, for $j = 1,2$ and the jump assumptions presented above, the alternative jump-related term dynamics and solution are

$$\frac{\partial C(\tau)}{\partial \tau} = n_{f_j}(\tau) - iu\, m_{f_j}(\tau), \tag{1.39}$$

$$C(\tau) = n_{F_j}(\tau) - iu\, m_{F_j}(\tau). \tag{1.40}$$

The analytical expressions followed by the expected value terms ($m_{f_1}, m_{f_2}, m_{F_1}$ and m_{F_2}) and the transform terms ($n_{f_1}, n_{f_2}, n_{F_1}$ and n_{F_2}) are represented in Table 1.5.

1.4 Model Estimation

We directly define our model dynamics under $\mathbb{Q}$ and, therefore, the parameter estimation is performed under this measure. We use the least-square fit to calibrate our parameters. This section describes the market data we use for this analysis and the calibration method we follow.

Market Data

We consider West Texas Intermediate (WTI) light sweet crude oil data listed on the New York Mercantile Exchange (NYMEX), which we obtain from Refinitive Eikon (formerly Thomson-Reuters Datastream). The data set consists of observations of closing prices (quoted in USD) and open interest for futures prices, and market implied (Black) volatilities for the corresponding options.

The period considered spans from May 27^{th}, 2010 to September 30^{th}, 2020 and is at monthly and daily frequency, making it 125 monthly and 2,618 daily observations, respectively. Only ATM and OTM options are utilised. We select ATM options plus those 15 OTM closer to the ATM level, which we label as ATM$\pm 0.5, 1, ..., 7, 7.5$ USD, with ATM the futures price. This makes 32 options per contract and observation.

The trading of futures contracts terminates three business days prior to the 25^{th} calendar day of the month prior to the contract month (i.e., delivery month). Futures contracts that mature on those termination dates exist for a wide variety of maturities. In deciding which maturity futures contracts to use, we select contracts based on higher open interest, as detailed in (Trolle & Schwartz 2009, p. 5,6). This procedure leaves seven generic futures contracts out of the first 60 available nominal ones: the second- to the sixth-month contracts (M2-M6) and the following two with expiration in either March, June, September or December (Q1-Q2). This represents 868 futures contracts in total. The trading of standard European options terminates six business days prior to the 25^{th} calendar day of the month prior to the contract month.

Calibration Method

The inputs to the calibration algorithm are the underlying futures prices, the option strikes and the discount factors. Additionally, as a proxy for the instantaneous variance, we use the square of ATM volatilities that corresponds to the shorter maturity contract (in our case, the contract labeled M2) – that is, a unique volatility value v_0 per observation date.

We use a least-squares fitting with the objective of minimising the root mean squared error in volatilities RMSE. With the calibrated parameters, for comparative purposes, we also report

MAEs in option volatilities. All the results reported in this Section are in terms of MAE(σ). The expressions followed by these error statistics read

$$MAE(\sigma) = \frac{\sum_{t=1}^{N} |\hat{\sigma}_t - \sigma_t|}{N}, \tag{1.41}$$

$$RMSE(\sigma) = \sqrt{\frac{\sum_{t=1}^{N} (\hat{\sigma}_t - \sigma_t)^2}{N}}. \tag{1.42}$$

We apply Feller's condition to all models with stochastic volatility, that is, all models considered except Mer76. Hes93 and Bat96 assume that $\sigma_S = 1$. Following this assumption, we also assume that $\sigma_S = 1$ in TS09-SV1, Tro14 and our model in the original set-up, $\sigma_S = 0$ in the alternative set-up. We calibrate the parameters for the models listed in Subsection 1.2.2 and for our model.

Following Carr & Madan (1999), the integral in the pricing functions (1.31)-(1.32) is numerically computed using Simpson's rule (using Matlab's built-in function $simps$). We compare the performance of other integration methods and we find Simpson's rule to be the best. For the sake of brevity, we do not present this analysis in this work, but the results are available upon request. We have carried out an equivalent analysis to choose the optimal value of α to be used in equations (1.31)-(1.32). When performing a numerical calibration, we use a standard fourth order Runge-Kutta algorithm to solve the system of ODEs (1.18)-(1.20) (using Matlab's built-in function $ode45$). We consider an integral step of $1/10$ and an upper bound of 60, which implies 600 evaluation points. Experiments are implemented on an HP laptop computer on a CPU Intel Core i7 2.60 GHz 16.0 GB RAM SSD hard drive machine, running on Windows 10 64 bits, with Matlab version R2020b and Microsoft Office 64 bits.

1.4.1 Monthly Observations

The observation period considered makes 125 end of month observations, which are taken on the last business day of the month in the period considered. As a result, we consider the seven futures contracts and their 32 corresponding ATM and OTM options for each observation, which represent 28,000 options. Because of data issues, 3,570 options are discarded, making it a final number of 24,430 options (87.25% of the total number).

Figure 1.1 focuses on the period May 2010 to September 2020; it considers the contracts labeled M2, Q1, Q2 only. Sub-figure 1.1(a) shows the evolution of futures prices per contracts, Sub-figure 1.1(b) shows futures returns, Sub-figure 1.1(c) shows Black volatilities for ATM call options, and Sub-figure 1.1(d) presents a histogram of futures returns compared with those normally-distributed. In the histogram, the presence of skewness and kurtosis (fat tails) is evident. In Sub-figure (c), we also observe that volatility is stochastic. In the period considered, the jump in 2011 corresponds to the Arab spring; the biggest downward jump occurring in 2014 corresponds to the territorial gains made by ISIS in Iraq and Syria, the surprising growth of US shale oil production (fracking) and the decision taken by the OPEC to maintain output. Futures prices plummeted in March 2020, which corresponds to the beginning of the Covid-19 pandemic.

A Jarque-Bera normality test demonstrates that futures returns are not Gaussian. Sub-table 1.3(a) presents the results of the test, contract by contract and for all contracts taken together. The values of the skewness and kurtosis signal the returns not to have a normal distribution, which supports the inclusion of stochastic variance as well as jumps.

1.4.2 Daily Observations

The observation period considered makes 2,618 daily observations. As a result, we consider the seven futures contracts and their 32 corresponding options for each observation, which represent 586,432 options. Because of data issues similar to the monthly observations, 74,194 options are discarded, making it a final number of 512,238 options (87.35% of the total number).

We omit plotting futures prices and returns, and options volatilities on daily observations to reduce clutter on the graphs. Again, a Jarque-Bera normality test demonstrates that futures returns are not Gaussian. Sub-table 1.3(b) presents the results.

1.5 Results

In this section we discuss the empirical pricing performance of our novel model presented in Subsection 1.2.1 and each of the extant models listed in Subsection 1.2.2. Black (1976) is the market model for pricing standard European options on futures prices. In fact, there is one equivalent Black volatility per quoted option; therefore, there is no benefit in calibrating this single-parameter model. Our benchmark model is TS09-SV1, which is deployed as a special case of ours, and our sub-specification SVSYJ^{a_1} corresponds to Tro14.

We compute the fair value of standard European call and put options contracts on different maturities and strike prices over a period of slightly over 10 years. Analytic results (estimated parameters values, pricing errors and computation time) are reported in Table 1.6. Sub-table (a) refers to monthly data and Sub-Table (b) refers to daily data of futures and option prices. Errors are expressed in terms of MAE(σ) and RMSE(σ), and computation time in hours.

We want to determine whether the addition of different types of jumps brings any benefit to the pricing performance of our model compared with our benchmark. In this section we will focus on results generated from daily observations; if results differ between one granularity and the other, we will explicitly discuss it.

Originally, TS09 was calibrated numerically applying the Fourier inversion theorem as in Duffie et al. (2000). This is the first empirical work in the literature we are aware of which prices plain vanilla options using the analytical solutions in Sitzia (2018). This innovation enables a much faster calibration of TS09-SV1 and our model. The alternative characterisation of the parameters is another novel feature, which reduces calibration time by approximately 50%.[9]

Our model presents the highest performance results (that is, the lowest values in terms of MAE(σ) and RSME(σ)) but also the longest computation times, as it contains the highest number of parameters. There is one exception on monthly (daily) data, where neither the benchmark nor our model can beat Bat96 (and Hes93) in terms or errors.[10] So that computational time and calibrated values are comparable, we use the same initial set of (common) parameter values throughout all of our model sub-specifications as well as for our TS09-SV1. We tried many different sets of initial parameter values until we reached the best possible local optimum. In all cases we beat the benchmark; this result is more evident using daily data where, on average, the outperformance reaches 0.57% in terms of MAE(σ) (0.0363 to 0.0306) and 0.72% in terms of RMSE(σ) (0.0601 to 0.0529). These results represent a noteworthy improvement in model performance. Considered along with the reduction in computation time through the analytical solution for the CF and the use of the FFT for option pricing, these improvements provide a significant benefit for practitioners.

To better understand the realism of the errors under each frequency scenario, we analyse the distribution of the errors which can be observed in Tables 1.7 to 1.10. These tables present the distribution of MAE(σ) along two dimensions, namely the 32 moneyness levels and the maturity of the seven futures contracts, considered individually and taken together. When the observations are taken monthly (daily), Tables 1.7 and 1.8 (1.9 and 1.10) present the performances obtained by our benchmark and our model. The first table refers to our i.i.d. sub-specification (1) and the latter to our more advanced model with time-dampening jumps (2). In Sub-tables (a) we present the benchmark errors, Sub-tables (b) present our model errors, and Sub-tables (c) represent how good or bad our model is compared with the benchmark. Where the inclusion of jumps improves the pricing accuracy of our model, the values in Sub-tables (c) are positive.

We subsequently study in detail the information displayed in Tables 1.9 and 1.10, which are based on the daily data set. Examining Sub-tables (a) and (b), the first insight is that contracts that report greater errors are found in the shorter maturity contracts (darker red cells). In terms of

[9]These values are available upon request.
[10]This particular fact is under current review.

moneyness, we find that the worst-performing contracts are the ones more distant from the ATM level; the worst of all correspond to options with lower strike level (that is, put options). For larger strike levels, the errors increase again for call options more distant from the ATM level. Furthermore, we observe that error performances are not symmetric. Examining Sub-tables (c) we observe that, on average, our model outperform the benchmark in nearly all contracts – all but one for SYSVJ^1, all but two for SYSVJ^2 (all being 32x7=224). The biggest improvements (darker blue) can be found in shorter contracts with lower strike levels and in OTM call options more distant from the ATM level. Improvements are not symmetric in this case, either. For SYSVJ^1, the model improvement reaches 2.28% and 2.22% for SYSVJ^2, which is noteworthy. The improvement in the aforementioned option contracts is consistent with the inclusion of jumps in the model. A priori, one would expected a positive effect in the short-term goodness of fit given that jumps (as opposed to volatilities) affect prices immediately; this effect is more clear in those contracts closer to maturity – a stylised fact in commodity markets.

Contrary to results from prior research[11] carried out with market data from past decades, when jumps were most of the times upwards (e.g., 1978-79: Iran cuts production and exports during its Revolution and cancels contrats with US companies; 1990: Iraq invades Kuwait; 1999: Asian demand recovers after 1997 crisis; early 2000's: production falls due to lack of investment; mid 2000's: Asia drives rising demand as production stagnates and Saudi spare capacity declines), we find that jumps in the WTI crude oil futures market over our sample period on average tend to be downwards. After the 2010's, we can observe another price increasing period starting in early December 2021 followed by a clear upward jump during the days preceding the Russian invasion of Ukraine on February 24th 2022, when the price of oil hit 100 USD per barrel for the first time since 2014. Of course, this price increase is after our data sample ends.

In Table 1.6 it can be observed that in jump models, the jump amplitude μ_J is negative, an empirical fact which can be observed in the heavier left tail in Sub-figure 1.1(d). Excluding Mer76, jump amplitudes (taken together in the case of jump assumptions (1) or (2)) are always higher in magnitude than -1. Their intensity rates are small, implying one jump every 10-12 years (depending on sub-specification and frequency). This results mainly from considering stochastic volatility within the models, which is the main driver of the non-Gaussian returns. Considering models with no jumps such as Hes93 and TS09-SV1, the correlation between the spot price and the volatility ρ_{Sv} is negative, whereas it is positive in all others. In models that allow for stochastic cost of carry, correlations between the cost of carry and the volatility ρ_{yv} are

[11] See, e.g., Trolle & Schwartz (2009) (time series spanning from January 1990 to May 2006) and Crosby (2008) (in Section 1, the author comments the rise in oil prices in 1990), among others.

positive in most cases. Correlations between the spot price and the cost of carry (convenience yield) ρ_{Sy} are negative (positive) in all cases; this goes in line with the results obtained in prior research.

The introduction of jumps complicates the calibration as parameters values are somewhat unstable; this fact can be observed in Table 1.6 in either frequency considered. In our model and for monthly data, we observe that with i.i.d jumps, jump volatilities σ_{J_S} and σ_{J_Y} are zero in all sub-specifications – they can all be considered as constant jumps providing similar performance no matter the jump type considered. Something similar occurs with time-dampening jumps, where the dampening factor b_Y hits zero in all sub-specifications (observe that jump assumption (a_2) is equivalent to (2) with $b_Y = 0$). Any type of jump outperforms our benchmark by 0.15%. For daily data and unlike the situation previously described, we can observe that jump parameters do not present null values: jump volatilities in i.i.d. jumps are clearly different from zero although small in magnitude, the jump-decay parameter in time-dependent jumps take reasonable values.

The extant jump models perform in an opposite way to our novel jump model. For monthly observations, the models of Bat96 and Mer76 have non-zero but quite small jump volatility values. On the contrary, these volatilities are zero for daily observations. In both frequencies, these findings lead us to think that jumps may not precisely be i.i.d.

In terms of model performance, MAE(σ) values are practically indistinguishable between the two sets of sub-specifications: those corresponding to i.i.d. jumps together with (a_2) hit 3.00%; those of (a_2) and (2) stay around 3.20%. Both values clearly outperform our benchmark. An insight discernible only in daily data is that sub-specifications that present time-dampening jumps do not perform better than those related to i.i.d. jumps. Although the time-dependency in jumps is an important stylised fact in commodity markets, we think it relevant to consider jumps variable rather than constant; a mixture of both types might deliver even better results. We conclude that our jump model performs better than our benchmark, especially for short maturity contracts and away from the ATM level.

1.6 Conclusions and Further Research

We have developed a novel term-structure model for commodity futures prices which presents stochastic spot prices, forward cost of carry curves and variance. The novel feature in our model is the presence of simultaneous jumps in the spot prices and the cost or carry, either i.i.d. or following a time-dampening form. We model futures dynamics under $\mathbb{Q}$, compute the CF and price plain vanilla option using the FFT algorithm with an analytic expression. We calibrate parameters for five extant models (Mer76, Hes93, Bat96, TS09-SV1 and Tro14) plus the six sub-specifications of our model SYSVJ, with the objective of analysing pricing performances.

This is the first empirical work in the literature which prices options with TS09-SV1 using analytical expressions. We prove that our model produces better results (that is, lower error values in terms of MAE(σ) and RSME(σ)) than our benchmark model TS09-SV1, specially for short maturity contracts and away from the ATM level. Our model outperforms the benchmark by 0.57% in terms of MAE(σ) and 0.72% in terms of RMSE(σ). Considered along with the reduction in computation time due to (i) the analytical solution for the CF, (ii) and the use of the FFT for option pricing and (iii) the alternative set-up, these improvements provide a significant benefit for practitioners.

Contrary to results from prior research, we find that jumps in the WTI crude oil futures market over our sample period on average tend to be downwards.

Future lines of research will include, firstly, the extension of TS09-SV1 to capture the dynamics of seasonal energy assets (e.g. natural gas) in the variance. Secondly, we also aim to price calendar spread options on WTI using a joint CF for the two futures contracts involved in each option, within the framework of the model presented in this work. We expect to also obtain analytical solutions for the new transforms, and analytical expressions to price both types of options.

1.7 Figures and Tables

Figure 1.1: Futures prices and returns, ATM call options implied volatilities – monthly data

(a) Futures prices

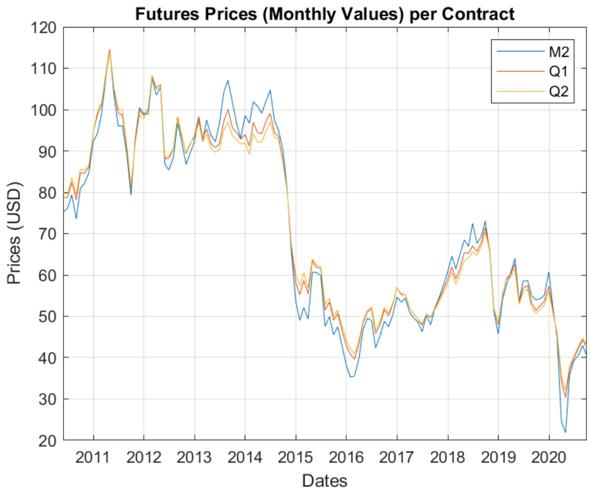

(b) Futures returns

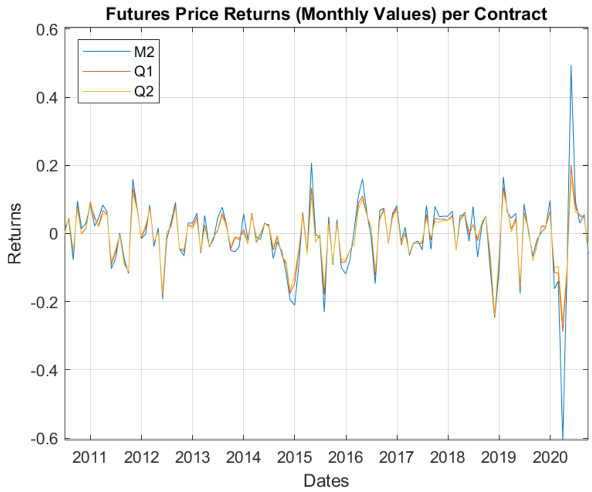

(c) Black volatilities for ATM call options

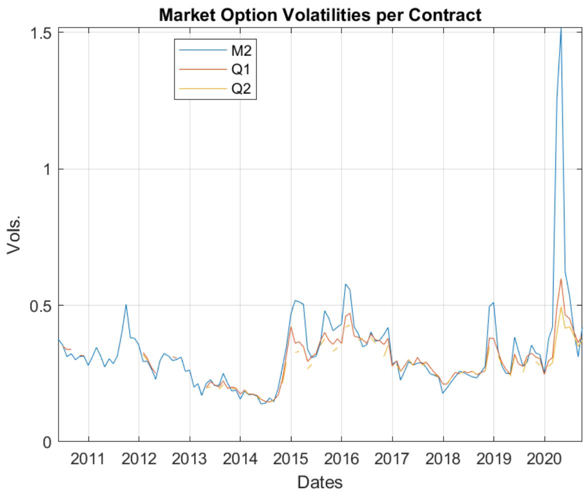

(d) Histogram of futures returns

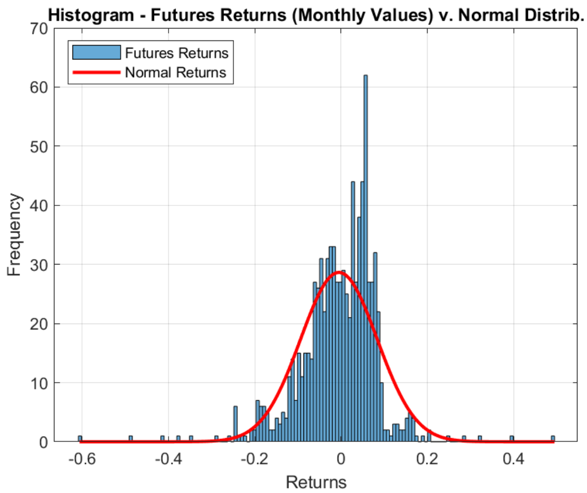

NOTES: This figure presents values that correspond to the futures contracts labeled M2, Q1, Q2 for the period May 2010 to September 2020. Sub-figure (a) presents futures prices, Sub-figure (b) presents futures returns, Sub-figure (c) presents implied volatilities for ATM call options, and Sub-figure (d) presents a histogram for aggregated futures returns.

Table 1.1: Models dynamics

Model	Dynamics
Mer76	$\frac{dS_t}{S_t} = \left(y_t - \lambda E_t^{\mathbb{Q}}\left[e^{J_S}-1\right]\right)dt + \sigma_S dW_t^S + \left(e^{J_S}-1\right)dN_t$ $\frac{dF(t,T)}{F(t,T)} = -\lambda E_t^{\mathbb{Q}}\left[e^{J_S}-1\right]dt + \sigma_S dW_t^S + \left(e^{J_S}-1\right)dN_t$
Hes93	$\frac{dS_t}{S_t} = y_t dt + \sqrt{v_t}dW_t^S$ $dv_t = \kappa\left(\theta - v_t\right)dt + \sigma_v\sqrt{v_t}dW_t^v$ $\frac{dF(t,T)}{F(t,T)} = \sqrt{v_t}dW_t^S$
Bat96	$\frac{dS_t}{S_t} = \left(y_t - \lambda E_t^{\mathbb{Q}}\left[e^{J_S}-1\right]\right)dt + \sqrt{v_t}dW_t^S + \left(e^{J_S}-1\right)dN_t$ $dv_t = \kappa\left(\theta - v_t\right)dt + \sigma_v\sqrt{v_t}dW_t^v$ $\frac{dF(t,T)}{F(t,T)} = -\lambda E_t^{\mathbb{Q}}\left[e^{J_S}-1\right]dt + \sqrt{v_t}dW_t^S + \left(e^{J_S}-1\right)dN_t$
TS09-SV1	$\frac{dS_t}{S_t} = y_t dt + \sigma_S\sqrt{v_t}dW_t^S$ $dy(t,T) = \mu_y(t,T)dt + \sigma_y(t,T)\sqrt{v_t}dW_t^y$ $dv_t = \kappa\left(\theta - v_t\right)dt + \sigma_v\sqrt{v_t}dW_t^v$ $\frac{dF(t,T)}{F(t,T)} = \sqrt{v_t}\left(\sigma_S dW_t^S + \sigma_Y(t,T)dW_t^y\right)$
TS09-SV1*	$\frac{dF(t,T)}{F(t,T)} = \sqrt{v_t}\sigma_F(t,T)dW_t^F$
Tro14	$\frac{dS_t}{S_t} = \left(y_t - \lambda E_t^{\mathbb{Q}}\left[e^{J_S}-1\right]\right)dt + \sigma_S\sqrt{v_t}dW_t^S + \left(e^{J_S}-1\right)dN_t$ $dy(t,T) = \mu_y(t,T)dt + \sigma_y(t,T)\sqrt{v_t}dW_t^y$ $dv_t = \kappa\left(\theta - v_t\right)dt + \sigma_v\sqrt{v_t}dW_t^v$ $\frac{dF(t,T)}{F(t,T)} = -\lambda E_t^{\mathbb{Q}}\left[e^{J_S}-1\right]dt + \sqrt{v_t}\left(\sigma_S dW_t^S + \sigma_Y(t,T)dW_t^y\right) + \left(e^{J_S}-1\right)dN_t$
Tro14*	$\frac{dF(t,T)}{F(t,T)} = -\lambda E_t^{\mathbb{Q}}\left[e^{J_S}-1\right]dt + \sqrt{v_t}\sigma_F(t,T)dW_t^F + \left(e^{J_S}-1\right)dN_t$
SYSVJ	$\frac{dS_t}{S_t} = \left(y_t - \lambda E_t^{\mathbb{Q}}\left[e^{J_S}-1\right]\right)dt + \sigma_S\sqrt{v_t}\,dW_t^S + \left(e^{J_S}-1\right)dN_t$ $dy(t,T) = \left(\mu_y(t,T) - \lambda E_t^{\mathbb{Q}}\left[J_y(t,T)\right]\right)dt + \sigma_y(t,T)\sqrt{v_t}\,dW_t^y + J_y(t,T)\,dN_t$ $dv_t = \kappa\left(\theta - v_t\right)dt + \sigma_v\sqrt{v_t}\,dW_t^v$ $\frac{dF(t,T)}{F(t,T)} = -\lambda E_t^{\mathbb{Q}}\left[e^{J_S+J_Y(t,T)}-1\right]dt + \sqrt{v_t}\left(\sigma_S dW_t^S + \sigma_Y(t,T)dW_t^y\right) + \left(e^{J_S+J_Y(t,T)}-1\right)dN_t$
SYSVJ*	$\frac{dF(t,T)}{F(t,T)} = -\lambda E_t^{\mathbb{Q}}\left[e^{J_F(t,T)}-1\right]dt + \sqrt{v_t}\sigma_F(t,T)dW_t^F + \left(e^{J_F(t,T)}-1\right)dN_t$

NOTES: This table presents each model dynamics, the last equation refers to its corresponding futures price dynamics. Those models presenting an alternative characterisation of the parameters (i.e., TS09-SV1, Tro14 and SYSVJ) appear with the superscript $\star$.

Table 1.2: Factors and features per model

Model	**Stochastic Factors**				**Jumps**			**Parameter**	**Analytical**
	S_t	$y(t,T)$	$F(t,T)$	v_t	S_t	$y(t,T)$	$F(t,T)$	**Count**	**Solution**
Mer76	✓				✓			4	✓
Hes93	✓			✓				4	✓
Bat96	✓			✓	✓			7	✓
TS09-SV1	✓	✓	$\star$	✓				9(6)	✓
SYSVJ^{a_1}	✓	✓		✓	✓			12	✓
SYSVJ^{b_1}	✓	✓		✓		✓		12	✓
SYSVJ^{1}	✓	✓	$\star$	✓	✓	✓	$\star$	14(9)	✓
SYSVJ^{a_2}	✓	✓		✓	✓			11	✓
SYSVJ^{b_2}	✓	✓		✓		✓		12	✓
SYSVJ^{2}	✓	✓	$\star$	✓	✓	✓	$\star$	13(9)	✓

NOTES: For each model, this table indicates the factors and jumps considered, the parameter count and if the model allows for an analytical solution for standard European option pricing. In those models presenting alternative set-up, $F(t,T)$ replaces S_t and $y(t,T)$; this is indicated with the symbols $\star$ (alternative set-up) and ✓ (original set-up). The parameter count for the alternative set-up is shown in brackets. SYSVJ^{a_1} corresponds to Tro14.

Table 1.3: Futures returns and Jarque-Bera test

(a) Monthly Observations

Contract	Min.	Max.	Mean	Std. Dev.	Skew.	Kurt.	JB Stat.	p-Value	Test
M2	49.49%	-60.62%	-0.50%	10.92%	-0.7948	12.2654	9.3739	0.0182	R
M3	39.57%	-48.78%	-0.50%	9.86%	-0.7081	8.4547	10.0370	0.0158	R
M4	32.32%	-41.76%	-0.50%	9.18%	-0.7223	6.4928	10.4806	0.0144	R
M5	28.16%	-37.66%	-0.51%	8.74%	-0.7326	5.6324	10.7459	0.0136	R
M6	25.16%	-34.86%	-0.51%	8.39%	-0.7536	5.1792	10.9373	0.0131	R
Q1	20.14%	-28.87%	-0.50%	7.64%	-0.7752	4.5381	11.2291	0.0123	R
Q2	16.47%	-25.85%	-0.50%	6.80%	-0.8589	4.4968	11.5409	0.0116	R
ALL	49.49%	-60.62%	-0.50%	8.87%	-0.7789	8.7694	2,343.644	0.0010	R

(b) Daily Observations

Contract	Min.	Max.	Mean	Std. Dev.	Skew.	Kurt.	JB Stat.	p-Value	Test
M2	58.12%	-56.86%	-0.02%	2.89%	-0.3230	130.9346	194.4978	0.0010	R
M3	24.00%	-34.08%	-0.02%	2.40%	-1.3885	35.7670	208.6014	0.0010	R
M4	18.58%	-27.71%	-0.02%	2.25%	-1.2731	26.5330	217.2025	0.0010	R
M5	17.14%	-24.78%	-0.02%	2.15%	-1.1976	22.4633	222.6880	0.0010	R
M6	15.64%	-23.65%	-0.02%	2.07%	-1.1427	20.0304	226.8677	0.0010	R
Q1	14.32%	-22.57%	-0.02%	1.96%	-1.0530	17.5825	223.3093	0.0010	R
Q2	11.29%	-19.68%	-0.02%	1.80%	-1.0021	14.5854	240.9477	0.0010	R
ALL	58.12%	-56.86%	-0.02%	2.24%	-1.9807	69.5524	42,831.8384	0.0010	R

NOTES: JB accounts for the Jarque-Bera normality test. The null hypothesis refers to the normal distribution of futures returns. The critical value associated to a significance level of 0.05 is 5.991. When the value of Test is R (CR), we reject (cannot reject) the null hypothesis at 95%.

Table 1.4: Fourier transforms – ODEs and solutions

(a) ODEs

Model	$\partial A(\tau)/\partial\tau$	$\partial B(\tau)/\partial\tau$	$\partial C(\tau)/\partial\tau$
Mer76	$-\frac{\sigma_S^2}{2}(u^2+iu)$	$-$	$n_{a_1} - iu\, m_{a_1}$
Hes93	$B(\tau)\kappa\theta$	$-\frac{1}{2}(u^2+iu) + B(\tau)\left(-\kappa + iu\sigma_v\rho_{Sv}\right) + B^2(\tau)\frac{\sigma_v^2}{2}$	$-$
Bat96	$B(\tau)\kappa\theta$	$-\frac{1}{2}(u^2+iu) + B(\tau)\left(-\kappa + iu\sigma_v\rho_{Sv}\right) + B^2(\tau)\frac{\sigma_v^2}{2}$	$n_{a_1} - iu\, m_{a_1}$
TS09-SV1($\star$)	$B(\tau)\kappa\theta$	$b_0 + b_1B(\tau) + b_2B^2(\tau)$	$-$
SYSVJ	$B(\tau)\kappa\theta$	$b_0 + b_1B(\tau) + b_2B^2(\tau)$	$n_{a_jb_j} - iu\, m_{a_jb_j}$
SYSVJ*	$B(\tau)\kappa\theta$	$b_0 + b_1B(\tau) + b_2B^2(\tau)$	$n_{f_j} - iu\, m_{f_j}$

(b) Solution to ODEs

Model	$A(\tau)$	$B(\tau)$	$C(\tau)$
Mer76	$-\frac{\sigma_S^2}{2}(u^2+iu)\tau$	$-$	$n_{A_1} - iu\, m_{A_1}$
Hes93	$\frac{\kappa\theta}{\sigma_v^2}\left((\kappa - iu\sigma_v\rho_{Sv} + d)\tau - 2\ln\frac{1-ge^{d\tau}}{1-g}\right)$	$\frac{\kappa - iu\rho_{Sv}\sigma_v + d}{\sigma_v^2}\left(\frac{1-e^{d\tau}}{1-ge^{d\tau}}\right)$	$-$
Bat96	$\frac{\kappa\theta}{\sigma_v^2}\left((\kappa - iu\sigma_v\rho_{Sv} + d)\tau - 2\ln\frac{1-ge^{d\tau}}{1-g}\right)$	$\frac{\kappa - iu\rho_{Sv}\sigma_v + d}{\sigma_v^2}\left(\frac{1-e^{d\tau}}{1-ge^{d\tau}}\right)$	$n_{A_1} - iu\, m_{A_1}$
TS09-SV1($\star$)	$\frac{2\kappa\theta}{\sigma_v^2}\left(\beta\gamma\tau - \mu z - \ln g(z)\right) + k_3$	$\frac{2\gamma}{\sigma_v^2}\left(\beta + \mu z + z\frac{g'(z)}{g(z)}\right)$	$-$
SYSVJ	$\frac{2\kappa\theta}{\sigma_v^2}\left(\beta\gamma\tau - \mu z - \ln g(z)\right) + k_3$	$\frac{2\gamma}{\sigma_v^2}\left(\beta + \mu z + z\frac{g'(z)}{g(z)}\right)$	$n_{A_jB_j} - iu\, m_{A_jB_j}$
SYSVJ*	$\frac{2\kappa\theta}{\sigma_v^2}\left(\beta\gamma\tau - \mu z - \ln g(z)\right) + k_3$	$\frac{2\gamma}{\sigma_v^2}\left(\beta + \mu z + z\frac{g'(z)}{g(z)}\right)$	$n_{F_j} - iu\, m_{F_j}$

NOTES: This table presents the expressions followed by each of the ODEs and their solutions as they can be found in the literature. As per our model, these expressions correspond to equations (1.18)-(1.20). $m_\bullet$ is the expected value at time t under $\mathbb{Q}$ of the jump assuming the jump assumption $\bullet$; $n_\bullet$ is the transform of the jump assuming the jump assumption $\bullet$. For TS09-SV1 and our model SYSVJ, the values for $k_3, g(z), g'(z), \beta$ and μ are shown in equations (1.24) and (1B.4)-(1B.6). Tro14 corresponds to SYSVJ(a_1). In each Sub-table, the superscript $\star$ after the model refers to the alternative characterisation of the parameters. For Hes93 and Bat96, we have that

$$g = \frac{\kappa - iu\sigma_v\rho_{Sv} + d}{\kappa - iu\sigma_v\rho_{Sv} - d}, \qquad d = \sqrt{(\kappa - iu\sigma_v\rho_{Sv})^2 + \sigma_v^2(u^2+iu)}. \tag{1.43}$$

Table 1.5: Jump assumptions, corresponding expected values and jump transforms

Jump	Set-up	Expected Value	Transform
(a_1)	✓	$m_{a_1} \equiv E_t^{\mathbb{Q}}\left[e^{J_S}-1\right] = e^{\mu_{J_S}+\frac{1}{2}\sigma^2_{J_S}}-1$	$n_{a_1} \equiv e^{iu\mu_{J_S}-\frac{u^2}{2}\sigma^2_{J_S}}-1$
		$m_{A_1} \equiv E_t^{\mathbb{Q}}\left[\int_t^T \left(e^{J_S}-1\right)du\right] = (T-t)m_{a_1}$	$n_{A_1} = (T-t)n_{a_1}$
(b_1)	✓	$m_{b_1} \equiv E_t^{\mathbb{Q}}\left[e^{J_y(t,T)}-1\right] = e^{\mu_{J_Y}+\frac{1}{2}\sigma^2_{J_Y}}-1$	$n_{b_1} \equiv e^{iu\mu_{J_Y}-\frac{u^2}{2}\sigma^2_{J_Y}}-1$
		$m_{B_1} \equiv E_t^{\mathbb{Q}}\left[\int_t^T \left(e^{J_y(t,T)}-1\right)du\right] = (T-t)m_{b_1}$	$n_{B_1} = (T-t)n_{b_1}$
(1)	✓	$m_{a_1b_1} \equiv E_t^{\mathbb{Q}}\left[e^{J_S+J_y(t,T)}-1\right] = (m_{a_1}+1)(m_{b_1}+1)-1$	$n_{a_1b_1} \equiv (n_{a_1}+1)(n_{b_1}+1)-1$
		$m_{A_1B_1} \equiv E_t^{\mathbb{Q}}\left[\int_t^T \left(e^{J_S+J_y(t,T)}-1\right)du\right] = (T-t)m_{a_1b_1}$	$n_{A_1B_1} \equiv (T-t)n_{a_1b_1}$
(1)	$\star$	$m_{f_1} \equiv E_t^{\mathbb{Q}}\left[e^{J_f(t,T)}-1\right] = e^{\mu_{J_F}+\frac{1}{2}\sigma^2_{J_F}}-1$	$n_{f_1} \equiv e^{iu\mu_{J_F}-\frac{u^2}{2}\sigma^2_{J_F}}-1$
		$m_{F_1} \equiv E_t^{\mathbb{Q}}\left[\int_t^T \left(e^{J_f(t,T)}-1\right)du\right] = (T-t)m_{f_1}$	$n_{F_1} = (T-t)n_{f_1}$
(a_2)	✓	$m_{a_2} \equiv E_t^{\mathbb{Q}}\left[e^{J_S}-1\right] = e^{\mu_{J_S}}-1$	$n_{a_2} \equiv e^{iu\mu_{J_S}}-1$
		$m_{A_2} \equiv E_t^{\mathbb{Q}}\left[\int_t^T \left(e^{J_S}-1\right)du\right] = (T-t)m_{a_2}$	$n_{A_2} = (T-t)n_{a_2}$
(b_2)	✓	$m_{b_2} \equiv E_t^{\mathbb{Q}}\left[e^{J_y(t,T)}-1\right] = e^{ae^{-b(T-t)}}-1$	$n_{b_2} \equiv e^{iuae^{-iub(T-t)}}-1$
		$m_{B_2} \equiv E_t^{\mathbb{Q}}\left[\int_t^T \left(e^{J_y(t,T)}-1\right)du\right] = e^{\frac{a}{b}\left(1-e^{-b(T-t)}\right)}-(T-t)$	$n_{B_2} \equiv e^{iu\frac{a}{b}\left(1-e^{-iub(T-t)}\right)}-(T-t)$
(2)	✓	$m_{a_2b_2} \equiv E_t^{\mathbb{Q}}\left[e^{J_S+J_y(t,T)}-1\right] = (m_{a_2}+1)(m_{b_2}+1)-1$	$n_{a_2b_2} \equiv (n_{a_2}+1)(n_{b_2}+1)-1$
		$m_{A_2B_2} \equiv E_t^{\mathbb{Q}}\left[\int_t^T \left(e^{J_S+J_y(t,T)}-1\right)du\right] = (T-t)m_{a_2b_2}$	$n_{A_2B_2} \equiv (T-t)n_{a_2b_2}$
(2)	$\star$	$m_{f_2} \equiv E_t^{\mathbb{Q}}\left[e^{J_f(t,T)}-1\right] = e^{ae^{-b(T-t)}}-1$	$n_{f_2} \equiv e^{iuae^{-iub(T-t)}}-1$
		$m_{F_2} \equiv E_t^{\mathbb{Q}}\left[\int_t^T \left(e^{J_f(t,T)}-1\right)du\right] = e^{\frac{a}{b}\left(1-e^{-b(T-t)}\right)}-(T-t)$	$n_{F_2} \equiv e^{iu\frac{a}{b}\left(1-e^{-iub(T-t)}\right)}-(T-t)$

NOTES: The expressions followed by $J_y(t,T)$ and $J_Y(t,T)$ can be found in equations (1.5) and (1.10), respectively. The expressions followed by $J_f(t,T)$ and $J_F(t,T)$ can be found in equations (1.35) and (1.36), respectively. The term $m_\bullet$ is the expected value at time t under $\mathbb{Q}$ of the jump in $\bullet$. The term $n_\bullet$ is the transform of the jump in $\bullet$. When $\bullet$ is a capital letter, it accounts for the integral from t to T of the jump in the corresponding assumption. The different jump assumptions can be found in column Jump. The symbol $\star$ in the column Set-up accounts for the alternative characterisation of the parameters whereas the symbol ✓ refers to the original set-up. Tro14 corresponds to SYSVJ(a_1).

Table 1.6: Estimated parameters, errors and computation time

(a) Monthly observations

Model			**SYSVJ**				**TS09-SV1**	**Bat96**	**Hes93**	**Mer76**
Jump Type	2	b_2	a_2	1	b_1	a_1				
σ_S	1.0000	1.0000	1.0000	1.0000	1.0000	1.0000	1.0000	–	–	0.2209
α	0.7209	0.1087	0.5418	0.4854	0.7692	0.5373	0.4516	–	–	–
γ	2.0851	0.4586	1.0796	0.9962	2.0267	2.0065	0.0882	–	–	–
κ	1.9029	2.7783	1.9105	1.9478	1.5101	1.0283	0.9387	3.0953	2.0095	–
θ	0.0060	0.0070	0.0076	0.0085	0.0074	0.0062	0.1618	0.0061	0.0773	–
σ_v	0.1048	0.1869	0.1013	0.1059	0.1037	0.1115	0.2859	0.1878	0.5574	–
ρ_{Sy}	-0.7697	-0.6356	-0.8325	-0.8746	-0.9386	-0.7363	-0.9916	–	–	–
ρ_{Sv}	0.9999	0.6595	1.0000	0.9778	0.9851	1.0000	-0.7435	-1.0000	-0.5648	–
ρ_{yv}	0.9714	-0.0492	0.8520	0.9540	0.3150	0.9847	-0.5937	–	–	–
λ	0.0919	0.0843	0.0875	0.0879	0.0914	0.0896	–	0.1040	–	0.4592
μ_{J_S}	-0.8664	–	-1.8480	-0.9041	–	-1.8256	–	-1.2911	–	-0.2689
σ_{J_S}	–	–	–	0.0002	–	0.0002	–	0.0175	–	0.0061
μ_{J_Y}	–	–	–	-0.9787	-1.7286	–	–	–	–	–
σ_{J_Y}	–	–	–	0.0000	0.0000	–	–	–	–	–
a_Y	-0.8664	-1.8608	–	–	–	–	–	–	–	–
b_Y	0.0000	0.0000	–	–	–	–	–	–	–	–
Parameter Count	13	12	11	14	12	12	9	7	4	4
MAE(σ)	0.0278	0.0279	0.0280	0.0280	0.0278	0.0280	0.0295	0.0277	0.0306	0.0805
RMSE(σ)	0.0547	0.0550	0.0549	0.0548	0.0548	0.0549	0.0590	0.0543	0.0606	0.1262
Computation Time	0.3926	0.2369	0.2445	0.1873	0.4383	0.2050	0.3266	0.0981	0.0459	0.0941

(b) Daily observations

Model			**SYSVJ**				**TS09-SV1**	**Bat96**	**Hes93**	**Mer76**
Jump Type	2	b_2	a_2	1	b_1	a_1				
σ_S	1.0000	1.0000	1.0000	1.0000	1.0000	1.0000	1.0000	–	–	0.2180
α	0.3742	0.3707	0.7727	0.8002	0.9693	0.8935	0.3745	–	–	–
γ	0.6933	0.8335	0.1047	0.1137	0.1180	0.0995	0.1365	–	–	–
κ	2.2080	2.3895	0.6158	0.5724	0.3381	0.4455	0.9943	2.7686	1.9003	–
θ	0.0243	0.0269	0.0265	0.0223	0.0333	0.0292	0.1414	0.0023	0.0683	–
σ_v	0.3228	0.3565	0.1246	0.1275	0.1248	0.1059	0.2775	0.1131	0.2731	–
ρ_{Sy}	-0.4214	-0.2987	-0.9961	-0.9949	-0.9991	-0.9991	-0.9096	–	–	–
ρ_{Sv}	0.0579	0.0653	0.3030	0.4882	0.5686	0.5657	-0.6657	1.0000	-1.0000	–
ρ_{yv}	0.1075	0.0183	0.3505	0.1346	0.6384	0.6391	-0.7219	–	–	–
λ	0.0705	0.0795	0.1000	0.1005	0.1037	0.0997	–	0.0960	–	0.6502
μ_{J_S}	-0.9069	–	-1.2891	-0.6762	–	-1.4818	–	-1.3793	–	-0.2263
σ_{J_S}	–	–	–	0.0256	–	0.1480	–	0.0000	–	0.0001
μ_{J_Y}	–	–	–	-0.6762	-1.4677	–	–	–	–	–
σ_{J_Y}	–	–	–	0.0256	0.0802	–	–	–	–	–
a_Y	-0.7358	-1.2668	–	–	–	–	–	–	–	–
b_Y	0.0680	0.0668	–	–	–	–	–	–	–	–
Parameter Count	13	12	11	14	12	12	9	7	4	4
MAE(σ)	0.0318	0.0321	0.0301	0.0300	0.0297	0.0298	0.0363	0.0250	0.0280	0.0803
RMSE(σ)	0.0542	0.0540	0.0526	0.0526	0.0519	0.0521	0.0601	0.0489	0.0539	0.1228
Computation Time	5.1864	3.0470	3.2148	5.2096	6.1521	4.3336	4.2462	8.2889	1.3871	5.4152

NOTES: MAE(σ) represents the mean absolute pricing error in option volatilities, RMSE(σ) represents the square root of the quadratic mean of errors in option volatilities. The pricing errors are expressed in parts per unit (e.g., 0.0805 means 8.05%). The computation time is calculated using the analytical solutions to the models displayed in Sub-table 1.4(b); the values are expressed in hours. Tro14 corresponds to SYSVJ(a_1).

Table 1.7: Model performance of SYSVJ[1] – monthly observations

(a) TS09-SV1

MAE(σ)	M2	M3	M4	M5	M6	Q1	Q2	ALL
p – 7.5	0.0426	0.0265	0.0289	0.0321	0.0328	0.0428	0.0420	0.0354
p – 7	0.0392	0.0253	0.0285	0.0317	0.0335	0.0422	0.0411	0.0345
p – 6.5	0.0362	0.0238	0.0274	0.0310	0.0336	0.0422	0.0418	0.0337
p – 6	0.0333	0.0229	0.0273	0.0301	0.0330	0.0425	0.0425	0.0331
p – 5.5	0.0307	0.0220	0.0271	0.0307	0.0328	0.0422	0.0411	0.0324
p – 5	0.0281	0.0217	0.0262	0.0301	0.0334	0.0419	0.0416	0.0319
p – 4.5	0.0264	0.0210	0.0254	0.0305	0.0326	0.0413	0.0417	0.0313
p – 4	0.0235	0.0204	0.0251	0.0295	0.0325	0.0414	0.0424	0.0307
p – 3.5	0.0214	0.0197	0.0247	0.0291	0.0322	0.0410	0.0419	0.0300
p – 3	0.0195	0.0187	0.0246	0.0286	0.0320	0.0421	0.0425	0.0297
p – 2.5	0.0185	0.0186	0.0242	0.0284	0.0323	0.0420	0.0421	0.0294
p – 2	0.0164	0.0182	0.0244	0.0287	0.0314	0.0412	0.0412	0.0288
p – 1.5	0.0156	0.0178	0.0243	0.0284	0.0316	0.0399	0.0410	0.0284
p – 1	0.0138	0.0174	0.0237	0.0281	0.0313	0.0414	0.0425	0.0283
p – 0.5	0.0127	0.0172	0.0238	0.0284	0.0313	0.0405	0.0410	0.0278
ATM p	0.0120	0.0166	0.0235	0.0281	0.0312	0.0409	0.0420	0.0277
ATM c	0.0120	0.0169	0.0237	0.0281	0.0313	0.0408	0.0414	0.0277
c + 0.5	0.0112	0.0167	0.0237	0.0282	0.0315	0.0392	0.0416	0.0274
c + 1	0.0109	0.0170	0.0233	0.0280	0.0308	0.0407	0.0417	0.0275
c + 1.5	0.0107	0.0170	0.0241	0.0281	0.0309	0.0389	0.0410	0.0272
c + 2	0.0112	0.0171	0.0234	0.0277	0.0306	0.0395	0.0420	0.0274
c + 2.5	0.0119	0.0176	0.0240	0.0281	0.0312	0.0393	0.0412	0.0276
c + 3	0.0125	0.0175	0.0241	0.0279	0.0310	0.0388	0.0411	0.0276
c + 3.5	0.0133	0.0184	0.0242	0.0284	0.0318	0.0395	0.0406	0.0280
c + 4	0.0138	0.0184	0.0246	0.0282	0.0311	0.0388	0.0410	0.0280
c + 4.5	0.0141	0.0190	0.0246	0.0286	0.0313	0.0389	0.0411	0.0282
c + 5	0.0150	0.0190	0.0251	0.0283	0.0310	0.0400	0.0413	0.0285
c + 5.5	0.0154	0.0195	0.0254	0.0288	0.0315	0.0387	0.0405	0.0285
c + 6	0.0159	0.0199	0.0253	0.0288	0.0322	0.0394	0.0420	0.0291
c + 6.5	0.0166	0.0200	0.0256	0.0294	0.0326	0.0406	0.0418	0.0295
c + 7	0.0173	0.0208	0.0258	0.0295	0.0324	0.0399	0.0417	0.0296
c + 7.5	0.0192	0.0219	0.0264	0.0303	0.0335	0.0402	0.0416	0.0304
ALL	0.0191	0.0195	0.0251	0.0291	0.0319	0.0406	0.0416	0.0295

(b) SYSVJ[1]

MAE(σ)	M2	M3	M4	M5	M6	Q1	Q2	ALL
p – 7.5	0.0464	0.0307	0.0306	0.0322	0.0339	0.0371	0.0406	0.0359
p – 7	0.0416	0.0278	0.0291	0.0307	0.0328	0.0364	0.0376	0.0337
p – 6.5	0.0378	0.0249	0.0271	0.0290	0.0318	0.0364	0.0371	0.0320
p – 6	0.0344	0.0226	0.0260	0.0276	0.0308	0.0376	0.0382	0.0310
p – 5.5	0.0312	0.0209	0.0252	0.0280	0.0307	0.0377	0.0379	0.0302
p – 5	0.0286	0.0201	0.0237	0.0277	0.0311	0.0383	0.0390	0.0298
p – 4.5	0.0268	0.0192	0.0228	0.0278	0.0302	0.0382	0.0384	0.0290
p – 4	0.0237	0.0184	0.0226	0.0270	0.0304	0.0386	0.0388	0.0285
p – 3.5	0.0217	0.0176	0.0223	0.0267	0.0300	0.0387	0.0385	0.0279
p – 3	0.0199	0.0165	0.0221	0.0262	0.0300	0.0403	0.0401	0.0279
p – 2.5	0.0187	0.0164	0.0218	0.0261	0.0302	0.0405	0.0407	0.0278
p – 2	0.0167	0.0159	0.0218	0.0263	0.0296	0.0399	0.0406	0.0272
p – 1.5	0.0160	0.0156	0.0216	0.0206	0.0295	0.0390	0.0397	0.0268
p – 1	0.0146	0.0154	0.0210	0.0256	0.0293	0.0403	0.0407	0.0267
p – 0.5	0.0140	0.0152	0.0211	0.0257	0.0292	0.0396	0.0390	0.0262
ATM p	0.0136	0.0147	0.0208	0.0253	0.0290	0.0400	0.0402	0.0262
ATM c	0.0136	0.0152	0.0210	0.0253	0.0291	0.0400	0.0398	0.0263
c + 0.5	0.0136	0.0149	0.0209	0.0254	0.0290	0.0381	0.0406	0.0261
c + 1	0.0137	0.0153	0.0204	0.0250	0.0284	0.0398	0.0409	0.0262
c + 1.5	0.0142	0.0156	0.0210	0.0248	0.0280	0.0378	0.0401	0.0259
c + 2	0.0151	0.0162	0.0208	0.0242	0.0278	0.0380	0.0398	0.0260
c + 2.5	0.0163	0.0169	0.0212	0.0245	0.0278	0.0374	0.0386	0.0261
c + 3	0.0176	0.0171	0.0216	0.0242	0.0276	0.0366	0.0380	0.0261
c + 3.5	0.0189	0.0180	0.0218	0.0246	0.0278	0.0370	0.0376	0.0265
c + 4	0.0200	0.0187	0.0221	0.0244	0.0277	0.0357	0.0380	0.0266
c + 4.5	0.0209	0.0193	0.0222	0.0248	0.0274	0.0354	0.0380	0.0268
c + 5	0.0218	0.0201	0.0230	0.0243	0.0271	0.0359	0.0383	0.0272
c + 5.5	0.0225	0.0208	0.0236	0.0251	0.0273	0.0343	0.0366	0.0272
c + 6	0.0229	0.0215	0.0234	0.0250	0.0281	0.0344	0.0372	0.0275
c + 6.5	0.0233	0.0219	0.0239	0.0257	0.0285	0.0352	0.0360	0.0278
c + 7	0.0233	0.0228	0.0242	0.0256	0.0280	0.0340	0.0355	0.0276
c + 7.5	0.0235	0.0238	0.0256	0.0264	0.0291	0.0339	0.0351	0.0282
ALL	0.0221	0.0191	0.0230	0.0262	0.0293	0.0376	0.0387	0.0280

(c) Diff. SYSVJ[1] – TS09-SV1

MAE(σ)	M2	M3	M4	M5	M6	Q1	Q2	ALL
p – 7.5	-0.0038	-0.0042	-0.0017	-0.0001	-0.0011	0.0056	0.0015	-0.0005
p – 7	-0.0024	-0.0024	-0.0006	0.0010	0.0007	0.0058	0.0036	0.0008
p – 6.5	-0.0017	-0.0011	0.0003	0.0020	0.0018	0.0058	0.0047	0.0017
p – 6	-0.0010	0.0002	0.0013	0.0025	0.0022	0.0049	0.0043	0.0021
p – 5.5	-0.0006	0.0011	0.0019	0.0026	0.0021	0.0044	0.0031	0.0021
p – 5	-0.0005	0.0016	0.0025	0.0024	0.0023	0.0037	0.0026	0.0021
p – 4.5	-0.0004	0.0019	0.0026	0.0026	0.0023	0.0031	0.0033	0.0022
p – 4	-0.0002	0.0020	0.0025	0.0025	0.0021	0.0028	0.0036	0.0022
p – 3.5	-0.0003	0.0021	0.0024	0.0024	0.0022	0.0022	0.0034	0.0021
p – 3	-0.0003	0.0022	0.0025	0.0024	0.0020	0.0019	0.0024	0.0019
p – 2.5	-0.0003	0.0023	0.0024	0.0024	0.0021	0.0015	0.0014	0.0017
p – 2	-0.0003	0.0023	0.0026	0.0024	0.0019	0.0013	0.0006	0.0015
p – 1.5	-0.0004	0.0022	0.0027	0.0025	0.0021	0.0009	0.0012	0.0016
p – 1	-0.0008	0.0020	0.0027	0.0025	0.0020	0.0010	0.0018	0.0016
p – 0.5	-0.0013	0.0020	0.0027	0.0027	0.0021	0.0010	0.0020	0.0016
ATM p	-0.0017	0.0018	0.0027	0.0028	0.0021	0.0008	0.0018	0.0015
ATM c	-0.0017	0.0018	0.0028	0.0027	0.0022	0.0008	0.0015	0.0014
c + 0.5	-0.0023	0.0018	0.0028	0.0028	0.0025	0.0010	0.0009	0.0014
c + 1	-0.0029	0.0017	0.0028	0.0030	0.0024	0.0008	0.0008	0.0012
c + 1.5	-0.0035	0.0014	0.0031	0.0033	0.0029	0.0011	0.0009	0.0013
c + 2	-0.0039	0.0010	0.0026	0.0034	0.0028	0.0015	0.0022	0.0014
c + 2.5	-0.0045	0.0008	0.0028	0.0036	0.0034	0.0019	0.0026	0.0015
c + 3	-0.0052	0.0004	0.0024	0.0037	0.0035	0.0023	0.0031	0.0015
c + 3.5	-0.0056	0.0005	0.0024	0.0038	0.0040	0.0025	0.0030	0.0015
c + 4	-0.0062	-0.0003	0.0024	0.0038	0.0034	0.0031	0.0030	0.0013
c + 4.5	-0.0068	-0.0002	0.0024	0.0038	0.0039	0.0035	0.0031	0.0014
c + 5	-0.0068	-0.0012	0.0021	0.0039	0.0039	0.0041	0.0030	0.0013
c + 5.5	-0.0070	-0.0014	0.0018	0.0037	0.0041	0.0044	0.0038	0.0013
c + 6	-0.0071	-0.0016	0.0018	0.0039	0.0042	0.0050	0.0048	0.0016
c + 6.5	-0.0067	-0.0019	0.0016	0.0037	0.0042	0.0054	0.0058	0.0017
c + 7	-0.0060	-0.0020	0.0016	0.0038	0.0044	0.0059	0.0063	0.0020
c + 7.5	-0.0043	-0.0019	0.0008	0.0039	0.0043	0.0063	0.0065	0.0022
ALL	-0.0030	0.0005	0.0021	0.0029	0.0027	0.0030	0.0029	0.0016

NOTES: This table reports model accuracy in terms of MAE(σ) within each moneyness-maturity category; the estimations performed on the monthly data set. p – (c +) i refers to put (call) options with strike equal to the ATM strike minus (plus) i USD – the strikes are, therefore, increasing. Only the central rows display ATM options, all others display OTM options. Sub-table (a) refers to TS09-SV1, Sub-table (b) refers to SYSVJ[1] (both models follow the original characterisation of the parameters); observe that the darker the color of the cell (red), the worse the model performance. Sub-table (c) displays the difference between both models (compares models accuracy), that is, TS09-SV1 – SYSVJ[1]; observe that the darker the color of the cell (blue), the more accurate our model is (the better our model performance).

Table 1.8: Model performance of SYSVJ^2 – monthly observations

(a) TS09-SV1

MAE(σ)	M2	M3	M4	M5	M6	Q1	Q2	ALL
p – 7.5	0.0426	0.0265	0.0289	0.0321	0.0328	0.0428	0.0420	0.0354
p – 7	0.0392	0.0253	0.0285	0.0317	0.0335	0.0422	0.0411	0.0345
p – 6.5	0.0362	0.0238	0.0274	0.0310	0.0336	0.0422	0.0418	0.0337
p – 6	0.0333	0.0229	0.0273	0.0301	0.0330	0.0425	0.0425	0.0331
p – 5.5	0.0307	0.0220	0.0271	0.0307	0.0328	0.0422	0.0411	0.0324
p – 5	0.0281	0.0217	0.0262	0.0301	0.0334	0.0419	0.0416	0.0319
p – 4.5	0.0264	0.0210	0.0254	0.0305	0.0326	0.0413	0.0417	0.0313
p – 4	0.0235	0.0204	0.0251	0.0295	0.0325	0.0414	0.0424	0.0307
p – 3.5	0.0214	0.0197	0.0247	0.0291	0.0322	0.0410	0.0419	0.0300
p – 3	0.0195	0.0187	0.0246	0.0286	0.0320	0.0421	0.0425	0.0297
p – 2.5	0.0185	0.0186	0.0242	0.0284	0.0323	0.0420	0.0421	0.0294
p – 2	0.0164	0.0182	0.0244	0.0287	0.0314	0.0412	0.0412	0.0288
p – 1.5	0.0156	0.0178	0.0243	0.0284	0.0316	0.0399	0.0410	0.0284
p – 1	0.0138	0.0174	0.0237	0.0281	0.0313	0.0414	0.0425	0.0283
p – 0.5	0.0127	0.0172	0.0238	0.0284	0.0313	0.0405	0.0410	0.0278
ATM p	0.0120	0.0166	0.0235	0.0281	0.0312	0.0409	0.0420	0.0277
ATM c	0.0120	0.0169	0.0237	0.0281	0.0313	0.0408	0.0414	0.0277
c + 0.5	0.0112	0.0167	0.0237	0.0282	0.0315	0.0392	0.0416	0.0274
c + 1	0.0109	0.0170	0.0233	0.0280	0.0308	0.0407	0.0417	0.0275
c + 1.5	0.0107	0.0170	0.0241	0.0281	0.0309	0.0389	0.0410	0.0272
c + 2	0.0112	0.0171	0.0234	0.0277	0.0306	0.0395	0.0420	0.0274
c + 2.5	0.0119	0.0176	0.0240	0.0281	0.0312	0.0393	0.0412	0.0276
c + 3	0.0125	0.0175	0.0241	0.0279	0.0310	0.0388	0.0411	0.0276
c + 3.5	0.0133	0.0184	0.0242	0.0284	0.0318	0.0395	0.0406	0.0280
c + 4	0.0138	0.0184	0.0246	0.0282	0.0311	0.0388	0.0410	0.0280
c + 4.5	0.0141	0.0190	0.0246	0.0286	0.0313	0.0389	0.0411	0.0282
c + 5	0.0150	0.0190	0.0251	0.0283	0.0310	0.0400	0.0413	0.0285
c + 5.5	0.0154	0.0195	0.0254	0.0288	0.0315	0.0387	0.0405	0.0285
c + 6	0.0159	0.0199	0.0253	0.0288	0.0322	0.0394	0.0420	0.0291
c + 6.5	0.0166	0.0200	0.0256	0.0294	0.0326	0.0406	0.0418	0.0295
c + 7	0.0173	0.0208	0.0258	0.0295	0.0324	0.0399	0.0417	0.0296
c + 7.5	0.0192	0.0219	0.0264	0.0303	0.0335	0.0402	0.0416	0.0304
ALL	0.0191	0.0195	0.0251	0.0291	0.0319	0.0406	0.0416	0.0295

(b) SYSVJ^2

MAE(σ)	M2	M3	M4	M5	M6	Q1	Q2	ALL
p – 7.5	0.0475	0.0315	0.0311	0.0326	0.0343	0.0374	0.0417	0.0366
p – 7	0.0425	0.0285	0.0294	0.0310	0.0331	0.0365	0.0384	0.0342
p – 6.5	0.0386	0.0256	0.0273	0.0292	0.0319	0.0364	0.0373	0.0323
p – 6	0.0350	0.0233	0.0262	0.0278	0.0308	0.0376	0.0381	0.0313
p – 5.5	0.0318	0.0213	0.0253	0.0282	0.0307	0.0376	0.0376	0.0303
p – 5	0.0291	0.0204	0.0239	0.0278	0.0311	0.0382	0.0386	0.0299
p – 4.5	0.0271	0.0194	0.0229	0.0280	0.0302	0.0380	0.0380	0.0291
p – 4	0.0240	0.0186	0.0227	0.0272	0.0304	0.0385	0.0384	0.0286
p – 3.5	0.0219	0.0177	0.0224	0.0269	0.0299	0.0387	0.0381	0.0280
p – 3	0.0200	0.0166	0.0222	0.0264	0.0300	0.0402	0.0395	0.0279
p – 2.5	0.0188	0.0164	0.0218	0.0262	0.0302	0.0405	0.0399	0.0277
p – 2	0.0167	0.0159	0.0219	0.0264	0.0296	0.0399	0.0396	0.0271
p – 1.5	0.0159	0.0156	0.0217	0.0261	0.0295	0.0390	0.0388	0.0267
p – 1	0.0144	0.0152	0.0211	0.0257	0.0293	0.0403	0.0399	0.0266
p – 0.5	0.0137	0.0149	0.0211	0.0258	0.0292	0.0395	0.0383	0.0261
ATM p	0.0132	0.0144	0.0208	0.0254	0.0290	0.0400	0.0397	0.0261
ATM c	0.0132	0.0148	0.0209	0.0254	0.0291	0.0400	0.0392	0.0261
c + 0.5	0.0130	0.0145	0.0208	0.0254	0.0289	0.0381	0.0401	0.0258
c + 1	0.0132	0.0149	0.0203	0.0251	0.0283	0.0398	0.0404	0.0260
c + 1.5	0.0135	0.0152	0.0208	0.0248	0.0279	0.0378	0.0394	0.0256
c + 2	0.0143	0.0156	0.0205	0.0243	0.0277	0.0379	0.0391	0.0256
c + 2.5	0.0154	0.0163	0.0209	0.0244	0.0276	0.0373	0.0379	0.0257
c + 3	0.0168	0.0165	0.0214	0.0242	0.0274	0.0365	0.0375	0.0257
c + 3.5	0.0181	0.0174	0.0215	0.0245	0.0275	0.0369	0.0370	0.0261
c + 4	0.0192	0.0179	0.0217	0.0242	0.0276	0.0355	0.0373	0.0262
c + 4.5	0.0202	0.0186	0.0218	0.0246	0.0272	0.0352	0.0373	0.0264
c + 5	0.0212	0.0194	0.0226	0.0241	0.0269	0.0357	0.0379	0.0268
c + 5.5	0.0219	0.0201	0.0232	0.0248	0.0271	0.0341	0.0360	0.0267
c + 6	0.0224	0.0208	0.0230	0.0247	0.0279	0.0342	0.0366	0.0271
c + 6.5	0.0228	0.0212	0.0236	0.0254	0.0282	0.0349	0.0355	0.0274
c + 7	0.0229	0.0221	0.0237	0.0254	0.0278	0.0337	0.0349	0.0272
c + 7.5	0.0232	0.0231	0.0251	0.0261	0.0289	0.0336	0.0346	0.0278
ALL	0.0219	0.0189	0.0229	0.0262	0.0292	0.0375	0.0382	0.0278

(c) Diff. SYSVJ^2 – TS09-SV1

MAE(σ)	M2	M3	M4	M5	M6	Q1	Q2	ALL
p – 7.5	-0.0049	-0.005	-0.0022	-0.0004	-0.0015	0.0054	0.0003	-0.0012
p – 7	-0.0033	-0.0032	-0.0009	0.0008	0.0004	0.0057	0.0027	0.0003
p – 6.5	-0.0024	-0.0017	0.0001	0.0017	0.0016	0.0058	0.0045	0.0014
p – 6	-0.0016	-0.0004	0.0011	0.0023	0.0022	0.0049	0.0044	0.0018
p – 5.5	-0.0011	0.0007	0.0018	0.0025	0.0022	0.0046	0.0035	0.0020
p – 5	-0.0010	0.0013	0.0024	0.0023	0.0023	0.0038	0.0030	0.0020
p – 4.5	-0.0007	0.0016	0.0024	0.0025	0.0024	0.0032	0.0037	0.0021
p – 4	-0.0005	0.0018	0.0024	0.0023	0.0021	0.0029	0.0040	0.0021
p – 3.5	-0.0005	0.0020	0.0023	0.0022	0.0022	0.0022	0.0039	0.0020
p – 3	-0.0005	0.0021	0.0024	0.0022	0.0020	0.0019	0.0030	0.0019
p – 2.5	-0.0003	0.0022	0.0023	0.0022	0.0021	0.0015	0.0021	0.0017
p – 2	-0.0003	0.0023	0.0025	0.0022	0.0018	0.0013	0.0016	0.0016
p – 1.5	-0.0003	0.0023	0.0026	0.0023	0.0021	0.0008	0.0022	0.0017
p – 1	-0.0007	0.0022	0.0026	0.0024	0.0020	0.0011	0.0026	0.0017
p – 0.5	-0.0010	0.0023	0.0027	0.0026	0.0020	0.0010	0.0027	0.0017
ATM p	-0.0012	0.0022	0.0028	0.0027	0.0022	0.0008	0.0023	0.0017
ATM c	-0.0012	0.0021	0.0028	0.0027	0.0022	0.0008	0.0022	0.0017
c + 0.5	-0.0018	0.0022	0.0029	0.0028	0.0026	0.0010	0.0015	0.0016
c + 1	-0.0023	0.0021	0.0030	0.0030	0.0025	0.0008	0.0013	0.0015
c + 1.5	-0.0029	0.0018	0.0033	0.0032	0.0030	0.0010	0.0016	0.0016
c + 2	-0.0030	0.0015	0.0029	0.0034	0.0029	0.0016	0.0029	0.0017
c + 2.5	-0.0036	0.0013	0.0031	0.0037	0.0036	0.0020	0.0033	0.0019
c + 3	-0.0043	0.0010	0.0027	0.0037	0.0037	0.0023	0.0037	0.0018
c + 3.5	-0.0048	0.0010	0.0027	0.0040	0.0043	0.0026	0.0036	0.0019
c + 4	-0.0054	0.0004	0.0028	0.0040	0.0036	0.0033	0.0036	0.0018
c + 4.5	-0.0060	0.0005	0.0028	0.0040	0.0041	0.0036	0.0037	0.0018
c + 5	-0.0062	-0.0004	0.0025	0.0042	0.0041	0.0043	0.0034	0.0017
c + 5.5	-0.0065	-0.0006	0.0022	0.0040	0.0044	0.0046	0.0044	0.0018
c + 6	-0.0065	-0.0009	0.0022	0.0041	0.0044	0.0052	0.0054	0.0020
c + 6.5	-0.0062	-0.0012	0.0020	0.0040	0.0044	0.0057	0.0063	0.0021
c + 7	-0.0056	-0.0014	0.0020	0.0041	0.0046	0.0062	0.0068	0.0024
c + 7.5	-0.0040	-0.0013	0.0013	0.0042	0.0046	0.0066	0.0069	0.0026
ALL	-0.0028	0.0007	0.0021	0.0029	0.0027	0.0031	0.0033	0.0017

NOTES: This table reports model accuracy in terms of MAE(σ) within each moneyness-maturity category; the estimations performed on the monthly data set. p – (c +) i refers to put (call) options with strike equal to the ATM strike minus (plus) i USD – the strikes are, therefore, increasing. Only the central rows display ATM options, all others display OTM options. Sub-table (a) refers to TS09-SV1, Sub-table (b) refers to our more advanced model SYSVJ^2 (both models follow the original characterisation of the parameters); observe that the darker the color of the cell (red), the worse the model performance. Sub-table (c) displays the difference between both models (compares models accuracy), that is, TS09-SV1 – SYSVJ^2; observe that the darker the color of the cell (blue), the more accurate our model is.

Table 1.9: Model performance of SYSVJ[1] – daily observations

(a) TS09-SV1

MAE(σ)	M2	M3	M4	M5	M6	Q1	Q2	ALL
p – 7.5	0.0770	0.0524	0.0411	0.0372	0.0370	0.0373	0.0392	0.0459
p – 7	0.0732	0.0509	0.0403	0.0367	0.0370	0.0371	0.0390	0.0449
p – 6.5	0.0701	0.0492	0.0394	0.0362	0.0370	0.0365	0.0392	0.0440
p – 6	0.0672	0.0473	0.0385	0.0354	0.0366	0.0365	0.0393	0.0430
p – 5.5	0.0644	0.0457	0.0378	0.0353	0.0364	0.0361	0.0394	0.0422
p – 5	0.0618	0.0441	0.0371	0.0345	0.0363	0.0361	0.0391	0.0413
p – 4.5	0.0594	0.0425	0.0364	0.0339	0.0357	0.0360	0.0397	0.0405
p – 4	0.0569	0.0410	0.0358	0.0332	0.0353	0.0359	0.0398	0.0397
p – 3.5	0.0546	0.0397	0.0350	0.0327	0.0349	0.0356	0.0398	0.0389
p – 3	0.0524	0.0385	0.0342	0.0321	0.0346	0.0359	0.0397	0.0382
p – 2.5	0.0503	0.0373	0.0335	0.0317	0.0339	0.0359	0.0402	0.0375
p – 2	0.0483	0.0362	0.0329	0.0313	0.0335	0.0359	0.0396	0.0368
p – 1.5	0.0465	0.0352	0.0323	0.0310	0.0330	0.0354	0.0398	0.0362
p – 1	0.0447	0.0341	0.0316	0.0305	0.0325	0.0357	0.0397	0.0355
p – 0.5	0.0431	0.0333	0.0309	0.0303	0.0321	0.0353	0.0396	0.0349
ATM p	0.0417	0.0324	0.0304	0.0301	0.0320	0.0349	0.0402	0.0345
ATM c	0.0416	0.0323	0.0304	0.0300	0.0320	0.0352	0.0394	0.0344
c + 0.5	0.0405	0.0317	0.0298	0.0298	0.0316	0.0351	0.0398	0.0340
c + 1	0.0394	0.0311	0.0294	0.0295	0.0314	0.0348	0.0395	0.0336
c + 1.5	0.0387	0.0305	0.0290	0.0294	0.0311	0.0344	0.0392	0.0332
c + 2	0.0380	0.0301	0.0287	0.0292	0.0311	0.0344	0.0391	0.0329
c + 2.5	0.0375	0.0297	0.0284	0.0291	0.0310	0.0342	0.0387	0.0327
c + 3	0.0372	0.0294	0.0282	0.0290	0.0308	0.0340	0.0385	0.0324
c + 3.5	0.0371	0.0293	0.0280	0.0288	0.0309	0.0340	0.0388	0.0324
c + 4	0.0372	0.0293	0.0278	0.0286	0.0308	0.0338	0.0387	0.0323
c + 4.5	0.0375	0.0294	0.0278	0.0285	0.0311	0.0337	0.0385	0.0324
c + 5	0.0380	0.0297	0.0277	0.0285	0.0309	0.0337	0.0384	0.0324
c + 5.5	0.0386	0.0300	0.0278	0.0286	0.0311	0.0336	0.0387	0.0326
c + 6	0.0394	0.0305	0.0280	0.0284	0.0310	0.0336	0.0388	0.0328
c + 6.5	0.0405	0.0310	0.0282	0.0287	0.0312	0.0337	0.0390	0.0332
c + 7	0.0418	0.0317	0.0284	0.0285	0.0314	0.0337	0.0389	0.0335
c + 7.5	0.0437	0.0325	0.0288	0.0287	0.0314	0.0342	0.0393	0.0341
ALL	0.0481	0.0359	0.0320	0.0311	0.0330	0.0351	0.0393	0.0363

(b) SYSVJ[1]

MAE(σ)	M2	M3	M4	M5	M6	Q1	Q2	ALL
p – 7.5	0.0542	0.0348	0.0289	0.0291	0.0303	0.0351	0.0400	0.0361
p – 7	0.0519	0.0336	0.0280	0.0282	0.0298	0.0345	0.0386	0.0350
p – 6.5	0.0502	0.0324	0.0273	0.0276	0.0296	0.0338	0.0379	0.0341
p – 6	0.0489	0.0314	0.0268	0.0271	0.0291	0.0337	0.0374	0.0335
p – 5.5	0.0476	0.0307	0.0266	0.0272	0.0293	0.0334	0.0370	0.0331
p – 5	0.0466	0.0301	0.0264	0.0270	0.0294	0.0334	0.0366	0.0328
p – 4.5	0.0456	0.0294	0.0262	0.0269	0.0292	0.0334	0.0370	0.0325
p – 4	0.0445	0.0287	0.0261	0.0267	0.0292	0.0333	0.0370	0.0322
p – 3.5	0.0434	0.0281	0.0257	0.0266	0.0293	0.0331	0.0369	0.0319
p – 3	0.0424	0.0276	0.0255	0.0264	0.0294	0.0334	0.0369	0.0317
p – 2.5	0.0413	0.0271	0.0252	0.0263	0.0292	0.0334	0.0372	0.0314
p – 2	0.0401	0.0265	0.0251	0.0262	0.0291	0.0334	0.0370	0.0311
p – 1.5	0.0390	0.0260	0.0248	0.0260	0.0291	0.0329	0.0373	0.0307
p – 1	0.0378	0.0254	0.0245	0.0257	0.0288	0.0331	0.0373	0.0304
p – 0.5	0.0366	0.0249	0.0241	0.0256	0.0286	0.0327	0.0374	0.0300
ATM p	0.0355	0.0244	0.0238	0.0253	0.0285	0.0324	0.0377	0.0297
ATM c	0.0354	0.0243	0.0238	0.0253	0.0286	0.0326	0.0374	0.0297
c + 0.5	0.0346	0.0240	0.0234	0.0252	0.0282	0.0326	0.0375	0.0293
c + 1	0.0337	0.0236	0.0231	0.0248	0.0281	0.0323	0.0374	0.0290
c + 1.5	0.0329	0.0232	0.0228	0.0247	0.0277	0.0319	0.0371	0.0286
c + 2	0.0322	0.0228	0.0225	0.0244	0.0276	0.0318	0.0370	0.0283
c + 2.5	0.0317	0.0225	0.0222	0.0244	0.0274	0.0317	0.0365	0.0280
c + 3	0.0312	0.0222	0.0221	0.0242	0.0269	0.0316	0.0361	0.0278
c + 3.5	0.0308	0.0221	0.0220	0.0240	0.0267	0.0315	0.0362	0.0276
c + 4	0.0307	0.0219	0.0219	0.0239	0.0266	0.0313	0.0359	0.0275
c + 4.5	0.0306	0.0219	0.0219	0.0238	0.0265	0.0311	0.0355	0.0273
c + 5	0.0306	0.0219	0.0219	0.0237	0.0262	0.0311	0.0351	0.0272
c + 5.5	0.0307	0.0220	0.0219	0.0241	0.0262	0.0309	0.0351	0.0273
c + 6	0.0310	0.0221	0.0221	0.0238	0.0261	0.0308	0.0349	0.0272
c + 6.5	0.0314	0.0222	0.0222	0.0241	0.0261	0.0307	0.0346	0.0273
c + 7	0.0320	0.0224	0.0223	0.0240	0.0263	0.0305	0.0345	0.0274
c + 7.5	0.0328	0.0227	0.0225	0.0243	0.0262	0.0307	0.0343	0.0277
ALL	0.0381	0.0257	0.0242	0.0255	0.0281	0.0324	0.0367	0.0300

(c) Diff. SYSVJ[1] – TS09-SV1

MAE(σ)	M2	M3	M4	M5	M6	Q1	Q2	ALL
p – 7.5	0.0228	0.0176	0.0122	0.0081	0.0067	0.0022	-0.0008	0.0098
p – 7	0.0213	0.0173	0.0123	0.0085	0.0072	0.0026	0.0004	0.0099
p – 6.5	0.0199	0.0167	0.0121	0.0086	0.0074	0.0027	0.0013	0.0098
p – 6	0.0183	0.0159	0.0117	0.0083	0.0075	0.0028	0.0019	0.0095
p – 5.5	0.0168	0.0150	0.0112	0.0080	0.0072	0.0028	0.0023	0.0090
p – 5	0.0153	0.0141	0.0107	0.0075	0.0069	0.0027	0.0025	0.0085
p – 4.5	0.0138	0.0131	0.0102	0.0070	0.0065	0.0026	0.0027	0.0080
p – 4	0.0124	0.0123	0.0097	0.0065	0.0061	0.0026	0.0028	0.0075
p – 3.5	0.0112	0.0115	0.0092	0.0061	0.0056	0.0025	0.0029	0.0070
p – 3	0.0100	0.0108	0.0087	0.0057	0.0052	0.0025	0.0028	0.0065
p – 2.5	0.0091	0.0102	0.0082	0.0054	0.0047	0.0025	0.0030	0.0061
p – 2	0.0082	0.0097	0.0078	0.0051	0.0043	0.0025	0.0026	0.0058
p – 1.5	0.0075	0.0092	0.0075	0.0050	0.0040	0.0025	0.0025	0.0054
p – 1	0.0069	0.0087	0.0071	0.0048	0.0037	0.0026	0.0023	0.0052
p – 0.5	0.0065	0.0083	0.0068	0.0047	0.0035	0.0026	0.0023	0.0050
ATM p	0.0061	0.0080	0.0066	0.0047	0.0034	0.0025	0.0025	0.0048
ATM c	0.0062	0.0080	0.0066	0.0047	0.0034	0.0026	0.0019	0.0048
c + 0.5	0.0059	0.0077	0.0064	0.0046	0.0034	0.0025	0.0023	0.0047
c + 1	0.0058	0.0075	0.0063	0.0047	0.0034	0.0025	0.0022	0.0046
c + 1.5	0.0057	0.0074	0.0062	0.0047	0.0034	0.0025	0.0021	0.0046
c + 2	0.0058	0.0073	0.0062	0.0048	0.0035	0.0026	0.0021	0.0046
c + 2.5	0.0058	0.0072	0.0061	0.0047	0.0037	0.0025	0.0022	0.0046
c + 3	0.0060	0.0072	0.0061	0.0048	0.0039	0.0024	0.0024	0.0047
c + 3.5	0.0063	0.0072	0.0060	0.0048	0.0041	0.0025	0.0025	0.0048
c + 4	0.0066	0.0073	0.0059	0.0047	0.0042	0.0025	0.0028	0.0049
c + 4.5	0.0069	0.0075	0.0058	0.0047	0.0046	0.0025	0.0030	0.0050
c + 5	0.0074	0.0077	0.0058	0.0047	0.0047	0.0027	0.0032	0.0052
c + 5.5	0.0078	0.0081	0.0058	0.0046	0.0048	0.0027	0.0036	0.0054
c + 6	0.0084	0.0084	0.0059	0.0046	0.0049	0.0028	0.0039	0.0056
c + 6.5	0.0091	0.0088	0.0060	0.0046	0.0051	0.0030	0.0044	0.0058
c + 7	0.0098	0.0093	0.0061	0.0045	0.0051	0.0032	0.0044	0.0061
c + 7.5	0.0109	0.0099	0.0062	0.0044	0.0051	0.0035	0.0050	0.0064
ALL	0.0100	0.0102	0.0078	0.0056	0.0049	0.0026	0.0026	0.0063

NOTES: This table reports model accuracy in terms of MAE(σ) within each moneyness-maturity category; the estimations performed on the daily data set. p – (c +) i refers to put (call) options with strike equal to the ATM strike minus (plus) i USD – the strikes are, therefore, increasing. Only the central rows display ATM options, all others display OTM options. Sub-table (a) refers to TS09-SV1, Sub-table (b) refers to SYSVJ[1] (both models follow the original characterisation of the parameters); observe that the darker the color of the cell (red), the worse the model performance. Sub-table (c) displays the difference between both models (compares models accuracy), that is, TS09-SV1 – SYSVJ[1]; observe that the darker the color of the cell (blue), the more accurate our model is (the better our model performance).

Table 1.10: Model performance of SYSVJ^2 – daily observations

(a) TS09-SV1

MAE(σ)	M2	M3	M4	M5	M6	Q1	Q2	ALL
p – 7.5	0.0770	0.0524	0.0411	0.0372	0.0370	0.0373	0.0392	0.0459
p – 7	0.0732	0.0509	0.0403	0.0367	0.0370	0.0371	0.0390	0.0449
p – 6.5	0.0701	0.0492	0.0394	0.0362	0.0370	0.0365	0.0392	0.0440
p – 6	0.0672	0.0473	0.0385	0.0354	0.0366	0.0365	0.0393	0.0430
p – 5.5	0.0644	0.0457	0.0378	0.0353	0.0364	0.0361	0.0394	0.0422
p – 5	0.0618	0.0441	0.0371	0.0345	0.0363	0.0361	0.0391	0.0413
p – 4.5	0.0594	0.0425	0.0364	0.0339	0.0357	0.0360	0.0397	0.0405
p – 4	0.0569	0.0410	0.0358	0.0332	0.0353	0.0359	0.0398	0.0397
p – 3.5	0.0546	0.0397	0.0350	0.0327	0.0349	0.0356	0.0398	0.0389
p – 3	0.0524	0.0385	0.0342	0.0321	0.0346	0.0359	0.0397	0.0382
p – 2.5	0.0503	0.0373	0.0335	0.0317	0.0339	0.0359	0.0402	0.0375
p – 2	0.0483	0.0362	0.0329	0.0313	0.0335	0.0359	0.0396	0.0368
p – 1.5	0.0465	0.0352	0.0323	0.0310	0.0330	0.0354	0.0398	0.0362
p – 1	0.0447	0.0341	0.0316	0.0305	0.0325	0.0357	0.0397	0.0355
p – 0.5	0.0431	0.0333	0.0309	0.0303	0.0321	0.0353	0.0396	0.0349
ATM p	0.0417	0.0324	0.0304	0.0301	0.0320	0.0349	0.0402	0.0345
ATM c	0.0416	0.0323	0.0304	0.0300	0.0320	0.0352	0.0394	0.0344
c + 0.5	0.0405	0.0317	0.0298	0.0298	0.0316	0.0351	0.0398	0.0340
c + 1	0.0394	0.0311	0.0294	0.0295	0.0314	0.0348	0.0395	0.0336
c + 1.5	0.0387	0.0305	0.0290	0.0294	0.0311	0.0344	0.0392	0.0332
c + 2	0.0380	0.0301	0.0287	0.0292	0.0311	0.0344	0.0391	0.0329
c + 2.5	0.0375	0.0297	0.0284	0.0291	0.0310	0.0342	0.0387	0.0327
c + 3	0.0372	0.0294	0.0282	0.0290	0.0308	0.0340	0.0385	0.0324
c + 3.5	0.0371	0.0293	0.0280	0.0288	0.0309	0.0340	0.0388	0.0324
c + 4	0.0372	0.0293	0.0278	0.0286	0.0308	0.0338	0.0387	0.0323
c + 4.5	0.0375	0.0294	0.0278	0.0285	0.0311	0.0337	0.0385	0.0324
c + 5	0.0380	0.0297	0.0277	0.0285	0.0309	0.0337	0.0384	0.0324
c + 5.5	0.0386	0.0300	0.0278	0.0286	0.0311	0.0336	0.0387	0.0326
c + 6	0.0394	0.0305	0.0280	0.0284	0.0310	0.0336	0.0388	0.0328
c + 6.5	0.0405	0.0310	0.0282	0.0287	0.0312	0.0337	0.0390	0.0332
c + 7	0.0418	0.0317	0.0284	0.0285	0.0314	0.0337	0.0389	0.0335
c + 7.5	0.0437	0.0325	0.0288	0.0287	0.0314	0.0342	0.0393	0.0341
ALL	0.0481	0.0359	0.0320	0.0311	0.0330	0.0351	0.0393	0.0363

(b) SYSVJ^2

MAE(σ)	M2	M3	M4	M5	M6	Q1	Q2	ALL
p – 7.5	0.0548	0.0359	0.0295	0.0290	0.0302	0.0344	0.0404	0.0363
p – 7	0.0533	0.0356	0.0294	0.0288	0.0304	0.0342	0.0394	0.0359
p – 6.5	0.0523	0.0351	0.0292	0.0288	0.0306	0.0338	0.0390	0.0355
p – 6	0.0513	0.0344	0.0291	0.0287	0.0305	0.0339	0.0386	0.0352
p – 5.5	0.0503	0.0340	0.0292	0.0291	0.0308	0.0338	0.0384	0.0351
p – 5	0.0494	0.0336	0.0293	0.0290	0.0311	0.0339	0.0379	0.0349
p – 4.5	0.0485	0.0331	0.0292	0.0291	0.0311	0.0340	0.0382	0.0347
p – 4	0.0475	0.0325	0.0293	0.0291	0.0311	0.0340	0.0380	0.0345
p – 3.5	0.0463	0.0319	0.0290	0.0290	0.0313	0.0338	0.0377	0.0342
p – 3	0.0452	0.0313	0.0288	0.0288	0.0314	0.0341	0.0375	0.0339
p – 2.5	0.0440	0.0308	0.0285	0.0288	0.0312	0.0341	0.0379	0.0336
p – 2	0.0427	0.0301	0.0284	0.0287	0.0312	0.0341	0.0373	0.0332
p – 1.5	0.0415	0.0295	0.0281	0.0285	0.0310	0.0336	0.0375	0.0328
p – 1	0.0402	0.0288	0.0277	0.0282	0.0307	0.0338	0.0374	0.0324
p – 0.5	0.0389	0.0282	0.0272	0.0280	0.0306	0.0334	0.0374	0.0320
ATM p	0.0377	0.0275	0.0269	0.0278	0.0305	0.0330	0.0381	0.0316
ATM c	0.0377	0.0275	0.0269	0.0277	0.0305	0.0333	0.0373	0.0316
c + 0.5	0.0367	0.0270	0.0264	0.0275	0.0301	0.0333	0.0378	0.0312
c + 1	0.0356	0.0265	0.0260	0.0271	0.0300	0.0329	0.0377	0.0308
c + 1.5	0.0348	0.0259	0.0256	0.0269	0.0295	0.0326	0.0376	0.0304
c + 2	0.0340	0.0254	0.0252	0.0264	0.0294	0.0325	0.0375	0.0301
c + 2.5	0.0334	0.0249	0.0247	0.0263	0.0291	0.0324	0.0371	0.0297
c + 3	0.0328	0.0245	0.0244	0.0260	0.0286	0.0323	0.0368	0.0294
c + 3.5	0.0324	0.0242	0.0241	0.0257	0.0284	0.0323	0.0370	0.0291
c + 4	0.0322	0.0239	0.0238	0.0254	0.0281	0.0320	0.0368	0.0289
c + 4.5	0.0320	0.0238	0.0236	0.0253	0.0281	0.0319	0.0366	0.0288
c + 5	0.0321	0.0237	0.0235	0.0251	0.0276	0.0319	0.0363	0.0286
c + 5.5	0.0321	0.0236	0.0233	0.0252	0.0275	0.0317	0.0365	0.0286
c + 6	0.0323	0.0236	0.0233	0.0249	0.0274	0.0316	0.0364	0.0285
c + 6.5	0.0327	0.0236	0.0233	0.0251	0.0273	0.0315	0.0363	0.0286
c + 7	0.0333	0.0238	0.0233	0.0249	0.0274	0.0314	0.0361	0.0286
c + 7.5	0.0340	0.0240	0.0233	0.0251	0.0272	0.0316	0.0363	0.0288
ALL	0.0401	0.0284	0.0265	0.0273	0.0297	0.0330	0.0375	0.0318

(c) Diff. SYSVJ^2 – TS09-SV1

MAE(σ)	M2	M3	M4	M5	M6	Q1	Q2	ALL
p – 7.5	0.0222	0.0164	0.0116	0.0082	0.0068	0.0029	-0.0012	0.0095
p – 7	0.0199	0.0153	0.0109	0.0079	0.0066	0.0029	-0.0004	0.0090
p – 6.5	0.0179	0.0141	0.0102	0.0075	0.0063	0.0027	0.0002	0.0084
p – 6	0.0159	0.0129	0.0094	0.0068	0.0061	0.0025	0.0007	0.0077
p – 5.5	0.0141	0.0117	0.0086	0.0062	0.0056	0.0023	0.0010	0.0071
p – 5	0.0124	0.0105	0.0078	0.0054	0.0052	0.0021	0.0013	0.0064
p – 4.5	0.0109	0.0094	0.0072	0.0048	0.0047	0.0020	0.0015	0.0058
p – 4	0.0094	0.0085	0.0065	0.0042	0.0042	0.0019	0.0018	0.0052
p – 3.5	0.0083	0.0077	0.0059	0.0037	0.0036	0.0018	0.0021	0.0047
p – 3	0.0072	0.0071	0.0054	0.0032	0.0032	0.0018	0.0022	0.0043
p – 2.5	0.0063	0.0066	0.0049	0.0029	0.0027	0.0018	0.0023	0.0039
p – 2	0.0056	0.0061	0.0045	0.0026	0.0023	0.0018	0.0023	0.0036
p – 1.5	0.0050	0.0057	0.0042	0.0025	0.0020	0.0018	0.0022	0.0033
p – 1	0.0045	0.0053	0.0039	0.0023	0.0017	0.0018	0.0023	0.0031
p – 0.5	0.0042	0.0051	0.0037	0.0023	0.0016	0.0019	0.0022	0.0030
ATM p	0.0039	0.0049	0.0036	0.0023	0.0015	0.0019	0.0021	0.0029
ATM c	0.0039	0.0049	0.0035	0.0023	0.0015	0.0019	0.0021	0.0029
c + 0.5	0.0038	0.0047	0.0035	0.0023	0.0014	0.0019	0.0020	0.0028
c + 1	0.0038	0.0046	0.0034	0.0024	0.0015	0.0019	0.0018	0.0028
c + 1.5	0.0039	0.0046	0.0035	0.0026	0.0016	0.0019	0.0017	0.0028
c + 2	0.0040	0.0047	0.0035	0.0027	0.0017	0.0018	0.0016	0.0029
c + 2.5	0.0041	0.0047	0.0036	0.0028	0.0019	0.0018	0.0016	0.0030
c + 3	0.0044	0.0049	0.0037	0.0030	0.0022	0.0017	0.0017	0.0031
c + 3.5	0.0047	0.0051	0.0039	0.0031	0.0025	0.0017	0.0018	0.0032
c + 4	0.0050	0.0053	0.0040	0.0032	0.0027	0.0017	0.0019	0.0034
c + 4.5	0.0054	0.0056	0.0041	0.0033	0.0030	0.0018	0.0019	0.0036
c + 5	0.0059	0.0060	0.0043	0.0034	0.0033	0.0018	0.0020	0.0038
c + 5.5	0.0064	0.0064	0.0045	0.0034	0.0035	0.0019	0.0022	0.0041
c + 6	0.0070	0.0069	0.0047	0.0035	0.0037	0.0020	0.0024	0.0043
c + 6.5	0.0078	0.0073	0.0049	0.0035	0.0039	0.0022	0.0027	0.0046
c + 7	0.0086	0.0079	0.0052	0.0036	0.0040	0.0023	0.0028	0.0049
c + 7.5	0.0097	0.0086	0.0055	0.0036	0.0042	0.0026	0.0029	0.0053
ALL	0.0080	0.0075	0.0054	0.0038	0.0033	0.0020	0.0017	0.0045

NOTES: This table reports model accuracy in terms of MAE(σ) within each moneyness-maturity category; the estimations performed on the daily data set. p – (c +) i refers to put (call) options with strike equal to the ATM strike minus (plus) i USD – the strikes are, therefore, increasing. Only the central rows display ATM options, all others display OTM options. Sub-table (a) refers to TS09-SV1, Sub-table (b) refers to our more advanced model SYSVJ^2 (both models follow the original characterisation of the parameters); observe that the darker the color of the cell (red), the worse the model performance. Sub-table (c) displays the difference between both models (compares models accuracy), that is, TS09-SV1 – SYSVJ^2; observe that the darker the color of the cell (blue), the more accurate our model is.

Bibliography

Amin, K., Ng, V. & Pirrong, C. (1995), 'Valuing energy derivatives', *Managing Energy Price Risk* **3**, 50–70. 2

Andersen, L. (2010), 'Markov models for commodity futures: theory and practice', *Quantitative Finance* **10**(8), 831–854. 2

Bates, D. S. (1996), 'Jumps and stochastic volatility: Exchange rate processes implicit in deutsche mark options', *Review of Financial Studies* **9**(1), 69–107. 3, 5, 11, 12

Black, F. (1976), 'The pricing of commodity contracts', *Journal of Financial Economics* **3**(1), 167–179. 18

Black, F. & Scholes, M. (1973), 'The pricing of options and corporate liabilities', *Journal of Political Economy* **81**(3), 637–654. 11

Brennan, M. J. (1991), The price of convenience and the valuation of commodity contingent claims, *in* 'Stochastic models and option values', Lund, D. and Øksendal, B., Elsever North Holland. 2

Brennan, M. J. & Schwartz, E. S. (1985), 'Evaluating natural resource investments', *The Journal of Business* **58**(2), 135–157. 2

Carr, P. & Madan, D. B. (1999), 'Option valuation using the fast Fourier transform', *Journal of Computational Finance* **2**(4), 61–73. 13, 17

Clewlow, L. & Strickland, C. (1999a), Valuing energy options in a one factor model fitted to forward prices, Research Paper Series 10, Quantitative Finance Research Centre, University of Technology, Sydney. 2

Clewlow, L. & Strickland, C. (1999b), A multi-factor model for energy derivatives, Research Paper Series 28, Quantitative Finance Research Centre, University of Technology, Sydney. 2

Cont, R. & Tankov, P. (2003), *Financial Modelling with Jump Processes*, Chapman and Hall/CRC Financial Mathematics Series. 7

Cortázar, G. & Schwartz, E. S. (1994), 'The valuation of commodity contingent claims', *Journal of Derivatives* **1**(4), 27–39. 2

Cortázar, G. & Schwartz, E. S. (2003), 'Implementing a stochastic model for oil futures prices', *Journal of Energy Economics* **25**(3), 215–238. 2

Cox, J. C., Ingersoll, J. E. & Ross, S. A. (1985), 'A theory of the term structure of interest rates', *Econometrica* **53**(2), 385–407. 4

Crosby, J. (2008), 'A multi-factor jump-diffusion model for commodities', *Quantitative Finance* **8**(2), 181–200. 2, 3, 6, 14, 20

Duffie, D. (2001), *Dynamic Asset Pricing Theory*, Princeton University Press. 7

Duffie, D., Pan, J. & Singleton, K. (2000), 'Transform analysis and asset pricing for affine jump-diffusions', *Econometrica* **68**, 1343–1376. 3, 13, 19, 42

Gibson, R. & Schwartz, E. S. (1990), 'Stochastic convenience yield and the pricing of oil contingent claims', *Journal of Finance* **45**(3), 959–976. 2

Heath, D., Jarrow, R. & Morton, A. (1992), 'Bond pricing and the term structure of interest rates: a new methodology for contingent claims valuation', *Econometrica* **60**(1), 77–105. 2, 7

Heston, S. L. (1993), 'A closed-form solution for options with stochastic volatility with applications to bond and currency options', *Review of Financial Studies* **6**(2), 327–343. 5, 11, 13

Hilliard, J. E. & Reis, J. (1998), 'Valuation of commodity futures and options under stochastic convenience yields, interest rates, and jump diffusions in the spot', *Journal of Financial and Quantitative Analysis* **33**(1), 61–86. 2

Merton, R. (1976), 'Option pricing when underlying stock returns are discontinuous', *Journal of Financial Economics* **3**(1-2), 125–144. 3, 5, 6, 11

Miltersen, K. R. (2003), 'Commodity price modelling that matches current observables: a new approach', *Quantitative Finance* **3**(1), 51–58. 2

Miltersen, K. R. & Schwartz, E. S. (1998), 'Pricing of options on commodity futures with stochastic term structures of convenience yields and interest rates', *Journal of Financial and Quantitative Analysis* **33**(1), 33–59. 2

Nielsen, M. J. & Schwartz, E. S. (2004), 'Theory of storage and the pricing of commodity claims', *Review of Derivatives Research* **7**(1), 5–24. 2

Reisman, H. (1991), Movements of the term structure of commodity futures and pricing of commodity claims, Unpublished manuscript, Haifa University, Israel. 2

Richter, M. & Sørensen, C. (2002), Stochastic volatility and seasonality in commodity futures and options: the case of soybeans, Working Paper 4, Copenhagen Business School, Department of Finance.
URL: *http://ssrn.com/abstract=301994* 2

Schwartz, E. S. (1997), 'The stochastic behavior of commodity prices: Implications for valuation and hedging', *Journal of Finance* **52**(3), 923–973. 2

Sitzia, N. (2018), 'The analytical solution of Trolle-Schwartz model, MSc. thesis, École Polytechnique Fédérale de Lausanne'.
URL: *https://ssrn.com/abstract=3121906* 9, 19, 44

Trolle, A. B. (2014), *Efficient Pricing of Energy Derivatives*, Marcel Prokopczuk, Ed.: Energy Pricing Models: Recent Advances, Methods and Tools, Palgrave Macmillan. 3, 5, 10, 11, 12

Trolle, A. B. & Schwartz, E. S. (2009), 'Unspanned stochastic volatility and the pricing of commodity derivatives', *Review of Financial Studies* **22**(11), 4423–4461. 1, 3, 4, 5, 9, 10, 11, 12, 16, 20

Yan, X. (2002), 'Valuation of commodity derivatives in a new multi-factor model', *Review of Derivatives Research* **5**(3), 251–271. 2

Appendix

1A Appendix for Proofs

1A.1 Proof of Proposition 1.1

From applying Itô's Lemma for jump diffusion processes to $F(t,T)$ in (1.6) we have that

$$\frac{dF(t,T)}{F(t,T)} = \Big(\int_t^T \mu_y(t,u)du + v_t\Big(\frac{\sigma_Y^2(t,T)}{2} + \sigma_S\sigma_Y(t,T)\rho_{Sy}\Big) - \lambda E_t^{\mathbb{Q}}\left[e^{J_S} + J_Y(t,T) - 1\right]\Big)dt$$
$$+ \sqrt{v_t}\big(\sigma_S dW_t^S + \sigma_Y(t,T)dW_t^y\big) + \big(e^{J_S+J_Y(t,T)} - 1\big)dN_t. \tag{1A.1}$$

In an arbitrage-free framework and given that, by definition, futures prices are martingales, the drift term in equation (1A.1) must equal zero. Therefore we group together

(i) those terms whose expected value equals zero

$$\sqrt{v_t}\big(\sigma_S dW_t^S + \sigma_Y(t,T)dW_t^y\big) + \big(e^{J_S+J_Y(t,T)} - 1\big)dN_t - \lambda E_t^{\mathbb{Q}}\left[e^{J_S+J_Y(t,T)} - 1\right]dt, \tag{1A.2}$$

(ii) the remaining terms whose expected value, therefore, also equals zero

$$\int_t^T \mu_y(t,u)du + v_t\Big(\frac{\sigma_Y^2(t,T)}{2} + \sigma_S\sigma_Y(t,T)\rho_{Sy}\Big) - \lambda E_t^{\mathbb{Q}}\left[e^{J_S} + J_Y(t,T) - 1\right]$$
$$+ \lambda E_t^{\mathbb{Q}}\left[e^{J_S+J_Y(t,T)} - 1\right] \tag{1A.3}$$

Observe that we had to artificially retrieve a new drift correction term in (i) so that the expected value of the jump terms offset one another. The very same term had to be incorporated in (ii).

For equation (1A.1) to be a martingale, it must hold that

$$\frac{1}{dt}E_t^{\mathbb{Q}}\left[\frac{dF(t,T)}{F(t,T)}\right] = \int_t^T \mu_y(t,u)du + v_t\Big(\frac{\sigma_Y^2(t,T)}{2} + \sigma_S\sigma_Y(t,T)\rho_{Sy}\Big)$$
$$- \lambda E_t^{\mathbb{Q}}\left[e^{J_S} + J_Y(t,T) - 1\right] + \lambda E_t^{\mathbb{Q}}\left[e^{J_S+J_Y(t,T)} - 1\right] = 0. \tag{1A.4}$$

Setting those terms in (ii) to zero and differentiating with respect to T lets us obtain the expression followed by the drift of $y(t,T)$ in (1.2)

$$\mu_y(t,T) = -v_t\sigma_y(t,T)\big(\sigma_Y(t,T)+\sigma_S\rho_{Sy}\big)+\lambda E_t^{\mathbb{Q}}\left[\big(e^{J_S}+J_y(t,T)-1\big)-\big(e^{J_S+J_y(t,T)}-1\big)\right]. \tag{1A.5}$$

Thus, the dynamics of the futures under the martingale condition becomes

$$\frac{dF(t,T)}{F(t,T)} = \sqrt{v_t}\big(\sigma_S dW_t^S+\sigma_Y(t,T)dW_t^y\big)-\lambda E_t^{\mathbb{Q}}\left[e^{J_S+J_Y(t,T)}-1\right]dt+\big(e^{J_S+J_Y(t,T)}-1\big)dN_t. \tag{1A.6}$$

From equation (1A.6), if one were to momentarily assume that there is only one jump in S_t but no jump in $y(t,T)$, $F(t,T)$ would change by $F(t,T)(e^{J_S}-1)$; with one jump only in $y(t,T)$ but no jump in S_t, $F(t,T)$ would change by $F(t,T)(e^{J_Y(t,T)}-1)$; with one jump in both S_t and $y(t,T)$, $F(t,T)$ would change by $F(t,T)(e^{J_S+J_Y(t,T)}-1)$.

We define the processes $s_t \equiv \ln S_t$ and $f(t,T) \equiv \ln F(t,T)$. Therefore, we have

$$df(t,T) = ds_t + dY(t,T). \tag{1A.7}$$

From applying Itô's Lemma for jump diffusion processes to s_t and Leibniz's rule to equation (1.2), we have

$$\begin{aligned} ds_t = \frac{\partial s_t}{\partial S_t}dS_t + \frac{1}{2}\frac{\partial^2 s_t}{\partial S_t^2}dS_t^2 + J_S dN_t &= \Big(y_t - \frac{\sigma_S^2}{2}v_t - \lambda E_t^{\mathbb{Q}}\left[e^{J_S}-1\right]\Big)dt + \sigma_S\sqrt{v_t}dW_t^S \\ &\quad + J_S dN_t, \end{aligned} \tag{1A.8}$$

$$dY(t,T) = \Big(\int_t^T \mu_y(t,u)du - \lambda E_t^{\mathbb{Q}}\left[J_Y(t,T)\right] - y_t\Big)dt + \sigma_Y(t,T)\sqrt{v_t}dW_t^y + J_Y(t,T)dN_t, \tag{1A.9}$$

with $\sigma_Y(T,t)$ and $J_Y(t,T)$ as in (1.8) and (1.10), respectively. By substituting (1A.8) and (1A.9) into (1A.7) we have

$$\begin{aligned} df(t,T) = &\Big(\int_t^T \mu_y(t,u)du - \frac{\sigma_S^2}{2}v_t - \lambda E_t^{\mathbb{Q}}\left[e^{J_S}+J_Y(t,T)-1\right]\Big)dt \\ &+ \sqrt{v_t}\left(\sigma_S dW_t^S + \sigma_Y(t,T)dW_t^y\right) + \big(J_S + J_Y(t,T)\big)dN_t. \end{aligned} \tag{1A.10}$$

1A.2 Proof of Proposition 1.2

Integrating (1.2) over t between t and 0, we obtain the expression followed by $y(t,T)$

$$\begin{aligned} y(t,T) = y(0,T) + \int_0^t \mu_y(u,T)du + \int_0^t \sqrt{v_u}\sigma_y(u,T)dW_u^y - \lambda\int_0^t E_u^{\mathbb{Q}}\left[J_y(u,T)\right]du \\ + \int_0^t J_y(u,T)dN_u, \end{aligned} \tag{1A.11}$$

and substituting T for t into (1A.11) yields the expression followed by y_t

$$y_t = y(0,t) + \int_0^t \mu_y(u,t)du + \int_0^t \sqrt{v_u}\sigma_y(u,t)dW_u^y - \lambda \int_0^t E_u^{\mathbb{Q}}\left[J_y(u,t)\right]du + \int_0^t J_y(u,t)dN_u. \tag{1A.12}$$

For all $0 \le s \le t$, we consider the following state variables χ_t and ϕ_t

$$\chi_t = e^{-\gamma(t-s)}\chi_s - \int_s^t v_u\Big(\frac{\alpha}{\gamma} + \sigma_S\rho_{Sy}\Big)e^{-\gamma(t-u)}du + \int_s^t \sqrt{v_u}e^{-\gamma(t-u)}dW_u^y, \tag{1A.13}$$

$$\phi_t = e^{-2\gamma(t-s)}\phi_s + \int_s^t v_u\frac{\alpha}{\gamma}e^{-2\gamma(t-u)}du, \tag{1A.14}$$

which dynamics are obtained by applying Itô's Lemma to (1A.13) and (1A.14) and subject to $\phi_0 = \chi_0 = 0$

$$d\chi_t = -\Big(\gamma\chi_t + v_t\Big(\sigma_S\rho_{Sy} + \frac{\alpha}{\gamma}\Big)\Big)dt + \sqrt{v_t}dW_t^y, \tag{1A.15}$$

$$d\phi_t = \Big(v_t\frac{\alpha}{\gamma} - 2\gamma\phi_t\Big)dt. \tag{1A.16}$$

Then, (1A.11) and (1A.12) are affine jump-diffusion functions of χ_t, ϕ_t and the jump-related terms

$$y(t,T) = y(0,T) + \sigma_y(t,T)\chi_t + \frac{\sigma_y^2(t,T)}{\alpha}\phi_t - \lambda\int_0^t E_u^{\mathbb{Q}}\left[J_y(u,T)\right]du + \int_0^t J_y(u,T)dN_u, \tag{1A.17}$$

$$y_t = y(0,t) + \alpha\left(\chi_t + \phi_t\right) - \lambda\int_0^t E_u^{\mathbb{Q}}\left[J_y(u,t)\right]du + \int_0^t J_y(u,t)dN_u. \tag{1A.18}$$

1A.3 Proof of Proposition 1.3

Integrating the expression followed by ds_t in (1A.8) and after applying exponentials, we have

$$S_t = S_0\exp\left\{\int_0^t \Big(y_u - \frac{\sigma_S^2}{2}v_u - \lambda E_u^{\mathbb{Q}}\left[e^{J_S}-1\right]\Big)du + \sigma_S\int_0^t \sqrt{v_u}dW_u^S + J_S\int_0^t dN_u\right\}. \tag{1A.19}$$

From equations (1.6), (1.11) and (1.15), we have that the futures price $F(t,T)$ is given by

$$\begin{aligned}
F(t,T) &= S_t\exp\left\{\int_t^T\Big(y(0,u) + \sigma_y(t,u)\chi_t + \frac{\sigma_y^2(t,u)}{\alpha}\phi_t - \lambda\int_0^t E_s^{\mathbb{Q}}\left[J_y(s,u)\right]ds\Big)du\right\} \\
&\quad \times\exp\left\{\int_t^T\int_0^t J_y(s,u)dN_s du\right\} \\
&= S_t\frac{F(0,T)}{F(0,t)}\exp\left\{\sigma_Y(t,T)\chi_t + \frac{\hat\sigma_Y(t,T)}{\alpha}\phi_t - \lambda\int_0^t E_u^{\mathbb{Q}}\left[J_Y(u,T)\right]du + \int_0^t J_Y(u,T)dN_u\right\} \\
&= S_0\frac{F(0,T)}{F(0,t)}\exp\left\{\sigma_Y(t,T)\chi_t + \frac{\hat\sigma_Y(t,T)}{\alpha}\phi_t + \int_0^t\Big(y_u - \frac{\sigma_S^2}{2}v_u\Big)du + \sigma_S\int_0^t\sqrt{v_u}dW_u^S\right\} \\
&\quad \exp\left\{-\lambda\int_0^t E_u^{\mathbb{Q}}\left[e^{J_S} + J_Y(u,T) - 1\right]du + \int_0^t\big(J_S + J_Y(u,T)\big)dN_u\right\},
\end{aligned} \tag{1A.20}$$

with

$$\hat{\sigma}_Y(t,T) \equiv \int_t^T \sigma_y^2(t,u)du = \frac{\alpha^2}{2\gamma}\left(1 - e^{-2\gamma(T-t)}\right). \tag{1A.21}$$

It is convenient to use $s_t \equiv \ln S_t$ instead of S_t as a state variable. In this case, the log futures prices $f(t,T) \equiv \ln F(t,T)$ are an affine jump-diffusion function of the following for state variables χ_t, ϕ_t, s_t and the jump-related terms

$$\begin{aligned} f(t,T) = s_t + f(0,T) - f(0,t) + \sigma_Y(t,T)\chi_t + \frac{\hat{\sigma}_Y(t,T)}{\alpha}\phi_t + \int_0^t \left(y_u - \frac{\sigma_S^2}{2}v_u\right)du \\ + \sigma_S \int_0^t \sqrt{v_u}dW_u^S - \lambda \int_0^t E_u^{\mathbb{Q}}\left[e^{J_S} + J_Y(u,T) - 1\right]du + \int_0^t \left(J_S + J_Y(u,T)\right)dN_u. \end{aligned} \tag{1A.22}$$

Rewriting equation (1A.22) in its integral form lets us see the evolution of the price of a futures contract

$$\begin{aligned} F(t,T) = F(0,T)\times \\ \exp\left\{\int_0^t \left(\sqrt{v_u}\left(\sigma_S dW_u^S + \sigma_Y(u,T)dW_u^y\right) - \frac{v_u}{2}\left(\sigma_S dW_u^S + \sigma_Y(u,T)dW_u^y\right)^2\right)du\right\} \\ \exp\left\{-\lambda\int_0^t E_u^{\mathbb{Q}}\left[e^{J_S} + J_Y(u,T) - 1\right]du + \int_0^t \left(e^{J_S + J_Y(u,T)} - 1\right)dN_u\right\}, \end{aligned} \tag{1A.23}$$

which shows that $F(t,T)$ and $F(t,t) \equiv S_t$ are Markov in a finite number of state variables.

1A.4 Proof of Proposition 1.4

We find the expressions followed by the terms $A(\tau), B(\tau)$ and $C(\tau)$ similarly to Duffie et al. (2000). The proof consists of showing that the CF $\psi(t) \equiv \psi(iu, t, T_{Opt}, T)$ is a martingale under $\mathbb{Q}$. To this end, we conjecture that $\psi(iu, t, T_{Opt}, T)$ is of the form in expression (1.17). From applying Itô's Lemma for jump diffusion processes to $\psi(t)$, we obtain the following PIDE

$$\begin{aligned} \frac{d\psi(t)}{\psi(t)} = \left(-\frac{\partial A(\tau)}{\partial \tau} - \frac{\partial B(\tau)}{\partial \tau}v_t - \frac{\partial C(\tau)}{\partial \tau}\lambda\right)dt + B(\tau)dv_t + iu\frac{dF(t,T)}{F(t,T)} + \frac{B^2(\tau)}{2}dv_t^2 \\ - \frac{u^2 + iu}{2}\left(\frac{dF(t,T)}{F(t,T)}\right)^2 + iuB(\tau)dv_t\frac{dF(t,T)}{F(t,T)} + \lambda\int_{-\infty}^{+\infty}[\psi(t,J) - \psi(t)]\varpi(J)\,dN_t, \end{aligned} \tag{1A.24}$$

where $\tau \equiv T_{Opt} - t$, $J \equiv J_S + J_y(t,T)$ is the jump size, $\varpi(J)$ is the distribution function of the random variable J, and $\lambda > 0$ is the constant intensity parameter of the Poisson process N_t. Based on the fact that the jump size J is independent of $f(t,T)$, we consider the jump integral term in (1A.24)

$$\int_{-\infty}^{+\infty} [\psi(t,J) - \psi(t)]\, \varpi(J)\, dN_t = \int_{-\infty}^{+\infty} \Big(E_t^{\mathbb{Q}}[e^{iu(f(t,T)+J)}] - E_t^{\mathbb{Q}}[e^{iuf(t,T)}]\Big)\, \varpi(J)\, dN_t$$
$$= \int_{-\infty}^{+\infty} E_t^{\mathbb{Q}}[e^{iuf(t,T)}] E_t^{\mathbb{Q}}[e^{iuJ} - 1] \varpi(J)\, dN_t$$
$$= n_{a_j b_j}(\tau) - iu\, m_{a_j b_j}(\tau). \tag{1A.25}$$

For $\psi(t)$ to be a martingale, it must hold that

$$\frac{1}{dt} E_t^{\mathbb{Q}} \left[\frac{d\psi_t}{\psi_t}\right] = \Big(-\frac{\partial A(\tau)}{\partial \tau} + B(\tau)\kappa\theta\Big) + \Big(-\frac{\partial C(\tau)}{\partial \tau} + n_{a_j b_j}(\tau) - iu\, m_{a_j b_j}(\tau)\Big)\lambda$$
$$+ \Big(-\frac{\partial B(\tau)}{\partial \tau} + b_0 + B(\tau) b_1 + B^2(\tau) b_2\Big) v_t = 0, \tag{1A.26}$$

with b_0, b_1 and b_2 as in (1.21) and subject to the initial conditions $A(0) = B(0) = C(0) = 0$. Since equation (1A.26) holds for all t, $f(t,T)$, v_t and λ, then the terms in each parentheses must vanish, reducing the problem to solving three much simpler ODEs

$$\frac{\partial A(\tau)}{\partial \tau} = B(\tau)\kappa\theta, \tag{1A.27}$$
$$\frac{\partial B(\tau)}{\partial \tau} = b_0 + B(\tau) b_1 + B^2(\tau) b_2, \tag{1A.28}$$
$$\frac{\partial C(\tau)}{\partial \tau} = n_{a_j b_j}(\tau) - iu\, m_{a_j b_j}(\tau), \tag{1A.29}$$

for $j = 1, 2$ and following the jump assumptions listed in Subsection 1.2.1. The expressions followed by the terms $n_{a_1 b_1}, n_{a_2 b_2}, m_{a_1 b_1}$ and $m_{a_2 b_2}$ are in Table 1.5.

1B Appendix for Analytic Expressions

1B.1 Analytic Expression for $B(\tau)$

We apply the following change of variable $B(\tau) = -\frac{y'(\tau)}{y(\tau) d_2(\tau)}$ to (1.19) so that it becomes

$$\Big(-\frac{y'(\tau)}{y(\tau) b_2}\Big)' = b_0(\tau) + b_1(\tau)\Big(-\frac{y'(\tau)}{y(\tau) b_2}\Big) + b_2\Big(-\frac{y'(\tau)}{y(\tau) b_2}\Big)^2. \tag{1B.1}$$

Given that b_2 is constant, it simplifies and we get the following homogeneous second order ODE

$$y''(\tau) - \big(c_0(\tau) + c_1(\tau) e^{-\gamma\tau}\big) y'(\tau) + \big(d_0(\tau) + d_1(\tau) e^{-\gamma\tau} + d_2(\tau) e^{-2\gamma\tau}\big) y(\tau) = 0. \tag{1B.2}$$

Equation (1.19) has an analytical solution which is given by

$$B(\tau) = \frac{2\gamma}{\sigma_v^2}\Big(\beta + \mu z + z\frac{g'(z)}{g(z)}\Big), \tag{1B.3}$$

where the function $g(z)$ is a linear combination of Kummer's (M) and Tricomi's (U) hypergeometric functions

$$g(z) = k_1 M(a,b,z) + k_2 U(a,b,z), \tag{1B.4}$$
$$g'(z) = \frac{a}{b} k_1 M(a+1,b+1,z) - a k_2 U(a+1,b+1,z), \tag{1B.5}$$

with coefficients

$$\begin{aligned} a &= -\mu b - \beta c_1 \frac{\omega}{\gamma} - d_1 \frac{\omega}{\gamma^2}, & b &= 1 + 2\beta + \frac{c_0}{\gamma}, \\ \mu &= -\frac{1}{2}\Big(1 + \frac{c_1 \omega}{\gamma}\Big), & \beta &= \frac{-c_0 \pm \sqrt{c_0^2 - 4d_0}}{2\gamma}, \\ \omega &= \pm \frac{\gamma}{\sqrt{c_1^2 - 4d_2}}, & z &= \frac{e^{-\gamma\tau}}{\omega}, \end{aligned} \tag{1B.6}$$

and

$$\begin{aligned} c_0 &= -\kappa + iu\sigma_v \Big(\rho_{Sv}\sigma_S + \rho_{yv}\frac{\alpha}{\gamma}\Big), & d_0 &= -\frac{\sigma_v^2(u^2+iu)}{4}\Big(\sigma_S^2 + \frac{\alpha^2}{\gamma^2} + 2\sigma_S\rho_{Sy}\frac{\alpha}{\gamma}\Big), \\ c_1 &= -iu\sigma_v\rho_{yv}\frac{\alpha}{\gamma} e^{-\gamma(T-T_{Opt})}, & d_1 &= +\frac{\sigma_v^2(u^2+iu)}{2}\frac{\alpha}{\gamma}\Big(\frac{\alpha}{\gamma} + \rho_{Sy}\sigma_S\Big) e^{-\gamma(T-T_{Opt})}, \\ & & d_2 &= -\frac{\sigma_v^2(u^2+iu)}{4}\frac{\alpha^2}{\gamma^2} e^{-2\gamma(T-T_{Opt})}. \end{aligned} \tag{1B.7}$$

In particular, if the initial condition is $B(0) = 0$, we have

$$\begin{aligned} k_1 &= \frac{-\beta\omega - \mu + a\frac{U(a+1,b+1,\frac{1}{\omega})}{U(a,b,\frac{1}{\omega})}}{\frac{a}{b}M(a+1,b+1,\frac{1}{\omega}) + aM(a,b,\frac{1}{\omega})\frac{U(a+1,b+1,\frac{1}{\omega})}{U(a,b,\frac{1}{\omega})}}, \\ k_2 &= \frac{1 - k_1 M(a,b,\frac{1}{\omega})}{U(a,b,\frac{1}{\omega})}. \end{aligned} \tag{1B.8}$$

The proof is in Sitzia (2018).

1B.2 Analytic Expression for the Alternative $B(\tau)$

Given that $\sigma_S = 0$ and $\rho_{yv} = \rho_{Fv}$, and alternatively to the expressions in (1B.7), the coefficients in $g(z)$ and $g'(z)$ become

$$\begin{aligned} c_0 &= -\kappa + iu\sigma_v\rho_{Fv}\frac{\alpha}{\gamma}, & d_0 &= -\frac{\sigma_v^2(u^2+iu)}{4}\frac{\alpha^2}{\gamma^2}, \\ c_1 &= -iu\sigma_v\rho_{Fv}\frac{\alpha}{\gamma} e^{-\gamma(T-T_{Opt})}, & d_1 &= +\frac{\sigma_v^2(u^2+iu)}{2}\frac{\alpha^2}{\gamma^2} e^{-\gamma(T-T_{Opt})}, \\ & & d_2 &= -\frac{\sigma_v^2(u^2+iu)}{4}\frac{\alpha^2}{\gamma^2} e^{-2\gamma(T-T_{Opt})}. \end{aligned} \tag{1B.9}$$

The expressions followed by a, b, μ, β, ω and z remain as in (1B.6) under the original set-up.

CHAPTER

2

Seasonality in Commodity Prices: New Approaches for Pricing Plain Vanilla Options

Abstract[1]

In this work we present a new term-structure model for commodity futures prices based on Trolle & Schwartz (2009), which we extend by incorporating seasonal stochastic volatility represented with two different sinusoidal expressions. We obtain a quasi-analytical representation of the characteristic function of the futures log-prices and closed-form expressions for standard European options' prices using the fast Fourier transform (FFT) algorithm. We price plain vanilla options on Henry Hub natural gas futures contracts, using our model and extant models. We obtain higher accuracy levels with our model than with the extant models.

[1]Co-author: Viviana Fanelli, University of Bari "Aldo Moro". This chapter refers to an article which is currently under review at the journal Annals of Operations Research. It can be found at SSRN (id=3944647).

2.1 Introduction

Over the last few years, natural gas has become one of the most utilised energy sources worldwide, second only to oil and coal, and is expected to overtake the latter by 2030. Natural gas is used to fuel electricity power plants, as well as industrial, commercial and domestic cooking and heating.

The countries with the largest production of natural gas are currently the United States, Russia, Iran, Qatar, Canada, China and Norway. All of these countries serve their domestic markets, and export excess around the world through pipelines or as liquefied natural gas. The demand for natural gas is very high in western Europe, north America and north Asia, where it is satisfied through dense pipeline networks.

The foremost global trading center is the Henry Hub (HH hereafter), located in the US. The HH is strategically situated in the state of Louisiana, a major onshore production region and close to offshore production. It is also connected to storage facilities, interstate and intrastate pipeline systems; therefore, its production can be easily moved from supply basins and exported to major consumption markets. These features make the HH the dominant global reference price for natural gas, especially for futures contracts.

Gas production in the US is steadily increasing, while gas storage level also plays a key role when looking at supply side. During periods of lower demand, production surplus can be injected into storage facilities in the form of liquefied natural gas, which can later provide a valuable cushion to meet demand peaks. However, liquefied natural gas storage can be utilised to meet sudden demand increase or decrease only up to a point. Natural gas supply is always affected by a relatively wide range of prices. Restrictions in the existing gas infrastructure impact additional flows, rendering the supply curve very inelastic when prices are high. Overall economic growth, weather and competing fuel prices are also significant factors in natural gas demand.

Major demand-side players include: (i) industrial organisations which use it to produce electricity due to its low price relative to coal, and as raw material to produce fertiliser, chemicals and hydrogen; (ii) transportation consumers using liquefied natural gas as vehicle fuel; (ii) industrial, commercial and domestic consumers using it as fuel for heating and in some cases cooling.

Weather is the main factor in natural gas price evolution, leading to seasonal price behaviour and stochastic volatility. During the northern hemisphere's fall and winter seasons, gas prices are higher due to increased demand for heating, and it is very volatile. In northern spring and summer, gas demand decreases, but production continues, as excess can be stored as liquefied natural gas, thus exhibiting less variability during this period. Considering the cyclical behaviour of natural gas prices is key to predict winter demand; therefore winter futures typically trade at a premium compared to summer ones. Understanding the seasonality in natural gas markets and the potential impact on its prices is useful for researchers and practitioners in the field of trading strategies.

The aim of our paper is to find a suitable model for pricing natural gas in the spot and futures markets, incorporating stochastic cost of carry and seasonal stochastic volatility. In this perspective, we review a great deal of literature on spot and futures models. In Table 2.1 we list the models for spot and futures prices we comment in this section in order to get a meaningful framework of the existing models and highlight the gap in the literature we fill with our work. Within it, we indicate what stochastic factors, volatility type and jumps they present, as well as the number of parameters included. In addition, we reference Fanelli (2020) to provide a concise survey of arbitrage pricing models for commodities.

In Black & Scholes (1973) (**BS73**) the spot price is modeled through a geometric Brownian motion. Merton (1976) (**Mer76**) defines the spot dynamics by using a stochastic process which includes iid jumps. Heston (1993) (**Hes93**) proposes a model with stochastic volatility for pricing contracts on spot prices. And Bates (1996) (**Bat96**) uses a combination of stochastic volatility and jump-diffusion processes for modeling spot prices when jump and volatility risks are systematic and non-diversifiable.

Geman & Nguyen (1995) (**GN95**) assume that the spot price is the sum of two components: one being seasonal and deterministic and the other stochastic and mean-reverting. Developing two- and three-state variable models, they obtain futures prices is through the classical spot-forward price relationship. Clewlow & Strickland (1999b) (**CS99b**) propose a one-factor model with a time-decaying volatility of the forward prices using two parameters, and Clewlow & Strickland (1999a) (**CS99a**) proposes the correspondent multi-dimensional model to Clewlow & Strickland (1999b). The main strength of Clewlow & Strickland (1999a) is that it develops a framework consistent with the market observable forward price curve as well as with the volatilities and correlations of forward prices. Clewlow & Strickland (2000) (**CS00**) add a long-term volatility parameter to the latter. In Sørensen (2002) (**Sor02**), commodity prices are modeled as a sum of a deterministic seasonal component, a non-stationary state-variable, and a stationary state-variable. Futures prices are established by standard no-arbitrage arguments. Under the risk-neutral probability measure, Lucia & Schwartz (2002) (**LS02**) propose one- and two-factor models for spot prices, and then a sinusoidal function to capture the seasonal behaviour of the futures curve directly implied in the spot price dynamics. Richter & Sørensen

(2002) (**RS02**) estimate a continuous-time stochastic volatility model for spot prices, reflecting seasonality patterns in both the spot price and the volatility.

Trolle & Schwartz (2009) (**TS09**) develop a parsimonious and highly tractable model for pricing commodity derivatives in the presence of unspanned stochastic volatility. They use two factors to model the movements of the future prices under the risk-neutral probability measure, the spot price and the forward cost of carry curve, and one or two variance factors to frame their three- and four-factor model specification, namely SV1 or SV2. They then obtain an affine model for futures curves and price standard American options on crude oil.

Back, Prokopczuk, Paschke & Rudolf (2013) (**BPP13**) propose one- and two-factor models for the logarithm of the spot price, which shows a seasonal pattern. In particular, the spot price is composed by two stochastic components which are mean-reverting and have seasonal volatility, and an additional seasonal component. The forward dynamics is obtained by applying the spot-forward price relationship. Arismendi, Back, Prokopczuk, Paschke & Rudolf (2016) (**ABP16**) model the futures price under the risk-neutral measure where the instantaneous variance of futures returns is described through a mean-reverting square-root process, where the long-term parameter is seasonal.

Fanelli, Maddalena & Musti (2016) (**FMM16**) considers a seasonal path-dependent volatility for electricity futures returns in the trading date, which is modeled following the Heath, Jarrow & Morton (1992) framework, and they obtain the dynamics of futures prices. Fanelli & Schmeck (2019) (**FS19**) focuses on the seasonality found in the implied volatility of electricity option prices in the delivery period.

Schneider & Tavin (2018) (**ST18**) propose a multi-factor stochastic volatility model for commodity futures contracts, with an expiry-dependent volatility term. This model is able to capture the Samuelson volatility effect. Schneider & Tavin (2021) (**ST21**) extend their previous model by incorporating a seasonal mean-reverting level in the variance (they propose five different expressions for this seasonal component).

We propose a three-factor model which we refer to as **SYSSV**[2] for futures prices with three stochastic factors: the spot price, the cost of carry curve and the instantaneous variance. The variance follows a mean-reverting square-root process which incorporates the seasonality in its long-run mean-reversion level. We obtain the futures prices in the original framework and also propose an alternative characterisation or set-up of the parameters. We price standard European options on HH natural gas futures contracts, with maturities ranging from approximately one to two months up to one year. Our benchmark model is the three-factor version of TS09, which on average we outperform slightly. However, a more granular analysis evidences that our model

[2]SYSSV stands for Stochastic cost of carry curve $Y(t,T)$ and Seasonal Stochastic Volatility v_t.

clearly outperforms the benchmark for short maturities and deep OTM (ATM and close to the ATM) options under the original (alternative) set-up. In particular and for montly observations, gains in model performance hit 1.74% when the set-up is the original and 3.53% when the set-up is the alternative. Our model also outperforms ST21 especially for the short maturities and deeper OTM put contracts, hitting a gain of a 3.13% (alternative set-up and simple harmonic pattern). An additional benefit provided by the alternative set-up is that the calibration is much quicker.

The remainder of this article is structured as follows: in Section 2.2 we present a novel model formulation based on the unspanned stochastic volatility model of TS09, which we extend by introducing seasonality in the variance, and we derive the correspondent characteristic function of the futures prices; in Section 2.3 we obtain the expression followed by standard European call and put options by means of the fast Fourier transform algorithm; in Section 2.4 we describe how we perform the parameter estimation; in Section 2.5 we comment our model's results and those of other extant ones that are well known in the literature; and in Section 2.6 we present our conclusions and indicate future lines of research.

2.2 A New Three-Factor Model for Futures Prices on Commodities

In this work we derive a futures-based model which can exactly match any given futures curve by specifying the futures initial values without incorporating any of the other model parameters. It fits the initial futures curve by construction, which means that the seasonality in prices is already incorporated. Moreover, our model is term-structured, presenting a seasonality pattern in the dynamics of the futures variance. This new element affects the option pricing but not the expression followed by the expected value of the futures prices.

In this section we formalise the dynamics of the futures prices in our novel model specification, compute the corresponding characteristic function, and indicate the technical conditions under which the dynamics of the variance factor are defined. Let S_t denote the time-t spot price of the commodity, and let $y(t,T)$ denote the time-t instantaneous forward cost of carry maturing at time T, with $y(t,t) = y_t$ the time-t instantaneous spot cost of carry. We model the evolution of the entire futures curve by specifying one process for S_t and another process for $y(t,T)$. Also, let v_t denote the instantaneous variance, which follows a mean-reverting process as in Cox, Ingersoll & Ross (1985).

2.2.1 The Model Under the Risk-Neutral Measure $\mathbb{Q}$

Consider the following three-factor model. Let $(\Omega, \mathcal{F}, \mathbb{Q})$ be a probability space on which three Brownian motion processes, W_t^S, W_t^y and W_t^v, are defined for all $0 \leq t \leq T$. Let $\mathcal{F}$ be the filtration generated by these Brownian motions. The absence of arbitrage implies the existence of a risk-neutral or equivalent martingale measure $\mathbb{Q}$ under which the processes followed by $S_t, y(t,T)$ and v_t are governed by the following dynamics

$$\frac{dS_t}{S_t} = y_t dt + \sigma_S \sqrt{v_t}\, dW_t^S, \tag{2.1}$$

$$dy(t,T) = \mu_y(t,T)dt + \sigma_y(t,T)\sqrt{v_t}\, dW_t^y, \tag{2.2}$$

$$dv_t = \kappa\left(\theta_t - v_t\right) dt + \sigma_v \sqrt{v_t}\, dW_t^v, \tag{2.3}$$

with $S_t, v_t > 0$, and allowing W_t^S, W_t^y and W_t^v to be correlated with ρ_{Sy}, ρ_{Sv} and ρ_{yv}, which denote pairwise correlations. θ_t is the time-varying long-run mean-reversion variance level. The volatility of the spot price S_t is represented by σ_S, the volatility of the variance v_t is represented by σ_v, and the volatility of the forward cost of carry curve $y(t,T)$, which we assume that follows a time-dampening form, is represented by

$$\sigma_y(t,T) \equiv \alpha e^{-\gamma(T-t)}, \tag{2.4}$$

with $\sigma_S, \sigma_v, \kappa, \theta_t, \alpha$ and $\gamma > 0$.

This novel model formulation consists of an expansion of the three-factor model specification of TS09 with seasonal stochastic volatility (SSV hereafter). This seasonality is captured in the deterministic expression followed by θ_t, which particular form we address in Section 2.2.1.

Volatility in (2.4) reflects the so-called Samuelson effect, which describes an empirical observation of the variations in futures prices increasing as the expiration date gets closer (see also Samuelson (1965)).[3] Figure 2.2a shows the time dependency for the implied volatilities in the HH natural gas market. These volatilities are grouped by the contracts' maturity month and then averaged. An inverse time-dependent pattern can be clearly observed in the data, providing evidence of the Samuelson effect in this market.

[3] This applies for a fixed maturity. Similarly, this effect can be seen in the futures variations which are, on a fixed date, higher for those contracts with longer maturities. When t approaches T, the term converges to 1 and the full volatility enters the dynamics. On the contrary, the volatility decreases when the time to maturity increases. This approach is typically captured with a term-structure alteration in the diffusion of the futures dynamics of the form followed by $\sigma_y(t,T)$ in expression (2.4).

Seasonality Specifications

In Hylleberg (1992), the seasonality is defined as "...the systematic, although not necessarily regular, intra-year movement caused by the changes of the weather, the calendar, and timing of decisions, directly or indirectly through the production and consumption decisions made by agents of the economy. These decisions are influenced by endowments, the expectations and preferences of the agents, and the production techniques available in the economy." Several models incorporate SSV in the trading date t, such as GN95, RS02, ABP16, FMM16 and ST21. The first two are spot models which explicitly present seasonality in prices and variance; the last three are term-structure models which implicitly incorporate it in prices, explicitly in the variance. Other models such as FS19 explicitly present it in the variance in the delivery period rather than in the trade date, which is reasonable in electricity markets.

As indicated in BPR13, implied volatilities in option prices reflect how market participants assess the future volatility pattern. In Figure 2.2b we show the seasonality for the quoted volatilities in the HH natural gas market. These volatilities are grouped by the options' trade month and then averaged. A trigonometric function describes the seasonal pattern in implied volatilities with reasonable accuracy. Thus we present two seasonality functions for θ_t that can be used as parametric forms to model seasonal variations of futures prices's volatility. These functions are deterministic and work with the following parameters: $a^\theta > 0$; $b^\theta, c^\theta \neq 0$ and $t_0 \in [0, 1[$. The parameter a^θ determines the basic volatility level, b^θ and c^θ govern the magnitude of the seasonality pattern, and t_0 refers to the time of the year when the volatility reaches its maximum. The simple (S) and multiple (M) harmonic expressions are defined as follows

$$\theta_t^S \equiv a^\theta + b^\theta \cos\big(2\pi(t - t_0)\big), \tag{2.5}$$

$$\theta_t^M \equiv a^\theta + b^\theta \cos\big(2\pi(t - t_0)\big) + c^\theta \sin\big(2\pi(t - t_0)\big), \tag{2.6}$$

which are continuous functions, differentiable everywhere and spend the same amount of time low and high.

Using the property of complementary angles, adapting the expression followed by θ_t^S in (2.5) is straightforward in terms of using the sinus instead of the cosinus of the angle.[4] With regards to the combined harmonic expression, the expression followed by θ_t^M in (2.6) is inspired in Rogel-Salazar & Sapsford (2014).

The specification followed by the variance dynamics can only guarantee the positiveness of the factor at all times if the Feller condition is met.[5] In our model, the sufficient condition to

[4] By adding $3/12$ to the value of t_0.

[5] In Hes93, the parameters obey that $2\kappa\theta > \sigma_v^2$, which is when the values of v_t are strictly positive. We also consider this restriction is met in all other multi-factor models analysed in this work.

enforce the positivity of the variance is $2\kappa(a^{\theta} - b^{\theta}) > \sigma_v^2$ for the simple harmonic expression.[6]

In Figure 2.3 we can observe futures prices and options volatilities for seven HH natural gas contracts labeled M2-M8, spanning from January 2011 to December 2020. Sub-figure 2.3a represents the time series for futures prices and Sub-figure 2.3b represents the ATM call option volatilities. In Figure 2.4 we refer to the same futures contracts previously described; in Sub-figure 2.4a we plot the futures' returns, and in Sub-figure 2.4b we represent the histogram of frequencies assigned to these returns. Directly related to what we can observe in this figure, Table 2.2 provides evidence of the non-Gaussian returns by rejecting the null hypothesis of normal prices returns by means of the Jarque-Bera test, applicable to each contract individually and all contracts taken together.

We also want to highlight the importance of distinguishing between choosing a jump model or a model presenting seasonality, when returns are non-Gaussian. A detailed analysis of the data set has to lead us to correctly and realistically pick the type of model which best matches the features of each particular asset.

Futures Dynamics

In this section we present a novel formulation for the futures' dynamics, which consists of an extension of TS09-SV1 that includes SSV. The form followed by this seasonality is inspired in the work of FS19 and ST21.

Let $F(t,T)$ denote the time-t price of a futures contract that matures at time T. By definition we have

$$F(t,T) \equiv S_t e^{\int_t^T y(t,u)du} = S_t e^{Y(t,T)} \tag{2.7}$$

with dynamics of S_t and $y(t,T)$ as in equations (2.1) and (2.2). In absence of arbitrage opportunities, the process followed by $F(t,T)$ must be a martingale under the risk-neutral measure $\mathbb{Q}$ (see Duffie (2001)). We define $f(t,T) \equiv \ln F(t,T)$, with $F(0,T) > 0$, $f(0,T) \neq 0$. As observed in TS09, from applying Itô's Lemma to the futures price in equation (2.7) and setting the drift to zero, it follows that the dynamics of $F(t,T)$ and $f(t,T)$, and the accumulated volatility of $y(t,T)$ are given by

$$\frac{dF(t,T)}{F(t,T)} = \sqrt{v_t}\Big(\sigma_S dW_t^S + \sigma_Y(t,T)dW_t^y\Big), \tag{2.8}$$

$$df(t,T) = \sqrt{v_t}\Big(\sigma_S dW_t^S + \sigma_Y(t,T)dW_t^y\Big) - \frac{v_t}{2}\Big(\sigma_S^2 + \sigma_Y^2(t,T) + 2\rho_{Sy}\sigma_S\sigma_Y(t,T)\Big)dt, \tag{2.9}$$

$$\sigma_Y(t,T) \equiv \int_t^T \sigma_y(t,u)du = \frac{\alpha}{\gamma}\left(1 - e^{-\gamma(T-t)}\right). \tag{2.10}$$

[6] For the multiple harmonic expression, the condition depends on the minimum value achieved by a combination of the sinus and cosinus functions, reaching their minimum in different points.

We define the futures dynamics based on firstly describing the dynamics of the spot price and the forward cost of carry curve, to then modify the diffusion term in the futures dynamics accordingly by introducing the accumulated volatility expression instead; that is, $\sigma_Y(t,T)$ in expression (2.10). Our model for futures prices is then defined by equations (2.8) and (2.3). Rewriting the dynamics in equations (2.8) and (2.9) in their integral form time 0 up to time $t \leq T$ lets us see the evolution of the futures prices and log-prices

$$F(t,T) = F(0,T)\exp\left\{\int_0^t \left(\sqrt{v_u}(\sigma_S dW_u^S + \sigma_Y(u,T)dW_u^y) - \frac{v_u}{2}(\sigma_S dW_u^S + \sigma_Y(u,T)dW_u^y)^2\right)du\right\}, \tag{2.11}$$

$$f(t,T) = f(0,T) + \int_0^t \left(\sqrt{v_u}(\sigma_S dW_u^S + \sigma_Y(u,T)dW_u^y) - \frac{v_u}{2}(\sigma_S dW_u^S + \sigma_Y(u,T)dW_u^y)^2\right)du. \tag{2.12}$$

Following (Crosby & Frau 2021, Sec. 3), we refer to this set-up as the original set-up of the parameters, where the expressions are defined in terms of S_t and $y(t,T)$: σ_S, $\sigma_Y(t,T)$, ρ_{Sy}, ρ_{Sv} and ρ_{vy}.

Alternative Characterisation of the Parameters

As initially indicated at the beginning of Sub-section 2.2.1 and shown in Sub-figure 2.2a, evidence[7] supports considering that the volatility of the futures $\sigma_f(t,T)$ follows a time-dampening form such as

$$\sigma_f(t,T) = \alpha_0 + \alpha e^{-\gamma(T-t)}. \tag{2.13}$$

Therefore, the expression which describes the volatility of the futures dynamics is

$$\sigma_F(t,T) \equiv \int_t^T \sigma_f(t,u)du = \alpha_0(T-t) + \frac{\alpha}{\gamma}\left(1 - e^{-\gamma(T-t)}\right). \tag{2.14}$$

This leads to more compact expressions defining the dynamics of the futures prices and log-prices

$$\frac{dF(t,T)}{F(t,T)} = \sqrt{v_t}\sigma_F(t,T)dW_t^F, \tag{2.15}$$

$$df(t,T) = \sqrt{v_t}\sigma_F(t,T)dW_t^F - \frac{1}{2}v_t\sigma_F^2(t,T)dt. \tag{2.16}$$

[7] We refer again to the so-called Samuelson effect, see Samuelson (1965). Recent works incorporating this stylised fact are BPR13 and ST18, among others.

Rewriting the dynamics in equations (2.15) and (2.16) in their integral form from time 0 up to time $t \leq T$ lets us see the evolution of the futures prices and log-prices

$$F(t,T) = F(0,T)\exp\Big\{\int_0^t \sqrt{v_u}\sigma_F(u,T)dW_u^F - \frac{1}{2}\int_0^t v_u\sigma_F^2(u,T)du\Big\}, \tag{2.17}$$

$$f(t,T) = f(0,T) + \int_0^t \sqrt{v_u}\sigma_F(u,T)dW_u^F - \frac{1}{2}\int_0^t v_u\sigma_F^2(u,T)du. \tag{2.18}$$

Following (Crosby & Frau 2021, Sec. 3), we refer to this set-up as the alternative characterisation of the parameters, where the expressions are defined in terms of $F(t,T)$. TS09-SV1 needs only 7 parameters instead of the original 9

$$\Phi^{\checkmark} \equiv \{\sigma_S, \alpha, \gamma, \kappa, \theta, \sigma_v, \rho_{Sy}, \rho_{Sv}, \rho_{yv}\},$$
$$\Phi^{\star} \equiv \{\alpha_0, \alpha, \gamma, \kappa, \theta, \sigma_v, \rho_{Fv}\},$$

whereas our model needs up to 8-9 instead of the original 10-11, depending on the expression chosen for θ_t

$$\Phi^{\checkmark} \equiv \{\alpha_0, \alpha, \gamma, \kappa, a^\theta, b^\theta, (c^\theta), \sigma_v, \rho_{Sy}, \rho_{Sv}, \rho_{yv}\},$$
$$\Phi^{\star} \equiv \{\sigma_S, \alpha, \gamma, \kappa, a^\theta, b^\theta, (c^\theta), \sigma_v, \rho_{Fv}\}.$$

Therefore, our model is capable of replicating values generated with the original set-up using two parameters less, which makes calibration much quicker as can be observed in Table 2.8.

2.2.2 Deriving the Characteristic Function

Options on natural gas expire (T_{Opt}) one business day before the expiration date of the underlying futures contract T, that is, $T_{Opt} = T - 1/252$. The Fourier transform for the time-t standard European option price can be expressed in terms of the characteristic function (CF hereafter) $\psi(iu, t, T_{Opt}, T)$, so it can be obtained by applying the Fourier inversion theorem. To price options on futures we introduce the transform

$$\psi(iu; t, T_{Opt}, T) \equiv E_t^{\mathbb{Q}}[e^{iuf(T_{Opt},T)}], \tag{2.19}$$

with futures log-price dynamics as in equations (2.9) for the original set-up or (2.16) for the alternative one. We define $\tau \equiv T_{Opt} - t$. The transform (2.19) has an exponential affine solution as demonstrated in the following proposition:

Proposition 2.1 *The Fourier transform in equation (2.19) is given by*

$$\psi(iu; t, T_{Opt}, T) = e^{A(\tau)+B(\tau)v_t+iuf(t,T)}. \tag{2.20}$$

$A(\tau)$ and $B(\tau)$ solve the following system of ODEs

$$\frac{\partial A(\tau)}{\partial \tau} = B(\tau)\kappa\theta_t, \tag{2.21}$$

$$\frac{\partial B(\tau)}{\partial \tau} = b_0 + b_1 B(\tau) + b_2 B^2(\tau), \tag{2.22}$$

subject to the initial conditions $A(0) = B(0) = 0$, θ_t as in (2.5) or (2.6). The expressions followed by the terms b_0, b_1 and b_2 conditional to the original set-up (left column) and the alternative set-up (right column) are

$$\begin{aligned} b_0 &= -\frac{1}{2}(u^2+iu)\big(\sigma_S^2 + \sigma_Y^2(t,T) + 2\rho_{Sy}\sigma_S\sigma_Y(t,T)\big), & b_0 &= -\frac{1}{2}(u^2+iu)\sigma_F^2(t,T), \\ b_1 &= -\kappa + iu\sigma_v\big(\rho_{Sv}\sigma_S + \rho_{yv}\sigma_Y(t,T)\big), & b_1 &= -\kappa + iu\sigma_v\rho_{Fv}\sigma_F(t,T), \\ b_2 &= \frac{\sigma_v^2}{2}, & b_2 &= \frac{\sigma_v^2}{2}. \end{aligned} \tag{2.23}$$

Proof. See Appendix 2A.1 for proof. ■

The analytic expression followed by $B(\tau)$ in equation (2.20) is not affected by θ_t and reads

$$B(\tau) = \frac{2\gamma}{\sigma_v^2}\left(\beta + \mu z + z\frac{g'(z)}{g(z)}\right), \tag{2.24}$$

and the expressions followed by $\beta, \mu, z, g(z)$ and $g'(z)$ can be found in Appendix 2B.1.

The following two propositions provide the analytic expressions followed by $A(\tau)$ in equation (2.20).

Proposition 2.2 *When θ_t follows a single sinusoidal form as in expression (2.5), ODE (2.21) has a quasi-analytical solution which is given by*

$$A(\tau) = m\big(A_1(\tau) + A_2(\tau) + A_3(\tau) + A_4(\tau) + k_3\big), \tag{2.25}$$

with

$$\begin{aligned} A_1(\tau) &= a^\theta\left(\beta\tau - \frac{\mu z + \ln g(z)}{\gamma}\right), \\ A_2(\tau) &= -b^\theta\frac{\beta y_\tau^s}{2\pi}, \\ A_3(\tau) &= b^\theta\mu z\frac{y_\tau^c - 2\pi\gamma y_\tau^s}{4\pi^2+\gamma^2}, \\ A_4(\tau) &= b^\theta\frac{\tau}{\omega}\Big(y_0^c g'(\omega^{-1}) - \frac{\tau}{2}\big(g'(\omega^{-1})\,(y_0^c\zeta_1 - 2\pi y_0^s) + y_0^c\zeta_2\big)\Big), \end{aligned} \tag{2.26}$$

with $a, b, \beta, \mu, z, g(z)$ and $g(z)$ as defined in Appendix 2B.1, with

$$\begin{aligned} &m = 2\kappa\gamma/\sigma_v^2, \\ &y_\tau^c = \cos\left(2\pi\left(T_0 - \tau - t_0\right)\right), \quad y_0^c = \cos\left(2\pi\left(T_0 - t_0\right)\right), \\ &y_\tau^s = \sin\left(2\pi\left(T_0 - \tau - t_0\right)\right), \quad y_0^s = \sin\left(2\pi\left(T_0 - t_0\right)\right), \\ &\zeta_1 = \gamma(1 + k_1 n_1 + k_2 n_2), \qquad \zeta_2 = \gamma(k_1 n_3 + k_2 n_4), \end{aligned} \tag{2.27}$$

and

$$\begin{aligned}
n_1 &= (a-b)\big(M(a-1,b,\omega^{-1}) - M(a,b,\omega^{-1})\big) + M(a,b,\omega^{-1})\omega^{-1},\\
n_2 &= a\big(U(a,b,\omega^{-1}) + (b-a-1)\,U(a+1,b,\omega^{-1})\big),\\
n_3 &= \frac{a}{b}\Big((a-b)\big(M(a+1,b+1,\omega^{-1}) - M(a,b+1,\omega^{-1})\big) + M(a+1,b+1,\omega^{-1})\omega^{-1}\Big),\\
n_4 &= a\big(U(a,b,\omega^{-1}) + \big(b-\omega^{-1}\big)\,U(a+1,b+1,\omega^{-1})\big).
\end{aligned} \tag{2.28}$$

M and U are Kummer's and Tricomi's hypergeometric functions, as defined in Appendix 2B.1.

In particular, if the initial condition is $A(0) = 0$, we have that

$$\begin{aligned}
k_3 &= x_0 + x_0^s y_0^s + x_0^c y_0^c,\\
x_0 &= a^\theta \frac{\mu}{\omega},\\
x_0^s &= b^\theta \left(\frac{\beta}{2\pi} - \frac{2\pi\mu}{\omega(4\pi^2+\gamma^2)}\right),\\
x_0^c &= -b^\theta \frac{\mu\gamma}{\omega(4\pi^2+\gamma^2)}.
\end{aligned} \tag{2.29}$$

Proof. See Appendix 2A.2 for proof. ■

Proposition 2.3 *When θ_t follows a mixed sinusoidal form as in expression (2.6), ODE (2.21) has a quasi-analytical solution which is given by*

$$A(\tau) = m\big(A_1(\tau) + A_2(\tau) + A_3(\tau) + A_4(\tau) + A_5(\tau) + A_6(\tau) + A_7(\tau) + k_3\big), \tag{2.30}$$

with $A_1(\tau), A_2(\tau), A_3(\tau)$ and $A_4(\tau)$ as in Proposition 2.2, with

$$\begin{aligned}
A_5(\tau) &= c^\theta \beta \frac{y_\tau^c}{2\pi},\\
A_6(\tau) &= c^\theta \mu z \frac{2\pi y_\tau^s - \gamma y_\tau^c}{4\pi^2+\gamma^2},\\
A_7(\tau) &= c^\theta \frac{\tau}{\omega}\Big(y_0^s g'(\omega^{-1}) - \frac{\tau}{2}\big(g'(\omega^{-1})\,(y_0^s\zeta_1 + 2\pi y_0^c) + y_0^s\zeta_2\big)\Big),
\end{aligned} \tag{2.31}$$

with $\beta, \mu, z, g(z)$ and $g(z)$ as defined in Appendix 2B.1; $m, y_\tau^c, y_0^c, y_\tau^s, y_0^s, \zeta_1$ and ζ_2 as in expression (2.27).

In particular, if the initial condition is $A(0) = 0$, we have that

$$\begin{aligned}
k_3 &= x_0 + x_0^s\, y_0^s + x_0^c\, y_0^c,\\
x_0 &= a^\theta \frac{\mu}{\omega},\\
x_0^s &= b^\theta \left(\frac{\beta}{2\pi} + \frac{2\pi\mu}{\omega(4\pi^2+\gamma^2)}\right) - c^\theta \frac{\mu\gamma}{\omega(4\pi^2+\gamma^2)},\\
x_0^c &= -b^\theta \frac{\mu\gamma}{\omega(4\pi^2+\gamma^2)} + c^\theta \left(\frac{\beta}{2\pi} + \frac{2\pi\mu}{\omega(4\pi^2+\gamma^2)}\right).
\end{aligned} \tag{2.32}$$

Proof. See Appendix 2A.3 for proof. ■

In Proposition 2.2, if $b^\theta = 0$ we then have that $\theta_t = a^\theta$, $A_2(\tau) = A_3(\tau) = A_4(\tau) = 0$, and $A(\tau) = A_1(\tau)$. In Proposition 2.3, if $b^\theta = c^\theta = 0$ we have that $\theta_t = a^\theta$, $A_2(\tau) = A_3(\tau) = A_4(\tau) = A_5(\tau) = A_6(\tau) = A_7(\tau) = 0$, and therefore $A(\tau) = A_1(\tau)$. Under either situation, our model is equivalent to TS09-SV1 and $A(\tau)$ reads

$$\begin{aligned} A(\tau) &= m(A_1(\tau) + k_3^{TS}), \\ k_3^{TS} &= x_0 = a^\theta \frac{\mu}{\omega}. \end{aligned} \tag{2.33}$$

Independently of the harmonic expression chosen and based on evidence, we assume that in the long-run mean-reverting parameter θ_t there is only one peak per year.

Extant Models

The naturally nested models respective to ours is TS09-SV1. Additionally, we also consider other extant models such as Mer76, Hes93 and Bat96. We compare the performance of our model to jump-diffusion models to avoid mis interpreting cycles in prices as jumps. We also include ST18 and ST21 in the list of extant models, the latter presenting SSV.[8]

Modeling the futures dynamics using jumps and stochastic volatility results in the futures prices having non-Gaussian returns – a stylised fact in the energy markets. In Table 2.2 we present the values for the four first moments of the distribution, and we perform the Jarque-Bera normality test on monthly data. We reject the null hypothesis of normality in returns for each of the labeled contracts M2-M8, and all contracts taken together. This implies that some source of structure in the variance such as stochastic volatility is required, providing skewness and/or kurtosis to the distribution of returns. Many earlier models include stochastic volatility in their specification.

We consider one-, two- and three-factor extant models, a mix of spot-based and term-structure models. To compare them from a commodity perspective, we transform the original spot-based specification in Mer76, Hes93 and Bat96 to their corresponding futures prices dynamics.[9] Hereafter we will refer to their futures-equivalent specification, but naming them in their original form. In this work we consider a panel of six extant models plus ours; in Section 2.5 we compare their pricing performances.

For each model, next we describe the components of the Fourier transform described in equation (2.20). BS73 models the spot prices requiring only the independent term $A(\tau)$; Mer76 extends BS73 incorporating iid jumps in the spot price, the jump-related terms are included in

[8] In this work, we consider the one-dimensional form of both models.
[9] Option prices for commodities's futures are quoted in the markets using Black (1976).

$A(\tau)$; Hes93 extends BS73 with stochastic variance, it uses $A(\tau)$ and the stochastic variance-related term $B(\tau)$; Bat96 extends Hes93 with iid jumps in the spot price, it uses $A(\tau)$ and $B(\tau)$; TS09, ST18, ST21 and our model are term-structure models with stochastic prices and variances, which require both terms $A(\tau)$ and $B(\tau)$. For instance, ST21 and our model incorporate seasonality in the variance, whereas TS09 and ST18 do not. Both TS09 as well as our model describe the dynamics of the spot price and the cost of carry before obtaining the futures prices' dynamics.

In Table 2.3 we present the dynamics followed by the models in the above list as well as ours. This table is complemented by Figure 2.1, which visually represents the links between the different models in terms of factors, seasonality and jumps. The expressions followed by the dynamics of $A(\tau)$ and $B(\tau)$ in equation (2.20) and their solutions can be found in Tables 2.4 and 2.5, respectively.

Key advantages of the most recent models including ours include improved approximation to the real price behaviour and better description of the implied volatility surface. In our case, adding up to three seasonality-related parameters provides more flexibility to replicate the volatility surface quoted in the market, allowing for a wider range of possible shapes (e.g., the Samuelson effect and the seasonal temperatures affecting the natural gas demand). The implementation is not straightforward; it does not require the addition of new terms to the CF in TS09, but the variance term $B(\tau)$ must be modified due to the seasonal component introduced.

2.3 Pricing of Standard European Options

In this section we price standard European options on futures contracts using the CF previously computed. Let $\mathcal{C}(t, T_{Opt}, T, K)$ and $\mathcal{P}(t, T_{Opt}, T, K)$ denote the time-t prices of a standard European call (hereafter, call) and a standard European put (hereafter, put) option expiring at time T_{Opt} with strike K on a futures contract expiring at time T, with $0 < t < T < T_{Opt}$. This option can be priced quasi-analytically within the framework we describe in this section. In our empirical work and from the different pricing approaches based on the CF, we follow the fast Fourier transform (FFT) methodology.[10]

2.3.1 The Fast Fourier Transform

Carr & Madan (1999) obtain a pricing formula for options which enables a computationally efficient FFT algorithm. Its popularity stems from its remarkable speed: while prior computation approaches require N^2 operations, the FFT requires only $N \ln(N)$ steps.

[10] See, e.g., Schmelzle (2010) for a classification of the different Fourier-based approaches.

In the following proposition we present the expressions followed by the prices of standard European call and put options prices:

Proposition 2.4 *The time-t price of a call and a put option expiring at time T_{Opt} with strike K on a time-t futures contract expiring at time T is given by*

$$\begin{aligned}\mathcal{C}(t, T_{Opt}, T, K) &= P(t, T_{Opt})\frac{e^{-\alpha \ln(K)}}{\pi}\int_0^\infty \Re\left[\frac{e^{-iu\ln(K)}\psi_t(u - i(1+\alpha), t, T_{Opt}, T)}{\alpha(\alpha+1) - u^2 + iu(1+2\alpha)}\right] du,\\ \mathcal{P}(t, T_{Opt}, T, K) &= P(t, T_{Opt})\frac{e^{-\alpha \ln(K)}}{\pi}\int_0^\infty \Re\left[\frac{e^{-iu\ln(K)}\psi_t(u - i(1-\alpha), t, T_{Opt}, T)}{\alpha(\alpha-1) - u^2 + iu(1-2\alpha)}\right] du,\end{aligned} \tag{2.34}$$

where $P(T_{Opt}, t)$ is the time-t price of a zero-coupon bond maturing at T_{Opt} and α is the control parameter.[11]

Proof. The proof is in Carr & Madan (1999). ■

This approach presents two advantages: firstly, it permits the use of the computationally efficient FFT; secondly, it only requires the evaluation of one integral, as opposed to the two integrals required when using former perspectives as in Hes93 or Duffie, Pan & Singleton (2000).

2.4 Market Data and Parameters Estimation

Market Data

We consider HH natural gas futures and options traded on the New York Mercantile Exchange (NYMEX), which we obtain from Refinitiv Eikon (formerly, Thomson-Reuters' Datastream). The data set consist of observations of closing prices (quoted in USD) for futures and market implied volatilities for the corresponding options. There are monthly contracts listed for the current year and the next 12 calendar years for both futures and options. For futures, trading months are the 72 consecutive months commencing with the next calendar month, and trading terminates three business days prior to the first calendar day of the delivery month. For options, trading months are the 12 consecutive months plus contracts extending up to 72 months and traded in a quarterly manner, and trading terminates at the close of business on the business day preceding the expiration of the underlying futures contract. There are 20 strike prices in

[11] α has to be chosen to ensure it makes the modified option price square-integrable and to obtain good numerical accuracy – a sufficient condition for the Fourier transform to exist. This parameter has to be wisely chosen as it might produce very oscillatory arguments of the integral if too big, or it might approach a point mass around 0 if too small.

increments of 0.05 USD above and below the ATM strike price in all months. The ATM strike price is nearest to previous day's close of the underlying futures contract.[12]

The 10-year period considered spans from January 3^{rd} 2011 to December 31^{st} 2020 and the market data set is at monthly and daily frequency. When the data is observed on a monthly basis, the observations correspond to the last business day of each month in the considered period. We are considering seven futures contracts labeled M2, M3, . . . , M8[13] and their correspondent ATM and OTM quoted options, call and put, for 16 degrees of moneyness (ATM plus 15 degrees of moneyness, from the ATM level $\pm 0.05\, i$ USD, for $i = 1 : 15$ (that is, $\pm 0, 0.05, 0.1 \ldots 0.75$)), making it 32 options per contract and 224 options per observation date.

The number of monthly (daily) observations equals 120 (2,521), making it 840 (17,647) futures prices and 26,880 (564,480) options volatilities. From these volatilities, we consider 21,972 (526,142) as valid after a cleansing process, which results in 81.74% (93.21%).

Parameters Estimation

We define our model dynamics directly under $\mathbb{Q}$, therefore the parameter estimation is performed under this measure. Subject to the original characterisation of the parameters, the 10 parameters in our model are $\Phi_t^{\checkmark} \equiv \{\sigma_S, \alpha, \gamma, \kappa, a^\theta, b^\theta, c^\theta, \rho_{Sy}, \rho_{Sv}, \rho_{yv}\}$, whereas conditional to the alternative set-up, the 8 parameters are $\Phi_t^{\star} \equiv \{\alpha_0, \alpha, \gamma, \kappa, a^\theta, b^\theta, c^\theta, \rho_{Fv}\}$.

In this work we study the empirical pricing performance of the models using the least-squares estimation method, under which the procedure to obtain the parameter estimates $\Phi_t^\star$ for every observation date t is defined as

$$\begin{aligned} \Phi_t^\star &= \arg\min_{\Phi_t} MAE_t^\sigma(\Phi_t) = \underset{arg\, min}{\Phi_t} \frac{1}{N_t} \sum_{i=1}^{N_t} \left| \hat{\sigma}_{t,i}(\Phi_t) - \sigma_{t,i} \right|, \\ \Phi_t^\star &= \arg\min_{\Phi_t} RMSE_t^\sigma(\Phi_t) = \underset{arg\, min}{\Phi_t} \sqrt{\frac{1}{N_t} \sum_{i=1}^{N_t} \left(\hat{\sigma}_{t,i}(\Phi_t) - \sigma_{t,i} \right)^2}, \end{aligned} \tag{2.35}$$

where $\sigma_{t,i}$ is the observed market volatility of option i out of N_t used for the estimation at time t, and $\hat{\sigma}_{t,i}(\Phi_t)$ is the theoretical model volatility based on a set of parameters. We compute implied volatilities employing the standard model of Black (1976). Parameters are not allowed to take values that are inconsistent with the model framework. Disregarding the seasonality, the following restrictions are applied for the original set-up: $\sigma_S = 1; \alpha, \gamma, \kappa, \sigma_v > 0; \rho_{Sy}, \rho_{Sv}, \rho_{yv} \in (-1, 1)$; for the alternative set-up: $\alpha = 1; \alpha_0, \gamma, \kappa, \sigma_v > 0; \rho_{Fv} \in (-1, 1)$. Furthermore, the

[12]Contract specifications for futures and options on HH natural gas can be found at CME home.
[13]They are the second to the eighth available maturity contracts.

parameters governing the seasonality are restricted to ensure their uniqueness: $a^\theta > 0, a^\theta \geq |b^\theta|, a^\theta \geq |c^\theta|$ and $t_0 \in [0, 1[$, with January 1^{st} representing the time origin.

We fix the value of the parameter t_0 based on the evidence in the seasonal behaviour of our underlying asset, the HH natural gas futures' prices. In order to obtain this evidence, we analyse the ATM Black volatilities quoted in the market for the shortest available contract (in the case that these volatilitites were not available, we consider the contract for the following available maturity and so on, until we find values).[14] For model sub-specification S (single sinusoidal pattern), we calibrate the values for a^θ and b^θ for 12 different values of t_0 $(1/12, 2/12, \ldots, 12/12)$ in order to obtain the correspondent values of R^2. We find that the highest values are obtained when the peak corresponds to the end of October, that is, $t_0 = 10/12$. For sub-specification M (multiple sinusoidal pattern), we proceed in a similar way with the three parameters involved. In this case, the value of t_0 does not affect the value of the R^2. Therefore we set $t_0 = 10/12$. The results of this analysis can be found in Table 2.6.

2.5 Results

In this section we implement our novel term-structure model SSYSV described in Sections 2.2 and 2.3, which displays stochastic spot prices and forward cost of carry curves (equivalent to stochastic futures prices) as well as SSV. For a panel of models, we calibrate their parameters for pricing ATM and OTM options, spanning different strikes and maturities, over a time period of exactly 10 years. The results are obtained using analytical expressions for the CF of the futures log-prices. Following Carr & Madan (1999), we use Simpson's rule to calculate the integral in the pricing functions (2.34) numerically, for which we use Matlab's built-in function $simps$. We use a standard fourth order Runge-Kutta algorithm to solve the system of ODEs (2.21)-(2.22), for which we use Matlab's built-in function $ode45$. We consider an integral step of $1/10$ and an upper bound of 60, which implies 600 evaluation points. We set the value of the control parameter α to 0.75. The experiments are implemented in a HP laptop computer configured with an Intel Core i7 2.60 GHz 16 GB RAM and SSD hard drive, running Windows 10 64 bits, Matlab version R2020b 64 bits and Microsoft Office 365 64 bits.

On Deciding the Value for the Seasonal Peak

In Table 2.6 we present a detailed analysis based on the values of R^2 when regressing the market variance v_t in terms of a cosinus only (S), sinus only ($M(b^\theta = 0)$) and both harmonic functions

[14] We have not chosen the shorter maturity contract M2 due to the lack of many ATM option values in the entire time series, especially during the first half of the sample.

(M). The values that t_0 can get are described in Section 2.4.

We start by calculating the values of R^2 per peak value, considering the whole sample period.[15] The values we obtain are quite small but it provides direction for t_0 in the gas market. The highest value for R^2 (5.95% for the single patter, 6.15% for the mixed pattern) is obtained for $t_0 = 10/12$ (end of October), and is aligned with the gas market performance. Sub-table 2.6a considers the whole period 2011-2020 and checks the effect of each value of t_0. For the simple S specification of the seasonality, best results are obtained when $t_0 = 4/12, 10/12$ ($R^2 = 5.95\%$ for the single pattern, 6.15% for the mixed pattern). October is easily identified as peak and April is the valley, so we set $t_0 = 10/12$. For the mixed M specification, all values perform equally. There is a clear explanation for the small overall value of R^2 considering the whole time series, as we did not isolate other economic factors from the analysis such as economic news, among others.

Subsequently we calculate the values of R^2 per individual year, already considering $t_0 = 10/12$ as peak. We can see the results in Sub-table 2.6b. The value for R^2 is clearly larger for the mixed pattern, which allows us to identify what years adjust best to a pure harmonic pattern, though not considering other elements. Some years present very good adjustment, such as 2012 ($R^2 = 74.89\%$) and 2019 ($R^2 = 84.85\%$); others display very poor performance, such as 2011 ($R^2 = 10.01\%$) and 2013 ($R^2 = 14.16\%$). Taking all the years together might not be the best analysis perspective; however, the value delivered for t_0 works quite well overall when there is no noise in the time series.

Lastly, we perform an extra analysis taking averages per trade month in the variance v_t for the whole period and all contracts. The results can be found in Sub-table 2.6c. We check the effect of each month as peak of the variance series once more, where as the best performances in terms of R^2 correspond to $t_0 = 4/12, 10/12$ (54.40% for the single pattern, 56.28% for the mixed pattern). We identify October as peak and April as valley again due to the same initial drivers. In complement to this, Figure 2.2b presents the regression of the market variance in terms of the cosinus function (single pattern).

Results in Table 2.7 are in line with those in Table 2.6. In it we provide evidence of our model's peak value for best performance compared to our benchmark TS09-SV1. As expected, we identify the biggest improvement when $t_0 = 10/12$. The smallest error corresponds to $t_0 = 10/12$ for the single pattern; for the mixed one the smallest error is identified for different values of t_0. One of these corresponds to the month with the smallest error for the single pattern, therefore we refer to this value of t_0 as the best performing month for both patterns, with lowest errors in both cases (4.26% and 4.25%). Additionally and following results in Sub-table 2.6b,

[15] In Table 2.6 we only consider the futures contract labeled M3.

we perform an equivalent analysis based on two individual years (2019 and 2020) for which results are reported in Table 2.9.

All these analyses are performed using monthly observations and the original parameters set-up. Similar results are obtained using daily observations and the alternative set-up.[16]

On Interpreting the Pricing Errors

Based on $t_0 = 10/12$ and for the period described in Section 2.4, our calibration results are reported in Table 2.8. We perform two sets of analysis: Sub-table (a) considers monthly data, whereas Sub-table (b) focuses on daily data. For each model considered, we display the parameters' estimates, the pricing errors MAE(σ) and RMSE(σ), and the computation times. Under the original (alternative) set-up, the average MAE(σ) for our model is 4.18% (4.25%), this is a 0.15% (0.09%) less than TS09-SV1,[17] almost identical error values. Lastly, we carry out a transverse analysis of the distribution of the errors between our model and TS09-SV1.

Next we compare model performances based on the monthly data set by means of the MAE(σ) estimates. Tables 2.10 and 2.11 (2.12 and 2.13) follow the original (alternative) characterisation of the parameters. Sub-tables (a) display the errors using the benchmark model TS09-SV1; Sub-tables (b) display the errors using our model, following sub-specifications S and M respectively. Both models perform worst (that is, present larger errors) for shorter maturity contracts, after which the model performance improves for both. Sub-tables (c) display the difference in errors between both models, with larger values indicating that our model outperforms the benchmark. In this sub-table we observe the most significant improvement, specifically (i) for deeper OTM options, particularly puts in shorter maturity contracts (i.e. M2 and M3) dealing with the original set-up; and (ii) for closer-to-the-ATM options, particularly puts in the very short maturity contracts (i.e. M2) when we deal with the alternative set-up, where improvement reaches 3.5%. For longer maturity contracts, both models display similar performance. In particular and for montly observations, gains in model performance hit 1.30% when the set-up is the original for the simple harmonic pattern; 1.74% when the set-up is the original for the multiple harmonic pattern. 2.92% when the set-up is the alternative for the simple harmonic pattern; 3.53% when the set-up is the alternative for the multiple harmonic pattern.

In our panel we also include another very recent model which also presents seasonality in the futures' variance as well as its equivalent one without seasonality, these are ST21 and ST18. In Table 2.14 we compare ST21 with our model SYSSV^S, both from a futures' perspective and

[16] The proof is available by direct request to the authors.

[17] Our model consists of an extension of TS09, therefore we compare both performances.

with identical seasonality specification. We find that our model clearly outperforms ST21 for short maturities and deeper OTM put options where the gain reaches a 3.13% (alternative set-up and simple harmonic pattern).

We had initially expected Hes93 and more clearly Mer76 to underperform compared to our model and benchmark, given that jump models' parameters are quite unstable. We identify that the jump model in Bat96 slightly outperforms our model and its benchmark. The difference (in percentage) arises on the second digit and it is minor. A detailed analysis should be carried out in the difference in the statistic error surface in order to identify a pattern(s) per contract lengths and/or moneyness levels.

2.6 Conclusions and Further Research

Volatility in many commodity markets follows a pronounced seasonal pattern while also fluctuating stochastically. In this paper, we extend the stochastic volatility model of TS09 to allow volatility to vary with the seasonal cycle. We develop a model that enables deriving quasi-analytical solutions for pricing options on futures prices. We empirically study its performance in pricing Henry Hub natural gas standard European options. We estimate our model using a cross-section of options prices considering a series of 10 years of futures contracts. Results show that the SSV model we suggest increases the accuracy of pricing options on HH natural gas. When our models follow an original set-up, accuracy increases especially for shorter maturity contracts and deeper OTM options. We also propose an alternative set-up, whereby we obtain better pricing performance for shorter maturity contracts and closer to the ATM options. An additional benefit of this alternative set-up consists of improving the speed of calculation.

We conclude the paper by outlining areas for future research. Many commodity assets exhibit jumps not only in prices but also in volatility, especially the natural gas. We identify that the jump model in Bat96 slightly outperforms our model and its benchmark; we can leverage this finding to study the inclusion of jumps in a future line of research. We also consider modeling the jump intensity according to a seasonal function. Another research field of interest are calendar spread options which are also common in energy markets, and their pricing requires to know the expression followed by the joint CF for the two futures involved.

2.7 Figures and Tables

Figure 2.1: Diagram of extant models

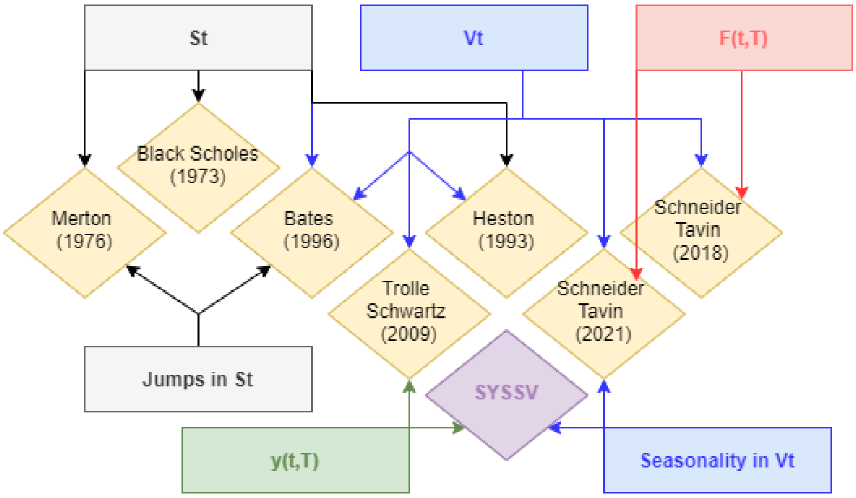

NOTES: In this figure we represent in a visual manner the factors affecting each of the considered models in this work, the existence of the type of seasonal effect and/or jumps. This figure complements the information in Section 2.2.2 and Table 2.3.

Figure 2.2: Stylised facts in the variance

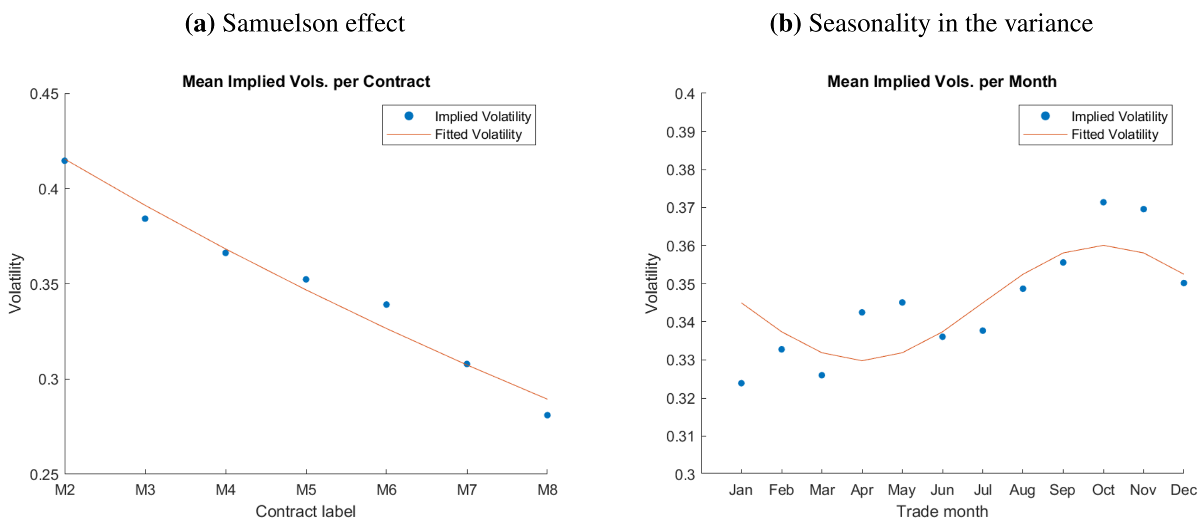

NOTES: This figure presents two stylised facts in the natural gas market. Sub-figure (a) shows the Samuelson effect of the implied volatilities of futures options grouped by contract (that is, from closest to maturity to more distant ones). Sub-figure (b) shows the seasonal pattern of the implied volatilities of futures options grouped by trade month. The seasonal volatility pattern is approximated by a trigonometric function following expression (2.5). For both sub-figures, the period considered spans from 01/2011 to 12/2020 (monthly observations), and only ATM options are considered. We compute implied volatilities employing the standard model of Black (1976).

Figure 2.3: Futures prices and ATM options volatilitites – monthly data

(a) Futures Prices

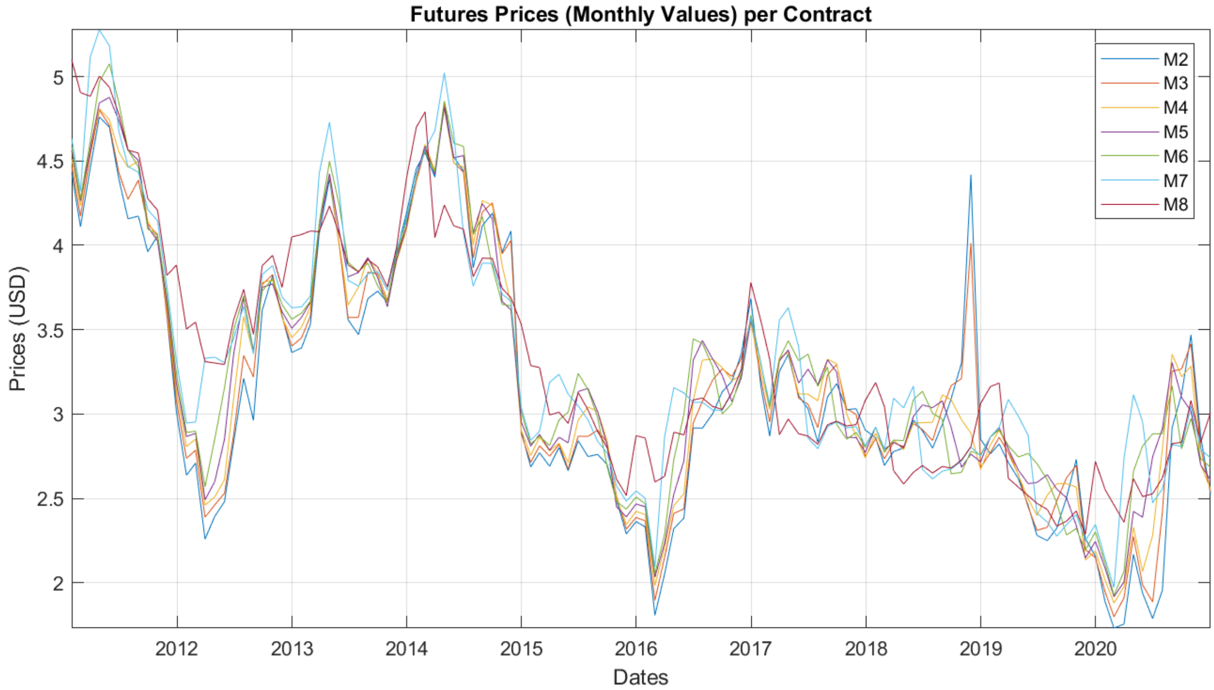

(b) Option Volatilities

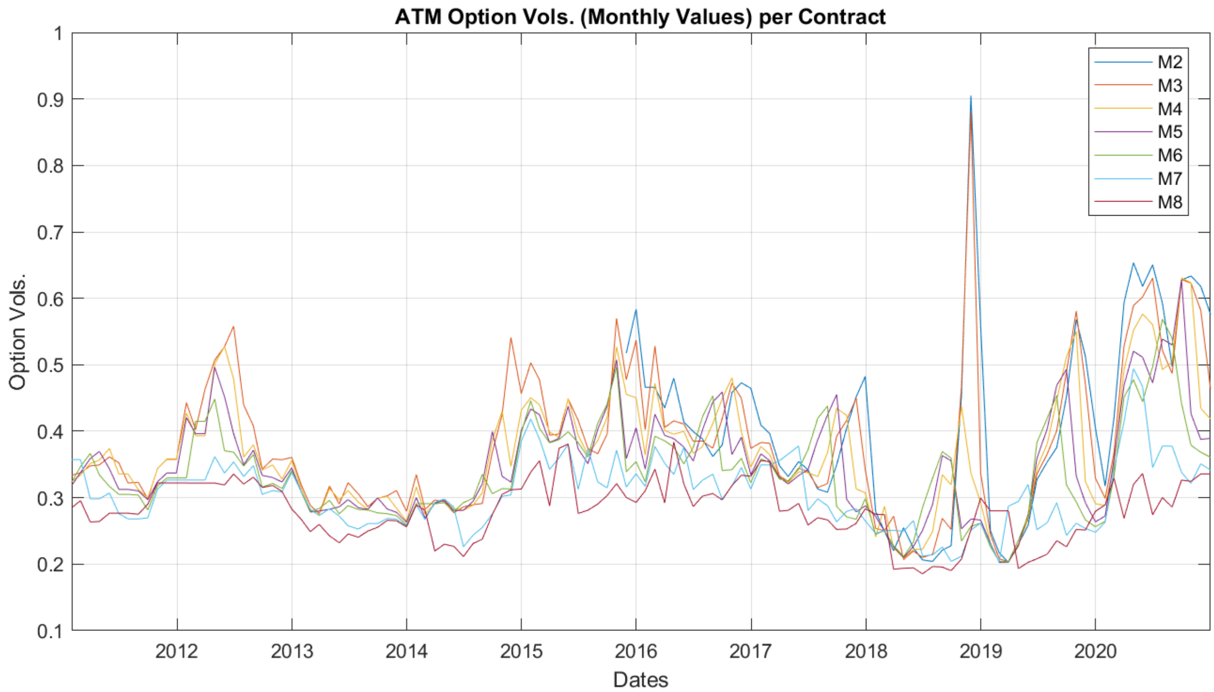

NOTES: Sub-figure (a) presents the prices of the futures contracts labeled M2-M8. Sub-figure (b) presents the volatilities of quoted ATM call options on the futures labeled M2-M8. All values correspond to monthly observations.

Figure 2.4: Futures returns – monthly data

(a) Futures Returns

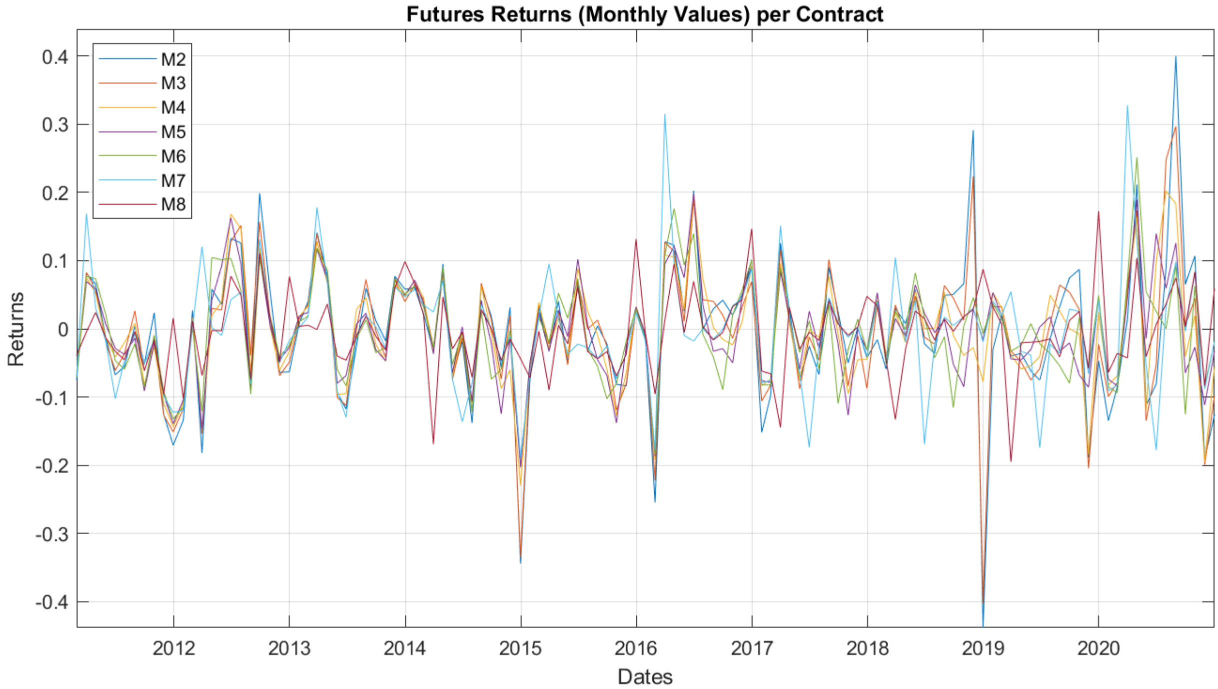

(b) Histogram of Returns

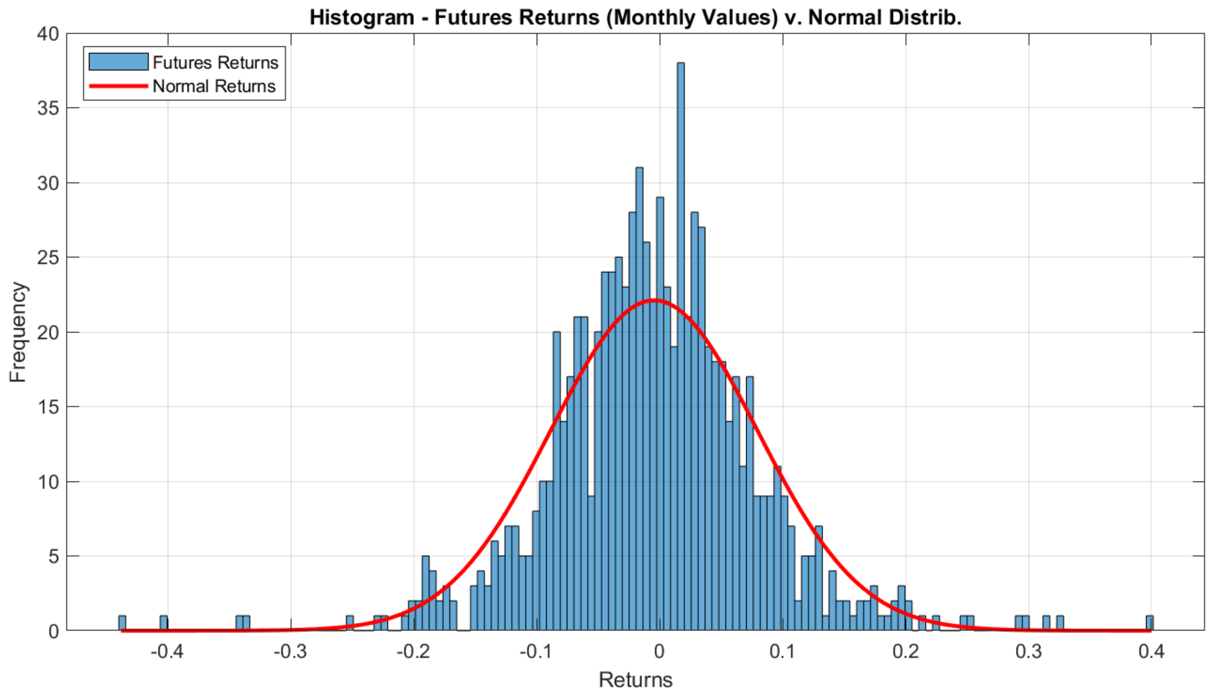

NOTES: Sub-figure (a) presents the returns of the futures contracts labeled M2-M8. In Sub-figure (b) we can see in blue the correspondent histogram to the returns in (a), the curve in red represents the equivalent PDF of a normal distribution with the same mean and standard deviation. All values correspond to monthly observations.

Table 2.1: Factors and features per model

Model	**Dimension**		**Stochastic Factors**				**Seasonality**			**Jumps**			**Parameter**
	Single	Mult.	S_t	$y(t,T)$	$F(t,T)$	v_t	Prices	Vols.	SSV	S_t	$y(t,T)$	v_t	**Count**
BS73	✓		✓										1
Mer76	✓		✓							✓			4
Hes93	✓		✓			✓							4
Bat96	✓		✓			✓				✓			7
GN95	✓		✓			✓	✓	✓	✓				17
CS99a		✓			✓								2
CS99b	✓				✓								2
CS00	✓				✓								3
LS02	✓		✓					✓					13
Sor02	✓		✓				✓						6
RS02	✓		✓			✓	✓	✓	✓				10
TS09-SV1	✓		✓	✓	$\star$	✓							9(7)
BPP13	✓		✓				✓	✓					7,8
ABP16	✓				✓	✓		✓	✓				5
FMM16	✓				✓			✓					36
FS19	✓				✓			✓	✓				15
ST18		✓			✓	✓							5
ST21		✓			✓	✓		✓	✓				6
SYSSV	✓		✓	✓	$\star$	✓		✓	✓				10,11(8,9)

NOTES: For each model mentioned in Section 2.1, this table enumerates the factors considered, the type of seasonality, the jumps and the parameter count. The column Dimension accounts for the dimensional setting of the model (single or multiple). The acronyms whereby we refer to the models can be found in Section 2.1. In those models presenting alternative characterisation of the parameters (as defined in Section 2.2.1) and in the columns for the stochastic factors, $F(t,T)$ replaces S_t and $y(t,T)$; this is indicated with the symbol $\star$ and the correspondent parameter count appears in brackets. We refer to our model as SYSSV. The number of parameters indicated for GN95 corresponds to the two-state variable model; for LS02 corresponds to the one-factor model.

Table 2.2: Futures returns and Jarque-Bera test

(a) Monthly Observations

Contract	Min.	Max.	Mean	Std. Dev.	Skew.	Kurt.	JB Stat.	p-Value	Test
M2	-43.82%	40.02%	-0.35%	10.61%	-0.2939	6.4480	5.929	0.0442	R
M3	-40.29%	29.69%	-0.34%	9.77%	-0.4977	5.7563	6.329	0.0396	R
M4	-22.97%	20.21%	-0.35%	7.98%	0.0011	3.3583	6.915	0.0331	R
M5	-20.31%	19.83%	-0.40%	7.35%	0.0527	3.1785	7.865	0.0258	R
M6	-18.99%	25.15%	-0.45%	7.29%	0.1753	3.4847	9.167	0.0190	R
M7	-18.90%	32.80%	-0.48%	8.19%	0.7649	5.9847	10.527	0.0142	R
M8	-19.50%	17.25%	-0.37%	5.97%	0.0752	4.3030	11.064	0.0127	R
ALL	-43.82%	40.02%	-0.39%	8.27%	-0.0700	6.0021	1,567.737	0.0010	R

(b) Daily Observations

Contract	Min.	Max.	Mean	Std. Dev.	Skew.	Kurt.	JB Stat.	p-Value	Test
M2	-20.21%	17.13%	-0.02%	2.43%	0.1865	9.0481	119.964	0.0010	R
M3	-37.70%	26.79%	-0.02%	2.34%	-0.8969	38.3860	128.552	0.0010	R
M4	-10.11%	22.96%	-0.02%	1.97%	0.6833	11.7360	143.408	0.0010	R
M5	-13.87%	14.89%	-0.02%	1.85%	0.0712	8.9002	175.663	0.0010	R
M6	-11.32%	13.26%	-0.03%	1.74%	0.1228	8.6686	213.328	0.0010	R
M7	-12.80%	14.00%	-0.03%	1.65%	-0.1090	9.0187	228.004	0.0010	R
M8	-14.84%	9.21%	-0.02%	1.85%	-0.7251	10.2528	227.048	0.0010	R
ALL	-37.70%	26.79%	-0.02%	1.96%	-0.1119	18.9926	33,600.777	0.0010	R

NOTES: JB accounts for the Jarque-Bera normality test. The null hypothesis refers to the normal distribution of futures returns. The critical value associated to a significance level of 0.05 is 5.991. When the value of Test is R (CR), we reject (cannot reject) the null hypothesis at 95%.

Table 2.3: Models dynamics

Model	Dynamics	Volatility
BS73	$\frac{dS_t}{S_t} = y_t dt + \sigma_S dW_t^S$	σ_S constant
	$\frac{dF(t,T)}{F(t,T)} = \sigma_F dW_t^F$	σ_S constant
Mer76	$\frac{dS_t}{S_t} = \left(y_t - \lambda E_t^{\mathbb{Q}}\left[e^{J_S} - 1\right]\right)dt + \sigma_S dW_t^S + \left(e^{J_S} - 1\right)dN_t$	σ_S constant
	$\frac{dF(t,T)}{F(t,T)} = -\lambda E_t^{\mathbb{Q}}\left[e^{J_F} - 1\right]dt + \sigma_F dW_t^F + \left(e^{J_F} - 1\right)dN_t$	σ_F constant
Hes93	$\frac{dS_t}{S_t} = y_t dt + \sqrt{v_t} dW_t^S$	$\sigma_S = 1$
	$dv_t = \kappa\left(\theta - v_t\right)dt + \sigma_v \sqrt{v_t} dW_t^v$	σ_v constant
	$\frac{dF(t,T)}{F(t,T)} = \sigma_F \sqrt{v_t} dW_t^F$	σ_F constant
Bat96	$\frac{dS_t}{S_t} = \left(y_t - \lambda E_t^{\mathbb{Q}}\left[e^{J_S} - 1\right]\right)dt + \sqrt{v_t} dW_t^S + \left(e^{J_S} - 1\right)dN_t$	$\sigma_S = 1$
	$dv_t = \kappa\left(\theta - v_t\right)dt + \sigma_v \sqrt{v_t} dW_t^v$	σ_v constant
	$\frac{dF(t,T)}{F(t,T)} = -\lambda E_t^{\mathbb{Q}}\left[e^{J_F} - 1\right]dt + \sqrt{v_t} dW_t^F + \left(e^{J_F} - 1\right)dN_t$	σ_F constant
TS09-SV1	$\frac{dS_t}{S_t} = y_t dt + \sigma_S \sqrt{v_t} dW_t^S$	σ_S constant
	$dy(t,T) = \mu_y(t,T)dt + \sigma_y(t,T)\sqrt{v_t} dW_t^y$	$\sigma_y(t,T) = \alpha e^{-\gamma(T-t)}$
	$dv_t = \kappa\left(\theta - v_t\right)dt + \sigma_v \sqrt{v_t} dW_t^v$	σ_v constant
	$\frac{dF(t,T)}{F(t,T)} = \sqrt{v_t}\left(\sigma_S dW_t^S + \sigma_Y(t,T) dW_t^y\right)$	$\sigma_Y(t,T) = \int_t^T \sigma_y(t,u)du$
TS09-SV1*	$\frac{dF(t,T)}{F(t,T)} = \sqrt{v_t}\sigma_F(t,T) dW_t^F$	$\sigma_f(t,T) = \alpha_0 + \alpha e^{-\gamma(T-t)}$, $\alpha = 1$
		$\sigma_F(t,T) = \int_t^T \sigma_f(t,u)du$
ST18	$\frac{dF(t,T)}{F(t,T)} = \sum_{i=1}^n \sigma_{F_i}(t,T)\sqrt{v_{i,t}} dW_t^{F_i}$	$\sigma_{F_i}(t,T) = e^{-\gamma_i(T-t)}$, $\alpha_i = 1$
	$dv_{i,t} = \kappa_i\left(\theta_i - v_{i,t}\right)dt + \sigma_{v_i}\sqrt{v_{i,t}} dW_t^{v_i}$	σ_{v_i} constant
ST21	$\frac{dF(t,T)}{F(t,T)} = \sum_{i=1}^n \sigma_{F_i}(t,T)\sqrt{v_{i,t}} dW_t^{F_i}$	$\sigma_{F_i}(t,T) = e^{-\gamma_i(T-t)}$, $\alpha_i = 1$
	$dv_{i,t} = \kappa_i\left(\theta_t - v_{i,t}\right)dt + \sigma_{v_i}\sqrt{v_{i,t}} dW_t^{v_i}$	σ_{v_i} constant
	$\theta_t = a^\theta + b^\theta \cos(2\pi(t + t_0))$	
SYSSV	$\frac{dS_t}{S_t} = y_t dt + \sigma_S \sqrt{v_t} dW_t^S$	σ_S constant
	$dy(t,T) = \mu_y(t,T)dt + \sigma_y(t,T)\sqrt{v_t} dW_t^y$	$\sigma_y(t,T) = \alpha e^{-\gamma(T-t)}$, $\alpha = 1$
	$dv_t = \kappa\left(\theta_t - v_t\right)dt + \sigma_v \sqrt{v_t} dW_t^v$	σ_v constant
	$\theta_t^S = a^\theta + b^\theta \cos(2\pi(t + t_0))$	
	$\theta_t^M = a^\theta + b^\theta \cos(2\pi(t + t_0)) + c^\theta \sin(2\pi(t + t_0))$	
	$\frac{dF(t,T)}{F(t,T)} = \sqrt{v_t}\left(\sigma_S dW_t^S + \sigma_Y(t,T) dW_t^y\right)$	$\sigma_Y(t,T) = \int_t^T \sigma_y(t,u)du$
SYSSV*	$\frac{dF(t,T)}{F(t,T)} = \sqrt{v_t}\sigma_F(t,T) dW_t^F$	$\sigma_f(t,T) = \alpha_0 + \alpha e^{-\gamma(T-t)}$, $\alpha = 1$
		$\sigma_F(t,T) = \int_t^T \sigma_f(t,u)du$

NOTES: This table presents the model dynamics and their correspondent volatility expressions for the models described in Section 2.2.2 andr model SYSSV. For the first four models, the last equation refers to their corresponding futures' price dynamics. Those models presenting an alternative set-up of the parameters (i.e., TS09-SV1 and SYSSV) appear with the symbol $\star$.

Table 2.4: Fourier transforms – ODEs and parameters

(a) ODEs

Model	$\partial A(\tau)/\partial\tau$	$\partial B(\tau)/\partial\tau$
BS73	b_0	–
Mer76	$b_0 + (n_J - ium_J)$	–
Hes93	$B(\tau)\kappa\theta$	$b_0 + b_1 B(\tau) + b_2 B^2(\tau)$
Bat96	$B(\tau)\kappa\theta + (n_J - ium_J)$	$b_0 + b_1 B(\tau) + b_2 B^2(\tau)$
TS09	$B(\tau)\kappa\theta$	$b_0 + b_1 B(\tau) + b_2 B^2(\tau)$
ST18	$B(\tau)\kappa\theta$	$b_0 + b_1 B(\tau) + b_2 B^2(\tau)$
ST21	$B(\tau)\kappa\theta_t$	$b_0 + b_1 B(\tau) + b_2 B^2(\tau)$
SYSSV	$B(\tau)\kappa\theta_t$	$b_0 + b_1 B(\tau) + b_2 B^2(\tau)$

(b) Parameters

Model	b_0	b_1	b_2
BS73	$-\frac{\sigma_S^2}{2}$	–	–
Mer76	$-\frac{\sigma_S^2}{2}$	–	–
Hes93	$-\frac{1}{2}(u^2 + iu)$	$-\kappa + iu\sigma_v\rho_{Sv}$	$\frac{\sigma_v^2}{2}$
Bat96	$-\frac{1}{2}(u^2 + iu)$	$-\kappa + iu\sigma_v\rho_{Sv}$	$\frac{\sigma_v^2}{2}$
TS09$^{\checkmark}$	$-\frac{1}{2}(u^2 + iu)(\sigma_S^2 + \sigma_Y^2(t,T) + 2\rho_{Sy}\sigma_S\sigma_Y(t,T))$	$-\kappa + iu\sigma_v(\rho_{Sv}\sigma_S + \rho_{yv}\sigma_Y(t,T))$	$\frac{\sigma_v^2}{2}$
TS09*	$-\frac{1}{2}(u^2 + iu)\sigma_F^2(t,T)$	$-\kappa + iu\sigma_v\rho_{Fv}\sigma_F(t,T)$	$\frac{\sigma_v^2}{2}$
ST18	$-\frac{1}{2}(u^2 + iu)\sigma_F^2(t,T)$	$-\kappa + iu\sigma_v\rho_{Fv}\sigma_F(t,T)$	$\frac{\sigma_v^2}{2}$
ST21	$-\frac{1}{2}(u^2 + iu)\sigma_F^2(t,T)$	$-\kappa + iu\sigma_v\rho_{Fv}\sigma_F(t,T)$	$\frac{\sigma_v^2}{2}$
SYSSV$^{\checkmark}$	$-\frac{1}{2}(u^2 + iu)(\sigma_S^2 + \sigma_Y^2(t,T) + 2\rho_{Sy}\sigma_S\sigma_Y(t,T))$	$-\kappa + iu\sigma_v(\rho_{Sv}\sigma_S + \rho_{yv}\sigma_Y(t,T))$	$\frac{\sigma_v^2}{2}$
SYSSV*	$-\frac{1}{2}(u^2 + iu)\sigma_F^2(t,T)$	$-\kappa + iu\sigma_v\rho_{Fv}\sigma_F(t,T)$	$\frac{\sigma_v^2}{2}$

NOTES: This table presents the expressions followed by the ODEs for the models described in Section 2.2.2 and our model SYSSV. Observe that BS73, Mer76, Hes93 and Bat96 are expressed in terms of the futures prices. The expression followed by $\sigma_F(t,T)$ in each model can be found in Table 2.3. The expressions followed by the jump terms are

$$n_J = e^{iu\mu_J - \frac{1}{2}\sigma_J^2 u^2} - 1, \qquad m_J = e^{\mu_J + \frac{1}{2}\sigma_J^2} - 1, \tag{2.36}$$

with μ_J and σ_J^2 corresponding to the mean and the variance of the jump in the price, respectively.

Table 2.5: Fourier transforms – solutions to ODEs

Model	$A(\tau)$	$B(\tau)$
BS73	$b_0\tau$	–
Mer76	$(b_0+n_J-ium_J)\tau$	–
Hes93	$\frac{\kappa\theta}{\sigma_v^2}\left((\kappa-iu\sigma_v\rho_{Fv}-d)\tau-2\ln\frac{1-ge^{-d\tau}}{1-g}\right)$	$\frac{\kappa-iu\sigma_v\rho_{Fv}-d}{\sigma_v^2}\left(\frac{1-e^{-d\tau}}{1-ge^{-d\tau}}\right)$
Bat96	$\frac{\kappa\theta}{\sigma_v^2}\left((\kappa-iu\sigma_v\rho_{Fv}-d)\tau-2\ln\frac{1-ge^{-d\tau}}{1-g}\right)+(n_J-ium_J)\tau$	$\frac{\kappa-iu\sigma_v\rho_{Fv}-d}{\sigma_v^2}\left(\frac{1-e^{-d\tau}}{1-ge^{-d\tau}}\right)$
TS09-SV1	$\frac{2\kappa\theta}{\sigma_v^2}\left(\beta\gamma\tau-\mu z-\ln g(z)\right)+k_3$	$\frac{2\gamma}{\sigma_v^2}\left(\beta+\mu z+z\frac{g'(z)}{g(z)}\right)$
ST18	$\frac{2\kappa\theta}{\sigma_v^2}\left(\beta\gamma\tau-\mu z-\ln g(z)\right)+k_3$	$\frac{2\gamma}{\sigma_v^2}\left(\beta+\mu z+z\frac{g'(z)}{g(z)}\right)$
ST21	$m(A_1(\tau)+A_2(\tau)+A_3(\tau)+A_4(\tau)+k_3)$	$\frac{2\gamma}{\sigma_v^2}\left(\beta+\mu z+z\frac{g'(z)}{g(z)}\right)$
SYSSV	$m(A_1(\tau)+A_2(\tau)+A_3(\tau)+A_4(\tau)+A_5(\tau)+A_6(\tau)+A_7(\tau)+k_3)$	$\frac{2\gamma}{\sigma_v^2}\left(\beta+\mu z+z\frac{g'(z)}{g(z)}\right)$
	$A_1(\tau)=a^\theta\left(\beta\tau-\frac{1}{\gamma}\left(\mu z+\ln g(z)\right)\right)$	
	$A_2(\tau)=-b^\theta\frac{\beta}{2\pi}y_\tau^s$	
	$A_3(\tau)=b^\theta\frac{\mu z}{4\pi^2+\gamma^2}\left(\gamma y_\tau^c-2\pi y_\tau^s\right)$	
	$A_4(\tau)=b^\theta\frac{\tau}{\omega}\left(y_0^c g'(\omega^{-1})-\frac{\tau}{2}\left(g'(\omega^{-1})\left(y_0^c\zeta_1-2\pi y_0^s\right)+y_0^c\zeta_2\right)\right)$	
	$A_5(\tau)=c^\theta\frac{\beta}{2\pi}y_\tau^c$	
	$A_6(\tau)=c^\theta\frac{\mu z}{4\pi^2+\gamma^2}\left(2\pi y_\tau^s-\gamma y_\tau^c\right)$	
	$A_7(\tau)=c^\theta\frac{\tau}{\omega}\left(y_0^s g'(\omega^{-1})-\frac{\tau}{2}\left(g'(\omega^{-1})\left(y_0^s\zeta_1+2\pi y_0^c\right)+y_0^s\zeta_2\right)\right)$	

NOTES: This table presents the correspondent solution to the ODEs presented in Table 2.4. Observe that BS73, Mer76, Hes93 and Bat96 are expressed in terms of the futures prices. As per our model SYSSV, these expressions correspond to (2.21)-(2.22). The terms b_0, b_1 and b_2 can be found in expressions (2.23). For TS09-SV1 and our model, $z, g(z), g'(z), \beta, \mu$ are in Appendix 2B.1; for ST18 and ST21, they are in Appendix 2B.2; m is as in expression (2.27). The expressions followed by k_3 in TS09-SV1 and SYSSV can be seen in equations (2.33) and (2.29) or (2.32), correspondingly. The values for n_J, m_J and b_0, b_1, b_2 can be found in Table 2.4. For BS73 and Mer96, observe that $\sigma_Y(t,T)=0$ (equivalently, $\sigma_F(t,T)=\sigma_S$). For Hes93 and Bat96, $\sigma_S=1$ and $\sigma_Y(t,T)=0$ (equivalently, $\sigma_F(t,T)=\sigma_S=1$); for these models, g and d read

$$g=\frac{\kappa-iu\sigma_v\rho_{Fv}+d}{\kappa-iu\sigma_v\rho_{Fv}-d},\qquad d=\sqrt{(\kappa-iu\sigma_v\rho_{Fv})^2+\sigma_v^2(u^2+iu)}. \tag{2.37}$$

Table 2.6: R^2 analysis

(a) R^2 per peak, years 2011-2020

R^2	**1/12**	**2/12**	**3/12**	**4/12**	**5/12**	**6/12**	**7/12**	**8/12**	**9/12**	**10/12**	**11/12**	**12/12**
S	0.66%	0.22%	2.63%	5.47%	5.95%	3.55%	0.66%	0.22%	2.63%	**5.95%**	5.47%	3.55%
$M(b^\theta = 0)$	5.47%	5.95%	3.55%	0.66%	0.22%	2.63%	5.47%	5.95%	3.55%	**0.22%**	0.66%	2.63%
M	6.15%	6.15%	6.15%	6.15%	6.15%	6.15%	6.15%	6.15%	6.15%	**6.15%**	6.15%	6.15%

(b) R^2 per year, peak $t_0 = 10/12$

R^2	**2011**	**2012**	**2013**	**2014**	**2015**	**2016**	**2017**	**2018**	**2019**	**2020**	**All**
S	0.08%	58.76%	7.13%	43.48%	10.09%	1.95%	38.21%	28.73%	**79.12%**	0.67%	5.95%
$M(b^\theta = 0)$	9.96%	14.60%	6.84%	12.66%	41.60%	38.19%	27.74%	9.42%	**6.38%**	23.00%	0.22%
M	10.01%	74.89%	14.16%	58.85%	52.51%	40.48%	66.93%	38.59%	**84.85%**	23.53%	6.15%

(c) R^2 per peak, years 2011-2020 – averaged values

R^2	**1/12**	**2/12**	**3/12**	**4/12**	**5/12**	**6/12**	**7/12**	**8/12**	**9/12**	**10/12**	**11/12**	**12/12**
S	1.78%	23.49%	49.85%	54.40%	32.79%	6.43%	1.78%	23.49%	49.85%	**54.40%**	32.79%	6.43%
$M(b^\theta = 0)$	54.50%	32.79%	6.43%	1.78%	23.49%	49.85%	54.50%	32.79%	6.43%	**1.78%**	23.49%	49.85%
M	56.28%	56.28%	56.28%	56.28%	56.28%	56.28%	56.28%	56.28%	56.28%	**56.28%**	56.28%	56.82%

NOTES: These tables present the values of R^2 calculated when regressing the series of ATM market variance v_t (squared of the quoted volatility) for the shortest futures contract available (in this case, M3) in terms of a cosinus and/or sinus functions. Sub-table (a) considers the whole sample period 2011-2020 and checks the effect of each month as peak of the volatility series. Sub-table (b) considers each year individually in the whole sample period and checks the effect of $t_0 = 10/12$ as peak of the series. Sub-table (c) considers the whole sample period and checks the effect of each month as peak of the series, on averaged values. With $M(b^\theta = 0)$ we refer to a new simple pattern based only on the sinus. In bold we highlight those cases which present higher R^2 values for the simple sinusoidal pattern S.

Table 2.7: MAE(σ) analysis

$MAE(\sigma)$	**1/12**	**2/12**	**3/12**	**4/12**	**5/12**	**6/12**	**7/12**	**8/12**	**9/12**	**10/12**	**11/12**	**12/12**
Ø	4.34%	4.34%	4.34%	4.34%	4.34%	4.34%	4.34%	4.34%	4.34%	**4.34%**	4.34%	4.34%
S	4.35%	4.33%	4.28%	4.26%	4.29%	4.34%	4.33%	4.33%	4.29%	**4.26%**	4.29%	4.33%
M	4.28%	4.31%	4.28%	4.25%	4.25%	4.26%	4.28%	4.31%	4.28%	**4.25%**	4.25%	4.26%

NOTES: This table presents MAE(σ) errors performed by our model, calculated when regressing the series of ATM market variance v_t (squared of the quoted volatility) for the shortest futures contract available (in this case, M3) in terms of a cosinus and/or sinus functions. We use the symbol Ø to identify the lack of seasonality in the variance v_t, this is equivalent to a constant θ_t parameter, namely the TS09-SV1 model. In bold we highlight those cases which present smaller error values for the simple sinusoidal pattern S.

Table 2.8: Estimated parameters, errors and computation time – monthly and daily observations

(a) Monthly observations

Model	**SYSSV**				**ST21**	**ST18**	**TS09-SV1**		**Bat96**	**Hes93**	**Mer76**
Seasonality Type	Multiple		Simple								
Set-up	⋆	✓	⋆	✓			⋆	✓			
σ_S	–	1.0000	–	1.0000	–	–	–	1.0000	–	–	0.2591
α_0	1.5886	–	1.4311	–	–	–	2.4336	–	–	–	–
α	1.0000	1.5454	1.0000	1.5438	–	–	1.0000	1.5144	–	–	–
γ	22.9148	0.2921	13.9186	0.4525	1.2394	1.2475	18.6119	0.2804	–	–	–
κ	17.7878	1.1011	15.1016	1.1192	2.4543	2.4879	40.4542	1.2827	5.8069	5.6512	–
a^θ, θ	0.0276	0.5168	0.0335	0.5028	0.2294	0.2289	0.0100	0.4486	0.0152	0.0774	–
b^θ	0.0037	0.0007	0.0039	0.0013	-0.0070	–	–	–	–	–	–
c^θ	0.0018	-0.0002	–	–	–	–	–	–	–	–	–
σ_v	0.9916	0.5532	0.9175	0.5697	0.3308	0.2630	0.7934	0.5754	0.1375	0.0689	–
ρ_{Sy}	–	-1.0000	–	-1.0000	–	–	–	-1.0000	–	–	–
ρ_{Sv}	–	0.1144	–	0.1042	–	–	–	0.2191	-1.0000	0.9999	–
ρ_{yv}	–	-0.1300	–	-0.1092	–	–	–	-0.3845	–	–	–
ρ_{Fv}	0.0872	–	0.0972	–	0.1800	0.2242	0.1647	–	–	–	–
λ	–	–	–	–	–	–	–	–	5.3309	–	5.9153
μ_J	–	–	–	–	–	–	–	–	0.0451	–	0.0737
σ_J	–	–	–	–	–	–	–	–	0.0803	–	0.0013
Parameter Count	9	11	8	10	6	5	7	9	7	4	4
MAE(σ)	0.0416	0.0425	0.0420	0.0426	0.0434	0.0436	0.0433	0.0434	0.0432	0.0480	0.0766
RMSE(σ)	0.0586	0.0596	0.0591	0.0597	0.0607	0.0608	0.0600	0.0605	0.0611	0.0657	0.1002
Comput. Time	0.1474	0.1567	0.1149	0.0785	0.0394	0.0639	0.1219	0.1108	0.6661	0.0981	0.2204

(b) Daily observations

Model	**SYSSV**				**ST21**	**ST18**	**TS09-SV1**		**Bat96**	**Hes93**	**Mer76**
Seasonality Type	Multiple		Simple								
Set-up	⋆	✓	⋆	✓			⋆	✓			
σ_S	–	1.0000	–	1.0000	–	–	–	1.0000	–	–	0.2826
α_0	1.8058	–	1.4354	–	–	–	1.5586	–	–	–	–
α	1.0000	1.4060	1.0000	1.4268	–	–	1.0000	1.4082	–	–	–
γ	24.7212	0.4387	21.2379	0.2795	1.2230	1.2598	24.0451	0.2953	–	–	–
κ	21.4165	1.2444	13.9554	1.2389	2.1558	2.1077	16.1562	1.3894	5.6808	5.8078	–
a^θ, θ	0.0197	0.4190	0.0349	0.4507	0.3013	0.3435	0.0284	0.4150	0.0300	0.0893	–
b^θ	0.0018	-0.0000	0.0012	0.0002	-0.0095	–	–	–	–	–	–
c^θ	0.0023	-0.0003	–	–	–	–	–	–	–	–	–
σ_v	0.9191	0.5383	0.9870	0.6194	0.2579	0.2923	0.9548	0.6638	0.2324	0.0769	–
ρ_{Sy}	–	-0.9999	–	-0.9991	–	–	–	-0.9994	–	–	–
ρ_{Sv}	–	0.0240	–	0.0865	–	–	–	0.1214	-1.0000	0.9987	–
ρ_{yv}	–	-0.0184	–	-0.1076	–	–	–	-0.1875	–	–	–
ρ_{Fv}	0.1079	–	0.0918	–	0.1962	0.2471	0.0976	–	–	–	–
λ	–	–	–	–	–	–	–	–	1.1827	–	2.0685
μ_J	–	–	–	–	–	–	–	–	0.1816	–	0.1149
σ_J	–	–	–	–	–	–	–	–	0.0352	–	0.0000
Parameter Count	9	11	8	10	6	5	7	9	7	4	4
MAE(σ)	0.0437	0.0438	0.0443	0.0442	0.0445	0.0446	0.0442	0.0444	0.0439	0.0463	0.0670
RMSE(σ)	0.0620	0.0625	0.0625	0.0625	0.0626	0.0627	0.0624	0.0626	0.0632	0.0660	0.0950
Comput. Time	3.8576	5.9236	2.0122	2.0370	0.7694	0.6831	1.1509	1.1935	9.0950	2.3092	4.6260

NOTES: MAE(σ) represents the mean absolute pricing error in option volatilities, RMSE(σ) represents the square root of the quadratic mean of errors in option volatilities. For the computation time we use analytical solutions; values are expressed in hours.

Table 2.9: Estimated parameters, errors and computation time – monthly observations, single years

(a) 2019

Model	**SYSSV**				**ST21**	**ST18**	**TS09-SV1**		**Bat96**	**Hes93**	**Mer76**
Seasonality Type	Multiple		Simple								
Set-up	$\star$	✓	$\star$	✓			$\star$	✓			
σ_S	–	1.0000	–	1.0000	–	–	–	1.0000	–	–	0.2697
α_0	1.6432	–	1.5596	–	–	–	2.0264	–	–	–	–
α	1.0000	1.4298	1.0000	1.5470	–	–	1.0000	1.6168	–	–	–
γ	13.7456	0.3180	15.3799	0.3035	1.3576	1.4247	33.1492	0.3769	–	–	–
κ	19.7671	1.7262	17.9145	1.3992	2.5633	2.6944	26.9385	1.7346	6.8128	6.5113	–
a^θ, θ	0.0203	0.3175	0.0234	0.3936	0.2095	0.2168	0.0121	0.3478	0.0001	0.0661	–
b^θ	0.0027	0.0004	0.0032	0.0008	-0.0088	–	–	–	–	–	–
c^θ	0.0010	-0.0005	–	–	–	–	–	–	–	–	–
σ_v	0.8159	0.6970	0.9048	0.6954	0.7529	0.8017	0.6763	0.7550	0.0831	0.0733	–
ρ_{Sy}	–	-1.0000	–	-1.0000	–	–	–	-1.0000	–	–	–
ρ_{Sv}	–	0.0768	–	0.1028	–	–	–	0.1104	1.0000	0.7453	–
ρ_{yv}	–	-0.1668	–	-0.1999	–	–	–	-0.2431	–	–	–
ρ_{Fv}	0.1158	–	0.1013	–	0.0656	0.0657	0.1491	–	–	–	–
λ	–	–	–	–	–	–	–	–	3.1753	–	0.4189
μ_J	–	–	–	–	–	–	–	–	-0.0102	–	0.1473
σ_J	–	–	–	–	–	–	–	–	0.1304	–	0.0009
Parameter Count	9	11	8	10	6	5	7	9	7	4	4
MAE(σ)	0.0537	0.0536	0.0540	0.0549	0.0542	0.0544	0.0540	0.0544	0.0561	0.0601	0.0790
RMSE(σ)	0.0679	0.0677	0.0681	0.0686	0.0698	0.0697	0.0689	0.0691	0.0709	0.0766	0.1052
Comput. Time	0.0104	0.1781	0.0151	0.2136	0.0142	0.0130	0.0098	0.0754	0.0373	0.0182	0.0161

(b) 2020

Model	**SYSSV**				**ST21**	**ST18**	**TS09-SV1**		**Bat96**	**Hes93**	**Mer76**
Seasonality Type	Multiple		Simple								
Set-up	$\star$	✓	$\star$	✓			$\star$	✓			
σ_S	–	1.0000	–	1.0000	–	–	–	1.0000	–	–	0.3672
α_0	1.4472	–	1.3812	–	–	–	1.4591	–	–	–	–
α	1.0000	1.4651	1.0000	1.4677	–	–	1.0000	1.2039	–	–	–
γ	15.1775	0.5065	20.6621	0.5008	1.0145	0.9789	14.3886	0.2657	–	–	–
κ	14.3425	0.9107	12.7726	0.9857	2.0569	1.9654	10.0686	1.7874	4.4405	3.2484	–
a^θ, θ	0.0398	0.6223	0.0427	0.6390	0.2170	1.1986	0.0121	0.3501	0.0010	0.0161	–
b^θ	0.0105	0.0061	0.0037	0.0066	-0.0279	–	–	–	–	–	–
c^θ	0.0018	-0.0010	–	–	–	–	–	–	–	–	–
σ_v	0.3793	0.4924	0.0500	0.5079	0.1330	0.1562	0.0836	0.5801	0.0515	0.0749	–
ρ_{Sy}	–	-0.9992	–	-0.9998	–	–	–	-0.9979	–	–	–
ρ_{Sv}	–	0.0204	–	0.0379	–	–	–	0.1399	0.7723	0.9998	–
ρ_{yv}	–	0.0045	–	0.0147	–	–	–	-0.2782	–	–	–
ρ_{Fv}	0.2465	–	0.2249	–	0.5812	0.5417	0.9998	–	–	–	–
λ	–	–	–	–	–	–	–	–	7.0755	–	7.3694
μ_J	–	–	–	–	–	–	–	–	0.0762	–	0.0712
σ_J	–	–	–	–	–	–	–	–	0.0018	–	0.0009
Parameter Count	9	11	8	10	6	5	7	9	7	4	4
MAE(σ)	0.0543	0.0540	0.0538	0.0548	0.0577	0.0588	0.0554	0.0573	0.0601	0.0639	0.1052
RMSE(σ)	0.0684	0.0696	0.0681	0.00704	0.0757	0.0765	0.0701	0.0750	0.0766	0.0822	0.1276
Comput. Time	0.0107	0.2723	0.0155	0.2736	0.0112	0.0154	0.0126	0.0754	0.0481	0.0188	0.0215

NOTES: MAE(σ) represents the mean absolute pricing error in option volatilities, RMSE(σ) represents the square root of the quadratic mean of errors in option volatilities. For the computation time we use analytical solutions; values are expressed in hours.

Table 2.10: MAE(σ) – simple harmonic pattern and original set-up

(a) TS09-SV1

MAE(σ)	M2	M3	M4	M5	M6	M7	M8	ALL
p – 7.5	0.0798	0.0557	0.0502	0.0487	0.0424	0.0345	0.0328	0.0492
p – 7	0	0.0540	0.0504	0.0459	0.0425	0.0351	0.0337	0.0436
p – 6.5	0	0.0498	0.0486	0.0478	0.0420	0.0353	0.0327	0.0427
p – 6	0	0.0501	0.0483	0.0483	0.0447	0.0364	0.0327	0.0434
p – 5.5	0	0.0451	0.0478	0.0470	0.0440	0.0342	0.0320	0.0417
p – 5	0.0657	0.0445	0.0462	0.0465	0.0436	0.034	0.0326	0.0447
p – 4.5	0.0937	0.0427	0.0451	0.0453	0.0457	0.0345	0.0317	0.0484
p – 4	0.0532	0.0420	0.0444	0.0475	0.0438	0.0345	0.0316	0.0424
p – 3.5	0.0463	0.0410	0.0445	0.0464	0.0454	0.0343	0.0319	0.0414
p – 3	0.0424	0.0398	0.0437	0.0473	0.0457	0.0353	0.0314	0.0408
p – 2.5	0.0397	0.0389	0.0438	0.0478	0.0457	0.0358	0.0320	0.0405
p – 2	0	0.0372	0.0435	0.0472	0.0465	0.0337	0.0321	0.0400
p – 1.5	0.0388	0.0374	0.0444	0.0489	0.0494	0.0352	0.0327	0.0410
p – 1	0.0604	0.0367	0.0446	0.0491	0.0473	0.0375	0.0325	0.0440
p – 0.5	0.0378	0.0361	0.0443	0.0489	0.0480	0.0363	0.0318	0.0405
ATM p	0.0369	0.0354	0.0432	0.0472	0.0471	0.0351	0.0305	0.0393
ATM c	0.0371	0.0363	0.0445	0.0483	0.0471	0.0359	0.0324	0.0402
c + 0.5	0	0.0351	0.0430	0.0481	0.0476	0.0373	0.0315	0.0404
c + 1	0	0.0351	0.0434	0.0486	0.0481	0.0383	0.0317	0.0409
c + 1.5	0	0.0354	0.0434	0.0480	0.0481	0.0379	0.0323	0.0409
c + 2	0	0.0354	0.0442	0.0496	0.0490	0.0384	0.0325	0.0415
c + 2.5	0	0.0357	0.0442	0.0496	0.0501	0.0378	0.0337	0.0418
c + 3	0	0.0362	0.0447	0.0503	0.0499	0.0397	0.0342	0.0425
c + 3.5	0.0577	0.0368	0.0447	0.0502	0.0514	0.0389	0.0348	0.0449
c + 4	0	0.0369	0.0451	0.0519	0.0519	0.0405	0.0350	0.0436
c + 4.5	0.0605	0.0371	0.0452	0.0521	0.0529	0.0412	0.0351	0.0463
c + 5	0.0623	0.0375	0.0458	0.0513	0.0533	0.0411	0.0359	0.0467
c + 5.5	0	0.0380	0.0463	0.0520	0.0536	0.0424	0.0374	0.045
c + 6	0.0567	0.0387	0.0466	0.0532	0.0559	0.0433	0.0372	0.0474
c + 6.5	0	0.0386	0.0472	0.0524	0.0556	0.0426	0.0371	0.0456
c + 7	0	0.0389	0.0466	0.0545	0.0552	0.0438	0.0386	0.0463
c + 7.5	0.0671	0.0396	0.0478	0.0532	0.0557	0.0459	0.0387	0.0497
ALL	0.0551	0.0399	0.0455	0.0492	0.0484	0.0377	0.0335	0.0434

(b) SYSSV^S

MAE(σ)	M2	M3	M4	M5	M6	M7	M8	ALL
p – 7.5	0.0750	0.0497	0.0487	0.0488	0.0422	0.0337	0.0325	0.0472
p – 7	0	0.0474	0.0479	0.0459	0.0425	0.0341	0.0326	0.0417
p – 6.5	0	0.0464	0.0466	0.0479	0.0421	0.0347	0.032	0.0416
p – 6	0	0.0465	0.0466	0.0485	0.0446	0.0357	0.0315	0.0422
p – 5.5	0	0.0418	0.0459	0.0473	0.0440	0.0334	0.0309	0.0405
p – 5	0.0527	0.0414	0.0445	0.0464	0.0437	0.0333	0.0313	0.0419
p – 4.5	0.0870	0.0399	0.0433	0.0460	0.0459	0.0336	0.0308	0.0466
p – 4	0.0460	0.0391	0.0425	0.0481	0.0442	0.0337	0.0303	0.0406
p – 3.5	0.0416	0.0382	0.0430	0.0471	0.0455	0.0334	0.0310	0.0400
p – 3	0.0395	0.0372	0.0421	0.0475	0.0457	0.0344	0.0305	0.0396
p – 2.5	0.0373	0.0362	0.0426	0.0479	0.0460	0.0349	0.0312	0.0395
p – 2	0	0.0346	0.0420	0.0476	0.0467	0.0329	0.0310	0.0391
p – 1.5	0.0359	0.0350	0.0431	0.0494	0.0497	0.0344	0.0319	0.0399
p – 1	0.0558	0.0344	0.0436	0.0495	0.0477	0.0369	0.0316	0.0428
p – 0.5	0.0345	0.0341	0.0436	0.0493	0.0482	0.0356	0.0311	0.0395
ATM p	0.0338	0.0333	0.0423	0.0475	0.0474	0.0345	0.0305	0.0385
ATM c	0.0338	0.0343	0.0439	0.0487	0.0473	0.0351	0.0319	0.0393
c + 0.5	0	0.0331	0.0421	0.0486	0.0479	0.0366	0.0314	0.0400
c + 1	0	0.0333	0.0429	0.0491	0.0484	0.0377	0.0315	0.0405
c + 1.5	0	0.0339	0.0430	0.0486	0.0486	0.0374	0.0321	0.0406
c + 2	0	0.0341	0.0439	0.0503	0.0494	0.0379	0.0324	0.0413
c + 2.5	0	0.0346	0.0438	0.0505	0.0505	0.0374	0.0336	0.0417
c + 3	0	0.0353	0.0446	0.0512	0.0503	0.0393	0.0340	0.0425
c + 3.5	0.0568	0.0361	0.0447	0.0510	0.0518	0.0387	0.0343	0.0448
c + 4	0	0.0364	0.0452	0.0528	0.0523	0.0404	0.0345	0.0436
c + 4.5	0.0600	0.0367	0.0452	0.0530	0.0533	0.0409	0.0349	0.0463
c + 5	0.0616	0.0373	0.0464	0.0524	0.0536	0.0411	0.0354	0.0468
c + 5.5	0	0.038	0.0471	0.0530	0.0540	0.0422	0.0369	0.0452
c + 6	0.0558	0.0388	0.0475	0.0546	0.0565	0.0432	0.0368	0.0476
c + 6.5	0	0.0388	0.0482	0.0538	0.0560	0.0424	0.0366	0.0460
c + 7	0	0.0391	0.0477	0.0559	0.0556	0.0435	0.0382	0.0467
c + 7.5	0.0663	0.0397	0.0490	0.0544	0.0562	0.0457	0.0383	0.0499
ALL	0.0514	0.0380	0.0448	0.0498	0.0487	0.0371	0.0329	0.0426

(c) Diff. TS09-SV1 – SYSSV^S

MAE(σ)	M2	M3	M4	M5	M6	M7	M8	ALL
p – 7.5	0.0048	0.0059	0.0014	-0.0001	0.0002	0.0008	0.0003	0.0019
p – 7	0	0.0067	0.0025	0.0000	0.0000	0.0010	0.0010	0.0019
p – 6.5	0	0.0033	0.0020	0.0000	-0.0001	0.0007	0.0007	0.0011
p – 6	0	0.0037	0.0017	-0.0002	0.0001	0.0006	0.0012	0.0012
p – 5.5	0	0.0033	0.0020	-0.0003	0.0000	0.0008	0.0012	0.0012
p – 5	0.0130	0.0031	0.0016	0.0001	-0.0001	0.0007	0.0012	0.0028
p – 4.5	0.0068	0.0028	0.0018	-0.0007	-0.0002	0.0009	0.0009	0.0018
p – 4	0.0072	0.0029	0.0019	-0.0006	-0.0004	0.0008	0.0014	0.0019
p – 3.5	0.0047	0.0028	0.0015	-0.0006	0.0000	0.0009	0.0010	0.0015
p – 3	0.0029	0.0026	0.0016	-0.0003	0.0000	0.0008	0.0009	0.0012
p – 2.5	0.0024	0.0027	0.0012	-0.0001	-0.0003	0.0009	0.0008	0.0011
p – 2	0	0.0026	0.0015	-0.0003	-0.0002	0.0008	0.0010	0.0009
p – 1.5	0.0030	0.0024	0.0013	-0.0005	-0.0003	0.0008	0.0008	0.0011
p – 1	0.0046	0.0024	0.0009	-0.0004	-0.0005	0.0006	0.0010	0.0012
p – 0.5	0.0034	0.0020	0.0008	-0.0004	-0.0001	0.0007	0.0007	0.0010
ATM p	0.0031	0.0021	0.0009	-0.0003	-0.0003	0.0006	0.0001	0.0009
ATM c	0.0034	0.0021	0.0006	-0.0004	-0.0002	0.0008	0.0005	0.0010
c + 0.5	0	0.0020	0.0008	-0.0006	-0.0003	0.0007	0.0001	0.0005
c + 1	0	0.0019	0.0006	-0.0005	-0.0003	0.0006	0.0002	0.0004
c + 1.5	0	0.0016	0.0005	-0.0005	-0.0005	0.0006	0.0001	0.0003
c + 2	0	0.0013	0.0003	-0.0008	-0.0003	0.0005	0.0001	0.0002
c + 2.5	0	0.0011	0.0003	-0.0009	-0.0004	0.0004	0.0001	0.0001
c + 3	0	0.0009	0.0001	-0.0009	-0.0004	0.0004	0.0003	0.0000
c + 3.5	0.0010	0.0007	0.0001	-0.0008	-0.0004	0.0002	0.0004	0.0002
c + 4	0	0.0005	-0.0001	-0.0009	-0.0004	0.0002	0.0004	-0.0001
c + 4.5	0.0005	0.0004	0.0000	-0.0009	-0.0004	0.0003	0.0002	0.0000
c + 5	0.0007	0.0002	-0.0006	-0.0012	-0.0003	0.0000	0.0005	-0.0001
c + 5.5	0	0.0000	-0.0008	-0.0010	-0.0004	0.0002	0.0005	-0.0003
c + 6	0.0009	-0.0001	-0.0009	-0.0014	-0.0006	0.0001	0.0003	-0.0002
c + 6.5	0	-0.0002	-0.0010	-0.0014	-0.0005	0.0002	0.0005	-0.0004
c + 7	0	-0.0002	-0.0011	-0.0014	-0.0004	0.0003	0.0005	-0.0004
c + 7.5	0.0009	-0.0001	-0.0011	-0.0012	-0.0004	0.0003	0.0004	-0.0002
ALL	0.0037	0.0020	0.0007	-0.0006	-0.0003	0.0006	0.0006	0.0008

NOTES: This table reports model accuracy in terms if options MAE(σ) within each moneyness-maturity category, with the estimations performed on the monthly data set. p – (c +) i refers to the put (call) options with strike equal to the ATM strike – (+) i USD. Only the central row refers to ATM options, all the others refer to OTM options; strikes are increasing. Sub-table (a) refers to TS09-SV1 and Sub-table (b) refers to SYSSV^S, both models expressed following the original set-up of the parameters: observe that the darker the color of the cell (red), the worse the model performance. Sub-table (c) indicates the difference between both models; the darker the color of the cell (blue), the better the performance of our model. Values of 0 indicate the lack of quoted options for this combination of contract and moneyness.

Table 2.11: MAE(σ) – multiple harmonic pattern and original set-up

(a) TS09-SV1

MAE(σ)	M2	M3	M4	M5	M6	M7	M8	ALL
p – 7.5	0.0798	0.0557	0.0502	0.0487	0.0424	0.0345	0.0328	0.0492
p – 7	0	0.0540	0.0504	0.0459	0.0425	0.0351	0.0337	0.0436
p – 6.5	0	0.0498	0.0486	0.0478	0.0420	0.0353	0.0327	0.0427
p – 6	0	0.0501	0.0483	0.0483	0.0447	0.0364	0.0327	0.0434
p – 5.5	0	0.0451	0.0478	0.0470	0.0440	0.0342	0.0320	0.0417
p – 5	0.0657	0.0445	0.0462	0.0465	0.0436	0.0340	0.0326	0.0447
p – 4.5	0.0937	0.0427	0.0451	0.0453	0.0457	0.0345	0.0317	0.0484
p – 4	0.0532	0.0420	0.0444	0.0475	0.0438	0.0345	0.0316	0.0424
p – 3.5	0.0463	0.0410	0.0445	0.0464	0.0454	0.0343	0.0319	0.0414
p – 3	0.0424	0.0398	0.0437	0.0473	0.0457	0.0353	0.0314	0.0408
p – 2.5	0.0397	0.0389	0.0438	0.0478	0.0457	0.0358	0.0320	0.0405
p – 2	0	0.0372	0.0435	0.0472	0.0465	0.0337	0.0321	0.0400
p – 1.5	0.0388	0.0374	0.0444	0.0489	0.0494	0.0352	0.0327	0.0410
p – 1	0.0604	0.0367	0.0446	0.0491	0.0473	0.0375	0.0325	0.0440
p – 0.5	0.0378	0.0361	0.0443	0.0489	0.0480	0.0363	0.0318	0.0405
ATM p	0.0369	0.0354	0.0432	0.0472	0.0471	0.0351	0.0305	0.0393
ATM c	0.0371	0.0363	0.0445	0.0483	0.0471	0.0359	0.0324	0.0402
c + 0.5	0	0.0351	0.0430	0.0481	0.0476	0.0373	0.0315	0.0404
c + 1	0	0.0351	0.0434	0.0486	0.0481	0.0383	0.0317	0.0409
c + 1.5	0	0.0354	0.0434	0.0480	0.0481	0.0379	0.0323	0.0409
c + 2	0	0.0354	0.0442	0.0496	0.0490	0.0384	0.0325	0.0415
c + 2.5	0	0.0357	0.0442	0.0496	0.0501	0.0378	0.0337	0.0418
c + 3	0	0.0362	0.0447	0.0503	0.0499	0.0397	0.0342	0.0425
c + 3.5	0.0577	0.0368	0.0447	0.0502	0.0514	0.0389	0.0348	0.0449
c + 4	0	0.0369	0.0451	0.0519	0.0519	0.0405	0.0350	0.0436
c + 4.5	0.0605	0.0371	0.0452	0.0521	0.0529	0.0412	0.0351	0.0463
c + 5	0.0623	0.0375	0.0458	0.0513	0.0533	0.0411	0.0359	0.0467
c + 5.5	0	0.0380	0.0463	0.0520	0.0536	0.0424	0.0374	0.0450
c + 6	0.0567	0.0387	0.0466	0.0532	0.0559	0.0433	0.0372	0.0474
c + 6.5	0	0.0386	0.0472	0.0524	0.0556	0.0426	0.0371	0.0456
c + 7	0	0.0389	0.0466	0.0545	0.0552	0.0438	0.0386	0.0463
c + 7.5	0.0671	0.0396	0.0478	0.0532	0.0557	0.0459	0.0387	0.0497
ALL	0.0551	0.0399	0.0455	0.0492	0.0484	0.0377	0.0335	0.0434

(b) SYSSV^M

MAE(σ)	M2	M3	M4	M5	M6	M7	M8	ALL
p – 7.5	0.0623	0.0470	0.0473	0.0481	0.0416	0.0332	0.0321	0.0445
p – 7	0	0.0468	0.0461	0.0455	0.0423	0.0334	0.0327	0.0411
p – 6.5	0	0.0440	0.0453	0.0473	0.0420	0.0341	0.0318	0.0407
p – 6	0	0.0442	0.0455	0.0480	0.0442	0.0351	0.0315	0.0414
p – 5.5	0	0.0397	0.0446	0.0467	0.0436	0.0328	0.0310	0.0397
p – 5	0.0494	0.0393	0.0434	0.0460	0.0434	0.0328	0.0313	0.0408
p – 4.5	0.0785	0.0378	0.0422	0.0457	0.0457	0.0331	0.0306	0.0448
p – 4	0.0437	0.0369	0.0413	0.0477	0.0440	0.0332	0.0303	0.0396
p – 3.5	0.0396	0.0361	0.0420	0.0467	0.0452	0.0329	0.0308	0.0391
p – 3	0.0373	0.0354	0.0410	0.0470	0.0453	0.0339	0.0304	0.0386
p – 2.5	0.0347	0.0344	0.0417	0.0474	0.0456	0.0345	0.0310	0.0385
p – 2	0	0.0330	0.0410	0.0471	0.0464	0.0324	0.0309	0.0385
p – 1.5	0.0333	0.0334	0.0421	0.0489	0.0492	0.0338	0.0316	0.0389
p – 1	0.0513	0.0329	0.0427	0.0490	0.0472	0.0364	0.0315	0.0416
p – 0.5	0.0322	0.0327	0.0427	0.0488	0.0476	0.0351	0.0310	0.0386
ATM p	0.0318	0.0320	0.0415	0.0469	0.0468	0.0341	0.0304	0.0377
ATM c	0.0317	0.0329	0.0431	0.0480	0.0468	0.0345	0.0317	0.0384
c + 0.5	0	0.0319	0.0413	0.0480	0.0473	0.0361	0.0314	0.0393
c + 1	0	0.0321	0.0421	0.0485	0.0479	0.0372	0.0315	0.0399
c + 1.5	0	0.0328	0.0422	0.0479	0.0480	0.0370	0.0321	0.0400
c + 2	0	0.0331	0.0431	0.0495	0.0488	0.0375	0.0324	0.0408
c + 2.5	0	0.0337	0.0431	0.0495	0.0500	0.0372	0.0335	0.0412
c + 3	0	0.0344	0.0438	0.0503	0.0499	0.0390	0.0339	0.0419
c + 3.5	0.0557	0.0352	0.0438	0.0501	0.0515	0.0387	0.0342	0.0442
c + 4	0	0.0356	0.0444	0.0517	0.0519	0.0402	0.0344	0.0430
c + 4.5	0.0595	0.0360	0.0444	0.0519	0.0530	0.0404	0.0348	0.0457
c + 5	0.0613	0.0365	0.0454	0.0513	0.0534	0.0409	0.0352	0.0463
c + 5.5	0	0.0374	0.0461	0.0518	0.0538	0.0417	0.0368	0.0446
c + 6	0.0562	0.0383	0.0463	0.0532	0.0559	0.0428	0.0367	0.0471
c + 6.5	0	0.0383	0.0470	0.0523	0.0558	0.0419	0.0364	0.0453
c + 7	0	0.0387	0.0465	0.0544	0.0554	0.0428	0.0380	0.0460
c + 7.5	0.0657	0.0395	0.0478	0.0531	0.0559	0.0452	0.0381	0.0493
ALL	0.0485	0.0366	0.0438	0.0490	0.0483	0.0367	0.0328	0.0418

(c) Diff. TS09-SV1 – SYSSV^M

MAE(σ)	M2	M3	M4	M5	M6	M7	M8	ALL
p – 7.5	0.0174	0.0087	0.0029	0.0006	0.0007	0.0013	0.0007	0.0046
p – 7	0	0.0072	0.0043	0.0004	0.0002	0.0018	0.0010	0.0025
p – 6.5	0	0.0057	0.0033	0.0006	0.0000	0.0012	0.0009	0.0019
p – 6	0	0.0059	0.0029	0.0003	0.0005	0.0013	0.0011	0.0020
p – 5.5	0	0.0054	0.0032	0.0003	0.0003	0.0014	0.0011	0.0020
p – 5	0.0164	0.0052	0.0028	0.0006	0.0002	0.0012	0.0013	0.0039
p – 4.5	0.0153	0.0049	0.0028	-0.0004	0.0001	0.0014	0.0011	0.0036
p – 4	0.0095	0.0051	0.0030	-0.0002	-0.0001	0.0013	0.0013	0.0028
p – 3.5	0.0067	0.0049	0.0026	-0.0003	0.0002	0.0014	0.0011	0.0024
p – 3	0.0051	0.0045	0.0026	0.0002	0.0004	0.0014	0.0010	0.0022
p – 2.5	0.0050	0.0044	0.0022	0.0003	0.0001	0.0013	0.0010	0.0020
p – 2	0	0.0042	0.0025	0.0001	0.0001	0.0013	0.0011	0.0016
p – 1.5	0.0056	0.0040	0.0023	0.0000	0.0002	0.0014	0.0010	0.0021
p – 1	0.0090	0.0039	0.0018	0.0002	0.0001	0.0011	0.0010	0.0024
p – 0.5	0.0057	0.0034	0.0016	0.0000	0.0004	0.0011	0.0008	0.0019
ATM p	0.0051	0.0033	0.0017	0.0003	0.0002	0.0010	0.0001	0.0017
ATM c	0.0054	0.0034	0.0014	0.0003	0.0003	0.0014	0.0007	0.0018
c + 0.5	0	0.0032	0.0016	0.0001	0.0003	0.0012	0.0001	0.0011
c + 1	0	0.0030	0.0013	0.0001	0.0002	0.0011	0.0002	0.0010
c + 1.5	0	0.0026	0.0012	0.0001	0.0002	0.0009	0.0002	0.0009
c + 2	0	0.0023	0.0011	0.0000	0.0002	0.0009	0.0001	0.0008
c + 2.5	0	0.0020	0.0010	0.0001	0.0001	0.0006	0.0002	0.0007
c + 3	0	0.0018	0.0009	0.0000	0.0000	0.0007	0.0003	0.0006
c + 3.5	0.0021	0.0015	0.0009	0.0001	-0.0001	0.0002	0.0005	0.0007
c + 4	0	0.0013	0.0008	0.0001	0.0000	0.0003	0.0006	0.0005
c + 4.5	0.0010	0.0011	0.0008	0.0002	-0.0001	0.0008	0.0003	0.0006
c + 5	0.0010	0.0009	0.0004	0.0000	-0.0002	0.0002	0.0007	0.0004
c + 5.5	0	0.0006	0.0002	0.0001	-0.0002	0.0007	0.0006	0.0004
c + 6	0.0006	0.0005	0.0003	0.0000	0.0000	0.0005	0.0004	0.0003
c + 6.5	0	0.0003	0.0002	0.0001	-0.0002	0.0007	0.0007	0.0003
c + 7	0	0.0002	0.0001	0.0001	-0.0002	0.0010	0.0007	0.0003
c + 7.5	0.0014	0.0001	0.0000	0.0002	-0.0002	0.0008	0.0006	0.0004
ALL	0.0066	0.0033	0.0017	0.0001	0.0001	0.0010	0.0007	0.0016

NOTES: This table reports model accuracy in terms if options MAE(σ) within each moneyness-maturity category, with the estimations performed on the monthly data set. p – (c +) i refers to the put (call) options with strike equal to the ATM strike – (+) i USD. Only the central row refers to ATM options, the others refer to OTM options; strikes are increasing. Sub-table (a) refers to TS09-SV1 and Sub-table (b) refers to SYSSV^M, both models expressed following the original set-up of the parameters: observe that the darker the color of the cell (red), the worse the model performance. Sub-table (c) indicates the difference between both models; the darker the color of the cell (blue), the better the performance of our model. Values of 0 indicate the lack of quoted options for this combination of contract and moneyness.

Table 2.12: MAE(σ) – simple harmonic pattern and alternative set-up

(a) TS09-SV1

MAE(σ)	M2	M3	M4	M5	M6	M7	M8	ALL
p – 7.5	0.0672	0.0450	0.0499	0.0515	0.0456	0.0337	0.0307	0.0462
p – 7	0	0.0430	0.0496	0.0481	0.0450	0.0334	0.0315	0.0418
p – 6.5	0	0.0412	0.0478	0.0495	0.0434	0.0341	0.0309	0.0411
p – 6	0	0.0415	0.0474	0.0493	0.0463	0.0350	0.0310	0.0417
p – 5.5	0	0.0373	0.0467	0.0477	0.0451	0.0324	0.0306	0.0400
p – 5	0.0594	0.0367	0.0451	0.0475	0.0445	0.0324	0.0310	0.0424
p – 4.5	0.0593	0.0356	0.0438	0.0455	0.0463	0.0326	0.0308	0.0420
p – 4	0.0576	0.0346	0.0429	0.0478	0.0442	0.0328	0.0310	0.0416
p – 3.5	0.0580	0.0339	0.0433	0.0465	0.0459	0.0326	0.0315	0.0417
p – 3	0.0577	0.0337	0.0422	0.0473	0.0458	0.0336	0.0312	0.0416
p – 2.5	0.0593	0.0328	0.0426	0.0479	0.0456	0.0342	0.0318	0.0420
p – 2	0	0.0319	0.0422	0.0471	0.0466	0.0322	0.0321	0.0387
p – 1.5	0.0625	0.0324	0.0432	0.0485	0.0491	0.0337	0.0327	0.0431
p – 1	0.0506	0.0318	0.0436	0.0489	0.0471	0.0363	0.0335	0.0417
p – 0.5	0.0660	0.0323	0.0435	0.0487	0.0481	0.0351	0.0327	0.0438
ATM p	0.0662	0.0322	0.0423	0.0471	0.0472	0.0341	0.0320	0.0430
ATM c	0.0675	0.0327	0.0438	0.0484	0.0473	0.0346	0.0332	0.0439
c + 0.5	0	0.0324	0.0421	0.0478	0.0478	0.0362	0.0331	0.0399
c + 1	0	0.0332	0.0428	0.0484	0.0484	0.0372	0.0334	0.0406
c + 1.5	0	0.0343	0.0429	0.0480	0.0483	0.0371	0.0338	0.0407
c + 2	0	0.0348	0.0438	0.0492	0.0494	0.0378	0.0340	0.0415
c + 2.5	0	0.0356	0.0437	0.0494	0.0506	0.0374	0.0351	0.0420
c + 3	0	0.0366	0.0443	0.0501	0.0504	0.0393	0.0357	0.0427
c + 3.5	0.0604	0.0374	0.0444	0.0502	0.0519	0.0389	0.0358	0.0456
c + 4	0	0.0379	0.0448	0.0517	0.0525	0.0405	0.0366	0.0440
c + 4.5	0.0612	0.0382	0.0448	0.0521	0.0534	0.0408	0.0364	0.0467
c + 5	0.0610	0.0391	0.0456	0.0511	0.0541	0.0412	0.0372	0.0470
c + 5.5	0	0.0399	0.0463	0.0520	0.0543	0.0422	0.0390	0.0456
c + 6	0.0618	0.0402	0.0464	0.0529	0.0561	0.0432	0.0384	0.0485
c + 6.5	0	0.0405	0.0470	0.0522	0.0563	0.0424	0.0385	0.0462
c + 7	0	0.0404	0.0463	0.0546	0.0560	0.0433	0.0399	0.0467
c + 7.5	0.0626	0.0410	0.0475	0.0534	0.0565	0.0455	0.0394	0.0494
ALL	0.0611	0.0366	0.0448	0.0494	0.0490	0.0367	0.0339	0.0433

(b) SYSSV^S

MAE(σ)	M2	M3	M4	M5	M6	M7	M8	ALL
p – 7.5	0.0623	0.0470	0.0473	0.0481	0.0416	0.0332	0.0321	0.0445
p – 7	0	0.0468	0.0461	0.0455	0.0423	0.0334	0.0327	0.0411
p – 6.5	0	0.0440	0.0453	0.0473	0.0420	0.0341	0.0318	0.0407
p – 6	0	0.0442	0.0455	0.0480	0.0442	0.0351	0.0315	0.0414
p – 5.5	0	0.0397	0.0446	0.0467	0.0436	0.0328	0.0310	0.0397
p – 5	0.0494	0.0393	0.0434	0.0460	0.0434	0.0328	0.0313	0.0408
p – 4.5	0.0785	0.0378	0.0422	0.0457	0.0457	0.033	0.0306	0.0448
p – 4	0.0437	0.0369	0.0413	0.0477	0.0440	0.0332	0.0303	0.0396
p – 3.5	0.0396	0.0361	0.0420	0.0467	0.0452	0.0329	0.0308	0.0391
p – 3	0.0373	0.0354	0.0410	0.0470	0.0453	0.0339	0.0304	0.0386
p – 2.5	0.0347	0.0344	0.0417	0.0474	0.0456	0.0345	0.0310	0.0385
p – 2	0	0.0330	0.0410	0.0471	0.0464	0.0324	0.0309	0.0385
p – 1.5	0.0333	0.0334	0.0421	0.0489	0.0492	0.0338	0.0316	0.0389
p – 1	0.0513	0.0329	0.0427	0.0490	0.0472	0.0364	0.0315	0.0416
p – 0.5	0.0322	0.0327	0.0427	0.0488	0.0476	0.0351	0.0310	0.0386
ATM p	0.0318	0.0320	0.0415	0.0469	0.0468	0.0341	0.0304	0.0377
ATM c	0.0317	0.0329	0.0431	0.0480	0.0468	0.0345	0.0317	0.0384
c + 0.5	0	0.0319	0.0413	0.0480	0.0473	0.0361	0.0314	0.0393
c + 1	0	0.0321	0.0421	0.0485	0.0479	0.0372	0.0315	0.0399
c + 1.5	0	0.0328	0.0422	0.0479	0.0480	0.0370	0.0321	0.0400
c + 2	0	0.0331	0.0431	0.0495	0.0488	0.0375	0.0324	0.0408
c + 2.5	0	0.0337	0.0431	0.0495	0.0500	0.0372	0.0335	0.0412
c + 3	0	0.0344	0.0438	0.0503	0.0499	0.039	0.0339	0.0419
c + 3.5	0.0557	0.0352	0.0438	0.0501	0.0515	0.0387	0.0342	0.0442
c + 4	0	0.0356	0.0444	0.0517	0.0519	0.0402	0.0344	0.0430
c + 4.5	0.0595	0.036	0.0444	0.0519	0.0530	0.0404	0.0348	0.0457
c + 5	0.0613	0.0365	0.0454	0.0513	0.0534	0.0409	0.0352	0.0463
c + 5.5	0	0.0374	0.0461	0.0518	0.0538	0.0417	0.0368	0.0446
c + 6	0.0562	0.0383	0.0463	0.0532	0.0559	0.0428	0.0367	0.0471
c + 6.5	0	0.0383	0.0470	0.0523	0.0558	0.0419	0.0364	0.0453
c + 7	0	0.0387	0.0465	0.0544	0.0554	0.0428	0.0380	0.0460
c + 7.5	0.0657	0.0395	0.0478	0.0531	0.0559	0.0452	0.0381	0.0493
ALL	0.0485	0.0366	0.0438	0.0490	0.0483	0.0367	0.0328	0.0418

(c) Diff. TS09-SV1 – SYSSV^S

MAE(σ)	M2	M3	M4	M5	M6	M7	M8	ALL
p – 7.5	0.0049	-0.0019	0.0026	0.0034	0.0040	0.0005	-0.0014	0.0017
p – 7	0	-0.0038	0.0034	0.0026	0.0027	0.0001	-0.0012	0.0006
p – 6.5	0	-0.0028	0.0025	0.0022	0.0014	0.0000	-0.0009	0.0004
p – 6	0	-0.0028	0.0019	0.0013	0.0021	-0.0001	-0.0005	0.0003
p – 5.5	0	-0.0024	0.0021	0.0010	0.0015	-0.0004	-0.0003	0.0002
p – 5	0.0101	-0.0026	0.0017	0.0015	0.0011	-0.0004	-0.0003	0.0016
p – 4.5	-0.0192	-0.0022	0.0016	-0.0002	0.0006	-0.0004	0.0001	-0.0028
p – 4	0.0139	-0.0023	0.0016	0.0001	0.0002	-0.0004	0.0007	0.0020
p – 3.5	0.0184	-0.0023	0.0013	-0.0002	0.0007	-0.0004	0.0007	0.0026
p – 3	0.0204	-0.0017	0.0012	0.0002	0.0005	-0.0003	0.0008	0.0030
p – 2.5	0.0245	-0.0017	0.0010	0.0004	0.0000	-0.0003	0.0008	0.0035
p – 2	0	-0.0011	0.0012	0.0000	0.0002	-0.0002	0.0012	0.0002
p – 1.5	0.0292	-0.0010	0.0011	-0.0005	-0.0002	-0.0001	0.0011	0.0042
p – 1	-0.0007	-0.0011	0.0009	0.0000	-0.0001	-0.0001	0.002	0.0001
p – 0.5	0.0338	-0.0004	0.0008	-0.0002	0.0004	-0.0001	0.0017	0.0052
ATM p	0.0344	0.0002	0.0008	0.0002	0.0004	0.0000	0.0016	0.0054
ATM c	0.0358	-0.0002	0.0007	0.0003	0.0005	0.0001	0.0015	0.0055
c + 0.5	0	0.0006	0.0008	-0.0002	0.0005	0.0002	0.0017	0.0006
c + 1	0	0.0011	0.0007	-0.0001	0.0005	0.0000	0.0018	0.0007
c + 1.5	0	0.0014	0.0007	0.0000	0.0003	0.0001	0.0017	0.0007
c + 2	0	0.0017	0.0006	-0.0003	0.0006	0.0002	0.0016	0.0007
c + 2.5	0	0.0019	0.0006	-0.0001	0.0006	0.0002	0.0016	0.0008
c + 3	0	0.0021	0.0006	-0.0002	0.0006	0.0002	0.0018	0.0009
c + 3.5	0.0047	0.0022	0.0006	0.0002	0.0004	0.0002	0.0015	0.0014
c + 4	0	0.0023	0.0004	0.0000	0.0006	0.0003	0.0022	0.0010
c + 4.5	0.0017	0.0022	0.0003	0.0002	0.0004	0.0004	0.0016	0.0010
c + 5	-0.0004	0.0026	0.0002	-0.0002	0.0006	0.0003	0.002	0.0008
c + 5.5	0	0.0025	0.0001	0.0001	0.0006	0.0005	0.0022	0.0010
c + 6	0.0057	0.0019	0.0001	-0.0003	0.0002	0.0004	0.0017	0.0014
c + 6.5	0	0.0022	0.0000	-0.0001	0.0005	0.0005	0.0021	0.0009
c + 7	0	0.0016	-0.0002	0.0002	0.0006	0.0005	0.0020	0.0008
c + 7.5	-0.0032	0.0015	-0.0003	0.0003	0.0006	0.0004	0.0013	0.0001
ALL	0.0126	-0.0001	0.0010	0.0004	0.0007	0.0001	0.0011	0.0015

NOTES: This table reports model accuracy in terms if options MAE(σ) within each moneyness-maturity category, with the estimations performed on the monthly data set. p – (c +) i refers to the put (call) options with strike equal to the ATM strike - (+) i USD. Only the central row refers to ATM options, all the others refer to OTM options; strikes are increasing. Sub-table (a) refers to TS09-SV1 and Sub-table (b) refers to SYSSV^S, both models expressed following the original set-up of the parameters: observe that the darker the color of the cell (red), the worse the model performance. Sub-table (c) indicates the difference between both models; the darker the color of the cell (blue), the better the performance of our model. Values of 0 indicate the lack of quoted options for this combination of contract and moneyness.

Table 2.13: MAE(σ) – multiple harmonic pattern and alternative set-up

(a) TS09-SV1

MAE(σ)	M2	M3	M4	M5	M6	M7	M8	ALL
p – 7.5	0.0672	0.0450	0.0499	0.0515	0.0456	0.0337	0.0307	0.0462
p – 7	0	0.0430	0.0496	0.0481	0.0450	0.0334	0.0315	0.0418
p – 6.5	0	0.0412	0.0478	0.0495	0.0434	0.0341	0.0309	0.0411
p – 6	0	0.0415	0.0474	0.0493	0.0463	0.0350	0.0310	0.0417
p – 5.5	0	0.0373	0.0467	0.0477	0.0451	0.0324	0.0306	0.0400
p – 5	0.0594	0.0367	0.0451	0.0475	0.0445	0.0324	0.0310	0.0424
p – 4.5	0.0593	0.0356	0.0438	0.0455	0.0463	0.0326	0.0308	0.0420
p – 4	0.0576	0.0346	0.0429	0.0478	0.0442	0.0328	0.0310	0.0416
p – 3.5	0.0580	0.0339	0.0433	0.0465	0.0459	0.0326	0.0315	0.0417
p – 3	0.0577	0.0337	0.0422	0.0473	0.0458	0.0336	0.0312	0.0416
p – 2.5	0.0593	0.0328	0.0426	0.0479	0.0456	0.0342	0.0318	0.0420
p – 2	0	0.0319	0.0422	0.0471	0.0466	0.0322	0.0321	0.0387
p – 1.5	0.0625	0.0324	0.0432	0.0485	0.0491	0.0337	0.0327	0.0431
p – 1	0.0506	0.0318	0.0436	0.0489	0.0471	0.0363	0.0335	0.0417
p – 0.5	0.0660	0.0323	0.0435	0.0487	0.0481	0.0351	0.0327	0.0438
ATM p	0.0662	0.0322	0.0423	0.0471	0.0472	0.0341	0.0320	0.0430
ATM c	0.0675	0.0327	0.0438	0.0484	0.0473	0.0346	0.0332	0.0439
c + 0.5	0	0.0324	0.0421	0.0478	0.0478	0.0362	0.0331	0.0399
c + 1	0	0.0332	0.0428	0.0484	0.0484	0.0372	0.0334	0.0406
c + 1.5	0	0.0343	0.0429	0.0480	0.0483	0.0371	0.0338	0.0407
c + 2	0	0.0348	0.0438	0.0492	0.0494	0.0378	0.0340	0.0415
c + 2.5	0	0.0356	0.0437	0.0494	0.0506	0.0374	0.0351	0.0420
c + 3	0	0.0366	0.0443	0.0501	0.0504	0.0393	0.0357	0.0427
c + 3.5	0.0604	0.0374	0.0444	0.0502	0.0519	0.0389	0.0358	0.0456
c + 4	0	0.0379	0.0448	0.0517	0.0525	0.0405	0.0366	0.0440
c + 4.5	0.0612	0.0382	0.0448	0.0521	0.0534	0.0408	0.0364	0.0467
c + 5	0.0610	0.0391	0.0456	0.0511	0.0541	0.0412	0.0372	0.0470
c + 5.5	0	0.0399	0.0463	0.0520	0.0543	0.0422	0.0390	0.0456
c + 6	0.0618	0.0402	0.0464	0.0529	0.0561	0.0432	0.0384	0.0485
c + 6.5	0	0.0405	0.0470	0.0522	0.0563	0.0424	0.0385	0.0462
c + 7	0	0.0404	0.0463	0.0546	0.0560	0.0433	0.0399	0.0467
c + 7.5	0.0626	0.0410	0.0475	0.0534	0.0565	0.0455	0.0394	0.0494
ALL	0.0611	0.0366	0.0448	0.0494	0.0490	0.0367	0.0339	0.0433

(b) SYSSV^M

MAE(σ)	M2	M3	M4	M5	M6	M7	M8	ALL
p – 7.5	0.0609	0.0453	0.0479	0.0489	0.0426	0.0334	0.0308	0.0443
p – 7	0	0.0433	0.0476	0.0460	0.0427	0.0335	0.0307	0.0406
p – 6.5	0	0.0419	0.0467	0.0481	0.0423	0.0342	0.0306	0.0406
p – 6	0	0.0426	0.0470	0.0486	0.0449	0.0353	0.0300	0.0414
p – 5.5	0	0.0384	0.0464	0.0476	0.0441	0.0329	0.0296	0.0398
p – 5	0.0490	0.0378	0.0451	0.0467	0.0438	0.0329	0.0298	0.0407
p – 4.5	0.0580	0.0365	0.0439	0.0459	0.0459	0.0332	0.0298	0.0419
p – 4	0.0441	0.0355	0.0431	0.0482	0.0441	0.0333	0.0292	0.0396
p – 3.5	0.0413	0.0348	0.0436	0.0470	0.0455	0.0331	0.0300	0.0393
p – 3	0.0385	0.0341	0.0428	0.0477	0.0458	0.0341	0.0298	0.0390
p – 2.5	0.0366	0.0331	0.0433	0.0481	0.0460	0.0347	0.0305	0.0389
p – 2	0	0.0318	0.0428	0.0476	0.0467	0.0327	0.0305	0.0387
p – 1.5	0.0332	0.0323	0.0439	0.0495	0.0497	0.0342	0.0311	0.0391
p – 1	0.0181	0.0315	0.0443	0.0496	0.0476	0.0365	0.0313	0.0370
p – 0.5	0.0319	0.0315	0.0443	0.0492	0.0481	0.0354	0.0309	0.0388
ATM p	0.0316	0.0309	0.0430	0.0475	0.0473	0.0344	0.0310	0.0379
ATM c	0.0323	0.0316	0.0445	0.0486	0.0472	0.0349	0.0317	0.0387
c + 0.5	0	0.0309	0.0428	0.0485	0.0478	0.0367	0.0319	0.0398
c + 1	0	0.0315	0.0434	0.0490	0.0483	0.0376	0.0319	0.0403
c + 1.5	0	0.0323	0.0436	0.0484	0.0484	0.0374	0.0325	0.0404
c + 2	0	0.0326	0.0444	0.0501	0.0492	0.0381	0.0327	0.0412
c + 2.5	0	0.0332	0.0443	0.0502	0.0502	0.0376	0.0339	0.0415
c + 3	0	0.0343	0.0451	0.0509	0.0501	0.0395	0.0341	0.0423
c + 3.5	0.0408	0.0353	0.0451	0.0506	0.0515	0.0390	0.0344	0.0424
c + 4	0	0.036	0.0456	0.0525	0.0520	0.0407	0.0347	0.0436
c + 4.5	0.0472	0.0364	0.0456	0.0525	0.0530	0.0412	0.0352	0.0445
c + 5	0.0492	0.0374	0.0466	0.0519	0.0533	0.0414	0.0355	0.0450
c + 5.5	0	0.0383	0.0473	0.0524	0.0536	0.0426	0.0371	0.0452
c + 6	0.0507	0.0390	0.0476	0.0538	0.0560	0.0435	0.0372	0.0468
c + 6.5	0	0.0394	0.0484	0.0529	0.0556	0.0428	0.0367	0.0460
c + 7	0	0.0398	0.0477	0.0551	0.0553	0.0439	0.0384	0.0467
c + 7.5	0.0558	0.0405	0.0490	0.0536	0.0558	0.0461	0.0383	0.0484
ALL	0.0423	0.0359	0.0452	0.0496	0.0486	0.0371	0.0326	0.0416

(c) Diff. TS09-SV1 – SYSSV^M

MAE(σ)	M2	M3	M4	M5	M6	M7	M8	ALL
p – 7.5	0.0063	-0.0002	0.0020	0.0026	0.0030	0.0003	0.0000	0.0020
p – 7	0	-0.0003	0.0020	0.0021	0.0023	-0.0001	0.0007	0.0011
p – 6.5	0	-0.0006	0.0011	0.0014	0.0011	-0.0002	0.0003	0.0005
p – 6	0	-0.0012	0.0004	0.0007	0.0014	-0.0003	0.0010	0.0003
p – 5.5	0	-0.0011	0.0004	0.0001	0.0011	-0.0005	0.0010	0.0002
p – 5	0.0104	-0.0012	0.0000	0.0008	0.0007	-0.0005	0.0012	0.0016
p – 4.5	0.0012	-0.0010	-0.0001	-0.0004	0.0004	-0.0006	0.0010	0.0001
p – 4	0.0135	-0.0009	-0.0002	-0.0004	0.0001	-0.0005	0.0018	0.0019
p – 3.5	0.0167	-0.0009	-0.0004	-0.0005	0.0004	-0.0006	0.0015	0.0023
p – 3	0.0192	-0.0004	-0.0006	-0.0005	0.0001	-0.0005	0.0013	0.0027
p – 2.5	0.0227	-0.0004	-0.0007	-0.0002	-0.0004	-0.0005	0.0013	0.0031
p – 2	0	0.0001	-0.0006	-0.0005	-0.0002	-0.0005	0.0016	0.0000
p – 1.5	0.0292	0.0001	-0.0007	-0.0010	-0.0006	-0.0005	0.0016	0.0040
p – 1	0.0325	0.0003	-0.0007	-0.0007	-0.0005	-0.0003	0.0022	0.0047
p – 0.5	0.0342	0.0008	-0.0007	-0.0005	-0.0001	-0.0003	0.0018	0.0050
ATM p	0.0346	0.0014	-0.0007	-0.0004	-0.0001	-0.0003	0.0010	0.0051
ATM c	0.0353	0.0011	-0.0007	-0.0002	0.0001	-0.0004	0.0014	0.0052
c + 0.5	0	0.0016	-0.0007	-0.0007	0.0000	-0.0004	0.0012	0.0002
c + 1	0	0.0017	-0.0006	-0.0006	0.0001	-0.0004	0.0015	0.0003
c + 1.5	0	0.0019	-0.0007	-0.0005	-0.0001	-0.0003	0.0014	0.0003
c + 2	0	0.0022	-0.0007	-0.0008	0.0002	-0.0003	0.0014	0.0003
c + 2.5	0	0.0024	-0.0006	-0.0007	0.0004	-0.0002	0.0012	0.0004
c + 3	0	0.0023	-0.0007	-0.0007	0.0004	-0.0002	0.0016	0.0004
c + 3.5	0.0195	0.0021	-0.0008	-0.0004	0.0004	-0.0001	0.0014	0.0032
c + 4	0	0.0020	-0.0008	-0.0007	0.0005	-0.0002	0.0019	0.0004
c + 4.5	0.0140	0.0018	-0.0008	-0.0004	0.0004	-0.0004	0.0012	0.0023
c + 5	0.0117	0.0018	-0.0010	-0.0008	0.0008	-0.0002	0.0017	0.0020
c + 5.5	0	0.0016	-0.0010	-0.0005	0.0007	-0.0004	0.0019	0.0004
c + 6	0.0111	0.0013	-0.0012	-0.0009	0.0001	-0.0003	0.0013	0.0016
c + 6.5	0	0.0011	-0.0014	-0.0006	0.0007	-0.0004	0.0018	0.0002
c + 7	0	0.0006	-0.0015	-0.0005	0.0007	-0.0005	0.0016	0.0001
c + 7.5	0.0067	0.0005	-0.0015	-0.0002	0.0007	-0.0005	0.0011	0.0010
ALL	0.0188	0.0006	-0.0004	-0.0002	0.0005	-0.0003	0.0013	0.0017

NOTES: This table reports model accuracy in terms if options MAE(σ) within each moneyness-maturity category, with the estimations performed on the monthly data set. p – (c +) i refers to the put (call) options with strike equal to the ATM strike – (+) i USD. Only the central row refers to ATM options, all the others refer to OTM options; strikes are increasing. Sub-table (a) refers to TS09-SV1 and Sub-table (b) refers to SYSSV^M, both models expressed following the original set-up of the parameters: observe that the darker the color of the cell (red), the worse the model performance. Sub-table (c) indicates the difference between both models; the darker the color of the cell (blue), the better the performance of our model. Values of 0 indicate the lack of quoted options for this combination of contract and moneyness.

Table 2.14: MAE(σ) – simple harmonic patterns

(a) SYSSV^S

MAE(σ)	M2	M3	M4	M5	M6	M7	M8	ALL
p – 7.5	0.0623	0.0470	0.0473	0.0481	0.0416	0.0332	0.0321	0.0445
p – 7	0	0.0468	0.0461	0.0455	0.0423	0.0334	0.0327	0.0411
p – 6.5	0	0.0440	0.0453	0.0473	0.0420	0.0341	0.0318	0.0407
p – 6	0	0.0442	0.0455	0.0480	0.0442	0.0351	0.0315	0.0414
p – 5.5	0	0.0397	0.0446	0.0467	0.0436	0.0328	0.0310	0.0397
p – 5	0.0494	0.0393	0.0434	0.0460	0.0434	0.0328	0.0313	0.0408
p – 4.5	0.0785	0.0378	0.0422	0.0457	0.0457	0.0330	0.0306	0.0448
p – 4	0.0437	0.0369	0.0413	0.0477	0.0440	0.0332	0.0303	0.0396
p – 3.5	0.0396	0.0361	0.0420	0.0467	0.0452	0.0329	0.0308	0.0391
p – 3	0.0373	0.0354	0.0410	0.0470	0.0453	0.0339	0.0304	0.0386
p – 2.5	0.0347	0.0344	0.0417	0.0474	0.0456	0.0345	0.0310	0.0385
p – 2	0	0.0330	0.0410	0.0471	0.0464	0.0324	0.0309	0.0385
p – 1.5	0.0333	0.0334	0.0421	0.0489	0.0492	0.0338	0.0316	0.0389
p – 1	0.0513	0.0329	0.0427	0.0490	0.0472	0.0364	0.0315	0.0416
p – 0.5	0.0322	0.0327	0.0427	0.0488	0.0476	0.0351	0.0310	0.0386
ATM p	0.0318	0.0320	0.0415	0.0469	0.0468	0.0341	0.0304	0.0377
ATM c	0.0317	0.0329	0.0431	0.0480	0.0468	0.0345	0.0317	0.0384
c + 0.5	0	0.0319	0.0413	0.0480	0.0473	0.0361	0.0314	0.0393
c + 1	0	0.0321	0.0421	0.0485	0.0479	0.0372	0.0315	0.0399
c + 1.5	0	0.0328	0.0422	0.0479	0.0480	0.0370	0.0321	0.0400
c + 2	0	0.0331	0.0431	0.0495	0.0488	0.0375	0.0324	0.0408
c + 2.5	0	0.0337	0.0431	0.0495	0.0500	0.0372	0.0335	0.0412
c + 3	0	0.0344	0.0438	0.0503	0.0499	0.0390	0.0339	0.0419
c + 3.5	0.0557	0.0352	0.0438	0.0501	0.0515	0.0387	0.0342	0.0442
c + 4	0	0.0356	0.0444	0.0517	0.0519	0.0402	0.0344	0.0430
c + 4.5	0.0595	0.0360	0.0444	0.0519	0.0530	0.0404	0.0348	0.0457
c + 5	0.0613	0.0365	0.0454	0.0513	0.0534	0.0409	0.0352	0.0463
c + 5.5	0	0.0374	0.0461	0.0518	0.0538	0.0417	0.0368	0.0446
c + 6	0.0562	0.0383	0.0463	0.0532	0.0559	0.0428	0.0367	0.0471
c + 6.5	0	0.0383	0.0470	0.0523	0.0558	0.0419	0.0364	0.0453
c + 7	0	0.0387	0.0465	0.0544	0.0554	0.0428	0.0380	0.0460
c + 7.5	0.0657	0.0395	0.0478	0.0531	0.0559	0.0452	0.0381	0.0493
ALL	0.0485	0.0366	0.0438	0.0490	0.0483	0.0367	0.0328	0.0418

(b) ST21

MAE(σ)	M2	M3	M4	M5	M6	M7	M8	ALL
p – 7.5	0.0937	0.0574	0.0529	0.0507	0.0433	0.0326	0.0320	0.0518
p – 7	0	0.0544	0.0527	0.0472	0.0430	0.0331	0.0324	0.0438
p – 6.5	0	0.0503	0.0507	0.0489	0.0422	0.0338	0.0316	0.0429
p – 6	0	0.0506	0.0501	0.0487	0.0450	0.0351	0.0317	0.0435
p – 5.5	0	0.0455	0.0492	0.0473	0.0441	0.0328	0.0310	0.0417
p – 5	0.0574	0.0447	0.0474	0.0471	0.0437	0.0328	0.0317	0.0436
p – 4.5	0.0947	0.0430	0.0459	0.0452	0.0455	0.0332	0.0314	0.0484
p – 4	0.0491	0.0423	0.0450	0.0476	0.0435	0.0329	0.0310	0.0416
p – 3.5	0.0444	0.0411	0.0451	0.0462	0.0450	0.0328	0.0316	0.0409
p – 3	0.0423	0.0399	0.0442	0.0471	0.0454	0.0336	0.0312	0.0405
p – 2.5	0.0398	0.0389	0.0444	0.0477	0.0453	0.0340	0.0316	0.0402
p – 2	0	0.0373	0.0439	0.0469	0.0460	0.0326	0.0319	0.0398
p – 1.5	0.0383	0.0375	0.0449	0.0485	0.0489	0.0336	0.0327	0.0406
p – 1	0.0603	0.0369	0.0449	0.0489	0.0468	0.0364	0.0327	0.0438
p – 0.5	0.0367	0.0364	0.0447	0.0484	0.0476	0.0353	0.0321	0.0402
ATM p	0.0361	0.0356	0.0436	0.0470	0.0466	0.0341	0.0308	0.0391
ATM c	0.0360	0.0367	0.0449	0.0483	0.0466	0.0350	0.0324	0.0400
c + 0.5	0	0.0356	0.0435	0.0477	0.0472	0.0354	0.0318	0.0402
c + 1	0	0.0358	0.0440	0.0482	0.0477	0.0369	0.0321	0.0408
c + 1.5	0	0.0362	0.0439	0.0477	0.0477	0.0363	0.0327	0.0408
c + 2	0	0.0363	0.0447	0.0491	0.0485	0.0369	0.0332	0.0415
c + 2.5	0	0.0367	0.0448	0.0492	0.0496	0.0364	0.0340	0.0418
c + 3	0	0.0374	0.0453	0.0499	0.0494	0.0383	0.0348	0.0425
c + 3.5	0.0594	0.0380	0.0455	0.0499	0.0507	0.0377	0.0349	0.0452
c + 4	0	0.0383	0.0459	0.0515	0.0513	0.0393	0.0355	0.0436
c + 4.5	0.0631	0.0386	0.0462	0.0518	0.0523	0.0397	0.0355	0.0467
c + 5	0.0667	0.0391	0.0466	0.0508	0.0527	0.0397	0.0363	0.0474
c + 5.5	0	0.0397	0.0471	0.0516	0.0529	0.0406	0.0379	0.0450
c + 6	0.0625	0.0406	0.0475	0.0526	0.0550	0.0416	0.0376	0.0482
c + 6.5	0	0.0406	0.0477	0.0517	0.0548	0.0406	0.0376	0.0455
c + 7	0	0.0410	0.0472	0.0541	0.0544	0.0417	0.0388	0.0462
c + 7.5	0.0757	0.0421	0.0483	0.0527	0.0548	0.0438	0.0385	0.0508
ALL	0.0562	0.0408	0.0463	0.0491	0.0481	0.0362	0.0335	0.0434

(c) Diff. ST21 − SYSSV^S

MAE(σ)	M2	M3	M4	M5	M6	M7	M8	ALL
p – 7.5	0.0313	0.0104	0.0056	0.0026	0.0016	-0.0006	-0.0002	0.0073
p – 7	0	0.0076	0.0066	0.0016	0.0008	-0.0003	-0.0003	0.0027
p – 6.5	0	0.0063	0.0054	0.0016	0.0003	-0.0003	-0.0002	0.0022
p – 6	0	0.0064	0.0046	0.0007	0.0007	0.0000	0.0002	0.0021
p – 5.5	0	0.0058	0.0046	0.0006	0.0005	0.0001	0.0000	0.0019
p – 5	0.0081	0.0054	0.0040	0.0011	0.0004	0.0000	0.0005	0.0028
p – 4.5	0.0163	0.0052	0.0037	-0.0005	-0.0002	0.0001	0.0007	0.0036
p – 4	0.0054	0.0053	0.0037	-0.0001	-0.0004	-0.0003	0.0007	0.0020
p – 3.5	0.0048	0.0050	0.0032	-0.0005	-0.0002	-0.0001	0.0008	0.0018
p – 3	0.0050	0.0046	0.0032	0.0001	0.0002	-0.0003	0.0008	0.0019
p – 2.5	0.0050	0.0044	0.0027	0.0003	-0.0003	-0.0005	0.0006	0.0017
p – 2	0	0.0043	0.0029	-0.0002	-0.0004	0.0002	0.0010	0.0013
p – 1.5	0.0050	0.0041	0.0027	-0.0004	-0.0003	-0.0002	0.0010	0.0017
p – 1	0.0090	0.0040	0.0021	0.0000	-0.0003	-0.0001	0.0012	0.0023
p – 0.5	0.0045	0.0037	0.0020	-0.0005	0.0000	0.0002	0.0011	0.0016
ATM p	0.0043	0.0036	0.0021	0.0001	-0.0002	-0.0001	0.0004	0.0015
ATM c	0.0043	0.0038	0.0018	0.0002	-0.0002	0.0005	0.0008	0.0016
c + 0.5	0	0.0037	0.0021	-0.0003	-0.0001	-0.0006	0.0005	0.0009
c + 1	0	0.0036	0.0019	-0.0003	-0.0002	-0.0003	0.0006	0.0009
c + 1.5	0	0.0033	0.0017	-0.0002	-0.0003	-0.0007	0.0006	0.0007
c + 2	0	0.0032	0.0016	-0.0005	-0.0003	-0.0006	0.0008	0.0007
c + 2.5	0	0.0031	0.0017	-0.0004	-0.0005	-0.0008	0.0005	0.0006
c + 3	0	0.0029	0.0016	-0.0004	-0.0005	-0.0007	0.0009	0.0006
c + 3.5	0.0038	0.0028	0.0016	-0.0002	-0.0008	-0.0010	0.0007	0.0010
c + 4	0	0.0027	0.0015	-0.0002	-0.0006	-0.0009	0.0011	0.0006
c + 4.5	0.0035	0.0026	0.0017	-0.0001	-0.0006	-0.0008	0.0007	0.0010
c + 5	0.0053	0.0026	0.0012	-0.0005	-0.0008	-0.0012	0.0012	0.0011
c + 5.5	0	0.0024	0.0009	-0.0002	-0.0009	-0.0011	0.0011	0.0004
c + 6	0.0064	0.0024	0.0011	-0.0006	-0.0009	-0.0013	0.0008	0.0011
c + 6.5	0	0.0024	0.0007	-0.0006	-0.0010	-0.0013	0.0012	0.0002
c + 7	0	0.0023	0.0007	-0.0004	-0.0010	-0.0012	0.0009	0.0002
c + 7.5	0.0100	0.0026	0.0006	-0.0003	-0.0011	-0.0014	0.0004	0.0015
ALL	0.0078	0.0041	0.0025	0.0001	-0.0002	-0.0005	0.0006	0.0017

NOTES: This table reports model accuracy in terms if options MAE(σ) within each moneyness-maturity category, with the estimations performed on the monthly data set. p – (c +) i refers to the put (call) options with strike equal to the ATM strike – (+) i USD. The central row refers to ATM options, the others refer to OTM options; strikes are increasing. Sub-table (a) refers to our model SYSSV^S and Sub-table (b) refers to ST21. Our model is expressed following the alternative set-up, both models use a same simple harmonic function: the darker the color of the cell (red), the worse the performance. Sub-table (c) indicates the difference between both models; the darker the color of the cell (blue), the better the performance of our model. Values of 0 indicate the lack of quoted options for this combination of contract and moneyness.

Bibliography

Arismendi, J. C., Back, J., Prokopczuk, M., Paschke, R. & Rudolf, M. (2016), 'Seasonal stochastic volatility: Implications for the pricing of commodity options', *Journal of Banking and Finance* **66**, 53–65. 50

Back, J., Prokopczuk, M., Paschke, R. & Rudolf, M. (2013), 'Seasonality and the valuation of commodity options', *Journal of Banking and Finance* **37**, 273–290. 50

Bates, D. S. (1996), 'Jumps and stochastic volatility: Exchange rate processes implicit in deutsche mark options', *Review of Financial Studies* **9**(1), 69–107. 49

Black, F. (1976), 'The pricing of commodity contracts', *Journal of Financial Economics* **3**(1), 167–179. 59, 62, 67

Black, F. & Scholes, M. (1973), 'The pricing of options and corporate liabilities', *Journal of Political Economy* **81**(3), 637–654. 49

Carr, P. & Madan, D. B. (1999), 'Option valuation using the fast Fourier transform', *Journal of Computational Finance* **2**(4), 61–73. 60, 61, 63

Clewlow, L. & Strickland, C. (1999a), Valuing energy options in a one factor model fitted to forward prices, Research Paper Series 10, Quantitative Finance Research Centre, University of Technology, Sydney. 49

Clewlow, L. & Strickland, C. (1999b), A multi-factor model for energy derivatives, Research Paper Series 28, Quantitative Finance Research Centre, University of Technology, Sydney. 49

Clewlow, L. & Strickland, C. (2000), *Energy Derivatives: Pricing and Risk Management*, Lacima Publications. 49

Collin-Dufresne, P. & Goldstein, R. S. (2002), Generalizing the affine framework to HJM and random field models.
URL: *https://ssrn.com/abstract=410421* 87

Cox, J. C., Ingersoll, J. E. & Ross, S. A. (1985), 'A theory of the term structure of interest rates', *Econometrica* **53**(2), 385–407. 51

Crosby, J. & Frau, C. (2021), 'Jumps in commodity prices: New approaches for pricing plain vanilla options'.
URL: *https://ssrn.com/abstract=3754835* 55, 56

Duffie, D. (2001), *Dynamic Asset Pricing Theory*, Princeton University Press. 54

Duffie, D., Pan, J. & Singleton, K. (2000), 'Transform analysis and asset pricing for affine jump-diffusions', *Econometrica* **68**, 1343–1376. 61, 87

Fanelli, V. (2020), *Financial Modelling in Commodity Markets*, Chapman & Hall/CRC Press. 49

Fanelli, V., Maddalena, L. & Musti, S. (2016), 'Modelling electricity futures prices using seasonal path-dependent volatility', *Applied Energy* **173**, 92–102. 50

Fanelli, V. & Schmeck, M. D. (2019), 'On the seasonality in the implied volatility of electricity options', *Quantitative Finance* **19**(8), 1321–1337. 50

Geman, H. & Nguyen, V.-N. (1995), 'Soybean inventory and forward curve dynamics', *Management Science* **51**(7), 1015–1164. 49

Heath, D., Jarrow, R. & Morton, A. (1992), 'Bond pricing and the term structure of interest rates: a new methodology for contingent claims valuation', *Econometrica* **60**(1), 77–105. 50

Heston, S. L. (1993), 'A closed-form solution for options with stochastic volatility with applications to bond and currency options', *Review of Financial Studies* **6**(2), 327–343. 49

Hylleberg, S., ed. (1992), *Modelling Seasonality*, Oxford University Press. 53

Lucia, J. J. & Schwartz, E. (2002), 'Electricity prices and power derivatives: Evidence from the nordic power exchange', *Review of Derivatives Research* **5**(1), 5–50. 49

Merton, R. (1976), 'Option pricing when underlying stock returns are discontinuous', *Journal of Financial Economics* **3**(1-2), 125–144. 49

Richter, M. & Sørensen, C. (2002), Stochastic volatility and seasonality in commodity futures and options: the case of soybeans, Working Paper 4, Copenhagen Business School, Department of Finance.
URL: *http://ssrn.com/abstract=301994* 49

Rogel-Salazar, J. & Sapsford, N. (2014), 'Seasonal effects in natural gas prices and the impact of the economic recession', *Wilmott Magazine* **December**. 53

Samuelson, P. A. (1965), 'Proof that properly anticipated prices fluctuate randoml', *Industrial Management Review* **6**(2), 41–49. 52, 55

Schmelzle, M. (2010), 'Option pricing formulae using Fourier transform: theory and application'.
URL: *https://pfadintegral.com/docs/Schmelzle2010%20Fourier%20Pricing.pdf* 60

Schneider, L. & Tavin, B. (2018), 'From the Samuelson volatility effect to a Samuelson correlation effect: an analysis of crude oil calendar spread options', *Journal of Banking and Finance* **95**, 185–202. 50

Schneider, L. & Tavin, B. (2021), 'Seasonal volatility in agricultural markets: Modelling and empirical investigations', *Annals of Operational Research* . 50

Sitzia, N. (2018), 'The analytical solution of Trolle-Schwartz model, MSc. thesis, École Polytechnique Fédérale de Lausanne'.
URL: *https://ssrn.com/abstract=3121906* 89, 92

Sørensen, C. (2002), 'Modeling seasonality in agricultural commodity futures', *The Journal of Futures Markets* **22**(5), 394–426. 49

Trolle, A. B. & Schwartz, E. S. (2009), 'Unspanned stochastic volatility and the pricing of commodity derivatives', *Review of Financial Studies* **22**(11), 4423–4461. 47, 50

Appendix

2A Appendix for Proofs

2A.1 Proof of Proposition 2.1

We find the expressions followed by the terms $A(\tau)$ and $B(\tau)$ similarly to Duffie et al. (2000) and Collin-Dufresne & Goldstein (2002). The proof consists of showing that the process $\psi(t) \equiv \psi(iu; t, T_{Opt}, T)$ is a martingale under $\mathbb{Q}$. To this end, we conjecture that $\psi(iu; t, T_{Opt}, T)$ is of the form in equation (2.20). From applying Itô's Lemma for jump diffusion processes to $\psi(t)$, we obtain the following partial integro-differential equation (PIDE)

$$\begin{aligned}\frac{d\psi(t)}{\psi(t)} &= -\Big(\frac{\partial A(T_{Opt}-t)}{\partial(T_{Opt}-t)} + \frac{\partial B(T_{Opt}-t)}{\partial(T_{Opt}-t)}v_t\Big)dt + B(T_{Opt}-t)dv_t + iu\frac{dF(t,T)}{F(t,T)} \\ &\quad + \frac{1}{2}B^2(T_{Opt}-t)dv_t^2 - \frac{1}{2}(u^2+iu)\left(\frac{dF(t,T)}{F(t,T)}\right)^2 + iuB(T_{Opt}-t)dv_t\frac{dF(t,T)}{F(t,T)}. \qquad (2A.1)\end{aligned}$$

For $\psi(t)$ to be a martingale and with $\tau \equiv T_{Opt} - t$, it must hold that

$$\frac{1}{dt}E_t^{\mathbb{Q}}\left[\frac{d\psi(t)}{\psi(t)}\right] = \Big(-\frac{\partial A(\tau)}{\partial\tau} + B(\tau)\kappa\,\theta_t\Big) + \Big(-\frac{\partial B(\tau)}{\partial\tau} + b_0 + b_1B(\tau) + b_2B^2(\tau)\Big)v_t = 0. \qquad (2A.2)$$

Subject to the initial condition $B(0) = 0$ and conditional to the original parameters set-up, we have that

$$b_0 = -\frac{1}{2}(u^2+iu)\Big(\sigma_S^2 + \sigma_Y^2(t,T) + 2\rho_{Sy}\sigma_S\sigma_Y(t,T)\Big), \qquad (2A.3)$$

$$b_1 = -\kappa + iu\sigma_v\Big(\rho_{Sv}\sigma_S + \rho_{yv}\sigma_Y(t,T)\Big), \qquad (2A.4)$$

and conditional to our alternative set-up (as defined in Section 2.2.1), we have that

$$b_0 = -\frac{1}{2}(u^2+iu)\sigma_F^2(t,T), \qquad (2A.5)$$

$$b_1 = -\kappa + iu\sigma_v\rho_{Fv}\sigma_F(t,T), \qquad (2A.6)$$

and the constant term b_2 being unconditional to the set-up

$$b_2 = \frac{\sigma_v^2}{2}. \tag{2A.7}$$

Since equation (2A.2) holds for all t, $f(t,T)$ and v_t then the terms in each parentheses must vanish, reducing the problem to solving two much simpler ODEs

$$\frac{\partial A(\tau)}{\partial \tau} = B(\tau)\kappa\,\theta_t, \tag{2A.8}$$

$$\frac{\partial B(\tau)}{\partial \tau} = b_0 + b_1 B(\tau) + b_2 B^2(\tau). \tag{2A.9}$$

Hence, $\psi(t)$ is a martingale provided that $A(\tau)$ and $B(\tau)$ satisfy (2A.8) and (2A.9), respectively. The expression followed by $B(\tau)$ can be found in Appendix 2B.1. Depending on the functional form followed by θ_t, the solution to $A(\tau)$ can be found in Appendix 2A.2 (single sinusoidal pattern) or 2A.3 (mixed sinusoidal pattern).

2A.2 Proof of Proposition 2.2

With $B(\tau)$ as in equation (2.24) and θ_t following the single sinusoidal pattern defined in expression (2.5), equation (2.21) becomes[1]

$$\begin{aligned}
\frac{\partial A(\tau)}{\partial \tau} &= B(\tau)\kappa\Big(a^\theta + b^\theta \cos\big(2\pi(T_{Opt} - \tau - t_0)\big)\Big) \\
&= \frac{2\kappa\gamma}{\sigma_v^2}\Big(\beta + \mu z + z\frac{g'(z)}{g(z)}\Big)\Big(a^\theta + b^\theta \cos\big(2\pi(T_{Opt} - \tau - t_0)\big)\Big) \\
&= m\big(A_1'(\tau) + A_2'(\tau) + A_3'(\tau) + A_4'(\tau)\big),
\end{aligned} \tag{2A.10}$$

with the constant m and each integrand being

$$\begin{aligned}
m &= 2\kappa\gamma/\sigma_v^2, \\
A_1'(\tau) &= a^\theta\Big(\beta + \mu z + z\frac{g'(z)}{g(z)}\Big), \\
A_2'(\tau) &= b^\theta \beta \cos\big(2\pi(T_{Opt} - \tau - t_0)\big), \\
A_3'(\tau) &= b^\theta \mu \cos\big(2\pi(T_{Opt} - \tau - t_0)\big) z, \\
A_4'(\tau) &= b^\theta \cos\big(2\pi(T_{Opt} - \tau - t_0)\big) z\frac{g'(z)}{g(z)},
\end{aligned} \tag{2A.11}$$

the expressions followed by $\beta, \mu, z, g(z)$ and $g'(z)$ can be found in Appendix 2B.1.

Equation (2A.10) has a quasi-analytical solution which is given by[2]

$$A(\tau) = m\big(A_1(\tau) + A_2(\tau) + A_3(\tau) + A_4(\tau) + k_3\big). \tag{2A.12}$$

[1]Given that $\tau \equiv T_{Opt} - t$, we use the equality $t - t_0 = T_{Opt} - \tau - t_0$ in the expression followed by θ_t.
[2]We say that it is quasi-analytical due to expression followed by the term $A_4(\tau)$.

The proof for $A_1(\tau)$ is in Sitzia (2018), $A_2(\tau)$ is direct and $A_3(\tau)$ is calculated using integration by parts[3]

$$\begin{aligned}
A_1(\tau) &= +a^\theta\Big(\beta\tau - \frac{1}{\gamma}\big(\mu z + \ln g(z)\big)\Big), & A_1(0) &= -a^\theta\frac{\mu}{\gamma\omega},\\
A_2(\tau) &= -b^\theta\frac{\beta y^s_\tau}{2\pi}, & A_2(0) &= -b^\theta\frac{\beta y^s_0}{2\pi},\\
A_3(\tau) &= +b^\theta\frac{\mu z\big(\gamma y^c_\tau - 2\pi y^s_\tau\big)}{4\pi^2+\gamma^2}, & A_3(0) &= +b^\theta\mu\frac{\gamma y^c_0 - 2\pi y^s_0}{\omega(4\pi^2+\gamma^2)}.
\end{aligned} \tag{2A.13}$$

with $y^c_\tau, y^c_0, y^s_\tau, y^s_0$ and m as in (2.27). Since $A'_4(\tau)$ is not integrable, we cannot directly obtain an analytic expression for $A_4(\tau)$ but, alternatively, we can approximate $A'_4(\tau)$ as a polynomial around $\tau = 0$ using a second order Taylor expansion.[4] We compute the integral of each polynomial and we get

$$\begin{aligned}
A_{4,1}(\tau) &= +b^\theta\frac{\tau}{\omega}y^c_0 g'\left(\omega^{-1}\right),\\
A_{4,2}(\tau) &= -b^\theta\frac{\tau^2}{2\omega}\Big(g'\left(\omega^{-1}\right)\Big(-2\pi y^s_0 + \gamma y^c_0\big(1 + k_1n_1 + k_2n_2\big)\Big) + \gamma y^c_0\big(k_1n_3 + k_2n_4\big)\Big),\\
A_4(\tau) &= A_{4,1}(\tau) + A_{4,2}(\tau),
\end{aligned} \tag{2A.14}$$

with $A_{4,1}(0) = A_{4,2}(0) = A_{4,3}(0) = 0$; with n_1, n_2, n_3, n_4 as in (2.28).

In particular, if the initial condition is $A(0) = 0$ and given (2.25), we have that

$$k_3 = -(A_1(0) + A_2(0) + A_3(0) + A_4(0)) = x_0 + x^s_0 y^s_0 + x^c_0 y^c_0, \tag{2A.15}$$

where

$$\begin{aligned}
x_0 &= a^\theta\frac{\mu}{\gamma\omega},\\
x^s_0 &= b^\theta\Big(\frac{\beta}{2\pi} + \frac{2\pi\mu}{\omega(4\pi^2+\gamma^2)}\Big),\\
x^c_0 &= -b^\theta\frac{\mu\gamma}{\omega(4\pi^2+\gamma^2)}.
\end{aligned} \tag{2A.16}$$

2A.3 Proof of Proposition 2.3

With $B(\tau)$ as in equation (2.24) and θ_t following the multiple sinusoidal pattern defined in expression (2.6), equation (2.21) becomes[1]

$$\begin{aligned}
\frac{\partial A(\tau)}{\partial\tau} &= B(\tau)\kappa\Big(a^\theta + b^\theta\cos\big(2\pi(T_{Opt} - \tau - t_0)\big) + c^\theta\sin\big(2\pi(T_{Opt} - \tau - t_0)\big)\Big)\\
&= \frac{2\kappa\gamma}{\sigma^2_v}\Big(\beta + \mu z + z\frac{g'(z)}{g(z)}\Big)\Big(a^\theta + b^\theta\cos\big(2\pi(T_{Opt} - \tau - t_0)\big) + c^\theta\sin\big(2\pi(T_{Opt} - \tau - t_0)\big)\Big)\\
&= m\big(A'_1(\tau) + A'_2(\tau) + A'_3(\tau) + A'_4(\tau) + A'_5(\tau) + A'_6(\tau) + A'_7(\tau)\big),
\end{aligned} \tag{2A.17}$$

[3]The proof is available by direct request to the authors.

[4]This closed-form expression is found thanks to Matlab's Symbolic Maths Toobox.

the expressions followed by $\beta, \mu, z, g(z)$ and $g'(z)$ can be found in Appendix 2B.1, each integrand being

$$\begin{aligned} A_5'(\tau) &= c^\theta \sin\big(2\pi(T_{Opt} - \tau - t_0)\big)\beta, \\ A_6'(\tau) &= c^\theta \sin\big(2\pi(T_{Opt} - \tau - t_0)\big)\mu z, \\ A_7'(\tau) &= c^\theta \sin\big(2\pi(T_{Opt} - \tau - t_0)\big) z \frac{g'(z)}{g(z)}. \end{aligned} \tag{2A.18}$$

Equation (2A.17) has a quasi-analytical solution which is given by[5]

$$A(\tau) = m\big(A_1(\tau) + A_2(\tau) + A_3(\tau) + A_4(\tau) + A_5(\tau) + A_6(\tau) + A_7(\tau) + k_3\big). \tag{2A.19}$$

The expressions followed by $A_1'(\tau)$-$A_4'(\tau)$ and $A_1(\tau)$-$A_4(\tau)$ are the same as in Appendix 2A.2, $A_5(\tau)$ is direct and $A_6(\tau)$ is calculated using integration by parts[3]

$$\begin{aligned} A_5(\tau) &= c^\theta \frac{\beta y_\tau^c}{2\pi}, & A_5(0) &= c^\theta \frac{\beta y_0^c}{2\pi}, \\ A_6(\tau) &= c^\theta \frac{\mu z\big(2\pi y_\tau^s + \gamma y_\tau^c\big)}{4\pi^2 + \gamma^2}, & A_6(0) &= c^\theta \frac{\mu(2\pi y_0^c + \gamma y_0^s)}{\omega(4\pi^2 + \gamma^2)}, \end{aligned} \tag{2A.20}$$

with $y_\tau^c, y_0^c, y_\tau^s, y_0^s$ and m as in expressions (2.27). Similarly to what occurred with $A_4'(\tau)$, $A_7'(\tau)$ is not integrable, and we approximate it using a second order Taylor expansion around $\tau = 0$.[4] We compute the integral of each polynomial and we get the following expressions

$$\begin{aligned} A_{7,1}(\tau) &= +c^\theta \frac{\tau}{\omega} y_0^s g'\left(\omega^{-1}\right), \\ A_{7,2}(\tau) &= -c^\theta \frac{\tau^2}{2\omega}\Big(g'\left(\omega^{-1}\right)\Big(2\pi y_0^c + \gamma y_0^s\big(1 + k_1 n_1 + k_2 n_2\big)\Big) + \gamma y_0^S\left(k_1 n_3 + k_2 n_4\right)\Big), \\ A_7(\tau) &= A_{7,1}(\tau) + A_{7,2}(\tau), \end{aligned} \tag{2A.21}$$

with $A_{7,1}(0) = A_{7,2}(0) = A_{7,3}(0) = 0$; with n_1, n_2, n_3, n_4 as in (2.28).

In particular, if the initial condition is $A(0) = 0$ and given (2A.19), we have that

$$k_3 = -(A_1(0) + A_2(0) + A_3(0) + A_4(0) + A_5(0) + A_6(0) + A_7(0)) = x_0 + x_0^s y_0^s + x_0^c y_0^c, \tag{2A.22}$$

where

$$\begin{aligned} x_0 &= a^\theta \frac{\mu}{\gamma\omega}, \\ x_0^s &= -c^\theta \frac{\mu\gamma}{\omega(4\pi^2 + \gamma^2)} + b^\theta\Big(\frac{\beta}{2\pi} + \frac{2\pi\mu}{\omega(4\pi^2 + \gamma^2)}\Big), \\ x_0^c &= -b^\theta \frac{\mu\gamma}{\omega(4\pi^2 + \gamma^2)} + c^\theta\Big(\frac{\beta}{2\pi} + \frac{2\pi\mu}{\omega(4\pi^2 + \gamma^2)}\Big), \end{aligned} \tag{2A.23}$$

and with $A_1(0)$-$A_4(0)$ as in Appendix 2A.2.

[5]We say that it is quasi-analytical due to expressions followed by the terms $A_4(\tau)$ and $A_7(\tau)$.

2B Appendix for Analytic Expressions

2B.1 Analytic Expression for $B(\tau)$

Equation (2.22) has an analytical solution which is given by

$$B(\tau) = \frac{2\gamma}{\sigma_v^2}\left(\beta + \mu z + z\frac{g'(z)}{g(z)}\right), \tag{2B.1}$$

where the function $g(z)$ is a linear combination of Kummer's (M) and Tricomi's (U) hypergeometric functions, whilst k_1 and k_2 are constants determined by the initial conditions of the differential equation

$$g(z) = k_1 M(a,b,z) + k_2 U(a,b,z), \tag{2B.2}$$

$$g'(z) = \frac{a}{b}k_1 M(a+1,b+1,z) - ak_2 U(a+1,b+1,z), \tag{2B.3}$$

with

$$a = -\left(\mu b + \beta c_1 \frac{\omega}{\gamma} + d_1 \frac{\omega}{\gamma^2}\right), \qquad \mu = -\frac{1}{2}\left(1 + \frac{c_1\omega}{\gamma}\right), \tag{2B.4}$$

$$b = 1 + 2\beta + \frac{c_0}{\gamma}, \qquad \beta = \frac{-c_0 \pm \sqrt{c_0^2 - 4d_0}}{2\gamma}, \tag{2B.5}$$

$$\omega = \pm\frac{\gamma}{\sqrt{c_1^2 - 4d_2}}, \qquad z = \frac{e^{-\gamma\tau}}{\omega}. \tag{2B.6}$$

From the pair of possible values for β and ω, we choose $\pm = +$ for β and $\pm = -$ for ω.

In particular, if the initial condition is $B(0) = 0$, we have the following constants

$$k_1 = \frac{a\frac{U(a+1,b+1,\frac{1}{\omega})}{U(a,b,\frac{1}{\omega})} - \beta\omega - \mu}{\frac{a}{b}M(a+1,b+1,\frac{1}{\omega}) + aM(a,b,\frac{1}{\omega})\frac{U(a+1,b+1,\frac{1}{\omega})}{U(a,b,\frac{1}{\omega})}}, \tag{2B.7}$$

$$k_2 = \frac{1 - k_1 M(a,b,\frac{1}{\omega})}{U(a,b,\frac{1}{\omega})}. \tag{2B.8}$$

We apply the change of variable $B(\tau) = -\frac{y'(\tau)}{y(\tau)b_2}$ to equation (2.22) and we get

$$\left(\frac{y'(\tau)}{y(\tau)}\right)^2 \frac{1}{b_2} - \frac{y''(\tau)}{y(\tau)}\frac{1}{b_2} = b_0 + \frac{y'(\tau)}{y(\tau)}\frac{b_1}{b_2} + \left(\frac{y'(\tau)}{y(\tau)}\right)^2 \frac{1}{b_2}, \tag{2B.9}$$

which leads to the following homogeneous second order ODE with no constant coefficients

$$y''(\tau) - \left(c_0 + c_1 e^{-\gamma\tau}\right)y'(\tau) + \left(d_0 + d_1 e^{-\gamma\tau} + d_2 e^{-2\gamma\tau}\right)y(\tau) = 0. \tag{2B.10}$$

Conditional to the original (alternative) characterisation[6], b_0, b_1 and b_2 are as in the left (right) column in expressions (2.23).[7] Conditional to the original set-up, the coefficients in $g(z)$ and $g'(z)$ are

$$\begin{aligned} c_0 &= -\kappa + iu\sigma_v\Big(\sigma_S\rho_{Sv} + \rho_{yv}\frac{\alpha}{\gamma}\Big), & d_0 &= -(u^2+iu)\frac{q_2}{2}\Big(\sigma_S^2 + \frac{\alpha^2}{\gamma^2} + 2\rho_{Sy}\sigma_S\frac{\alpha}{\gamma}\Big), \\ c_1 &= -iu\sigma_v\rho_{yv}\frac{\alpha}{\gamma}e^{-\gamma(T-T_{Opt})}, & d_1 &= q_2(u^2+iu)\frac{\alpha}{\gamma}\Big(\frac{\alpha}{\gamma} + \rho_{Sy}\sigma_S\Big)e^{-\gamma(T-T_{Opt})}, \\ & & d_2 &= -(u^2+iu)\frac{q_2}{2}\frac{\alpha^2}{\gamma^2}e^{-2\gamma(T-T_{Opt})}. \end{aligned} \tag{2B.11}$$

Alternatively, and conditional to the alternative set-up, the coefficients in $g(z)$ and $g'(z)$ are

$$\begin{aligned} c_0 &= -\kappa + iu\sigma_v\rho_{Fv}\frac{\alpha}{\gamma}, & d_0 &= -(u^2+iu)\frac{q_2}{2}\frac{\alpha^2}{\gamma^2}, \\ c_1 &= -iu\sigma_v\rho_{Fv}\frac{\alpha}{\gamma}e^{-\gamma(T-T_{Opt})}, & d_1 &= q_2(u^2+iu)\frac{\alpha^2}{\gamma^2}e^{-\gamma(T-T_{Opt})}, \\ & & d_2 &= -(u^2+iu)\frac{q_2}{2}\frac{\alpha^2}{\gamma^2}e^{-2\gamma(T-T_{Opt})}. \end{aligned} \tag{2B.12}$$

In the case of the original set-up, the proof is in Sitzia (2018). In the alternative set-up, we have followed the steps described in that work to obtain the correspondent expressions.[3]

2B.2 Solutions to Schneider-Tavin (2018, 2021)

For both models, the CF in (2.19) is given by the Fourier transform in equation (2.20).

$B(\tau)$ solves the ODE in (2.22), with b_0, b_1 and b_2 as in expressions (2.23), right column (alternative set-up). Following the methodology described in Sitzia (2018), we apply the change of variable $B(\tau) = -\frac{y'(\tau)}{y(\tau)b_2}$ to equation (2.22), so that it becomes

$$\Big(-\frac{y'(\tau)}{y(\tau)b_2}\Big)' = b_0(\tau) + b_1(\tau)\Big(-\frac{y'(\tau)}{y(\tau)b_2}\Big) + b_2\Big(-\frac{y'(\tau)}{y(\tau)b_2}\Big)^2. \tag{2B.13}$$

Grouping constant parameters and exponentials, we get to the following second order ODE[8]

$$y''(\tau) - \big(c_0 + c_1(\tau)\alpha e^{-\lambda\tau}\big)y'(\tau) + c_2(\tau)\left(\alpha e^{-\lambda\tau}\right)^2 y(\tau) = 0, \tag{2B.14}$$

with coefficients

$$\begin{aligned} c_0 &= -\kappa, \\ c_1 &= -iu\sigma_v\rho_{Fv}\alpha e^{-\lambda(T-T_{Opt})}, \\ c_2 &= -\frac{\sigma_v^2(u^2+iu)}{4}\left(\alpha e^{-\lambda(T-T_{Opt})}\right)^2. \end{aligned} \tag{2B.15}$$

[6]As defined in Section 2.2.1.
[7]Observe that the expression followed by b_2 is unconditional to the set-up.
[8]See that c_2 is d_2 in Sitzia (2018).

Now we apply a last substitution using some parameters ω, β and μ which will be determined in order to simplify the above equation into a confluent hypergeometric equation $g(z)$. These parameters are given by

$$\begin{aligned} \mu &= -\frac{1}{2}\left(1+\frac{c_1\omega}{\lambda}\right), \quad & \beta &= -\frac{c_0}{\lambda}, \\ \omega &= \frac{\gamma}{\sqrt{c_1^2-4d_2}}, & z &= \frac{e^{-\lambda\tau}}{\omega}. \end{aligned} \tag{2B.16}$$

The function $g(z)$ is a linear combination of Kummer's (M) and Tricomi's (U) hypergeometric functions

$$g(z) = k_1 M(a,b,z) + k_2 U(a,b,z), \tag{2B.17}$$

$$g'(z) = \frac{a}{b} k_1 M(a+1,b+1,z) - a k_2 U(a+1,b+1,z), \tag{2B.18}$$

with parameters

$$a = -\mu b + \omega \frac{c_0 c_1}{2\lambda}, \qquad b = 1-\beta. \tag{2B.19}$$

The expressions followed by k_1, k_2 and $B(\tau)$ are the same as in TS09 and our model, they can be found in Appendix 2B.1. In ST18, $A(\tau)$ solves the same ODE as for TS09. The integral is direct, its analytical solution and k_3 are given by equations (2.33). In ST21, $A(\tau)$ solves the same ODE (2.21) as in our model. While $A(\tau)$ depends on the specification of θ_t, in this work we only focus on their sinusoidal pattern, defined in equation (2.5). The integral of $A(\tau)$ is not direct any more. We provide it in Proposition 2.2 with proof in Appendix 2A.2.

CHAPTER

3

Spread Options on Commodity Prices

Abstract[1]

In this work we perform a pricing exercise of different types of European spread options; we particularly focus on calendar and crack spread options. We present the expressions followed by the joint characteristic functions of the underlying log-prices for a panel of bivariate processes. We follow different methodologies for option valuation, and compare accuracy and processing times obtained using each one.

[1]Co-authors: Gianluca Fusai, Bayes Business School, City University of London; and Ioannis Kyriakou, Bayes Business School, City University of London. This chapter refers to an article which is currently a work in progress.

3.1 Introduction

Spread options focus on spreads in the commodity markets, especially energy, both for spot and futures. In these markets, spread options are usually based on differences between prices of the same commodity at two different locations (location spreads, e.g., Brent crude oil delivered in the UK v. WTI crude oil delivered in the US) or at different times (calendar spreads), between the prices of inputs and outputs (production spreads), or between the prices of different grades of the same commodity (quality spreads). Other relevant spread options in the energy markets are crack spread options, which are defined by the difference between prices of refined oil qualities.

There is a specific literature analysing the price of spread options in energy markets. In it, the traditional approach to model the spread is by modeling each asset separately. Spread options have been thoroughly studied in a bivariate Black & Scholes (1973) framework deriving a formula for the price. Margrabe (1978) pioneered spread option pricing deriving an analytical solution for the price of an exchange option, equivalent to a spread option with zero strike value.

Other authors provide approximation formulas for any strike level to overcome that restriction. Kirk & Aron (1995) are the first to provide a solution still commonly used by practitioners. Assuming that the two underlying futures follow a bivariate geometric Brownian motion, they propose that the value of the second price plus the strike is log-normally distributed. In this context they obtain an approximation formula for the spread option generalising the Margrabe formula. Numerous extensions of the Kirk model have been proposed suggesting improvements, but all still based on similar assumptions. Bjerksund & Stlensland (2011) present a slight twist of Kirk's approach, deriving a formula for the spread value where the lower bound produced is extremely accurate, and the precision is much greater. Venkatramanan & Alexander (2011) express the price of a spread option as the sum of the prices of two compound options, deriving a new analytic approximation for the price of European spread options.

Dempster & Hong (2002) introduce an integration methodology based on the two-dimensional fast Fourier transform (henceforth FFT) approach for spread option pricing that is effcient for geometric Brownian motion and more sophisticated price processes.

Hurd & Zhou (2010) introduce a new formula for general spread option pricing based on Fourier analysis of the payoff function. They develop a numerical integration method for computing spread options in two dimensions using the FFT methods introduced by Carr & Madan (1999), and prove its effectiveness. Their methodology is applicable to a variety of spread option payoffs in any model for which the joint characteristic function (henceforth JCF) is given analytically.

Caldana & Fusai (2013) recently proposed a very fast one-dimensional Fourier method that extends the approximation given by Bjerksund & Stlensland (2011) to any model for which the JCF of the underlying assets forming the spread in known analytically. They propose an accurate method for pricing European spread options by extending the lower bound approximation of Bjerksund & Stlensland (2011). They perform a pricing exercise using bivariates processes for models including jumps and stochastic volatility. They test the models' performances comparing their results to Monte Carlo simulations and Hurd & Zhou (2010).

In line with the performance analysis carried out in Caldana & Fusai (2013), we also consider other noteworthy works. Alfeus & Schloegl (2018) perform an applied exercise on bivariate models including Black & Scholes (1973) and Heston (1993), among others. They explore the performance of the highly efficient Hurd & Zhou (2010) technique comparing it with Monte Carlo simulations and the lower bound approximation of Caldana & Fusai (2013). Schneider & Tavin (2018) introduce a futures-based model capable of capturing the main features of crude oil futures and options contracts, such as the Samuelson volatility effect and the volatility smile. They calculate the JCF of two futures contracts in the model and price calendar spread options. Devising an empirical application using the Caldana & Fusai (2013) methodology, they show that in contrast to simpler nested models, their model can be successfully calibrated to market prices of vanilla and calendar spread options.

To the best of our knowledge, Schneider & Tavin (2018) is the only work in the literature focused on pricing European calendar spread options by providing the JCF expressions on the term-structure model they present. In this work, we take that approach one step further to calculate them for two different types of European spread options, calendar and crack. We perform an applied pricing exercise on a panel of nine models, and compare the accuracy and computing times between the Carr & Madan (1999) and Caldana & Fusai (2013) methodologies.

The remainder of this article is structured as follows: in Section 3.2 we define what a Fourier transform is and how to price European options with it; in Section 3.4 we indicate the list of extant models which conform the panel for which we perform our pricing exercise, we present the JCFs followed by the underlying(s) involved in the calendar and crack spreads respectively, and for the panel of models; is Section 3.3 we introduce the spread options pricing methodologies we follow in this work; in Section 3.5 we present the pricing results we obtain using the Fourier inversion methods we follow and compare their corresponding computation times for illustration; and in Section 3.6 we present our conclusions and indicate future lines of research.

3.2 The Characteristic Function

Since Stein & Stein (1991) first used the Fourier inversion method to find the distribution of the underlying asset in a stochastic volatility model, the Fourier transform methods have become a very active field of financial mathematics. Heston (1993) applied the characteristic function approach to obtain an analytic representation for the valuation of standard European options in the Fourier domain. Duffie, Pan & Singleton (2000) produced a comprehensive survey indicating that Fourier transform methods are applicable to a wide range of stochastic processes in the form of exponential affine diffusions. Carr & Madan (1999) pioneered the use of the FFT technique by mapping the Fourier transform directly to option prices via the single characteristic function (SCF henceforth). Since then, many efficient numerical methods using FFT techniques have been proposed, and many authors have discussed these methods in rigorous detail.

3.2.1 The Fourier Transform

Let f be a random variable with a probability density function $g(f)$, a piecewise continuous real function over $\mathbb{R}$ which satisfies the integrability condition

$$\int_{-\infty}^{\infty} |g(f)| df < \infty. \tag{3.1}$$

With $u \in \mathbb{R}$, the Fourier transform of $g(f)$ is defined by

$$G(f) = \int_{-\infty}^{\infty} e^{iuf} g(f) df. \tag{3.2}$$

Given $G(f)$, $g(f)$ can be recovered by the Fourier inversion formula

$$g(f) = \frac{1}{2\pi} \int_{-\infty}^{\infty} e^{-iuf} G(u) du. \tag{3.3}$$

In our case, $f \equiv \ln F(t,T)$ represents the time-t log-price of a futures contract F maturing at time T. To price European options on futures contracts we introduce the transform $\Phi_F(u)$, which can be expressed in terms of the characteristic function of $g(f)$

$$\Phi_F(u) \equiv \mathbb{E}_0^{\mathbb{Q}}[e^{iuf(t,T)}] = \int_{-\infty}^{\infty} e^{iuf(t,T)} g(f) df. \tag{3.4}$$

3.2.2 Fourier Inversion Methods

Apart from Monte Carlo simulations, European options prices are also available by Fourier inversion methods since the expression followed by the SCF or the JCF is known.

Two major approaches exist in the literature to date for pricing standard European options. The first one delivers option prices with respect to the Fourier inversion of cumulative distribution functions in likeness to the classical Black-Scholes formula, as represented by Heston (1993) and Bakshi & Madan (2000). The alternative approach considers the pricing of options analogue to the Fourier inversion of the density function, as in Carr & Madan (1999) and Lewis (2001), among others. The Carr & Madan (1999) approach presents two advantages over the first one: it permits the use of the computationally efficient FFT; and only requires the evaluation of one integral (two integrals required in Heston (1993) or in Duffie et al. (2000)). Both Fourier inversion methodologies are applicable to a wide range of European options.

To price spread options, we are aware of three efficient methods. In Hurd & Zhou (2010), the JCF of the calendar payoff function with a strike $K = 1$ is calculated analytically, and the price of the corresponding option is then deduced from this result. This method needs a double integral to be evaluated numerically using the two-dimensional FFT. The formula in Bjerksund & Stlensland (2011) for a bivariate GBM process is generalised by Caldana & Fusai (2013) to models for which the JCF of the prices forming the spread is known analytically. These methods give a lower bound for the European spread option price. As commented in (Schneider & Tavin 2018, Sec. 3.1), this bound is very close to the actual price and therefore they regard it as the spread option price itself; moreover, the formula is exact when $K = 0$. This method relies on a one-dimensional Fourier inversion. The main point in this methodology is that the approximated option price is obtained through a univariate Fourier inversion. Le Courtois & Walter (2015) propose a third method which is more direct than former ones, but requires the marginals and JCF of the spread prices. A double integral of the payoff function times the joint density of the two contracts has to be evaluated.

In this work we focus on the pricing of European spread and plain vanilla options and we rely on two inversion methods to price them. We use the methodology described in Carr & Madan (1999) for both option types, and specifically for spread options we also use the one described in Caldana & Fusai (2013).

3.3 Pricing of Options

Let S_t be a spot price process and let $F(t,T)$ be a futures price process. By definition, we have that

$$F(t,T) \equiv S_t e^{\int_t^T y(t,u)du}, \tag{3.5}$$

where $y(t,T) = r(t,T) - q(t,T)$ denotes the forward cost of carry curve, $r(t,T)$ refers to the risk-free interest rate and $q(t,T)$ is the convenience yield forward curve. In the panel featured in Section 3.4 we consider models originally conceived for spot prices and others for futures prices. Depending on the market, in most of the cases commodity prices are quoted in the form of future prices, since spot prices are not always available. Therefore, we generalise our expressions' form of by assuming futures prices by default. Observe that in the case of $T = t$, time-t futures prices maturing instantaneously coincide with time-t spot prices, that is, $F(t,t) \equiv S_t$, therefore we can easily move from spot- to futures-based equations.

Since he option's expiration date T_{Opt} occurs prior to the expiration date of the underlying futures contract T, that is, $T_{Opt} < T$,[2] we are interested in considering the transforms in Section 3.4 when $t = T_{Opt}$. In order to evaluate options, the discounted expectation of the payoff must be calculated under the risk-neutral measure $\mathbb{Q}$. We define $P(t, T_{Opt})$ as the time-t price of a zero-coupon bond maturing at T_{Opt}, assuming a continuously compounded risk-free interest rate. Given that each asset's currency coincides, we assume a unique interest rate curve. We assume constant interest rates r, convenience yields q and, therefore, cost of carries y. Recall that we defined the futures log-prices $f(t,T) \equiv \ln F(t,T)$.

3.3.1 Plain Vanilla Options

A standard European call option on F pays at expiry time T_{Opt} the amount

$$\mathcal{C}^{PV}(T,K) = max(F_T - K, 0), \tag{3.6}$$

where F_T is a financial quantity on F observed and maturing at time T . We restrict to the case of one risky asset described by its corresponding SDEs as can be seen in Tables 3.1 and 3.2. The time-t arbitrage-free fair price of the call option is

$$\mathcal{C}^{PV}(t, T_{Opt}, T, K) = P(t, T_{Opt})\mathbb{E}^{\mathbb{Q}}[max(F_T - K, 0)]. \tag{3.7}$$

Consider the SCF $\Phi_F(u)$ in equation (3.4). Following Carr & Madan (1999) and with $\Phi_F(u)$ representing the SCF of the futures price, the time-t price of a standard European call option expiring at time T_{Opt} with strike K on a time-t futures contract expiring at time T $F(t,T)$ is given by

$$\mathcal{C}(t, T_{Opt}, T, K) = P(t, T_{Opt})\frac{e^{-\alpha \ln(K)}}{\pi}\int_t^{\infty} \Re\left[\frac{e^{-iu\ln(K)}\Phi_F(u - i(1+\alpha))}{\alpha(\alpha+1) - u^2 + iu(1+2\alpha)}\right] du, \tag{3.8}$$

with α being the control parameter.[3] The proof is in Carr & Madan (1999).

[2] One and three business days for the Henry Hub natural gas and for the West Texas Intermediate crude oil markets.
[3] It tunes an exponentially decaying term introduced to allow the integration in the Fourier space.

3.3.2 Spread Options

Spread options are derivatives whose payoff depends on the difference of two financial quantities. These can refer either to contracts on the same underlying asset with different maturities, or to contracts with the same maturity but on different assets. The former case is known as an intra-commodity calendar spread option. The latter is known as an inter-commodity spread, of which there are different varieties such as crack spreads and spark spreads. In this work we focus on calendar and crack types of European spread options.[4] We assume bivariate processes only for prices, and we make the assumption of common variances and cost of carry processes when they apply.

Calendar Spread Options

In commodity markets it is quite common to have options which depend on the value of a single underlying asset, which is evaluated at two particular future times $T_2 > T_1 > 0$. We assume that $\sigma_{F_{T_1}} = \sigma_{F_{T_2}} = \sigma_F$.

A European calendar spread call option on F pays at expiry time T_{Opt} the amount

$$\mathcal{C}^{Cal}(T_1, T_2, K) = max(F_{T_1} - F_{T_2} - K, 0), \tag{3.9}$$

where F_{T_1} and F_{T_2} are two financial quantities on F observed and maturing at times T_1 and T_2, respectively. We restrict to the case of one risky asset described by its SDEs. The expressions followed by the JCF terms can be found in Table 3.5b.

The time-t arbitrage-free fair price of the calendar call spread option is

$$\mathcal{C}^{Cal}(t, T_1, T_2, T_{Opt}, K) = P(t, T_{Opt})\mathbb{E}^{\mathbb{Q}}[max(F_{T_1} - F_{T_2} - K, 0)]. \tag{3.10}$$

Let $\mathbf{u} = (u_1, u_2)^\intercal \in \mathbb{R}^2$ and $\mathbf{F}(t, T_1, T_2) = \big(F(t, T_1), F(t, T_2)\big)^\intercal$. Consider the JCF

$$\Phi_{\mathbf{F}}(\mathbf{u}) \equiv \mathbb{E}_t^{\mathbb{Q}}[e^{iu_1 \ln F_{T_1} + iu_2 \ln F_{T_2}}] = \mathbb{E}_t^{\mathbb{Q}}[e^{i\mathbf{u}^\intercal \ln \mathbf{F}(T_1, T_2)}]. \tag{3.11}$$

For illustration purposes, a general bivariate GBM process for futures under $\mathbb{Q}$ is represented as

$$\frac{dF(t,T_1)}{F(t,T_1)} = \sigma_F dW_t^F, \qquad \frac{dF(t,T_2)}{F(t,T_2)} = \sigma_F dW_t^F, \tag{3.12}$$

and a bivariate Hes93 process for futures under $\mathbb{Q}$ is represented as

$$\begin{aligned} \frac{dF(t,T_1)}{F(t,T_1)} &= \sigma_F \sqrt{v_t} dW_t^F, \qquad \frac{dF(t,T_2)}{F(t,T_2)} = \sigma_F \sqrt{v_t} dW_t^F, \\ dv_t &= \kappa(\theta - v_t)dt + \sigma_v \sqrt{v_t} dW_t^v, \qquad \mathbb{E}_t[dW_t^F, dW_t^v] = \rho_{Fv} dt. \end{aligned} \tag{3.13}$$

[4]Information on traded spread options on energy futures can be found at CME home.

Crack Spread Options

Crack spread options are defined on two underlying assets observed at a common maturity date $T > 0$. We assume bivariate price processes (i.e., each asset presents its own price dynamics, which are correlated with ρ_{12}). For stochastic volatility models, we also consider a common variance factor.[5] However, the correlation between prices and variance can differ between assets, i.e. $\rho_{F_1 v} \neq \rho_{F_2 v}$; we assume that $\sigma_{F_{T_1}} \neq \sigma_{F_{T_2}}$. We define the log-future prices $f_1(t,T) \equiv \ln F_1(t,T)$ and $f_2(t,T) \equiv \ln F_2(t,T)$.

A European crack spread call option on F_1 and F_2 pays at expiry time T_{Opt} the amount

$$\mathcal{C}^{Cra}(T,K) = max(F_{1,T} - F_{2,T} - K, 0), \tag{3.14}$$

where $F_{1,T}$ and $F_{2,T}$ are two financial quantities on assets F_1 and F_2 respectively, observed and maturing at time T. We restrict to the case of two risky assets, described by their SDEs and subject to correlation $\left\langle dW_t^{F_1}, dW_t^{F_2} \right\rangle = \rho_{12} dt$. The expressions followed by the JCF terms can be found in Table 3.5b.

The time-t no-arbitrage fair price of the crack call spread option is

$$\mathcal{C}^{Cra}(t, T_{Opt}, T, K) = P(t, T_{Opt}) \mathbb{E}_t^{\mathbb{Q}}[max(F_{1,T} - F_{2,T} - K, 0)]. \tag{3.15}$$

Let $\mathbf{u} = (u_1, u_2)^\intercal \in \mathbb{R}^2$ and $\mathbf{F}(t,T) = \big(F_1(t,T), F_2(t,T)\big)^\intercal$. Consider the JCF

$$\Phi_{\mathbf{F}}(\mathbf{u}) \equiv \mathbb{E}_t^{\mathbb{Q}}[e^{iu_1 \ln F_{1,T} + iu_2 \ln F_{2,T}}] = \mathbb{E}_t^{\mathbb{Q}}[e^{i\mathbf{u}^\intercal \ln \mathbf{F}(T)}]. \tag{3.16}$$

For illustration purposes, a general bivariate GBM process for futures under $\mathbb{Q}$ is represented as

$$\frac{dF_1(t,T)}{F_1(t,T)} = \sigma_{F_1} dW_t^{F_1}, \qquad \frac{dF_2(t,T)}{F_2(t,T)} = \sigma_{F_2} dW_t^{F_2}, \qquad \mathbb{E}_t[dW_t^{F_1}, dW_t^{F_2}] = \rho_{12} dt, \tag{3.17}$$

and a bivariate Hes93 process for futures under $\mathbb{Q}$ is represented as

$$\begin{gathered} \frac{dF_1(t,T)}{F_1(t,T)} = \sigma_{F_1}\sqrt{v_t} dW_t^{F_1}, \qquad \frac{dF_2(t,T)}{F_2(t,T)} = \sigma_{F_2}\sqrt{v_t} dW_t^{F_2}, \qquad \mathbb{E}_t[dW_t^{F_1}, dW_t^{F_2}] = \rho_{12} dt, \\ dv_t = \kappa(\theta - v_t)dt + \sigma_v \sqrt{v_t} dW_t^v, \qquad \mathbb{E}_t[dW_t^{F_1}, dW_t^v] = \rho_{F_1 v} dt, \qquad \mathbb{E}_t[dW_t^{F_2}, dW_t^v] = \rho_{F_2 v} dt. \end{gathered} \tag{3.18}$$

Since the spread is defined on two different assets, the correlation between assets ρ_{12} plays a key role.

Consider the JCFs of the two futures forming the spread $\Phi_{\mathbf{F}}(\mathbf{u})$ in (3.11) for calendar spread options and (3.16) for crack spread options. Next we introduce two different methodologies for

[5]Meaning that the model parameters and the initial value of the variance process coincide.

pricing these options. Following Carr & Madan (1999), the time-t price of a European spread call option expiring at time T_{Opt} with strike K on these futures is given by

$$\mathcal{C}(t,T_{Opt},T,K) = P(t,T_{Opt})\frac{e^{-\alpha\ln K}}{\pi}\int_t^\infty \Re\left[\frac{e^{-iu\ln K}\Phi_{\mathbf{F}}(u_1-i(1+\alpha),u_2-i(1+\alpha))}{\alpha(\alpha+1)-(u_1+u_2)^2+i(u_1+u_2)(1+2\alpha)}\right]du, \tag{3.19}$$

with α being the control parameter.[3]

Following Caldana & Fusai (2013) and only if the JCF of the underlying assets forming the spread is known analytically, the time-t price of the approximate European spread call option expiring at time T_{Opt} with strike K on these futures is given by

$$\mathcal{C}(t,T_{Opt},T,K) = P(t,T_{Opt})\frac{e^{-\delta k}}{\pi}\left(\int_t^\infty e^{-iuk}\psi_F(u)du\right)^+, \tag{3.20}$$

where

$$\psi_F(u) = \frac{e^{i\eta\ln\Phi_{\mathbf{F}}(0,-i\alpha)}}{i\eta}\Big(\Phi_{\mathbf{F}}(\eta-i,-\alpha\eta)-\Phi_{\mathbf{F}}(\eta,-\alpha\eta-i)-K\Phi_{\mathbf{F}}(\eta,-\alpha\eta)\Big), \tag{3.21}$$

and

$$\eta = u-i\delta,\qquad \alpha=\frac{F_2}{F_2+K},\qquad k=\ln(F_2+K), \tag{3.22}$$

with δ being the control parameter.[3] The proof is in Caldana & Fusai (2013).

Whereas α and k strictly refer to the futures prices, the JCF $\Phi_{\mathbf{F}}(\mathbf{u})$ can refer to either the log-spot or log-futures prices. Note that F_2 strictly refers to a futures price (never a spot price). For calendar spread options, it represents the future's price maturing at the most distant date $F(t,T_2)$; for crack spread options, it refers to the future's price of the second asset involved in the spread $F_2(t,T)$.

For all types of options discussed in this section, the value of the equivalent European put option prices can be computed using the expression for the put-call parity.

3.4 Panel of Models

In the following sections we present the expressions followed by JCF terms for a panel of nine models. We blend non-Gaussian and multi-factor models, some of which present seasonal stochastic volatility or jumps. Our panel consists of the following models: Black & Scholes (1973) or **BS73**; Merton (1976) or **Mer76** extends BS73 by incorporating jumps in the spot price; Heston (1993) or **Hes93** extends BS73 by incorporating instantaneous stochastic volatility; Bates (1996) or **Bat96** is a combination of Mer76 and Hes93; Trolle & Schwartz (2009)-SV1 or **TS09** extends Hes93 by incorporating a stochastic cost of carry forward curve; Crosby

& Frau (2021) or **SYSVJ**[6] extends TS09 by incorporating jumps in the spot and in the cost of carry forward curve; Frau & Fanelli (2021) or **SYSSV**[7] extends TS09 by introducing seasonality in the variance; Schneider & Tavin (2018) or **ST18** presents a two-factor model for futures prices with stochastic volatility together with a time-decaying deterministic term accounting for the Samuelson effect; and Schneider & Tavin (2021) or **ST21** extends ST18 by introducing seasonality in the variance. A key difference between the pairs of models ST18 & ST21 and TS09 & SYSSV consists of the expression followed by the volatility of the futures prices: whereas the former pair are future-based models, the latter are spot-based models which futures dynamics are derived from applying Itô's Lemma to the futures dynamics as well as imposing the martingale condition.[8]

The first seven models are originally defined in terms of spot prices; we also present their dynamics in terms of futures' prices. Instead of presenting each of the models' price and log-price dynamics individually, they can all be found in Tables 3.1 and 3.2. The last two models were originally defined following a multi-dimensional set-up, but in this work we consider them in a uni-dimensional form. The main features of these models are summarised in Table 3.3. In Tables 3.4 and 3.5 we present the ODEs followed by each of the terms forming the SCF and the JCF, and their respective solutions.

In the case of spot-based models, the equations we obtain in Sections 3.4.2 and 3.4.3 can be directly applied to futures prices by replacing one price for the other and setting $y = r - q = 0$. Regarding jump models (i.e., Mer76, Bat96 and SYSVJ), we assume that there are only idiosyncratic jumps which are not correlated. In this panel we incorporate two recent extensions of the TS09 model: for SYSVJ we only consider i.i.d. jumps in spot prices; for SYSSV we only consider the simple sinusoidal form; and for ST21 we only consider the sinusoidal form.

ST18 and ST21 encompass Hes93 as a nested model: when $\gamma = 0$ in ST18, it reduces to Hes93 for futures curves. In ST18, the authors also derive closed-form solutions for the model, presenting the JCF followed by the log-futures aimed for pricing crack spread options. Alternatively and following Sitzia (2018), we present our own expressions so that the methodology we follow to obtain the expressions for $A(t;u,v)$, $B(t;u,v)$ and $C(t;u,v)$ in the characteristic function for TS09 and posterior models is the same.

Deriving the JCFs for the panel of models considered conforms a significant contribution of this work. This is inspired by the work by ST18 where the authors present the expressions

[6] Acronym for Stochastic cost of carry Y Stochastic Volatility and Jumps.

[7] Acronym for Stochastic cost of carry Y Seasonal Stochastic Volatility.

[8] In ST18 and ST21, the term correcting the square root of v_t is a time-decaying functional form composed of one single term. In TS09-SV1 and SYSSV, this term is comprised by two elements, one related to the spot price and another to the cost of carry, the latter being the integral of a time-decaying functional form.

followed by the terms in the JCF aimed for pricing European crack spread options. We take that approach one step further and calculate the correspondent JCFs aimed for pricing two different types of European spread options, in particular calendar and crack. Specifically, novel is the expression for the JCF in the case of calendar spread options; and novel are the expressions followed by the JCF's terms for the newer models (that is, TS09 and posterior) for either crack or calendar options.

In the remaining of this section we present the expression followed by the JCF with which we can price European plain vanilla, calendar spread and crack spread options on futures contracts. We differentiate between models presenting i.i.d. increments (BS73 and Mer76) and non-Gaussian or stochastic volatility models (all others). For bivariate processes, we present the general equations followed by the JCF, as can be seen in Propositions 3.1 and 3.2 (calendar spread options), 3.3 and 3.4 (crack spread options).

3.4.1 Plain Vanilla Options

The transform in (3.4) has an exponential affine solution, its form depending on the type of process followed by the risk factors.

Affine Processes with i.i.d. Increments

For an affine process with i.i.d. increments, the SCF at time $t \leq T$ for the futures price F_T is given by

$$\Phi_F(u) \equiv E_0^{\mathbb{Q}}\left[e^{iuf(t,T)}\right] = e^{A(t-0;u)+B(t-0;u)f(0,T)}. \tag{3.23}$$

For BS73 and Mer76, the SCF can be computed replacing the expressions in Sub-table 3.4b into equation (3.23).

Affine Processes with Stochastic Volatility

For an affine process with stochastic volatility, the SCF at time $t \leq T$ for the futures price and its variance is given by

$$\Phi_{F,V}(u,v) \equiv E_0^{\mathbb{Q}}\left[e^{iuf(t,T)+ivV_t}\right] = e^{A(t-0;u,v)+B(t-0;u,v)f(0,T)+C(t-0;u,v)V_0}. \tag{3.24}$$

For the remaining models, the SCF can be computed replacing the expressions in Sub-table 3.4b into equation (3.24).

For further details on the components, see Appendix 3A.

3.4.2 Calendar Spread Options

To the best of our knowledge, this is the first work in the literature which explicitly defines the general equations followed by the JCF, as can be seen in the following propositions.[9]

Affine Processes with i.i.d. Increments

The SCF of $F(t,T)$ at $t=0$ has an exponential affine solution which is given by equation (3.23). The following proposition provides the JCF for the two futures involved in the calendar spread for an i.i.d. process:

Proposition 3.1 *For an affine process with i.i.d. increments, the JCF at time $t \le T_1, T_2$ for the futures prices F_{T_1}, F_{T_2} is given by*

$$\Phi_{\boldsymbol{F}}(\boldsymbol{u}) \equiv E_0^{\mathbb{Q}}\left[e^{iu_1 f_{T_1}+iu_2 f_{T_2}}\right] = e^{A(T_2-T_1;u_2)}\Phi_{F_{t,T_1}}\big(u_1 - iB(T_2-T_1;u_2)\big). \tag{3.25}$$

The SCF of the first (second) maturity is given by setting $u_2 = 0$ $(u_1 = 0)$ in the JCF.

Proof. See Appendix 3B.1 for proof. ■

For BS73 and Mer76, the JCF can be computed replacing the expressions in Sub-table 3.5b into equation (3.25).

Affine Processes with Stochastic Volatility

The SCF of $F(t,T)$ and its variance V_t at $t=0$ has an exponential affine solution given by (3.24). The following proposition provides the JCF for the two futures involved in the calendar spread for a stochastic volatility process:

Proposition 3.2 *For an affine process with stochastic volatility, the JCF at time $t \le T_1, T_2$ for the futures prices F_{T_1}, F_{T_2} is given by*

$$\begin{aligned}\Phi_{F_{T_1},F_{T_2}}(u_1,u_2) &\equiv E_0^{\mathbb{Q}}\left[e^{iu_1 f_{T_1}+iu_2 f_{T_2}}\right]\\ &= e^{A(T_2-T_1;u_2,0)}\Phi_{F_{t,T_1}}\big(u_1 - iB(T_2-T_1;u_2,0); -iC(T_2-T_1;u_2,0)\big).\end{aligned} \tag{3.26}$$

The SCF of the first (second) maturity is given by setting $u_2 = 0$ $(u_1 = 0)$ in the JCF.

Proof. See Appendix 3B.2 for proof. ■

For the remaining models, the JCF can be computed replacing the expressions in Sub-table 3.5b into equation (3.26).

[9]For this option type and for their model only, ST18 present the expression followed by the JCF.

3.4.3 Crack Spread Options

We explicitly define the general equations followed by the JCF, as can be seen in the following propositions.

Affine Processes with i.i.d. Increments

The SCF of $F(t,T)$ at time $t=0$ has an exponential affine solution which is given by equation (3.23). The following proposition provides the JCF for the two futures involved in the crack spread for an i.i.d. process:

Proposition 3.3 *For an affine process with i.i.d. increments, the JCF at time $t \leq T$ for the futures prices $F_{1,T}, F_{2,T}$ is given by*

$$\Phi_{\boldsymbol{F}}(\boldsymbol{u}) \equiv E_0^{\mathbb{Q}}\left[e^{iu_1 f_{1,T}+iu_2 f_{2,T}}\right] = e^{A(T;u_1,u_2)+B_1(T;u_1)f_1(0,T)+B_2(T;u_2)f_2(0,T)}. \tag{3.27}$$

The SCF of the first (second) asset is given by setting $u_2=0$ $(u_1=0)$ in the JCF.

For BS73 and Mer76, the JCF can be computed replacing the expressions in Sub-table 3.5b into equaiton (3.27).

Affine Processes with Stochastic Volatility

The SCF of $F(t,T)$ and its variance V_t at $t=0$ has an exponential affine solution given by (3.24). The following proposition provides the JCF for the two futures involved in the crack spread for a stochastic volatility process:

Proposition 3.4 *For an affine process with stochastic volatility, the JCF at time $t \leq T$ for the futures prices $F_{1,T}, F_{2,T}$ is given by*

$$\Phi_{\boldsymbol{F}}(\boldsymbol{u}) \equiv E_0^{\mathbb{Q}}\left[e^{iu_1 f_{1,T}+iu_2 f_{2,T}}\right] = e^{A(T;u_1,u_2)+B_1(T;u_1)f_1(0,T)+B_2(T;u_2)f_2(0,T)+C(T;u_1,u_2)V_0}. \tag{3.28}$$

The SCF of the first (second) asset is given by setting $u_2=0$ $(u_1=0)$ in the JCF.

For the remaining models, the JCF can be computed replacing the expressions in Sub-table 3.5b into equation (3.28).

Following the newer models (that is, TS09 and extensions, ST18 and ST21), the expressions followed by the components of the variance term $C(\tau;u_1,u_2)$ can be found in Appendix 3C.2; those followed by the independent term $A(\tau;u_1,u_2)$ can be found in Appendix 3C.3. Observe that the expressions followed by all these terms in ST18 are as in TS09, and in ST21 are as in SYSSV, respectively.

3.5 Results

This section features a pricing exercise of different types of European options. Initial values for the factors involved can be found in Table 3.6 and model parameters can be found in Table 3.7.

We calculate options' values by means of two different techniques. Prices in columns $CM99$ are obtained using the methodology described in Carr & Madan (1999) as in (3.8) and (3.19); we use the FFT algorithm with 1,024 evaluation points and we set the value of $\alpha = 0.75$. Prices in columns $CF13$ are calculated using the technology described in Caldana & Fusai (2013) as in (3.20) and (3.21); we use the Gauss-Kronrod quadrature with $\delta = 0.75$.

For plain vanilla options, we use the SCF in (3.4), whereas for calendar and crack spread options, we use the JCFs in (3.11) and (3.16) respectively.

Table 3.8 presents the values we obtain for European crack and calendar spread options, as well as plain vanilla ones. Sub-table (a) refers to options on spot prices and Sub-table (b) refers to options on futures prices. In terms of results, we differentiate two groups of models: i) BS73, Mer76, Hes93 and Bat96; ii) TS09 and extensions (SYSVJ, SYSSV), ST18 and ST21. For the earlier models, prices obtained under both methodologies quickly and clearly converge: option values for the first group diverge in the fourth or fifth decimal place; prices for models in the second group diverge in the first or second decimal place. For this second group we follow the methodology described in Sitzia (2018), which requires the use of hypergeometric functions. The complexity in this type of solutions requires higher computation precision to obtain accurate results, and the number of integration points also affects the output. The identify these elements as drivers of divergence between methods.[10] In Sub-table (c) we display the calculation time expressed in seconds. We find that $CF13$ is, on average, 26.5 times quicker than $CM99$.

In Table 3.9 and for all the models in the panel, we extend the European call option prices discussed in the previous table to a vector of 11 strikes: for (calendar and crack) spread options we consider $K = [0 : 0.4, \ldots, 3.6 : 4]$, whereas for plain vanilla options they start from the ATM level and increase in the same magnitude as indicated for spread options. In this table we only consider options based on futures prices.

3.6 Conclusions and Further Research

Different types of spread options are quite common in commodity markets; in this work we focus on calendar and crack spread options. For both types, we derive the corresponding JCF

[10] This issue is under current investigation.

for the two futures involved in the spread and price European spread options on it. This paper's main contribution are two: the explicit expressions followed by the JCFs which are required for the pricing of calendar spread options, and the expressions followed by the JCF's terms for the newer models (TS09, extensions (SYSVJ, SYSSV), ST18 and ST21) which are required for the pricing of either type of spread options.

We follow the option pricing methodology described in $CM99$ and the one described in $CF13$, and then compare prices and computation times. The prices obtained with $CM99$ clearly converge with those obtained using $CF13$, especially for the earlier models, but there is a clear trade-off between accuracy and computational time. Moreover, $CF13$ provides prices on average 26.5 times quicker than $CM99$.

We outlining areas for future research. In order to achieve better accuracy between pricing methodologies we propose to implement the pricing exercise utilising higher precision computation (e.g., the Multiprecision Toolbox in Matlab). Additionally, we consider the implementation of Monte Carlo simulations to benchmark option prices. We also believe it valuable to use real market data for the pricing and calibrating each of the models to quoted options, especially in energy markets such as the West Texas Intermediate light sweet crude oil and the Henry Hub natural gas. This would enable comparing the goodness of fit for each of the models presented in this work, and observe which perform best.

3.7 Tables

Table 3.1: Dynamics under $\mathbb{Q}$

Model	**Dynamics**	**Volatility**
BS73	$\frac{dS_t}{S_t} = y_t dt + \sigma_S dW_t^S$	σ_S constant
	$\frac{dF(t,T)}{F(t,T)} = \sigma_F dW_t^F$	σ_F constant
Mer76	$\frac{dS_t}{S_t} = \left(y_t - \lambda \mathbb{E}^{\mathbb{Q}}\left[e^{J_S} - 1\right]\right)dt + \sigma_S dW_t^S + \left(e^{J_S} - 1\right)dN_t$	σ_S constant
	$\frac{dF(t,T)}{F(t,T)} = -\lambda \mathbb{E}^{\mathbb{Q}}\left[e^{J_F} - 1\right]dt + \sigma_F dW_t^F + \left(e^{J_F} - 1\right)dN_t$	σ_F constant
Hes93	$\frac{dS_t}{S_t} = y_t dt + \sigma_S \sqrt{v_t} dW_t^S$	σ_S constant
	$dv_t = \kappa\left(\theta - v_t\right)dt + \sigma_v \sqrt{v_t} dW_t^v$	σ_v constant
	$\frac{dF(t,T)}{F(t,T)} = \sigma_F \sqrt{v_t} dW_t^F$	σ_F constant
Bat96	$\frac{dS_t}{S_t} = \left(y_t - \lambda \mathbb{E}^{\mathbb{Q}}\left[e^{J_S} - 1\right]\right)dt + \sigma_S \sqrt{v_t} dW_t^S + \left(e^{J_S} - 1\right)dN_t$	σ_S constant
	$dv_t = \kappa\left(\theta - v_t\right)dt + \sigma_v \sqrt{v_t} dW_t^v$	σ_v constant
	$\frac{dF(t,T)}{F(t,T)} = -\lambda \mathbb{E}^{\mathbb{Q}}\left[e^{J_F} - 1\right]dt + \sigma_F \sqrt{v_t} dW_t^F + \left(e^{J_F} - 1\right)dN_t$	σ_F constant
TS09	$\frac{dS_t}{S_t} = y_t dt + \sigma_S \sqrt{v_t} dW_t^S$	σ_S constant
	$dy(t,T) = \mu_y(t,T)dt + \sigma_y(t,T)\sqrt{v_t} dW_t^y$	$\sigma_y(t,T) = \alpha e^{-\gamma(T-t)}$
	$dv_t = \kappa\left(\theta - v_t\right)dt + \sigma_v \sqrt{v_t} dW_t^v$	$\alpha = 1, \sigma_v$ constant
	$\frac{dF(t,T)}{F(t,T)} = \sqrt{v_t}\left(\sigma_S dW_t^S + \sigma_Y(t,T) dW_t^y\right)$	$\sigma_Y(t,T) = \int_t^T \sigma_y(t,u)du$
SYSVJ	$\frac{dS_t}{S_t} = \left(y_t - \lambda \mathbb{E}^{\mathbb{Q}}\left[e^{J_S} - 1\right]\right)dt + \sigma_S \sqrt{v_t} dW_t^S + \left(e^{J_S} - 1\right)dN_t$	σ_S constant
	$dy(t,T) = \left(\mu_y(t,T) - \lambda \mathbb{E}^{\mathbb{Q}}\left[J_y\right]\right)dt + \sigma_y(t,T)\sqrt{v_t} dW_t^y + J_y dN_t$	$\sigma_y(t,T) = \alpha e^{-\gamma(T-t)}$
	$dv_t = \kappa\left(\theta - v_t\right)dt + \sigma_v \sqrt{v_t} dW_t^v$	α, σ_v constant
	$\frac{dF(t,T)}{F(t,T)} = \sqrt{v_t}\left(\sigma_S dW_t^S + \sigma_Y(t,T) dW_t^y\right)$	$\sigma_Y(t,T) = \int_t^T \sigma_y(t,u)du$
	$\quad - \lambda E_t^{\mathbb{Q}}\left[e^{J_S + J_Y(t,T)} - 1\right]dt + \left(e^{J_S + J_Y(t,T)} - 1\right)dN_t$	
SYSSV	$\frac{dS_t}{S_t} = y_t dt + \sigma_S \sqrt{v_t} dW_t^S$	σ_S constant
	$dy(t,T) = \mu_y(t,T)dt + \sigma_y(t,T)\sqrt{v_t} dW_t^y$	$\sigma_y(t,T) = \alpha e^{-\gamma(T-t)}$
	$dv_t = \kappa\left(\theta_t - v_t\right)dt + \sigma_v \sqrt{v_t} dW_t^v$	$\alpha = 1, \sigma_v$ constant
	$\quad \theta_t = a^\theta + b^\theta \cos(2\pi(t + t_0))$	
	$\frac{dF(t,T)}{F(t,T)} = \sqrt{v_t}\left(\sigma_S dW_t^S + \sigma_Y(t,T) dW_t^y\right)$	$\sigma_Y(t,T) = \int_t^T \sigma_y(t,u)du$
ST18	$\frac{dF(t,T)}{F(t,T)} = \sum_{i=1}^n \sigma_{F_i}(t,T)\sqrt{v_{i,t}} dW_t^{F_i}$	$\sigma_{F_i}(t,T) = \alpha_i e^{-\gamma_i(T-t)}$
	$dv_{i,t} = \kappa_i\left(\theta_i - v_{i,t}\right)dt + \sigma_{v_i}\sqrt{v_{i,t}} dW_t^{v_i}$	$\alpha_i = 1, \sigma_{v_i}$ constant
ST21	$\frac{dF(t,T)}{F(t,T)} = \sum_{i=1}^n \sigma_{F_i}(t,T)\sqrt{v_{i,t}} dW_t^{F_i}$	$\sigma_{F_i}(t,T) = \alpha_i e^{-\gamma_i(T-t)}$
	$dv_{i,t} = \kappa_i\left(\theta_t - v_{i,t}\right)dt + \sigma_{v_i}\sqrt{v_{i,t}} dW_t^{v_i}$	$\alpha_i = 1, \sigma_{v_i}$ constant
	$\quad \theta_t = a^\theta + b^\theta \cos(2\pi(t + t_0))$	

NOTES: This table presents the dynamics and the volatility expressions for the models we study in this work. S_t and $F(t,T)$ denote the spot and futures prices; y_t denotes the instantaneous cost of carry $y_t = r_t - q_t$ with r_t, q_t denoting the instantaneous interest rate and convenience yield; v_t denotes the instantaneous variance.

Table 3.2: Log-price dynamics under $\mathbb{Q}$

Model	Dynamics	Drift
BS73	$d\ln S_t = \mu_t dt + \sigma_S dW_t^S$ $d\ln F(t,T) = (\mu_t - y_t)dt + \sigma_S dW_t^S$	$\mu_t = y_t - \frac{\sigma_S^2}{2}$
Mer76	$d\ln S_t = \mu_t dt + \sigma_S dW_t^S + (e^{J_S} - 1)dN_t$ $d\ln F(t,T) = (\mu_t - y_t)dt + \sigma_S dW_t^S + (e^{J_S} - 1)dN_t$	$\mu_t = y_t - \frac{\sigma_S^2}{2} - \lambda \mathbb{E}^{\mathbb{Q}}\left[e^{J_S} - 1\right]$
Hes93	$d\ln S_t = \mu_t dt + \sigma_S \sqrt{v_t} dW_t^S$ $d\ln F(t,T) = (\mu_t - y_t)dt + \sigma_S \sqrt{v_t} dW_t^S$	$\mu_t = y_t - \frac{\sigma_S^2}{2} v_t$
Bat96	$d\ln S_t = \mu_t dt + \sigma_S \sqrt{v_t} dW_t^S + (e^{J_S} - 1)dN_t$ $d\ln F(t,T) = (\mu_t - y_t)dt + \sigma_S \sqrt{v_t} dW_t^S + (e^{J_S} - 1)dN_t$	$\mu_t = y_t - \frac{\sigma_S^2}{2} v_t - \lambda \mathbb{E}^{\mathbb{Q}}\left[e^{J_S} - 1\right]$
TS09,SYSSV	$d\ln S_t = \mu_t dt + \sqrt{v_t}\left(\sigma_S dW_t^S + \sigma_Y(t,T) dW_t^y\right)$ $d\ln F(t,T) = (\mu_t - y_t)dt + \sqrt{v_t}\left(\sigma_S dW_t^S + \sigma_Y(t,T) dW_t^y\right)$	$\mu_t = y_t + \int_t^T \mu_y(t,u)du - \frac{\sigma_S^2}{2} v_t$
SYSVJ	$d\ln S_t = \mu_t dt + \sqrt{v_t}\left(\sigma_S dW_t^S + \sigma_Y(t,T) dW_t^y\right)$ $d\ln F(t,T) = (\mu_t - y_t)dt + \sqrt{v_t}\left(\sigma_S dW_t^S + \sigma_Y(t,T) dW_t^y\right)$ $+ \left(e^{J_S + J_Y(t,T)} - 1\right) dN_t$	$\mu_t = y_t + \int_t^T \mu_y(t,u)du - \frac{\sigma_S^2}{2} v_t$ $- \lambda \mathbb{E}^{\mathbb{Q}}\left[e^{J_S + J_Y(t,T)} - 1\right]$
ST18,ST21	$d\ln F(t,T) = \sum_{i=1}^n \left(\mu_{it} dt + \sigma_{F_i}(t,T)\sqrt{v_{i,t}} dW_t^{F_i}\right)$	$\mu_{i,t} = -\frac{1}{2}\sigma_{F_i}^2(t,T) v_{i,t}$

NOTES: In this table we present the equivalent log-price dynamics to the models displayed in Table 3.1.

Table 3.3: Factors and features per model

Model	**Dimension**		**Stochastic Factors**				**Seasonality**		**Jumps**		**Parameter**
	Single	Multiple	S_t	$y(t,T)$	$F(t,T)$	v_t	Prices	Vols.	Prices	Vols.	**Count**
BS73	✓		✓								1
Mer76	✓		✓						✓		4
Hes93	✓		✓			✓					5
Bat96	✓		✓			✓			✓		8
TS09	✓		✓	✓		✓					9
SYSVJ	✓		✓	✓		✓			✓		12
SYSSV	✓		✓	✓		✓		✓			10
ST18		✓			✓	✓					6
ST21		✓			✓	✓		✓			7

NOTES: In this table we present the main features presented by a panel of nine models. Seasonality refers to explicit seasonality in the model dynamics. Parameter Count refers to the number of parameters according to the specification we deal with in this work. Since ST18 and ST21 originally set $\alpha = 1$, we do not count it in. Alternatively, and although Hes93 and Bat96 originally set $\sigma = 1$, we let it differ, hence we count it in.

Table 3.4: Fourier transforms for univariate processes

(a) ODEs

Model	$\partial A(\tau;u)/\partial\tau$	$\partial C(\tau;u)/\partial\tau$
BS73	b_0	$-$
Mer76	$b_0+\lambda(n_J-ium_J)$	$-$
Bat96,SYSVJ	$C(\tau;u)\kappa\theta+\lambda(n_J-ium_J)$	$b_0+b_1C(\tau;u)+b_2C^2(\tau;u)$
Hes93,TS09,ST18	$C(\tau;u)\kappa\theta$	$b_0+b_1C(\tau;u)+b_2C^2(\tau;u)$
SYSSV,ST21	$C(\tau;u)\kappa\theta_t$	$b_0+b_1C(\tau;u)+b_2C^2(\tau;u)$

(b) Solutions to ODEs

Model	$A(\tau;u)$	$C(\tau;u)$
BS73	$b_0\tau$	$-$
Mer76	$b_0\tau+\lambda(n_J-ium_J)\tau$	$-$
Hes93	$-\frac{\kappa\theta}{\sigma_v^2}\left((b_1+d)\tau+2\ln\frac{1-ge^{-d\tau}}{1-g}\right)$	$-\frac{b_1+d}{\sigma_v^2}\left(\frac{1-e^{-d\tau}}{1-ge^{-d\tau}}\right)$
Bat96	$-\frac{\kappa\theta}{\sigma_v^2}\left((b_1+d)\tau+2\ln\frac{1-ge^{-d\tau}}{1-g}\right)+\lambda(n_J-ium_J)\tau$	$-\frac{b_1+d}{\sigma_v^2}\left(\frac{1-e^{-d\tau}}{1-ge^{-d\tau}}\right)$
TS09,ST18	$m(A_1(\tau)+k_3)$	$\frac{2\gamma}{\sigma_v^2}\left(\beta+\mu z+z\frac{g'(z)}{g(z)}\right)$
SYSVJ	$m(A_1(\tau)+k_3)+\lambda(n_J-ium_J)\tau$	$\frac{2\gamma}{\sigma_v^2}\left(\beta+\mu z+z\frac{g'(z)}{g(z)}\right)$
SYSSV,ST21	$m(A_1(\tau)+A_2(\tau)+A_3(\tau)+A_4(\tau)+k_3)$	$\frac{2\gamma}{\sigma_v^2}\left(\beta+\mu z+z\frac{g'(z)}{g(z)}\right)$
	$A_1(\tau)=a^\theta\left(\beta\tau-\frac{1}{\gamma}\left(\mu z+\ln g(z)\right)\right)$	
	$A_2(\tau)=-b^\theta\frac{\beta}{2\pi}y_\tau^s$	
	$A_3(\tau)=b^\theta\frac{\mu z}{4\pi^2+\gamma^2}\left(\gamma y_\tau^c-2\pi y_\tau^s\right)$	
	$A_4(\tau)=\frac{b^\theta}{\omega}\left(\tau y_0^c g'(\omega^{-1})-\frac{\tau^2}{2}\left(g'(\omega^{-1})\left(y_0^c\zeta_1-2\pi y_0^s\right)+y_0^c\zeta_2\right)\right)$	

(c) Parameters in ODEs

Model	b_0	b_1	b_2
BS73,Mer76	$-\frac{\sigma_S^2}{2}(u^2+iu)$	$-$	$-$
Hes93,Bat96	$-\frac{\sigma_S^2}{2}(u^2+iu)$	$-\kappa+iu\sigma_v\rho_{Sv}\sigma_S$	$\frac{\sigma_v^2}{2}$
TS09,SYSVJ,SYSSV	$-\frac{1}{2}(u^2+iu)(\sigma_S^2+\sigma_Y^2(t,T)+2\rho_{Sy}\sigma_S\sigma_Y(t,T))$	$-\kappa+iu\sigma_v(\rho_{Sv}\sigma_S+\rho_{yv}\sigma_Y(t,T))$	$\frac{\sigma_v^2}{2}$
ST18,ST21	$-\frac{1}{2}(u^2+iu)\sigma_F^2(t,T)$	$-\kappa+iu\sigma_v\rho_{Fv}\sigma_F(t,T)$	$\frac{\sigma_v^2}{2}$

NOTES: With $\tau\equiv T_{Opt}-t$, this table presents the expressions followed by the ODEs and their solution for our panel of models. Observe that the expressions correspondent to BS73, Mer76, Hes93 and Bat96 are expressed in terms of futures prices (alternatively and for spot prices, add $iuy=iu(r-q)$ to $A'(\tau;u)$ and $iuy\tau$ to $A(\tau;u)$). The expressions followed by $g(z),g'(z)$ can be found in (3A.6); z,β,μ depend on the model: for TS09 and extensions, they can be found in (3A.8), for ST18 and ST21, they can be found in (3A.12). Observe that for BS73, Mer96, Hes93 and Bat96, we have that $\sigma_Y(t,T)=0$ (equivalently, $\sigma_F(t,T)=\sigma_S$). The expressions followed by the jump terms in Mer76, Bat96 and SYSVJ can be found in (3A.4); those followed by d,g in Hes93 and Bat96 write

$$d=\sqrt{b_1^2+\sigma_v^2(\sigma_S^2u^2+iu\sigma_S)},\quad g=\frac{b_1-d}{b_1+d}. \tag{3.29}$$

The expression followed by m is as in (3A.14); k_3 is as in (3A.18) and depends on the model.

Table 3.5: Fourier transforms for bivariate processes

(a) ODEs

Model	$\partial A(\tau;u_1,u_2)/\partial\tau$	$\partial C(\tau;u_1,u_2)/\partial\tau$
BS73	b_0	–
Mer76	$b_0+\big(\lambda_1(n_{J_1}-iu_1m_{J_1})+\lambda_2(n_{J_2}-iu_2m_{J_2})\big)$	–
Bat96,SYSVJ	$C(\tau;u_1,u_2)\kappa\theta+\big(\lambda_1(n_{J_1}-iu_1m_{J_1})+\lambda_2(n_{J_2}-iu_2m_{J_2})\big)$	$b_0+b_1C(\tau;u_1,u_2)+b_2C^2(\tau;u_1,u_2)$
Hes93,TS09,ST18	$C(\tau;u_1,u_2)\kappa\theta$	$b_0+b_1C(\tau;u_1,u_2)+b_2C^2(\tau;u_1,u_2)$
SYSSV,ST21	$C(\tau;u_1,u_2)\kappa\theta_t$	$b_0+b_1C(\tau;u_1,u_2)+b_2C^2(\tau;u_1,u_2)$

(b) Solutions to ODEs

Model	$A(\tau;u_1,u_2)$	$C(\tau;u_1,u_2)$
BS73	$b_0\tau$	–
Mer76	$b_0\tau+\big(\lambda_1(n_{J_1}-iu_1m_{J_1})+\lambda_2(n_{J_2}-iu_2m_{J_2})\big)\tau$	–
Hes93	$-\frac{\kappa\theta}{\sigma_v^2}\big((b_1+d)\tau+2\ln\frac{1-ge^{-d\tau}}{1-g}\big)$	$-\frac{b_1+d}{\sigma_v^2}\big(\frac{1-e^{d\tau}}{1-ge^{-d\tau}}\big)$
Bat96	$-\frac{\kappa\theta}{\sigma_v^2}\big((b_1+d)\tau+2\ln\frac{1-ge^{-d\tau}}{1-g}\big)+\big(\lambda_1(n_{J_1}-iu_1m_{J_1})+\lambda_2(n_{J_2}-iu_2m_{J_2})\big)\tau$	$-\frac{b_1+d}{\sigma_v^2}\big(\frac{1-e^{d\tau}}{1-ge^{-d\tau}}\big)$
TS09,ST18	$m(A_1(\tau;u_1,u_2)+k_3)$	$\frac{2\gamma}{\sigma_v^2}\big(\beta+\mu z+z\frac{g'(z)}{g(z)}\big)$
SYSVJ	$m(A_1(\tau;u_1,u_2)+k_3)+\big(\lambda_1(n_{J_1}-iu_1m_{J_1})+\lambda_2(n_{J_2}-iu_2m_{J_2})\big)\tau$	$\frac{2\gamma}{\sigma_v^2}\big(\beta+\mu z+z\frac{g'(z)}{g(z)}\big)$
SYSSV,ST21	$m(A_1(\tau;u_1,u_2)+A_2(\tau;u_1,u_2)+A_3(\tau;u_1,u_2)+A_4(\tau;u_1,u_2)+k_3)$	$\frac{2\gamma}{\sigma_v^2}\big(\beta+\mu z+z\frac{g'(z)}{g(z)}\big)$
	$A_1(\tau;u_1,u_2)=a^\theta\left(\beta\tau-\frac{1}{\gamma}\big(\mu z+\ln g(z)\big)\right)$	
	$A_2(\tau;u_1,u_2)=-b^\theta\frac{\beta}{2\pi}y_\tau^s$	
	$A_3(\tau;u_1,u_2)=b^\theta\frac{\mu z}{4\pi^2+\gamma^2}\big(\gamma y_\tau^c-2\pi y_\tau^s\big)$	
	$A_4(\tau;u_1,u_2)=\tau\frac{b^\theta}{\omega}\Big(y_0^c g'(\omega^{-1})-\frac{\tau}{2}\big(g'(\omega^{-1})\,(y_0^c\zeta_1-2\pi y_0^s)+y_0^c\zeta_2\big)\Big)$	

(c) Parameters in ODEs

Model	b_0	b_1	b_2
BS73,Mer76	$-\frac{1}{2}\big(\sigma_{S_1}^2(u_1^2+iu_1)+\sigma_{S_2}^2(u_2^2+iu_2)+2\sigma_{S_1}u_1\sigma_{S_2}u_2\rho_{12}\big)$	–	–
Hes93,Bat96	$-\frac{1}{2}\big(\sigma_{S_1}^2(u_1^2+iu_1)+\sigma_{S_2}^2(u_2^2+iu_2)+2\sigma_{S_1}u_1\sigma_{S_2}u_2\rho_{12}\big)$	$-\kappa+i\sigma_v\big(u_1\sigma_{S_1}\rho_{S_1v}+u_2\sigma_{S_2}\rho_{S_2v}\big)$	$\frac{\sigma_v^2}{2}$
TS09,SYSVJ,SYSSV	$-\frac{1}{2}\big(\sigma_{S_1}^2(u_1^2+iu_1)+\sigma_{S_2}^2(u_2^2+iu_2)+2\sigma_{S_1}u_1\sigma_{S_2}u_2\rho_{12}\big)$	$-\kappa+i\sigma_v\big(u_1\sigma_{S_1}\rho_{S_1v}+u_2\sigma_{S_2}\rho_{S_2v}\big)$	$\frac{\sigma_v^2}{2}$
	$-\frac{1}{2}\big(u_1^2+u_2^2+i(u_1+u_2)\big)\sigma_Y^2$	$+i\sigma_v(u_1+u_2)\sigma_Y\rho_{yv}$	
	$-\big(\sigma_{S_1}(u_1^2+iu_1)+\sigma_{S_2}(u_2^2+iu_2)\big)\sigma_Y\rho_{Sy}$		
ST18,ST21	$-\frac{1}{2}\big(\sigma_{F_1}^2(u_1^2+iu_1)+\sigma_{F_2}^2(u_2^2+iu_2)+2\sigma_{F_1}u_1\sigma_{F_2}u_2\rho_{12}\big)$	$-\kappa+i\sigma_v\big(u_1\sigma_{F_1}\rho_{F_1v}+u_2\sigma_{F_2}\rho_{F_2v}\big)$	$\frac{\sigma_v^2}{2}$

NOTES: This table presents the expressions followed by each component of the JCF for the futures log-prices for our panel of models. Observe that they are expressed in terms of futures prices (for spot prices, add $iu_1y_1+iu_2y_2=iu_1(r-q_1)+iu_2(r-q_2)$ to $A'(\tau;u_1,u_2)$, and add $(iu_1y_1+iu_2y_2)\tau$ to $A(\tau;u_1,u_2)$). For affine processes with i.i.d. increments, the JCF can be computed replacing these expressions into (3.25) and (3.27) for calendar and crack spread options; for affine processes with stochastic volatility, it can be computed replacing these expressions into (3.26) and (3.28) for calendar and crack spread options. The expressions followed by $g(z),g'(z)$ can be found in (3A.6); m can be found in (3A.14) and the jump-related paramters in (3C.3). z,β,μ depend on the model: for TS09, SYSVJ and SYSSV they can be found in (3A.8); for ST18 and ST21, they can be found in (3A.12). d,g read

$$d=\sqrt{b_1^2+\sigma_v^2(\sigma_{S_1}^2u_1^2+\sigma_{S_2}u_2^2+2\sigma_{S_1}\sigma_{S_2}\rho_{12}+i(\sigma_{S_1}u_1+\sigma_{S_2}u_2))},\quad g=\frac{b_1-d}{b_1+d}. \tag{3.30}$$

For crack spread options, we define $\tau\equiv T_{Opt}-t$, with $T_1>T_{Opt}>t\geq 0$. For calendar spread options, the time argument can be $\tau\equiv T_1-t$ or $\tau\equiv T_{Opt}-T_1$, depending on the term in the JCF, with $T_2>T_{Opt}>T_1>t\geq 0$.

Table 3.6: Initial values for bivariate processes

(a) Crack Spread Options

Factor	Asset 1	Asset 2
S_t	$S_0 = 100$	$S_0 = 96$
$r_{t,T}$	$r_{0,T} = 0.10$	$r_{0,T} = 0.10$
$q_{t,T}$	$q_{0,T} = 0.05$	$q_{0,T} = 0.05$
$y_{t,T}$	$y_{0,T} = 0.05$	$y_{0,T} = 0.05$
$F(t,T)$	$F(0,T) = 105.1271$	$F(0,T) = 100.9220$
V_t	$V_0 = 0.04$	$V_0 = 0.04$

(b) Calendar Spread Options

Factor	Asset 1	Asset 2
S_t	$S_0 = 100$	$S_0 = 96$
$r_{t,T}$	$r_{0,T_1} = 0.10$	$r_{0,T_1} = 0.10$
	$r_{0,T_2} = 0.10$	$r_{0,T_2} = 0.10$
$q_{t,T}$	$q_{0,T_1} = 0.05$	$q_{0,T_1} = 0.05$
	$q_{0,T_2} = 0.05$	$q_{0,T_2} = 0.05$
$y_{t,T}$	$y_{0,T_1} = 0.05$	$y_{0,T_1} = 0.05$
	$y_{0,T_2} = 0.05$	$y_{0,T_2} = 0.05$
$F(t,T)$	$F(0,T_1) = 105.1271$	$F(0,T_1) = 100.9220$
	$F(0,T_2) = 110.5171$	$F(0,T_2) = 106.0964$
V_t	$V_0 = 0.04$	$V_0 = 0.04$

NOTES: We define $y_{t,T} \equiv r_{t,T} - q_{t,T}$. The values for all the futures prices are obtained using equation (3.5). For Crack Spread Options (a), we assume $T = 1$. For Calendar Spread Options (b), we assume $T_1 = 1, T_2 = 2$.

Table 3.7: Model parameters for bivariate processes

Model	SYSSV	SYSVJ	ST21	ST18	TS09	Bat96	Hes93	Mer76	BS73
σ_F	1.00	1.00	1.00	1.00	1.00	$1.00, 0.50$	$1.00, 0.50$	$0.20, 0.10$	$0.20, 0.10$
α	0.50	0.50	–	–	0.50	–	–	–	–
γ	0.75	0.75	1.25	1.25	0.75	–	–	–	–
κ	1.00	1.00	0.20	0.20	1.00	1.00	1.00	–	–
θ	0.04	0.04	0.03	0.03	0.04	0.04	0.04	–	–
b^θ	0.01	–	0.40	–	–	–	–	–	–
σ_v	0.05	0.05	0.75	0.75	0.05	0.05	0.05	–	–
ρ_{Fy}	-1.00	-1.00	–	–	-1.00	–	–	–	–
ρ_{Fv}	-0.50	-0.50	-0.10	-0.10	-0.50	$-0.50, 0.25$	$-0.50, 0.25$	–	–
ρ_{yv}	-0.75	-0.75	–	–	-0.75	–	–	–	–
λ	–	$0.20, +0.10$	–	–	–	$0.20, +0.10$	–	$0.20, +0.10$	–
μ_J	–	$0.02, -0.07$	–	–	–	$0.02, -0.07$	–	$0.02, -0.07$	–
σ_J	–	$0.06, +0.01$	–	–	–	$0.06, +0.01$	–	$0.06, +0.01$	–

NOTES: In this table we present the model parameters we use for option pricing. For jump models, we assume that only idiosyncratic jumps exist, with no correlation between them. For crack spread options, we set an asset correlation of $\rho_{12} = 0.5$. When there is a single value per parameter, it means that we have used the same value for each underlying asset. The subscript F in σ and ρ refers to price, for either a spot or a futures contract. The parameter θ converts to a^θ for SYSSV and ST21.

Table 3.8: Option prices and calculation time

(a) Options on Spot prices

OPTION	CRACK			CALENDAR						PLAIN VANILLA	
	Assets 1 – 2			Asset 1			Asset 2			Asset 1	Asset 2
Model	CM99	CF13	Abs. Diff.	CM99	CF13	Abs. Diff.	CM99	CF13	Abs. Diff.	CM99	CM99
BS73	8.5131	8.5132	0.0001	7.8750	7.8751	0.0001	2.9539	2.9540	0.0001	9.9409	6.2142
Mer76	8.6410	8.6411	0.0001	7.9835	7.9835	0.0001	3.1547	3.1548	0.0001	10.011	6.3236
Hes93	8.5427	8.5428	0.0001	6.1454	6.1455	0.0001	2.1479	2.1480	0.0001	9.9563	6.2429
Bat96	8.6670	8.6671	0.0001	6.2774	6.2774	0.0001	2.3886	2.3887	0.0001	10.025	6.3492
TS09	6.2602	6.2596	0.0006	3.4123	3.4131	0.0008	3.2758	3.2766	0.0008	8.6312	8.2860
SYSVJ	6.4413	6.4405	0.0008	3.6085	3.6094	0.0009	3.4641	3.4650	0.0009	8.7109	8.3367
SYSSV	5.7505	5.8169	0.0664	2.5588	2.6632	0.1044	2.4564	2.5566	0.1002	8.8722	8.5173

(b) Options on futures prices

OPTION	CRACK			CALENDAR						PLAIN VANILLA	
	Assets 1 – 2			Asset 1			Asset 2			Asset 1	Asset 2
Model	CM99	CF13	Abs. Diff.	CM99	CF13	Abs. Diff.	CM99	CF13	Abs. Diff.	CM99	CM99
BS73	8.5131	8.5132	0.0001	7.8750	7.8751	0.0001	2.9539	2.9540	0.0001	7.5771	3.6415
Mer76	8.6410	8.6411	0.0001	7.9835	7.9835	0.0001	3.1547	3.1548	0.0001	7.6526	3.7770
Hes93	8.5427	8.5428	0.0001	6.1454	6.1455	0.0001	2.1479	2.1480	0.0001	7.5497	3.6325
Bat96	8.6670	8.6671	0.0001	6.2774	6.2774	0.0001	2.3886	2.3887	0.0001	7.6251	5.5608
TS09	6.2602	6.2596	0.0006	3.4123	3.4131	0.0008	3.2758	3.2766	0.0008	6.1008	5.8568
SYSVJ	6.4413	6.4405	0.0008	3.6085	3.6094	0.0009	3.4641	3.4650	0.0009	6.1921	5.9109
SYSSV	5.7505	5.8169	0.0664	2.5588	2.6632	0.1044	2.4564	2.5566	0.1002	6.2574	6.0071

(c) Running Time

OPTION	CRACK			CALENDAR					
	Assets 1 – 2			Asset 1			Asset 2		
Model	CM99	CF13	**Ratio**	CM99	CF13	**Ratio**	CM99	CF13	**Ratio**
BS73	1.2487	0.0565	**26.3236**	1.3030	0.0439	**29.8900**	1.2886	0.0511	**27.0971**
Mer76	1.3882	0.0509	**28.2857**	1.4715	0.0518	**28.9777**	1.4452	0.0580	**26.7167**
Hes93	2.3197	0.0832	**28.2138**	2.7928	0.0982	**28.7154**	2.7212	0.1068	**26.0316**
Bat96	2.4315	0.0864	**28.2044**	2.9154	0.1053	**28.0560**	2.9080	0.1450	**24.6031**
TS09	185.6360	8.0146	**23.7643**	240.9856	9.7031	**24.9120**	238.4525	9.5027	**25.1305**
SYSVJ	183.8979	7.6811	**24.1235**	240.7162	9.6328	**25.1317**	237.5645	9.3911	**25.3402**
SYSSV	365.7018	14.8307	**24.7392**	585.1719	22.0355	**26.6296**	585.9564	22.2508	**26.4149**
Average			**26.2364**			**27.4732**			**25.9049**

NOTES: In this Table we present the values obtained for European call options using those values displayed in Tables 3.6 and 3.7. The model SYSVJ considers jumps only in S_t, that is, sub-specification (a_1). In Sub-tables (a) and (b) we present option values for spot and futures prices, respectively. For spread options, values correspond to a strike level $K = 0$; for plain vanilla options, the options are ATM. Header $CM99$ indicates that we follow the methodology in Carr & Madan (1999) together with the FFT algorithm with 1,024 evaluation points. Header $CF13$ indicates that we use the technology presented in Caldana & Fusai (2013) together with the Gauss-Kronrod quadrature. In Sub-table (c) we present the calculation time, which is expressed in seconds. On average, $CF13$ is 26.5 times quicker than $CM99$. This calculation has been performed using 10 repetitions of the pricing exercise.

Table 3.9: Option prices per vector of strikes

(a) Black & Scholes (1973)

BS73	**CRACK**			**CALENDAR**						**PLAIN VANILLA**	
	Assets 1 – 2			**Asset 1**			**Asset 2**			**Asset 1**	**Asset 2**
Strike	CM99	CF13	Abs. Diff.	CM99	CF13	Abs. Diff.	CM99	CF13	Abs. Diff.	CM99	CM99
0.0000	8.5131	8.5132	0.0001	7.8750	7.8751	0.0001	2.9539	2.9540	0.0001	7.5771	3.6415
0.4000	8.3125	8.3125	0.0001	7.7261	7.7261	0.0000	2.8330	2.8329	0.0001	7.4119	3.4706
0.8000	8.1150	8.1150	0.0000	7.5789	7.5789	0.0000	2.7152	2.7152	0.0000	7.2494	3.3054
1.2000	7.9208	7.9208	0.0000	7.4335	7.4335	0.0000	2.6010	2.6010	0.0000	7.0897	3.1458
1.6000	7.7299	7.7299	0.0000	7.2899	7.2898	0.0000	2.4901	2.4901	0.0000	6.9326	2.9918
2.0000	7.5423	7.5423	0.0000	7.1480	7.1480	0.0000	2.3826	2.3826	0.0000	6.7781	2.8433
2.4000	7.3580	7.3580	0.0000	7.0080	7.0080	0.0000	2.2784	2.2784	0.0000	6.6264	2.7003
2.8000	7.1769	7.1769	0.0000	6.8698	6.8698	0.0000	2.1775	2.1775	0.0000	6.4772	2.5626
3.2000	6.9991	6.9991	0.0000	6.7334	6.7334	0.0001	2.0798	2.0798	0.0000	6.3307	2.4301
3.6000	6.8245	6.8245	0.0000	6.5988	6.5987	0.0001	1.9853	1.9853	0.0000	6.1867	2.3029
4.0000	6.6531	6.6531	0.0000	6.4660	6.4659	0.0001	1.8940	1.8940	0.0000	6.0453	2.1808

(b) Merton (1976)

Mer76	**CRACK**			**CALENDAR**						**PLAIN VANILLA**	
	Assets 1 – 2			**Asset 1**			**Asset 2**			**Asset 1**	**Asset 2**
Strike	CM99	CF13	Abs. Diff.	CM99	CF13	Abs. Diff.	CM99	CF13	Abs. Diff.	CM99	CM99
0.0000	8.6410	8.6411	0.0001	7.9835	7.9835	0.0001	3.1547	3.1548	0.0001	7.6526	3.7770
0.4000	8.4412	8.4412	0.0001	7.8345	7.8344	0.0000	3.0327	3.0326	0.0001	7.4877	3.6072
0.8000	8.2445	8.2445	0.0000	7.6871	7.6871	0.0000	2.9138	2.9138	0.0000	7.3255	3.4428
1.2000	8.0510	8.0510	0.0000	7.5416	7.5416	0.0000	2.7982	2.7982	0.0000	7.1659	3.2839
1.6000	7.8608	7.8608	0.0000	7.3978	7.3978	0.0000	2.6859	2.6859	0.0000	7.0090	3.1304
2.0000	7.6738	7.6738	0.0000	7.2559	7.2558	0.0000	2.5768	2.5768	0.0000	6.8548	2.9822
2.4000	7.4900	7.4900	0.0000	7.1157	7.1156	0.0000	2.4709	2.4709	0.0000	6.7031	2.8393
2.8000	7.3094	7.3094	0.0000	6.9773	6.9772	0.0000	2.3682	2.3682	0.0000	6.5541	2.7016
3.2000	7.1319	7.1319	0.0000	6.8406	6.8406	0.0001	2.2686	2.2686	0.0000	6.4076	2.5690
3.6000	6.9577	6.9577	0.0000	6.7058	6.7057	0.0001	2.1721	2.1721	0.0000	6.2637	2.4414
4.0000	6.7866	6.7865	0.0000	6.5727	6.5726	0.0001	2.0786	2.0786	0.0000	6.1223	2.3188

(c) Heston (1993)

Hes93	**CRACK**			**CALENDAR**						**PLAIN VANILLA**	
	Assets 1 – 2			**Asset 1**			**Asset 2**			**Asset 1**	**Asset 2**
Strike	CM99	CF13	Abs. Diff.	CM99	CF13	Abs. Diff.	CM99	CF13	Abs. Diff.	CM99	CM99
0.0000	8.5427	8.5428	0.0001	6.1454	6.1455	0.0001	2.1479	2.1480	0.0001	7.5497	3.6325
0.4000	8.3375	8.3374	0.0001	6.0036	6.0036	0.0000	2.0365	2.0364	0.0001	7.3811	3.4583
0.8000	8.1353	8.1353	0.0000	5.8639	5.8639	0.0000	1.9289	1.9289	0.0000	7.2153	3.2898
1.2000	7.9365	7.9365	0.0000	5.7264	5.7264	0.0000	1.8254	1.8254	0.0000	7.0522	3.1270
1.6000	7.7409	7.7409	0.0000	5.5910	5.5910	0.0000	1.7259	1.7259	0.0000	6.8919	2.9698
2.0000	7.5485	7.5485	0.0000	5.4577	5.4577	0.0000	1.6304	1.6304	0.0000	6.7342	2.8182
2.4000	7.3594	7.3594	0.0000	5.3266	5.3266	0.0000	1.5387	1.5387	0.0000	6.5792	2.6721
2.8000	7.1735	7.1735	0.0000	5.1976	5.1976	0.0000	1.4508	1.4508	0.0000	6.4268	2.5315
3.2000	6.9909	6.9909	0.0000	5.0708	5.0708	0.0000	1.3666	1.3666	0.0000	6.2771	2.3963
3.6000	6.8114	6.8114	0.0000	4.9461	4.9460	0.0001	1.2861	1.2861	0.0000	6.1300	2.2665
4.0000	6.6352	6.6352	0.0000	4.8235	4.8234	0.0001	1.2092	1.2092	0.0000	5.9855	2.1418

Table 3.9: Option prices per vector of strikes – continued

(d) Bates (1996)

Bat96	**CRACK**			**CALENDAR**						**PLAIN VANILLA**	
	Assets 1 – 2			**Asset 1**			**Asset 2**			**Asset 1**	**Asset 2**
Strike	CM99	CF13	Abs. Diff.	CM99	CF13	Abs. Diff.	CM99	CF13	Abs. Diff.	CM99	CM99
0.0000	8.6670	8.6671	0.0001	6.2774	6.2774	0.0001	2.3886	2.3887	0.0001	7.6251	3.7671
0.4000	8.4628	8.4628	0.0000	6.1355	6.1355	0.0000	2.2757	2.2756	0.0001	7.4569	3.5942
0.8000	8.2617	8.2617	0.0000	5.9956	5.9956	0.0000	2.1664	2.1664	0.0000	7.2914	3.4269
1.2000	8.0638	8.0638	0.0000	5.8579	5.8579	0.0000	2.0609	2.0609	0.0000	7.1287	3.2650
1.6000	7.8691	7.8691	0.0000	5.7223	5.7223	0.0000	1.9592	1.9592	0.0000	6.9686	3.1086
2.0000	7.6775	7.6775	0.0000	5.5888	5.5888	0.0000	1.8613	1.8613	0.0000	6.8111	2.9576
2.4000	7.4892	7.4892	0.0000	5.4574	5.4574	0.0000	1.7670	1.7670	0.0000	6.6563	2.8120
2.8000	7.3040	7.3040	0.0000	5.3281	5.3281	0.0000	1.6762	1.6762	0.0000	6.5042	2.6717
3.2000	7.1220	7.1220	0.0000	5.2010	5.2009	0.0000	1.5890	1.5890	0.0000	6.3547	2.5365
3.6000	6.9432	6.9432	0.0000	5.0759	5.0758	0.0001	1.5053	1.5053	0.0000	6.2077	2.4066
4.0000	6.7676	6.7676	0.0000	4.9528	4.9528	0.0001	1.4249	1.4249	0.0000	6.0634	2.2816

(e) Trolle & Schwartz (2009)

TS09	**CRACK**			**CALENDAR**						**PLAIN VANILLA**	
	Assets 1 – 2			**Asset 1**			**Asset 2**			**Asset 1**	**Asset 2**
Strike	CM99	CF13	Abs. Diff.	CM99	CF13	Abs. Diff.	CM99	CF13	Abs. Diff.	CM99	CM99
0.0000	6.2602	6.2596	0.0006	3.4127	3.4131	0.0005	3.2761	3.2766	0.0005	6.1008	5.8568
0.4000	6.0299	6.0288	0.0011	3.2901	3.2906	0.0005	3.1536	3.1541	0.0005	5.9269	5.6830
0.8000	5.8042	5.8028	0.0013	3.1706	3.1711	0.0005	3.0344	3.0348	0.0004	5.7564	5.5127
1.2000	5.5834	5.5818	0.0016	3.0543	3.0547	0.0005	2.9183	2.9188	0.0004	5.5893	5.3459
1.6000	5.3676	5.3658	0.0019	2.9409	2.9414	0.0004	2.8054	2.8059	0.0004	5.4255	5.1826
2.0000	5.1569	5.1548	0.0021	2.8306	2.8310	0.0004	2.6957	2.6961	0.0004	5.2651	5.0228
2.4000	4.9512	4.9489	0.0023	2.7233	2.7237	0.0004	2.5890	2.5894	0.0004	5.1080	4.8664
2.8000	4.7506	4.7480	0.0025	2.6189	2.6193	0.0004	2.4855	2.4859	0.0004	4.9542	4.7135
3.2000	4.5551	4.5524	0.0027	2.5175	2.5179	0.0004	2.3850	2.3853	0.0004	4.8037	4.5640
3.6000	4.3647	4.3618	0.0028	2.4190	2.4193	0.0004	2.2875	2.2878	0.0003	4.6564	4.4180
4.0000	4.1794	4.1765	0.0029	2.3233	2.3237	0.0003	2.1929	2.1932	0.0003	4.5124	4.2752

(f) SYSVJ

SYSVJ	**CRACK**			**CALENDAR**						**PLAIN VANILLA**	
	Assets 1 – 2			**Asset 1**			**Asset 2**			**Asset 1**	**Asset 2**
Strike	CM99	CF13	Abs. Diff.	CM99	CF13	Abs. Diff.	CM99	CF13	Abs. Diff.	CM99	CM99
0.0000	6.4413	6.4405	0.0008	3.6086	3.6094	0.0008	3.4643	3.4650	0.0007	6.1921	5.9109
0.4000	6.2141	6.2129	0.0012	3.4850	3.4858	0.0008	3.3407	3.3415	0.0007	6.0189	5.7371
0.8000	5.9914	5.9900	0.0014	3.3645	3.3652	0.0007	3.2204	3.2211	0.0007	5.8490	5.5669
1.2000	5.7735	5.7719	0.0015	3.2469	3.2476	0.0007	3.1031	3.1038	0.0007	5.6824	5.4001
1.6000	5.5604	5.5587	0.0017	3.1322	3.1329	0.0007	2.9888	2.9895	0.0007	5.5191	5.2368
2.0000	5.3521	5.3503	0.0018	3.0205	3.0212	0.0007	2.8777	2.8783	0.0007	5.3591	5.0769
2.4000	5.1487	5.1468	0.0019	2.9116	2.9123	0.0007	2.7695	2.7701	0.0006	5.2024	4.9205
2.8000	4.9502	4.9482	0.0020	2.8057	2.8063	0.0007	2.6643	2.6649	0.0006	5.0490	4.7674
3.2000	4.7566	4.7545	0.0021	2.7025	2.7032	0.0006	2.5620	2.5626	0.0006	4.8988	4.6178
3.6000	4.5680	4.5658	0.0022	2.6022	2.6028	0.0006	2.4627	2.4633	0.0006	4.7518	4.4715
4.0000	4.3842	4.3820	0.0022	2.5047	2.5052	0.0006	2.3662	2.3668	0.0006	4.6080	4.3285

Table 3.9: Option prices per vector of strikes – continued

(g) SYSSV

SYSSV	CRACK			CALENDAR						PLAIN VANILLA	
	Assets 1 – 2			Asset 1			Asset 2			Asset 1	Asset 2
Strike	CM99	CF13	Abs. Diff.	CM99	CF13	Abs. Diff.	CM99	CF13	Abs. Diff.	CM99	CM99
0.0000	5.7505	5.8169	0.0664	2.5588	2.6632	0.1044	2.4564	2.5566	0.1002	6.2574	6.0071
0.4000	5.5162	5.5805	0.0643	2.4442	2.5461	0.1020	2.3418	2.4397	0.0978	6.0773	5.8270
0.8000	5.2868	5.3492	0.0624	2.3321	2.4324	0.1003	2.2300	2.3261	0.0961	5.9006	5.6506
1.2000	5.0626	5.1232	0.0606	2.2233	2.3219	0.0986	2.1216	2.2160	0.0944	5.7274	5.4778
1.6000	4.8437	4.9025	0.0588	2.1177	2.2146	0.0969	2.0164	2.1092	0.0928	5.5576	5.3085
2.0000	4.6302	4.6873	0.0571	2.0153	2.1106	0.0953	1.9145	2.0057	0.0912	5.3913	5.1428
2.4000	4.4219	4.4774	0.0554	1.9159	2.0096	0.0937	1.8159	1.9055	0.0896	5.2283	4.9806
2.8000	4.2191	4.2730	0.0539	1.8196	1.9118	0.0922	1.7204	1.8085	0.0881	5.0688	4.8220
3.2000	4.0217	4.0740	0.0524	1.7264	1.8171	0.0907	1.6281	1.7147	0.0866	4.9126	4.6668
3.6000	3.8297	3.8806	0.0510	1.6361	1.7254	0.0892	1.5389	1.6241	0.0852	4.7598	4.5152
4.0000	3.6431	3.6927	0.0496	1.5488	1.6366	0.0878	1.4528	1.5365	0.0837	4.6102	4.3670

NOTES: In these Tables we present the values obtained for European call options using those values displayed in Tables 3.6 and 3.7. We present option values where the underlying price is that of a futures contract. For spread options, values correspond to strike levels starting from $K = 0$ up to $K = 4$, increasing in 0.4; for plain vanilla options, the options start ATM and increase in 0.4. Header $CM99$ indicates that we follow the methodology in Carr & Madan (1999) together with the FFT algorithm with 1,024 evaluation points. Header $CF13$ indicates that we use the technology presented in Caldana & Fusai (2013) together with the Gauss-Kronrod quadrature. Each sub-table refers to a model in the panel. The model SYSVJ considers jumps only in S_t, that is, sub-specification (a_1).

Bibliography

Alfeus, M. & Schloegl, E. (2018), 'On numerical methods for spread options'.
URL: *https://ssrn.com/abstract=3099902* 97

Bakshi, G. & Madan, D. (2000), 'Spanning and derivative security valuation', *Journal of Financial Economics* **55**(2), 205–238. 99

Bates, D. S. (1996), 'Jumps and stochastic volatility: Exchange rate processes implicit in deutsche mark options', *Review of Financial Studies* **9**(1), 69–107. 103

Bjerksund, P. & Stlensland, G. (2011), 'Closed form spread option valuation', *Quantitative Finance iFirst* pp. 1–10. 96, 97, 99

Black, F. & Scholes, M. (1973), 'The pricing of options and corporate liabilities', *Journal of Political Economy* **81**(3), 637–654. 96, 97, 103

Caldana, R. & Fusai, G. (2013), 'A general closed-form spread option pricing formula', *Journal of Banking and Finance* **37**(12), 4893–4906. 96, 97, 99, 103, 108, 115, 118

Carr, P. & Madan, D. B. (1999), 'Option valuation using the fast Fourier transform', *Journal of Computational Finance* **2**(4), 61–73. 96, 97, 98, 99, 100, 103, 108, 115, 118

Crosby, J. & Frau, C. (2021), 'Jumps in commodity prices: New approaches for pricing plain vanilla options'.
URL: *https://ssrn.com/abstract=3754835* 103

Dempster, M. A. H. & Hong, S. S. G. (2002), *Spread Option Valuation and the Fast Fourier Transform*, Springer Berlin Heidelberg, pp. 203–220. 96

Duffie, D., Pan, J. & Singleton, K. (2000), 'Transform analysis and asset pricing for affine jump-diffusions', *Econometrica* **68**, 1343–1376. 98, 99

Frau, C. & Fanelli, V. (2021), 'Seasonality in commodity prices: New approaches for pricing plain vanilla options'.
URL: *https://ssrn.com/abstract=3944647* 104, 125

Heston, S. L. (1993), 'A closed-form solution for options with stochastic volatility with applications to bond and currency options', *Review of Financial Studies* **6**(2), 327–343. 97, 98, 99, 103

Hurd, T. & Zhou, Z. (2010), 'A Fourier transform method for spread option pricing', *SIAM Journal of Financial Mathematics* **1**, 142–157. 96, 97, 99

Kirk, E. & Aron, J. (1995), 'Correlation in the energy markets, managing energy price risk', *Risk Books* pp. 71–78. 96

Lewis, A. (2001), A simple option formula for general jump-diffusion and other exponential Lévy processe, Technical report.
URL: *http://www.optioncity.net* 99

Margrabe, W. (1978), 'The value of an option to exchange one asset for another', *Journal of Finance* **33**, 177–86. 96

Merton, R. (1976), 'Option pricing when underlying stock returns are discontinuous', *Journal of Financial Economics* **3**(1-2), 125–144. 103

Schneider, L. & Tavin, B. (2018), 'From the Samuelson volatility effect to a Samuelson correlation effect: an analysis of crude oil calendar spread options', *Journal of Banking and Finance* **95**, 185–202. 97, 99, 104

Schneider, L. & Tavin, B. (2021), 'Seasonal volatility in agricultural markets: Modelling and empirical investigations', *Annals of Operational Research* . 104

Sitzia, N. (2018), 'The analytical solution of Trolle-Schwartz model, MSc. thesis, École Polytechnique Fédérale de Lausanne'.
URL: *https://ssrn.com/abstract=3121906* 104, 108, 124, 129

Stein, E. & Stein, F. (1991), 'Stock price distribution with stochastic volatility: an analytic approach', *Review of Financial Studies* **4**, 727–752. 98

Trolle, A. B. & Schwartz, E. S. (2009), 'Unspanned stochastic volatility and the pricing of commodity derivatives', *Review of Financial Studies* **22**(11), 4423–4461. 103

Venkatramanan, A. & Alexander, C. (2011), 'Closed form approximations for spread options', *Applied Mathematical Finance* **18**(5), 447–472. 96

Appendix

3A Appendix for the Single Characteristic Function

For a time-t option price on a futures prices $F(t,T)$, we introduce the transform with its exponential affine solution, which is given by

$$\Phi_F(u) \equiv E_t^{\mathbb{Q}}[e^{iuf(T_{Opt},T)}] = e^{A(T_{Opt}-t;u)+iuf(t,T)+C(T_{Opt}-t;u)V_t}. \tag{3A.1}$$

3A.1 ODEs

In a more general form and with $\tau \equiv T_{Opt} - t$, $A(\tau;u)$ and $C(\tau;u)$ solve the following system of ODEs

$$\frac{\partial A(\tau;u)}{\partial \tau} = \kappa\theta_t C(\tau;u) + \lambda\big(n_J - ium_J\big), \tag{3A.2}$$

$$\frac{\partial C(\tau;u)}{\partial \tau} = b_0 + b_1 C(\tau;u) + b_2 C^2(\tau;u), \tag{3A.3}$$

subject to the initial conditions $A(0;u) = C(0;u) = 0$, with

$$m_J = e^{\mu_J + \frac{1}{2}\sigma_J^2} - 1, \quad n_J = e^{iu\mu_J - \frac{1}{2}\sigma_J^2 u^2} - 1. \tag{3A.4}$$

If the model does not present jumps, this general model reduces to SYSSV; if the model does not present seasonality in the variance either, it reduces to TS09. Observe that these elements only affect $A(\tau;u)$. This means that, for a given set of b_0, b_1, b_2, the solution to $C(\tau;u)$ remains the same. and ST21. Equation (3A.3) has an analytical solution given by

$$C(\tau;u) = \frac{2\gamma}{\sigma_v^2}\left(\beta + \mu z + z\frac{g'(z)}{g(z)}\right), \tag{3A.5}$$

where the function $g(z)$ is a linear combination of Kummer's M and Tricomi's U hypergeometric functions, whist k_1 and k_2 are constants determined by the initial conditions of the differential equation

$$\begin{aligned} g(z) &= k_1 M(a,b,z) + k_2 U(a,b,z), \\ g'(z) &= \frac{a}{b}k_1 M(a+1,b+1,z) - ak_2 U(a+1,b+1,z). \end{aligned} \tag{3A.6}$$

3A.2 Variance Term $C(\tau;u)$

Trolle-Schwartz (2009) and extensions (SYSVJ, SYSSV)

For the three models and with $\sigma_Y(t,T)$ as in Table 3.1, we have that

$$\begin{aligned} b_0 &= -\frac{1}{2}(u^2+iu)\big(\sigma_S^2+\sigma_Y^2(t,T)+2\rho_{Sy}\sigma_S\sigma_Y(t,T)\big),\\ b_1 &= -\kappa+iu\sigma_v\big(\rho_{Sv}\sigma_S+\rho_{yv}\sigma_Y(t,T)\big), \qquad b_2=\frac{\sigma_v^2}{2}. \end{aligned} \tag{3A.7}$$

The coefficients in $g(z)$ and $g'(z)$ are

$$\begin{aligned} a &= -\mu b-\beta c_1\frac{\omega}{\gamma}-d_1\frac{\omega}{\gamma^2}, \quad & b &= 1+2\beta+\frac{c_0}{\gamma}, \quad & z &= \frac{e^{-\gamma\tau}}{\omega},\\ \mu &= -\frac{1}{2}\Big(1+\frac{c_1\omega}{\gamma}\Big), & \beta &= \frac{-c_0+\sqrt{c_0^2-4d_0}}{2\gamma}, & \omega &= -\frac{\gamma}{\sqrt{c_1^2-4d_2}}, \end{aligned} \tag{3A.8}$$

with

$$\begin{aligned} c_0 &= -\kappa+iu\sigma_v\Big(\rho_{Sv}\sigma_S+\rho_{yv}\frac{\alpha}{\gamma}\Big), \quad & d_0 &= -\frac{\sigma_v^2}{4}(u^2+iu)\Big(\sigma_S^2+\frac{\alpha^2}{\gamma^2}+2\sigma_S\rho_{Sy}\frac{\alpha}{\gamma}\Big),\\ c_1 &= -iu\sigma_v\rho_{yv}\frac{\alpha}{\gamma}e^{-\gamma(T-T_{Opt})}, & d_1 &= +\frac{\sigma_v^2}{2}(u^2+iu)\frac{\alpha}{\gamma}\Big(\frac{\alpha}{\gamma}+\rho_{Sy}\sigma_S\Big)e^{-\gamma(T-T_{Opt})},\\ & & d_2 &= -\frac{\sigma_v^2}{4}(u^2+iu)\frac{\alpha^2}{\gamma^2}e^{-2\gamma(T-T_{Opt})}. \end{aligned} \tag{3A.9}$$

In particular, if the initial condition is $C(0;u)=0$, then

$$k_1=\frac{-\beta\omega-\mu+a\frac{U(a+1,b+1,\omega^{-1})}{U(a,b,\omega^{-1})}}{\frac{a}{b}M(a+1,b+1,\omega^{-1})+aM(a,b,\omega^{-1})\frac{U(a+1,b+1,\omega^{-1})}{U(a,b,\omega^{-1})}}, \quad k_2=\frac{1-k_1M(a,b,\omega^{-1})}{U(a,b,\omega^{-1})}. \tag{3A.10}$$

The three models present the same expressions for $C(\tau;u)$ and their components. The proof is in Sitzia (2018).

Schneider-Tavin (2018, 2021)

For both models and with $\sigma_F(t,T)$ as in Table 3.1, we have that

$$b_0=-\frac{1}{2}(u^2+iu)\sigma_F^2(t,T), \qquad b_1=-\kappa+iu\sigma_v\rho_{Fv}\sigma_F(t,T), \qquad b_2=\frac{\sigma_v^2}{2}. \tag{3A.11}$$

Following the methodology described in Sitzia (2018), the coefficients in $g(z), g'(z)$ are

$$\begin{aligned} a &= -\Big(\mu b+\omega\frac{\kappa c_1}{2\gamma}\Big), \quad & b &= 1-\beta, \quad & z &= \frac{e^{-\gamma\tau}}{\omega},\\ \mu &= -\frac{1}{2}\Big(1+\frac{c_1\omega}{\gamma}\Big), & \beta &= \frac{\kappa}{\gamma}, & \omega &= -\frac{\gamma}{\sqrt{c_1^2-4d_2}},\\ c_1 &= -iu\sigma_v\rho_{Fv}\sigma_F(T_{Opt},T), & & & d_2 &= -\frac{\sigma_v^2(u^2+iu)}{4}\sigma_F(T_{Opt},T)^2. \end{aligned} \tag{3A.12}$$

The expressions followed by k_1, k_2 are as those for TS09. The proof is in Frau & Fanelli (2021).

3A.3 Independent Term $A(\tau; u)$

Equation (3A.2) has an analytical solution given by

$$A(\tau) = m\big(A_1(\tau;u) + A_2(\tau;u) + A_3(\tau;u) + A_4(\tau;u) + k_3\big) + \lambda(n_J - ium_J)\tau, \tag{3A.13}$$

with

$$m = 2\kappa\gamma/\sigma_v^2, \tag{3A.14}$$

$$\begin{aligned} A_1(\tau;u) &= a^\theta\Big(\beta\tau - \frac{\mu z + \ln g(z)}{\gamma}\Big),\\ A_2(\tau;u) &= -b^\theta \frac{\beta y^s_\tau}{2\pi},\\ A_3(\tau;u) &= b^\theta \frac{y^c_\tau - 2\pi\gamma y^s_\tau}{4\pi^2+\gamma^2}\mu z,\\ A_4(\tau;u) &= b^\theta \frac{\tau}{\omega}\Big(y^c_0 g'\left(\omega^{-1}\right) - \frac{\tau}{2}\Big(g'\left(\omega^{-1}\right)\left(y^c_0\zeta_1 - 2\pi y^s_0\right) + y^c_0\zeta_2\Big)\Big), \end{aligned} \tag{3A.15}$$

where

$$\begin{aligned} y^c_\tau &= \cos\left(2\pi\left(T_0 - \tau - t_0\right)\right), \quad & y^c_0 &= \cos\left(2\pi\left(T_0 - t_0\right)\right),\\ y^s_\tau &= \sin\left(2\pi\left(T_0 - \tau - t_0\right)\right), \quad & y^s_0 &= \sin\left(2\pi\left(T_0 - t_0\right)\right),\\ \zeta_1 &= \gamma(1 + k_1 n_1 + k_2 n_2), & \zeta_2 &= \gamma(k_1 n_3 + k_2 n_4), \end{aligned} \tag{3A.16}$$

and

$$\begin{aligned} n_1 &= (a-b)\big(M(a-1,b,\omega^{-1}) - M(a,b,\omega^{-1})\big) + M(a,b,\omega^{-1})\omega^{-1},\\ n_2 &= a\big(U(a,b,\omega^{-1}) + (b-a-1)\,U(a+1,b,\omega^{-1})\big),\\ n_3 &= \frac{a}{b}\Big((a-b)\big(M(a+1,b+1,\omega^{-1}) - M(a,b+1,\omega^{-1})\big) + M(a+1,b+1,\omega^{-1})\omega^{-1}\Big),\\ n_4 &= a\big(U(a,b,\omega^{-1}) + \left(b-\omega^{-1}\right)U(a+1,b+1,\omega^{-1})\big). \end{aligned} \tag{3A.17}$$

In particular, if the initial condition is $A(0;u) = 0$, we have

$$\begin{aligned} &k_3 = x_0 + x^s_0 y^s_0 + x^c_0 y^c_0,\\ &x_0 = a^\theta \frac{\mu}{\omega}, \qquad x^s_0 = b^\theta\Big(\frac{\beta}{2\pi} - \frac{2\pi\mu}{\omega(4\pi^2+\gamma^2)}\Big), \qquad x^c_0 = -b^\theta \frac{\mu\gamma}{\omega(4\pi^2+\gamma^2)}. \end{aligned} \tag{3A.18}$$

Observe that $k_3 = x_0$ in TS09, SYSVJ and ST18. The proof is in Frau & Fanelli (2021).

With $b^\theta = 0$ (implying $A_2(\tau;u) = A_3(\tau;u) = A_4(\tau;u) = 0$) and $\lambda = 0$, we have the solution for TS09 and ST18. With $b^\theta = 0$, we have the solution for SYSVJ, m_J and n_J as in (3A.4). With only $\lambda = 0$, we have the solution for SYSSV and ST21. The expressions followed by $a, b, \beta, \mu, \omega, z$ depend on the model; they are defined in Appendix 3A.2.

3B Appendix for Proofs

3B.1 Proof of Proposition 3.1

For affine processes with i.i.d. increments, the SCF of the price $F(t, T)$ at time $T_0 = 0$ is given by

$$\Phi_{F_{t,T}}(u) \equiv \mathbb{E}_{T_0}^{\mathbb{Q}}\left[e^{iuf(t,T)}\right] = e^{A(t-T_0;u)+B(t-T_0;u)f(T_0,T)}. \tag{3B.1}$$

Using the tower expectations, the JCF of $F(t, T_1)$ and $F(t, T_2)$ is given by

$$\begin{aligned}
\Phi_{\mathbf{F}}(\mathbf{u}) &\equiv \mathbb{E}_{T_0}^{\mathbb{Q}}\left[e^{iu_1 f(t,T_1)+iu_2 f(t,T_2)}\right] \\
&= \mathbb{E}_{T_0}^{\mathbb{Q}}\left[e^{iu_1 f(t,T_1)}\mathbb{E}_{T_1}^{\mathbb{Q}}\left[e^{iu_2 f(t,T_2)}\right]\right] \\
&= \mathbb{E}_{T_0}^{\mathbb{Q}}\left[e^{iu_1 f(t,T_1)}e^{A(T_2-T_1;u_2)+B(T_2-T_1;u_2)f(t,T_1)}\right] \\
&= e^{A(T_2-T_1;u_2)}\mathbb{E}_{T_0}^{\mathbb{Q}}\left[e^{i(u_1-iB(T_2-T_1;u_2))f(t,T_1)}\right] \\
&= e^{A(T_2-T_1;u_2)+A(T_1-T_0;u_1-iB(T_2-T_1;u_2))+B(T_1-T_0,u_1-iB(T_2-T_1;u_2))f(T_0,T_1)} \\
&= e^{A(T_2-T_1;u_2)}\Phi_{F_{t,T_1}}\big(u_1 - iB(T_2 - T_1; u_2)\big),
\end{aligned} \tag{3B.2}$$

where

$$\begin{aligned}
B(T_2 - T_1; u_2) &= iu_2, \\
u_1 - iB(T_2 - T_1; u_2) &= u_1 + u_2, \\
A(T_1 - T_0; u_1 - iB(T_2 - T_1; u_2)) &= A(T_1 - T_0; u_1 + u_2), \\
B(T_1 - T_0; u_1 - iB(T_2 - T_1; u_2)) &= B(T_1 - T_0; u_1 + u_2) = i(u_1 + u_2).
\end{aligned} \tag{3B.3}$$

3B.2 Proof of Proposition 3.2

For affine processes with stochastic volatility, the SCF of the price $F(t, T)$ and its variance V_t at time $T_0 = 0$ is given by

$$\Phi_{F_{t,T},V_t}(u, v)\mathbb{E}_{T_0}^{\mathbb{Q}}\left[e^{iuf(t,T)+ivV_t}\right] = e^{A(t-T_0;u,v)+B(t-T_0;u,v)f(T_0,T)+C(t-T_0;u,v)V_{T_0}}. \tag{3B.4}$$

Using the tower expectations, the JCF of $F(t, T_1)$ and $F(t, T_2)$ is given by

$$\begin{aligned}
\Phi_{\mathbf{F}}(\mathbf{u}) &\equiv \mathbb{E}^{\mathbb{Q}}_{T_0}\left[e^{iu_1 f(t,T_1)+iu_2 f(t,T_2)}\right] \\
&= \mathbb{E}^{\mathbb{Q}}_{T_0}\left[e^{iu_1 f(t,T_1)}\mathbb{E}^{\mathbb{Q}}_{T_1}\left[e^{iu_2 f(t,T_2)}\right]\right] \\
&= \mathbb{E}^{\mathbb{Q}}_{T_0}\left[e^{iu_1 f(t,T_1)}e^{A(T_2-T_1;u_2,0)+i(-i)B(T_2-T_1;u_2,0)f(t,T_1)+i(-i)C(T_2-T_1;u_2,0)V_{T_1}}\right] \\
&= e^{A(T_2-T_1;u_2,0)}\mathbb{E}^{\mathbb{Q}}_{T_0}\left[e^{i(u_1-iB(T_2-T_1;u_2,0))f(t,T_1)+i(-i)C(T_2-T_1;u_2,0)V_{T_1}}\right] \\
&= e^{A(T_2-T_1;u_2,0)}e^{A(T_1-T_0;u_1-iB(T_2-T_1;u_2,0),(-i)C(T_2-T_1;u_2,0))} \\
&\times e^{B(T_1-T_0;u_1-iB(T_2-T_1;u_2,0),(-i)C(T_2-T_1;u_2,0))f(T_0,T_1)}e^{C(T_1-T_0;u_1-iB(T_2-T_1;u_2,0),(-i)C(T_2-T_1;u_2,0))V_{T_0}} \\
&= e^{A(T_2-T_1;u_2,0)}\Phi_{F_{t,T_1},V_t}\big(u_1 - iB(T_2-T_1;u_2,0), -iC(T_2-T_1;u_2,0)\big),
\end{aligned} \tag{3B.5}$$

where

$$\begin{aligned}
B(T_2-T_1;u_2,0) &= iu_2, \\
u_1 - iB(T_2-T_1;u_2,0) &= u_1+u_2, \\
-iC(T_2-T_1;u_2,0) &= 0, \\
A(T_1-T_0;u_1-iB(T_2-T_1;u_2),-iC(T_2-T_1;u_2,0)) &= A(T_1-T_0;u_1+u_2,0), \\
B(T_1-T_0;u_1-iB(T_2-T_1;u_2),-iC(T_2-T_1;u_2,0)) &= B(T_1-T_0;u_1+u_2,0) = i(u_1+u_2), \\
C(T_1-T_0;u_1-iB(T_2-T_1;u_2),-iC(T_2-T_1;u_2,0)) &= C(T_1-T_0;u_1+u_2,0).
\end{aligned} \tag{3B.6}$$

3C Appendix for the Joint Characteristic Function

For a time-t option price on a futures price $F(t, T)$, the JCF is given by equation (3B.5).

3C.1 ODEs

For crack spread options, we define $\tau \equiv T_{Opt} - t$, with $T_1 > T_{Opt} > t \geq 0$. For calendar spread options, we need to be careful with the time argument τ, since it can be $\tau \equiv T_1 - t$ or $\tau \equiv T_{Opt} - T_1$, depending on the term in the JCF, with $T_2 > T_{Opt} > T_1 > t \geq 0$.

In a more general form, $A(\tau; u_1, u_2)$ and $C(\tau; u_1, u_2)$ solve the system

$$\frac{\partial A(\tau;u)}{\partial \tau} = \kappa\theta_t C(\tau;u_1,u_2) + \lambda_1\big(n_{J_1} - iu_1 m_{J_1}\big) + \lambda_2\big(n_{J_2} - iu_2 m_{J_2}\big), \tag{3C.1}$$

$$\frac{\partial C(\tau;u)}{\partial \tau} = b_0 + b_1 C(\tau;u_1,u_2) + b_2 C^2(\tau;u_1,u_2), \tag{3C.2}$$

subject to the initial conditions $A(0; u_1, u_2) = C(0; u_1, u_2) = 0$ and with

$$\begin{aligned}
m_{J_1} &= e^{\mu_{J_1}+\frac{1}{2}\sigma^2_{J_1}} - 1, \quad n_{J_1} = e^{iu_1\mu_{J_1}-\frac{1}{2}\sigma^2_{J_1}u_1^2} - 1, \\
m_{J_2} &= e^{\mu_{J_2}+\frac{1}{2}\sigma^2_{J_2}} - 1, \quad n_{J_2} = e^{iu_2\mu_{J_2}-\frac{1}{2}\sigma^2_{J_2}u_2^2} - 1,
\end{aligned} \tag{3C.3}$$

If the model does not present jumps, this general model reduces to SYSSV; if the model does not present seasonality in the variance either, it reduces to TS09. Observe that these elements only affect $A(\tau; u_1, u_2)$. This means that, for a given set of b_0, b_1, b_2, the solution to $C(\tau; u_1, u_2)$ remains as in Appendix 3A.

3C.2 Variance Term $C(\tau; u)$

Trolle-Schwartz (2009) and extensions (SYSVJ, SYSSV)

With $\sigma_Y(t,T)$ as in Table 3.1, we have that

$$\begin{aligned}
b_0 &= -\frac{1}{2}\Big((u_1^2 + iu_1)\big(\sigma_{S_1}^2 + \sigma_Y^2(t,T) + 2\rho_{S_1 y}\sigma_{S_1}\sigma_Y(t,T)\big)\Big) \\
&\quad - \frac{1}{2}\Big((u_2^2 + iu_2)\big(\sigma_{S_2}^2 + \sigma_Y^2(t,T) + 2\rho_{S_2 y}\sigma_{S_2}\sigma_Y(t,T)\big)\Big), \\
b_1 &= -\kappa + i\sigma_v\Big(u_1\big(\rho_{S_1 v}\sigma_{S_1} + \rho_{yv}\sigma_Y(t,T)\big) + u_2\big(\rho_{S_2 v}\sigma_{S_2} + \rho_{yv}\sigma_Y(t,T)\big)\Big), \\
b_2 &= \frac{\sigma_v^2}{2}.
\end{aligned} \tag{3C.4}$$

The coefficients in $g(z), g'(z)$ are as in (3A.8), with

$$\begin{aligned}
c_0 &= -\kappa + i\sigma_v\Big(u_1\big(\rho_{S_1 v}\sigma_{S_1} + \rho_{yv}\frac{\alpha}{\gamma}\big) + u_2\big(\rho_{S_2 v}\sigma_{S_2} + \rho_{yv}\frac{\alpha}{\gamma}\big)\Big), \\
c_1 &= -\sigma_v\rho_{yv}\frac{\alpha}{\gamma}e^{-\gamma(T-T_{Opt})}i(u_1+u_2), \\
d_0 &= -\frac{\sigma_v^2}{4}\Big(\big(\sigma_{S_1}^2 + \frac{\alpha^2}{\gamma^2} + 2\sigma_{S_1}\rho_{S_1 y}\frac{\alpha}{\gamma}\big)(u_1^2 + iu_1) + \big(\sigma_{S_2}^2 + \frac{\alpha^2}{\gamma^2} + 2\sigma_{S_2}\rho_{S_2 y}\frac{\alpha}{\gamma}\big)(u_2^2 + iu_2)\Big), \\
d_1 &= +\frac{\sigma_v^2}{2}\frac{\alpha}{\gamma}e^{-\gamma(T-T_{Opt})}\Big(\big(\frac{\alpha}{\gamma} + \rho_{S_1 y}\sigma_{S_1}\big)(u_1^2 + iu_1) + \big(\frac{\alpha}{\gamma} + \rho_{S_2 y}\sigma_{S_2}\big)(u_2^2 + iu_2)\Big), \\
d_2 &= -\frac{\sigma_v^2}{4}\frac{\alpha^2}{\gamma^2}e^{-2\gamma(T-T_{Opt})}\left(u_1^2 + u_2^2 + i(u_1+u_2)\right).
\end{aligned} \tag{3C.5}$$

In particular, if the initial condition is $C(0; u_1, u_2) = 0$, then k_1, k_2 are as in (3A.10). The extensions of TS09 present exactly the same expressions for this term and their components.

Schneider-Tavin (2018, 2021)

With $\sigma_F(t,T)$ as in Table 3.1, we have that

$$\begin{aligned}
b_0 &= -\frac{1}{2}\Big((u_1^2 + iu_1)\sigma_{F_1}^2(t,T) + (u_2^2 + iu_2)\sigma_{F_2}^2(t,T)\Big), \\
b_1 &= -\kappa + i\sigma_v\Big(u_1\rho_{F_1 v}\sigma_{F_1}(t,T) + u_2\rho_{F_2 v}\sigma_{F_2}(t,T)\Big), \\
b_2 &= \frac{\sigma_v^2}{2}.
\end{aligned} \tag{3C.6}$$

Following the methodology described in Sitzia (2018), the coefficients in $g(z), g'(z)$ are as in (3A.12), and

$$c_1 = -i\sigma_v \Big(u_1 \rho_{F_1 v} \sigma_{F_1}(T_{Opt}, T) + u_2 \rho_{F_2 v} \sigma_{F_2}(T_{Opt}, T) \Big),$$
$$d_2 = -\frac{\sigma_v^2}{4} \Big((u_1^2 + iu_1)\sigma_{F_1}^2(T_{Opt}, T) + (u_2^2 + iu_2)\sigma_{F_2}^2(T_{Opt}, T) \Big). \tag{3C.7}$$

The expressions followed by k_1, k_2 are as those for TS09.

3C.3 Independent Term $A(\tau; u)$

Equation (3C.1) has an analytical solution given by

$$A(\tau; u_1, u_2) = \frac{2\kappa\gamma}{\sigma_v^2}\big(A_1(\tau; u_1, u_2) + A_2(\tau; u_1, u_2) + A_3(\tau; u_1, u_2) + A_4(\tau; u_1, u_2) + k_3 \big)$$
$$+ \lambda_1(n_{J_1} - iu_1 m_{J_1})\tau + \lambda_2(n_{J_2} - iu_2 m_{J_2})\tau, \tag{3C.8}$$

with $A_1(\tau; u_1, u_2)$–$A_4(\tau; u_1, u_2)$ as in (3A.15), k_3 as in (3A.18).